SMOS 3RD MISSION REPROCESSING CAMPAIGN

LEVEL 2 SM V700 OVERALL QUALIFICATION

Project code	SO-TN-CB-GS-0095
Version	2.a
Date	05/07/2021

	Role	Name	Date and signature
Written by :	**CESBIO**		
	Project Engineer	E. Bousquet	
	Lead Investigator	Y. Kerr	
	Project Engineer	A. Mahmoodi	
	Project Engineer	A. Mialon	
	Project Engineer	P. Richaume	
	FMI		
		M. Holmberg	
		J. Lemmetyinen	
		K. Rautiainen	
	Tor Vergata University		
		C. Vittucci	
	WSL-Gamma		
		D. Houtz	
		R. Naderpour	
		M. Schwank	

Approved by**:**			
Approved by :			

DOCUMENT STATUS SHEET

version / rev.	Date	Pages	Changes	Visa
1.0	14/12/2020		Early check initial issue	
2.a	25/05/2021		Whole 11 years REPR analysis draft issue	

DISTRIBUTION LIST

ESTEC:	

ESRIN:	
Klaus Scipal	
Roberto Sabia	

CNES	

Industry	
Argans	

ESLs	
CESBIO team	
Tor Vergata team	
Gamma team	
FMI team	

QWG	
All core members	

REFERENCES

[AD1] SM_ATBD_SO-TN-ESL-SM-GS-0001_4a_20190909

[AD2] SO-TN-CBSA-GS-0052_Soil_Moisture_Level_2_Products_Evaluation_Metrics-2.0_20190219

[AD3] SO-TN-CBSA-GS-0063_SMOS_Level_2_SM_650_Reprocessing_Canpaign_Overall_Qualification-1.0_20180119

[AD4] SO-TN-CBSA-GS-0083_L2L1_metric_L1C620_vs_L1C724_20200401

[AD5] H. Tang, and J. Armston, J."GEDI L2B ATBD for Footprint Canopy Cover and Vertical Profile Metrics", Goddard Space Flight Center, Greenbelt, MD, 2019. https://lpdaac.usgs.gov/documents/588/GEDI_FCCVPM_ATBD_v1.0.pdf

[AD6] P. Potapov, X. Li, A. Hernandez-Serna, A. Tyukavina, M. C. Hansen, A. Kommareddy, A. Pickens, S. Turubanova, H. Tang, C. Edibaldo Silva, et al., "Mapping global forest canopy height through integration of GEDI and Landsat data," Remote Sensing of Environment, vol. 253, Feb. 2021, Art. no. 112165.

[AD7] P. R. Stysley, D. B. Coyle, R. B., Kay, R. Frederickson, D. Poulios, K. Cory, and G. Clarke, "Long term performance of the high output maximum efficiency resonator (HOMER) laser for NASA' s global ecosystem dynamics investigation (GEDI) lidar,"Optics & Laser Technology, vol. 68, pp.67-72, 2015.

[AD8] Luthcke, S.B., T.J. Sabaka, J. Nicholas, S. Preaux and M. Hofton. 2021. Algorithm Theoretical Basis Document (ATBD) for GEDI L3 Gridded Land Surface Metrics. https://gedi.umd.edu/data/documents (Provided as companion file GEDI_ATBD_L3R01.pdf)

[AD9] Schwank, M., Kontu, A., Mialon, A., Naderpour, R., Houtz, D., Lemmetyinen, J., Rautiainen, K., Li, Q., Richaume, P., Kerr, Y., & Mätzler, C. (2021). Temperature Effects on L-band Vegetation Optical Depth of a Boreal Forest. Remote Sensing of Environment

[AD10] Mialon, A., Rodríguez-Fernández, N.J., Santoro, M., Saatchi, S., Mermoz, S., Bousquet, E., & Kerr, Y.H. (2020). Evaluation of the Sensitivity of SMOS L-VOD to Forest Above-Ground Biomass at Global Scale. Remote Sensing, 12, 1450

ACRONYMS

TABLE OF CONTENTS

1 INTRODUCTION

This technical note reports on the evaluation of the 3rd mission reprocessing from the Level 2 Soil Moisture v700 products perspective. It corresponds to DT2-5 deliverable.

On 2020/12/05 the 3rd mission reprocessing campaign for the soil moisture processor v700 started. Three parallel processing instances, starting for 2010 (S1), 2014 (S2) and 2018 (S3) have been used to produce the main reprocessing 20100501 to 20210524 data 11 years worth.

The catch-up, 20210201 up to the operational switch to v700 on 20210524, is only partly considered in this release.

The early check that built the v1.0 content of this technical note is kept in this report for shorter period perspectives. They refer to the segment S1 2010 (04,05,06,07,08,09), the segment S2 2014 (01,02,03 ,04 ,05 ,06) and 3 months of data for the segment S3 2018 (01 02, 03, 04). Note that S1 is a bit different from S2 and S3 as the RFI situation awareness was just starting; S1 contains much more RFI impact than the two others.

The general goal of this technical note is to report on the reprocessing health, the possible agreements/differences/divergences between v700 and v650 data and all findings indicating improvement/degradation of the v700 compared to the previous v650 similarly to [AD3] though with new perspectives offered by the enlarged ESLs expertise, the longer data period and our increased knowledge.

This report considers different perspectives: temporal, spatial, spatiotemporal on maps, stats and performances of retrieved v700 parameters SM, TauNadir, ACard, Chi2, PRFI12 against REPR v650 data against our expertise knowledge and expectations from past preliminary work, especially the blind-tests exercises outcomes.

The UDP, DAP, AUX_ECMWF and few others products were essentially used. They represent on overall ~350000 products for a volume of ~20TB (all multiplied by two as v700 and v650 are considered) of data to be mined, several time, partly or entirely, to obtain the different perspectives needed for this report.

This technical note is organized into 5 main sections, the section 1 being this introduction.

The section 2 describes the main characteristics of the L2SM v700 reprocessing campaign compared to the REPR/OPER L2SM v650, in terms of algorithms, ADFS, setup evolution and the expected differences we should observe.

The section 3 provides directly the main conclusions and findings: positive aspects, negative aspects, caveats, issues, further required insights. They are based on the detailed analysis provided by the following sections 4 and 5 which provide deeper analysis and details, maps, plots, etc … to look at.

The section 4 is dedicated to the overall features perspective; the big factual picture, while the section 5 is dedicated to more thematic perspectives providing insights on the VOD, the cryopshere and climatology.

Even if the included material is already very consequent, this technical note is to be considered as a draft version. Most of the time was invested to mine the data, produce outputs, refine them, do some interpretations etc … but not yet spending enough time to really step back and take all the necessary time to look at them, digest the information, look for additional specific focus and/or finer analysis when necessary.

An updated version will be issued with added insights. A larger amount of material than what can be reasonably reported in this (already huge) technical note has been produced (full resolution, specific areas, ascending, descending, meridional hovmöller, etc …). It is intended to make them all available in a repository for this future issue to offer any people the possibility to investigate them.

2 L2SM V700 REPROCESSING CAMPAIGN CHARACTERISTICS COMPARED TO V650

There are significant changes between the L2SM v700 reprocessing compared to v650 REPR/OPER:

1. algorithms changes involving processor code updates,
2. configuration changes, including algorithms parameters and ADFs content changes, new added ADFs fields to support the algorithms changes,
3. L1C v724 is used instead of the L1C V620

The two first points were studied upstream and were presented at various QWGs and PMs based on blind tests. All these past detailed exercises were made on evolutions that shaped the v700 from the L2SM v650 but on the basis of the same L1C v620.

The last point was studied using the L2 SM v650 comparing L1C v724 against L1C v620 on limited test data (4 months) and reported in the L2SM/L1C metric technical note [AD4].

The L2SM v700 are based on algorithms evolutions that contain significant number of changes compared to v650 with different expected impacts from the aforementioned past studies; they are marked as blue text following the algorithms changes below:

- The Bircher organic soil dielectric constant empirical model is added. Actually, the dielectric constant of all wet ground surfaces (FNO, FFO) is considered as a weighted mixture of mineral soil (Mironov model) and organic soil (Bircher model).

  Expectation: the general characteristic of SOM is to allow more water than mineral soils for the same emissivity. So it is by using the Bircher model compared to Minronov', retrieved soil moisture is expected to increase. However, this increase is *non-linear and for dry to low soil moisture conditions, both behave similarly. As the soil is wetting to moderate – high value, retrieved soil moisture is expected to become as significantly higher for SOM than for mineral.*

- The term is added to the cost function along with the RA^2. This term represents the average ripples, oscillations amplitude coming from image reconstructions errors. From the retrieval perspective these ripples are seen as unexplained extra variances along the BTs incidence angle profile. These extra observation variances generate in turn higher Chi2 than expected when we do account for them; it is the purpose of .
Expectation: this approach introduced in v700 has the same goal than the post rescaling Chi2 introduced in v650. However in v650 it is made on the Chi2 after the retrieval is over which mean that using it or not or with different scale factors does not change retrieved values. For v700 it is more naturally introduced in the cost function as an added component to the observation errors and thus it allows retrievals readjustments. Consequently differences in retrieved values between the two versions are expected, though small as variability with no systematic impacts.
- The nominal (FNO) and forest (FFO) are packed to a single fraction for the free parameters retrievals, still keeping the specific fixed parameters properties linked to each of these surfaces.
Expectation: more successful retrievals are expected on mixed NO-FO surface, particularly apparent at frontiers around dense forest. Significant changes in retrieved soil moisture and opacity, particularly for the latter that has the strongest non linear relationships with BTs. Besides, packing the two fractions together decreases the underlying presence of the landcover as the NO or FO fixed contribution disappear which results in a spatial smoothing effect on retrieved values.

The second aspect in v700 is algorithms configuration changes and ADFs changes.

- The original IGBP water fractions of the AUX_DFFFRA are replaced by water fraction derived from the ESA-CCI-Radar water body. As a consequence all other fractions increase/decrease proportionally.
Expectation: using ECA-CCI RADAR high resolution provides almost systematically and everywhere higher water fraction in our modelling. As a direct consequence with more contribution of colder BT in the aggregated modelling, retrieved soil moisture decrease in compensation. Change is retrieved opacity is also expected but with increased retrieved values though more complex interactions between the two quantities are also expected.
- The AUX_LANDCL single scattering albedo (ω) for low vegetation (FNO) is changed from 0 to 0.06 and their associated roughness (HRmax=0.1, HRmin=0.05) changed to (HRmax=0.3, HRmin=0.1).

Expectation: time series of retrieved soil moisture are expected to have a changed dynamic, at least improved when compared to in-situ measurements. As a direct mechanical effect in the Tau-Omega model, with decreased emissions from low vegetation NO model contribution it implies to raise the ground emission contribution by decreasing soil moisture in compensation. The effect is non-linearly function of the low vegetation opacity; higher the low vegetation opacity higher the decrease of retrieved soil moisture as the attenuation of vegetation increases.

- The RSOM field, the fraction of organic soil, is added to the AUX_DFFSOI to support the Bircher organic soil dielectric constant model.
  Expectation: the organic soil is strongly present at high Northern latitude and less in other places with some exceptions. Effects are thus expected to be more prominent especially for wet conditions in the north.

Last but not the least is the L1C evolutions brought by the v724 versus the v620 that add to the v700 L2SM evolutions. It makes the L2SM v700 3rd mission reprocessing more difficult than it was the case for the 2nd one where only L2SM versions were different. Expectation: as reported in [AD4] although the L1C v724 appears rather neutral in term of systematic differences at Global, but with significant variability with very structured spatial patterns is reported. This varaibility and structure are also changing depending on the orbits ascending/descending passes. These significant changes correspond also to specific areas, contrasted transition and forest for both retrieved soil moisture and opacity. Below dense forest L1C v724 based soil moisture and opacity tends to decrease but with associated decrease Chi2 as well. Dynamics of time series of retrieved parameters are also different, at least improved for soil moisture when compared to in-situ measurements but essentially for ascending orbits while descending ondes were reported more similar.

Final note on our expectations:

- the expectations reported at the previous paragraph are considered independently from each others. Reinforcements or cancellations of some effects are expected and potentially modulated in time for some of them like omega impact, from no impact to strong impact following low vegetation seasonality, like SOM impact both dependent on the SOM fraction but also dependent on wetness conditions.
- The Northern high latitude is expected to be complex areas where different effects are competing. It is for instance the case for omega, SOM, water fractions. At these Northern locations SOM is very present so with expected retrieved soil moisture increase. But it competes with retrieved soil moisture decrease as it is also a place with increased water fractions. And this is expected to be also modulated in time as for wet conditions SOM have more impact and may dominates. But if low vegetation is growing at the same time then decreased soil moisture is also reinforced.

- Other locations could seem easier, like dense tropical/equatorial forests where mostly the increased water fractions of river networks is dominating with simpler and much static signature on retrieved soil moisture and opacity. It is true, but they are also locations where L1C v724 impact is the strongest.

3 CONCLUSIONS AND WAYS FORWARD

We expected the L2SM v700 to be significantly different from the v650 and it is the case. The main source comes from the L2SM algorithms changes. However, the L1C724 is certainly not neutral though difficult to know exactly its relative impact without replaying a L2SM v700 REPR but using L1C v620 which is not feasible.

Most differences are in line with our expectations for wet soil retrievals i.e. NO/FO (DT11/12) which were the focus of all preliminary studies and evaluations.

It gives a first evident conclusion about the reprocessing campaign itself; over the ~11 years the 3rd SMOS mission reprocessing performed necessarily well.

Indeed, we observe in these v700 data compared to v650 ones the main characteristics enumerated in the previous section 2 but also added aspects.

The v700 has in general lower SM compared to v650, but not necessarily everywhere and not necessarily all the time and reduced dynamics (amplitude). By increasing omega value we traded bias to gain on correlation with respect to in-situ measurements. Around rivers networks, the CCI-RADAR water fractions used for v700 are higher that the IGBP ones of v650 and induce decreased retrieved soil moisture. On v700 SM maps rivers network mostly disappear compared to v650 SM maps which is a very good thing. In addition, the L1C v724 also decreases slightly the retrieved SM compared to the L1C v620 used for the v650.

Northern latitudes represent certainly the most complex area where the different algorithms changes compete, some time in opposite direction, and where NPEs (snow, frost) play also a strong role. For instance, increased water fractions is highly present and in association with increased omega when low vegetation is raising tends to sum-up in the decrease of retrieved soil moisture. But on another hand, rich organic soil is also highly present and tends to increase the retrieved soil moisture particularly in wet condition. They induce the most complex patterns in Hovmöller diagram compared to mid latitudes.

When compared to in-situ measurements the v700 lower retrieved soil moisture represents on average a decrease of ~-0.03 m^3/m^3 (ASC) ~-0.02 (DSC) m3/m3 compared to v650' however with expected improvements on correlation that increases by ~0.14 (ASC) ~0.13 (DSC) and on the STDD that decreases by ~-0.02 (ASC) ~ -0.01 (DSC). The v700 increase of correlation and the decrease of STDD are almost systematic for all the networks/sites. The v700 soil moisture decrease generates more variability across the sites regarding the biases. For networks/stations such as Watersheds, AMMA, some of SCAN for which the v650 was too wet, the lower v700 soil moisture actually improves the bias. The RMSD are more comparable, there are almost as many better for v700 than for v650. In a sense the evolutions made have traded on the fixed component of errors (bias), accepting potentially more, to gain on the random (or variational) components (correlation, standard deviation) but somewhat not changing drastically the total error budget (RMSD).

The retrieved v700 opacity is on average more similar to v650 than soil moisture but with strong local differences on mixed FFO/FNO areas due to the joint FNO+FFO retrieval. It is mostly visible as smoother spatial values, especially on transitions at the interface NO/FO (true as well for SM but to a lower extent). These v700 smoother VOD values appear more consistent when compared to AGB map, and compared to RH100 and PAI parameters retrieved by GEDI, the correlation coefficients are higher than the v650 ones.

The retrieved dielectric constant (ACard) is a new perspective in the evaluation of reprocessed data. ACard was introduced as an experimental retrieved parameter designed for diagnostic or for surfaces like frozen soil, ice, snow where soil moisture retrieval does not make sense. However the dielectric constant retrieval decision tree branches can represent ~45% of the land retrievals during the Northern winter season, with ~28% being obtained over snow, frost decision tree branches. At Northern summer season, the retrievals drops typically to ~22%, 4.5% being dedicated to snow, frost cases. Generally speaking, the retrieved dielectric constant follows the expected logic with a decrease of FO/NO retrieved area in favour to snow and frost soil retrieved increasing area during winter. The retrieved dielectric constants have reasonable values and seasonal variations but with differences between v650 and v700. Usually v700 reports more FO/NO cases, so less retrievals cases for snow/frost than v650 and when retrieved lower retrieved dielectric constant than v650. Compared to other information, L3FT products and AUX_ECMWF SWE, the retrieved dielectric constant should display expected connections. For freeze-thaw state, the overall behaviour is as expected. Lower retrieved dielectric constant for L3FT frost state is obtained than for L3FT taw state for the two versions. However, the amplitude between the two states retrieved dielectric constant variation is perhaps more evident with v650 and some disagreement exist. The retrieved dielectric constant should also decrease by the effect of dry snow. This characteristic can be clearly observed but not all the time. These two geophysical effects deserve more investigations.

Regarding the performances, the Chi2 and the success/failures, there are significant differences between the two versions.

The v700 Chi2 is slightly higher for RFI areas as the procedure to calibrate σ_{IRE} has been made on very strictly selected free of RFI data, which is a good thing. For other areas, RFI cleaner, it is in general the opposite with lower v700 Chi2 or similar Chi2 than v650', so better fits, which is also a good thing. It was not so clearly seen in blind tests as the exercises considered each algorithm move independently from each other and for a limited period of time and also using L1C v620 (no Gibbs2). With all options included and longer periods it becomes more apparent e.g. L1C 734 Gibbs2 pattern we know over Australia coast line, organic soil at northern latitudes …

The v700 retrievals performances (successful retrievals) are in general significantly increased, more actually than expected. The joint FNO+FFO retrievals for very mixed NO/FO, especially the transition FO/NO, are particularly factor in this gain. However, for ACard retrievals it is more balanced. There are specific areas but also time (season) where v650 retrievals performances are higher than v700 but also with lower magnitudes variations compared to the increased NO/FO performances.

At this stage, this technical report contains a lot of information. A large part of the time was taken in mining the large amount of data, producing plots, figures, iterating, refining etc… It was already a daunting exercise for the reprocessing campaign v650 vs. v620, it is even more the case with this reprocessing campaign.

We need now to step back and take the necessary time to look and analyze these results and certainly refine or complement some of them as there is a certain number of not addressed or partly addressed questions appearing.

For example, we always observed since the beginning of the mission ascending/descending differences but now impact the analysis VOD over forest for certain regions and also somewhat the cryosphere analysis. There are not yet explained anomalies in time series of VOD that could pinpoint algorithms or ADFs issues or because of other factors to determine.

The RFI is a severe issue that could blur results or create interpretation artifacts. However, with 11 years worth of data we could consider to redo some analysis with extreme RFI rejection. Even with the expense in spatial/time coverage, more 'natural' signatures could appear, being geophysical, algorithmic issues, ADFs issues or instrumental aspects.

4 OVERALL PERSPECTIVE

Compared to the 2nd mission reprocessing L2SM qualification, the 3rd is different in the sense that we have now two degrees of freedom. For the 2nd mission reprocessing the differences were only coming from L2SM updates; both L2SM v650 and L2SM v620 were using the same L1C v620.

For this 3rd mission reprocessing both L2SM v700 and L1C v724 updates are matter of changes compared to L2SM v650 + L1C v620.

We consider here the whole 11 years of reprocessing, 20100501 – 20210131, and the few months taken from the three segments of parallel reprocessing instances that were available in Dec 2019: S1: 20100601 – 20100905, S2: 20140201 – 20140524, S3: 20180201 – 20180414.

The whole integrated 11 years includes all the SMOS mission past story particularly the RFIs impact and evolution since 2010 while the S1, S2, S3 segments represent different shorter windows allowing to observe specific aspects.

The following subsections will look to the reprocessed data through different perspectives:

- Section 4.1: the Earth as seen by the AUX_DFFFRA and decision tree for the retrievals
- Section 4.2: the retrievals success/failure for SM/TauNadir, ACard/TauNadir retrievals: Numerical figures globally, per continental areas; Global maps; space-time through Global zonal Hovmöller.
- Section 4.3: focus on retrieved SM/TauNadir/Chi2/PRFI12 through SM retrieved times series versus in-situ SM time series; Global spatial maps and stats per continental areas; space-time as Global mean and std zonal Hovmöller plots.
- Section 4.4: focus on Ascending versus Descending

4.1 DECISION TREE AND FRACTIONS CHANGES

For this section the v700 and v620 SML2PP was run over 4 days with a specific configuration preventing any NPE events to occur: no soil freezing, no water body turned into ice, no dry, mixed, snow cover.

FM0 from DAP are extracted to access then the static (no NPE) FM0 radiometric fractions leading also to the static decision tree branches of the Earth.

The only but important change is the water fraction change introduced by the ESA CCI radar maps @250m for v700 vs. IGBP @ 1km. The landcover itself being the same (IGBP), the other fractions are just changing proportionally to the increase/decrease of FWO as it is shown Figure 1. This change is mostly an increase of FWO due to the higher 250m resolution among other factors with clearly dominant red colors in Figure 1 bottom left detailed with different ranges Figure 2. We can also observe that decrease of FWO can actually exist but for much more limited number and smaller areas with also more limited magnitudes change.

These FWO variations are taken from the other fractions for the same areas and appear mostly as dominant blue colors for the three other plots of Figure 1. They lead to the redistribution of fraction illustrated Figure 3.

However, these redistributed fractions impacts marginally the final decision tree branches with very close DT branches maps for v700 Figure 4 and v650 Figure 5. Actually redistributions of DT branches are limited to those shown Figure 6.

Water fraction change is an important factor in our aggregated BT modeling. Higher water fraction implies higher contribution of modeled cold BT in the total aggregated BT model. The direct expected consequence for the same SMOS observed BT, is that the retrieved BT model(s) have to increase in compensation. For bare soil it implies lower retrieved soil moisture. With the vegetation increasing possibly more complex interactions between retrieved soil moisture and retrieved opacity to compensate are expected. As the vegetation becomes more like forest with high opacity we expect though the retrieved opacity to increase as well (assuming no adverse interactions are playing e.g. coming from joint FO+NO retrieval along with omega increase for the NO part).

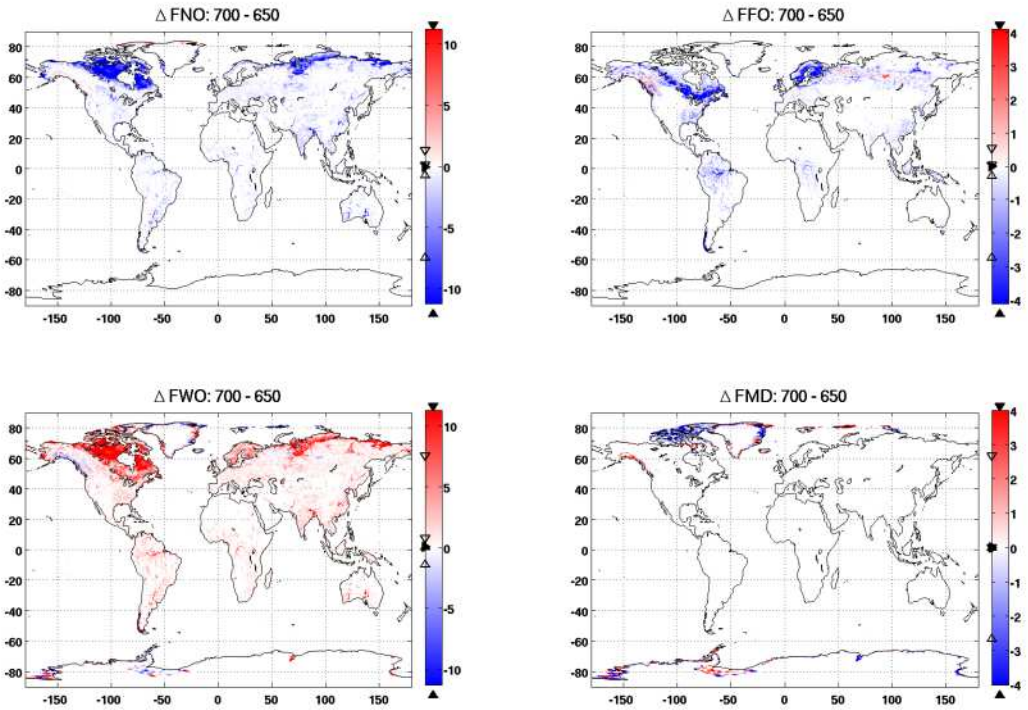

Figure 1: Working Area static radiometric fraction change, Δ=700 – 650, for FNO (top left), FFO (top right), FWO (bottom left) and all ACard MD fractions together (bottom right).

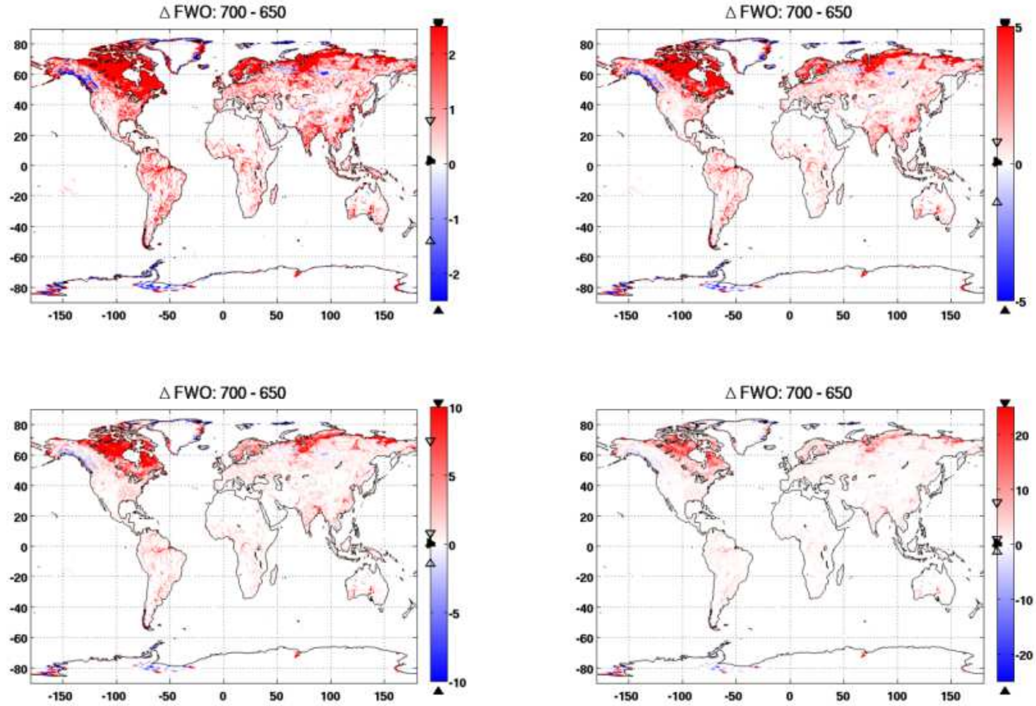

Figure 2: Working Area static radiometric water fraction change $\Delta = FWO_{700} - FWO_{650}$ focus.

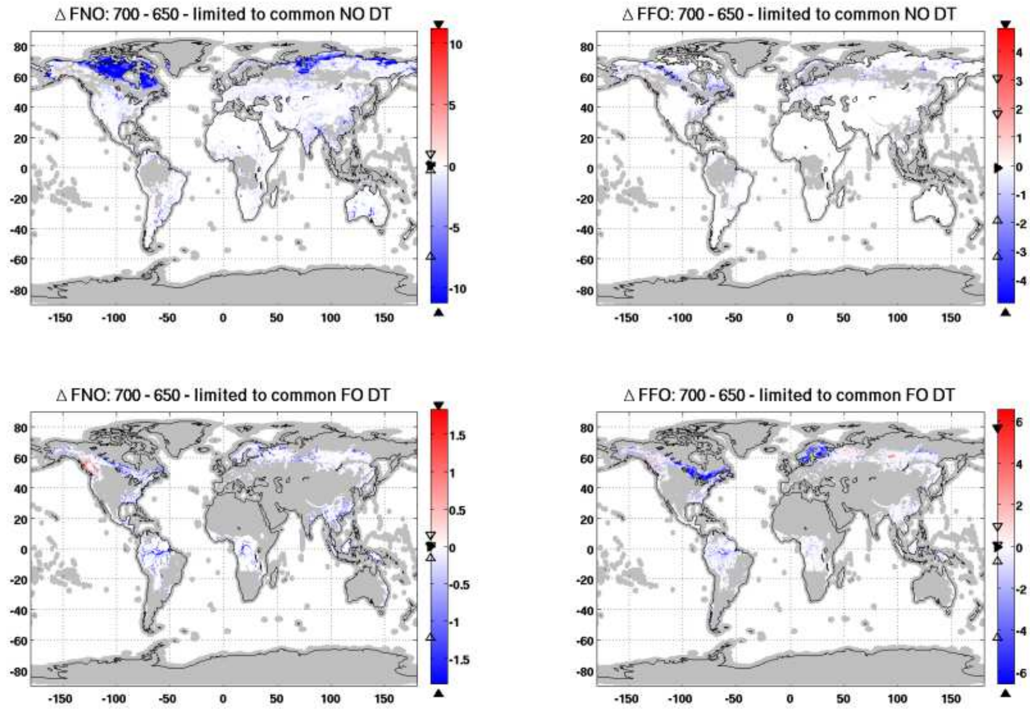

Figure 3: Redistribution NO/FO DT due to FWO change

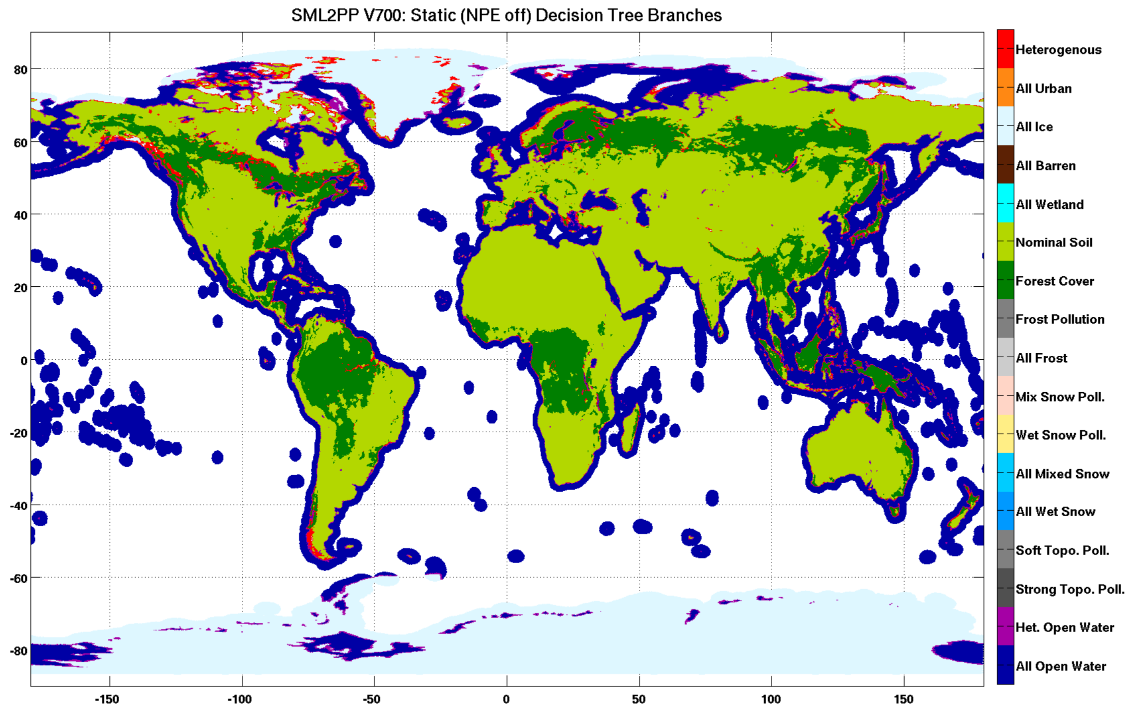

Figure 4: map of v700 static (all NPE off) decision tree branches.

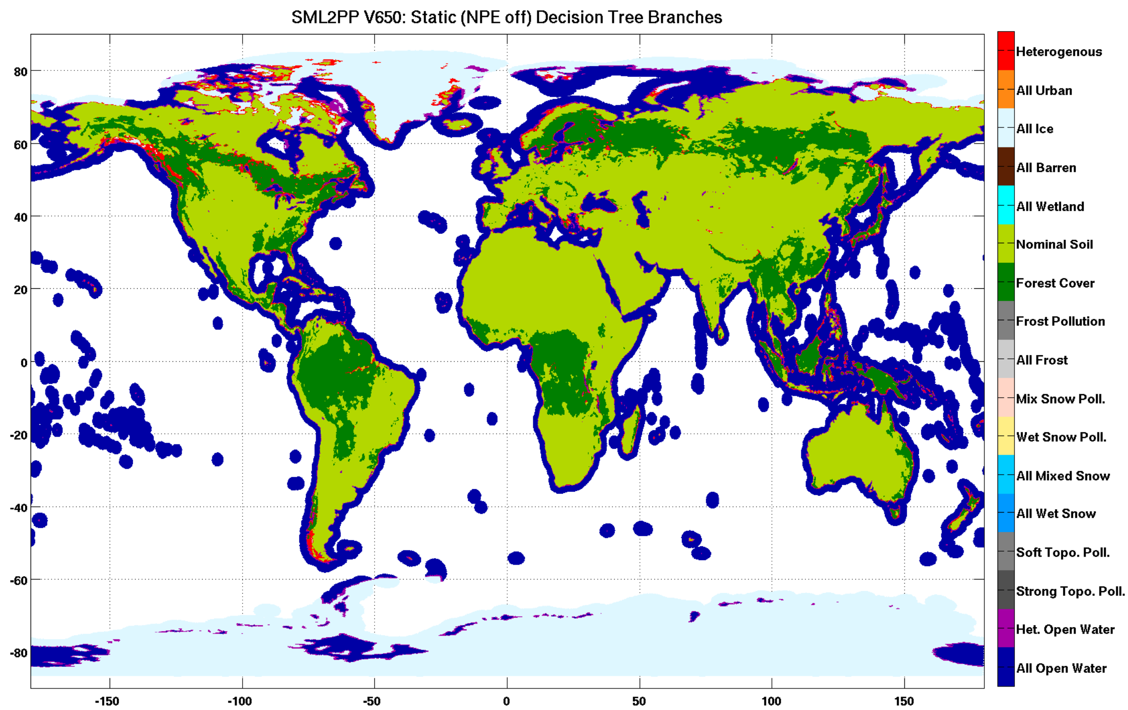

Figure 5: map of v650 static (all NPE off) decision tree branches.

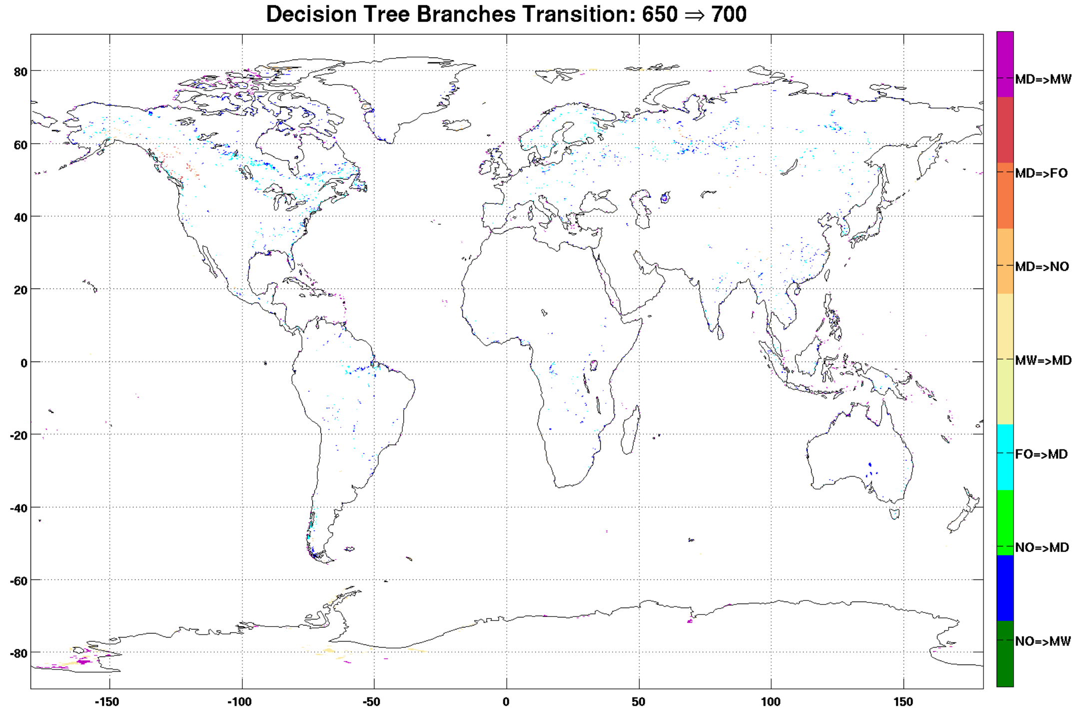

Figure 6: redistribution of decision tree branches between v700 and v650.

4.2 RETRIEVAL SUCCESS/FAILURE PERFORMANCES

This section focuses on the retrievals performances in term of success/failures.

The retrieval performance here is defined as the number of successful retrievals divided by the number of attempted retrievals = number of FL_NO_PROD=0 divided by the number of S_Tree_1≠0. It is important to not just divide by the number of available values as FL_NO_PROD=1 (so no product) is raised also for other reasons than retrievals failures. If we do so then the true success/failure performances of the retrievals will be underestimated.

Indeed the retrievals are not attempted when not enough L1C BTs are available, which is typically the case for the two following reasons:

- For the two ~100km outer swath edges and the two swath start/tips tips of L1C where naturally not enough BTs exists (roughly less than ~10) in BT profiles to guaranty good and stable retrievals.
- Everywhere DGGs are severely contaminated by RFI result in not enough number of BTs left after the L2SM BT filtering has been applied and technically falling into the previous case.

- All in one the two above reasons result in an overall ~18.5% of failing DGGs so raising FL_NO_PROD to 1 but not because of retrievals failures which were actually not attempted.

For such case the decision tree branches S_Tree_1 is equal to 0 as we skip the DGGID. We do not even enter the decision tree stage 1 which has the role to compute FM0 fractions and decides which decision tree branch (DT1 to DT17) is to be used.

The sections that follow focus on the performances per: 1) SM/TauNadir retrievals, so for NO/FO (DT11/DT12) and 2) for all other DTs cases corresponding to ACard/TauNadir retrieval. DT1 highly dominant FWO Tsurf e.g. far enough ocean side of coastline is not yet inspected.

4.2.1 SM/TAUNADIR RETRIEVALS (DT11-12)

This subsection focuses on retrieval success/failure performances for SM/TauNadir retrievals so for decision tree branches DT11 (FO) and DT12 (NO) surfaces. Numerical figure, Global maps & stats and space-time Hovmöller zonal of retrievals performances are given.

4.2.1.1 NUMERICAL

The tables below provide the successful percentages of retrievals considering only the decision tree 11 (FO) and 12 (NO) retrievals i.e. limited to the SMs retrievals DGGs subset so not considering ACard retrieval or water-body retrievals.

Over the whole 11 years:

- the v700 provide always significantly more successful retrievals than v650 on average, about 5%. Actually retrievals performances are above our expectations; we were expecting rather ~3% gain for v700 at Global
- However there is also strong variability across the 7 continental areas. The lowest, still positive, retrieval performance increase is +0.6% for descending orbits over Australia and the highest is +12.8% for West Europe descending orbits.
- Ascending versus descending orbits retrievals performances are also not equivalent.
    - At Global, ascending orbits have +1.8% than descending ones with also a strong variability across the 7 continental areas.
    - For the North America, Africa and Asia areas it is the opposite, descending orbits retrievals are more successful by few percent.
    - The remaining areas behave like the Global Earth though we sometimes high differences e.g. East Europe ascending orbits succeed with +14.4% compared to their descending orbits.

- This asymmetrical orbits passes performances, positive or negative, is a not a specificity of v700 but a common and consistent characteristic between v700 and v650 though with some magnitude variations.
- Most likely this asymmetrical characteristic is dominated by the impact of RFI on the SMOS system due to the tilted antenna; the same sources do not impact the same the retrievals depending if SMOS is flying toward them (long distance impact) or flying from them (short stopping impact).

Indeed, depending on the areas the increase of successful retrievals can reach quite high values, especially for not that-RFI-clean areas e.g. Asia, East Europe and West Europe. It needs particular attention as more successful retrievals is good but only if the added new retrieved values are also good.

However, it is also the first time that we can observe all-included updates of L2SM v700 but also along with the L1C v724 updates. All were independently factors or neutrals in added successful retrievals, they may have just sum up in a way.

Table 1: Whole reprocessing 20100501 - 20210131; overall spatio-temporal average successful retrieval performances of v700 versus v650 per continental areas

		Whole reprocessing (20100501 - 20210131) – Nominal (DT12) & Forest (DT11)							
		North America	**South America**	**West Europe**	**Africa**	**East Europe**	**Asia**	**Australia**	**Global**
ASC	**v700**	96.2 %	97.0 %	86.3 %	89.3 %	89.6 %	72.7 %	96.8 %	89.6 %
	v650	90.2 %	92.6 %	77.2 %	86.7 %	82.6 %	65.3%	96.1 %	84.2 %
	Δ7-6	**+6.0 %**	**+4.4%**	**+9.1 %**	**+2.6 %**	**+7.0 %**	**+7.4 %**	**+0.7 %**	**+5.4 %**
DSC	**v700**	96.7 %	94.8 %	74.0 %	92.1 %	75.2 %	73.3 %	96.1 %	87.8 %
	v650	91.6 %	91.1 %	61.2 %	90.8 %	66.5 %	65.9 %	95.5 %	82.6 %
	Δ7-6	**+5.1 %**	**+3.7 %**	**+12.8 %**	**+1.3 %**	**+8.7 %**	**+7.4 %**	**+0.6 %**	**+5.2 %**
v700 A-D		**-0.5 %**	**+2.2 %**	**+12.3 %**	**-2.8 %**	**+14.4 %**	**-0.6 %**	**+0.7 %**	**+1.8 %**
V650 A-D		**-1.4 %**	**+1.5 %**	**+16.0 %**	**-4.1 %**	**+16.1 %**	**-0.6 %**	**+0.6 %**	**+1.6 %**

Table 2: Reprocessing instance S1; overall spatio-temporal average successful retrieval performances of v700 versus v650 per continental areas

		Reprocessing instance S1 (20100601-20100905) – Nominal (DT12) & Forest (DT11)							
		North America	**South America**	**West Europe**	**Africa**	**East Europe**	**Asia**	**Australia**	**Global**
ASC	**v700**	89.3 %	96.1 %	79.8 %	87.6 %	89.1 %	59.1 %	97.7 %	86.0 %
	v650	85.6 %	91.7 %	71.2 %	85.5 %	84.9 %	54.5 %	97.5 %	82.0 %
	Δ7-6	**+4.3 %**	**+4.4 %**	**+8.6 %**	**+2.1 %**	**+4.2 %**	**+4.6 %**	**+0.2 %**	**+4.0 %**
DSC	**v700**	97.4 %	96.2 %	54.8 %	90.2 %	65.3 %	54.8 %	97.7 %	81.6 %
	v650	94.3 %	92.8 %	42.4 %	89.0 %	58.6 %	48.8 %	96.7 %	77.1 %
	Δ7-6	**+3.1 %**	**+3.4 %**	**+12.4 %**	**+1.2 %**	**+6.7 %**	**+6.0 %**	**+1.0 %**	**+4.5 %**
v700 A-D		**-8.1 %**	**-0.1 %**	**+25.0 %**	**-2.6 %**	**23.8 %**	**+4.3 %**	**+0.0 %**	**+4.4 %**
V650 A-D		**-8.7 %**	**-1.1 %**	**+28.8 %**	**-3.5 %**	**26.3 %**	**+5.7 %**	**+0.8 %**	**+4.9 %**

Table 3: Reprocessing instance S2; overall spatio-temporal average successful retrieval performances of v700 versus v650 per continental areas

		Reprocessing instance S2 (20140201-20140524) – Nominal (DT12) & Forest (DT11)							
		North America	**South America**	**West Europe**	**Africa**	**East Europe**	**Asia**	**Australia**	**Global**
ASC	**v700**	96.1 %	95.7 %	88.4 %	90.3 %	83.7 %	71.4 %	97.4 %	88.8 %
	v650	87.8 %	90.7 %	79.0 %	87.6 %	73.5 %	63.3 %	96.5 %	82.7 %
	Δ7-6	**+8.3 %**	**+5.0 %**	**+9.4 %**	**+2.7 %**	**+10.2 %**	**+8.1 %**	**+0.9 %**	**+5.8 %**
DSC	**v700**	94.8 %	93.7 %	68.2 %	92.7 %	63.1 %	70.2 %	97.1 %	86.3 %
	v650	87.8 %	89.5 %	54.0 %	91.6 %	52.3 %	62.3 %	95.9 %	80.8 %
	Δ7-6	**+7.0 %**	**+4.2 %**	**+14.0 %**	**+1.1 %**	**+10.8 %**	**+7.9 %**	**+1.2 %**	**+5.5 %**

v700 A-D	**+1.3 %**	**+2.0 %**	**+20.2 %**	**-2.4 %**	**+20.6 %**	**+1.2 %**	**+0.3 %**	**+2.5 %**
v650 A-D	**+0.0 %**	**+1.2 %**	**+25.0 %**	**-4.0 %**	**+21.2 %**	**+1.0 %**	**+0.6 %**	**+1.9 %**

Table 4: Reprocessing instance S3; overall spatio-temporal average successful retrieval performances of v700 versus v650 per continental areas

		Reprocessing instance S3 (20180201-20180414) – Nominal (DT12) & Forest (DT11)							
		North America	**South America**	**West Europe**	**Africa**	**East Europe**	**Asia**	**Australia**	**Global**
ASC	**v700**	94.2 %	97.6 %	89.0 %	89.6 %	83.1 %	75.6 %	97.2 %	89.5 %
	v650	83.5 %	93.5 %	77.9 %	86.8 %	65.5 %	65.7 %	96.1 %	82.5 %
	Δ7-6	**+10.7 %**	**+4.1 %**	**+11.1 %**	**+2.8 %**	**+17.6 %**	**+9.9 %**	**+1.1 %**	**+7.0 %**
DSC	**v700**	95.5 %	95.5 %	81.4 %	92.2 %	72.5 %	81.4 %	96.1 %	90.3 %
	v650	86.8 %	91.7 %	70.1 %	90.8 %	62.1 %	73.0 %	95.0 %	85.1 %
	Δ7-6	**+8.7 %**	**+3.8 %**	**+11.3 %**	**+ 1.4 %**	**+10.4 %**	**+8.4 %**	**+1.1 %**	**+5.2 %**
v700 A-D		**-2.3 %**	**+2.1 %**	**+7.6 %**	**-2.6 %**	**+10.6 %**	**-5.8 %**	**+1.1 %**	**-0.3 %**
v650 A-D		**-3.3 %**	**+1.8 %**	**+7.8 %**	**-4.0 %**	**+3.4 %**	**-7.3 %**	**+1.1 %**	**-2.6 %**

4.2.1.2 MAPS OVERALL REPR PERIOD 2010 – 2021

Putting aside RFI areas, the quite high overall retrievals performances for NO/FO areas is homogenous. It appears improved for the v700 in general, significantly improved for specific areas, transitions NO/FO, FO, quite visible on maps compared to v650. So generally speaking v700 gained on sustained performances spatially. This can be seen with more spatially homogenous dark red pattern v700 Figure 7 compared to v650 Figure 8.

However there is few degraded performance for v700 for some localized areas, though with less magnitude compared to the improved values. It is really visible when looking to the difference performances map v700-v650 Figure 9 as blue areas that appear also quite localized spatially. Further specific analysis is required to understand the reason.

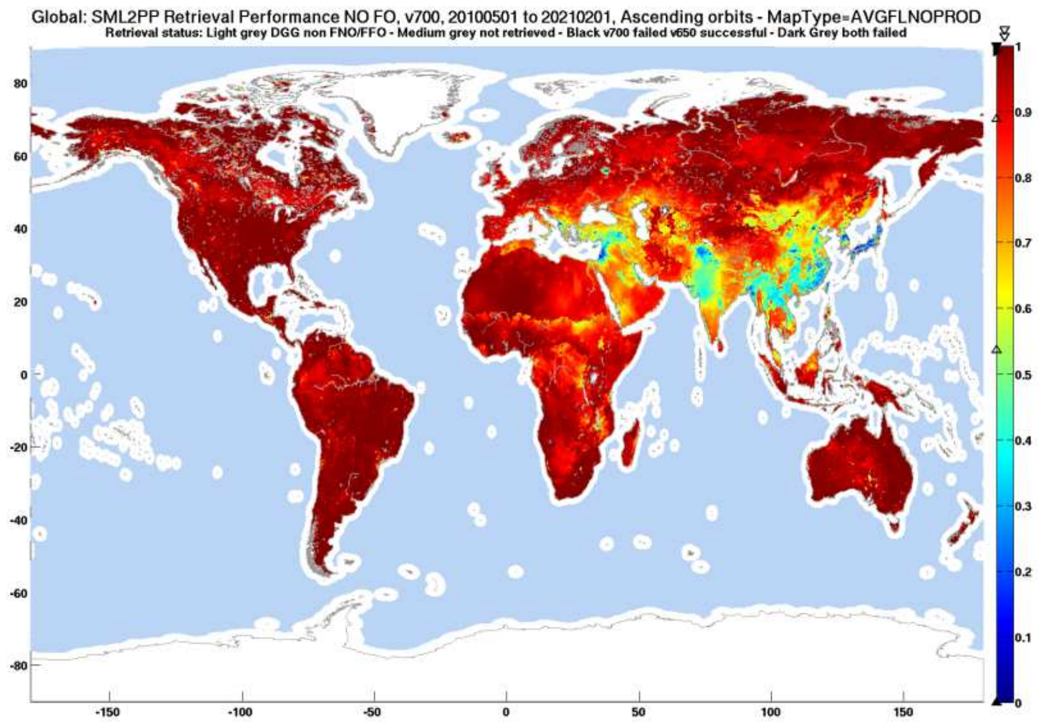

Figure 7: Map of NO/FO (DT 11,12) v700 retrieval performance for the overall reprocessing campaign, 20100501- 20210131

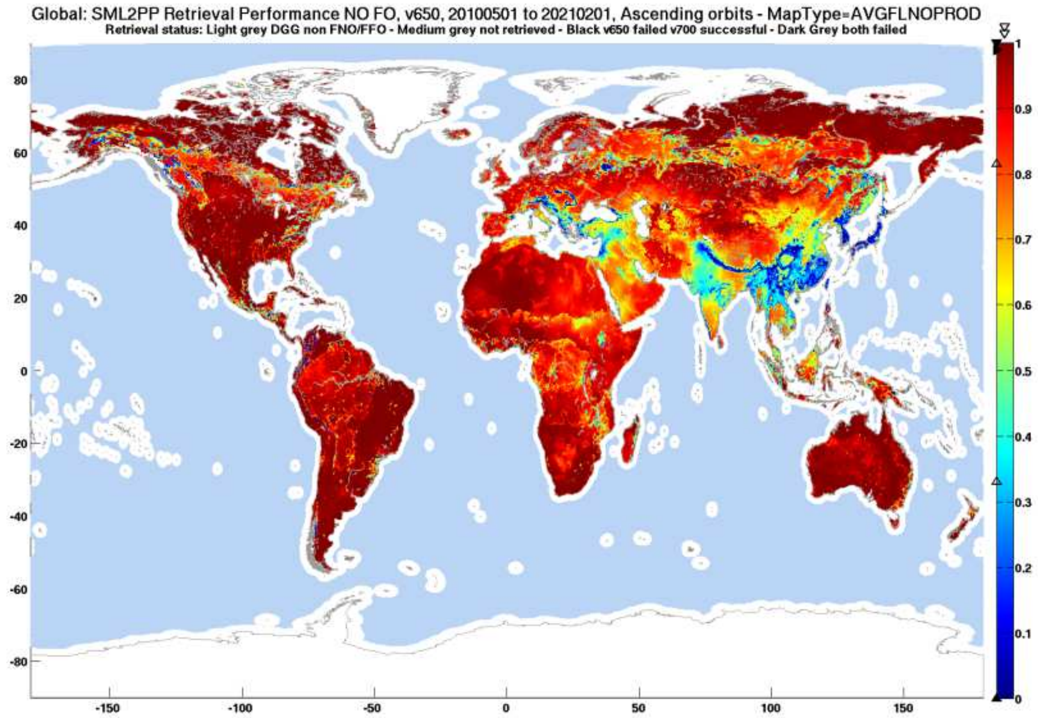

Figure 8: Map of NO/FO (DT 11,12) v650 retrieval performance for the overall reprocessing campaign, 20100501- 20210131, ascending orbits.

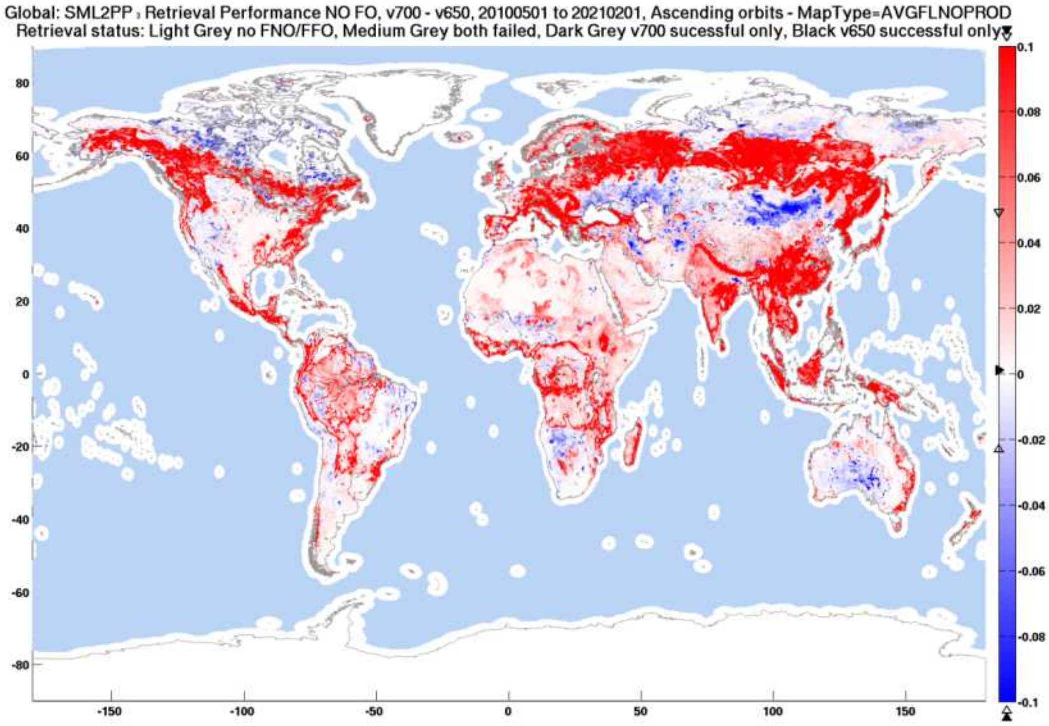

Figure 9: Map of NO/FO (DT 11,12) retrieval performance difference, v700 – v650, for the overall reprocessing campaign, 20100501- 20210131, ascending orbits.

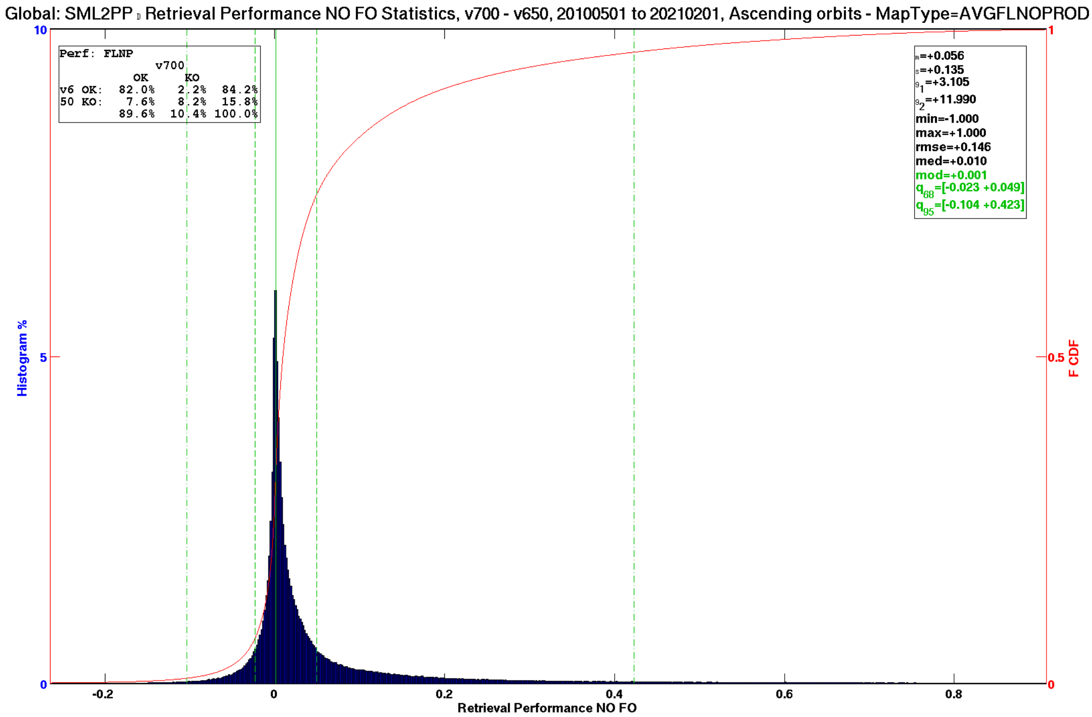

Figure 10: Histogram of NO/FO (DT 11,12) retrieval performance difference, v700 – v650, for the overall reprocessing campaign, 20100501- 20210131, ascending orbits.

4.2.1.3 SPACE TIME ZONAL HOVMÖLLER

In the previous section the spatial information integrated over time allows to locate spatial area of interest. However the past story of SMOS, particularly RFI events in time or specificity of seasonality on performances is lost.

At the expense of a full spatial perspective, Hovmöller plot adds the time perspective though averaging spatial information, here zonal i.e. average over bands of latitude and 4 days of time. The standard deviation over the latitude bands and 4 days of time is also given; it is not often produced information, but we think it also important spatial variability in time information to add to the traditional Hovmöller mean.

As for spatial maps, we interpret the Hovmöller mean zonal performance as the dark redder the better.

For the Hovmoller std zonal performance it is a bit more complex. Along with high Hovmöller mean zonal performance then the dark bluer is the better. It means that the high performance is steady for all DGGs of the latitude band compared to lighter blue if not red e.g. for RFI areas. On another hand when mean retrievals performances are poor, toward blue, associated blue std performance means that it is poor mostly everywhere on the band of latitude. The extreme case is a mean performance of 0 everywhere would have a std of 0 (dark blue) but no good at all... While red std in such case would give hope that within the band it exists better mean performances though in minority.

When comparing v700 vs. v660 Hovmöller, ∆Hovmoller mean zonal performances v700 – v650, redder the better for v700, bluer the better for v650.

∆Hovmoller std zonal performances v700 – v650 is again more complex with variable interpretation. However assuming lower std is better i.e. retrievals performances are more stable spatially then bluer the better for v700, redder the better for v650. As mention before, it does not work for low performances.

Obviously, v700 is dominantly better than v650 (delta Hovmoller) complementing the same spatial feeling but also at all times. Moreover, this increase of performance goes along with a decreased zonal std (dominantly blue) meaning that it spreads also all over the zonal bands.

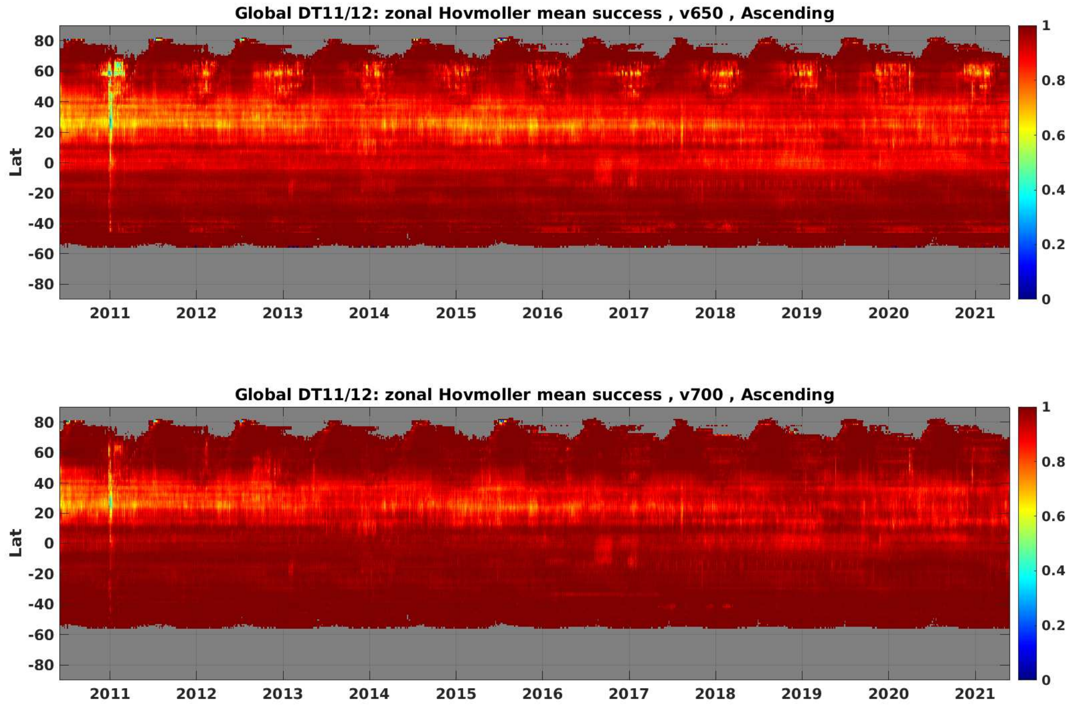

Figure 11: Global Hovmöller: mean zonal NO/FO (DT 11,12) retrieval performances in time, v650 (top), v700 (bottom), ascending orbits.

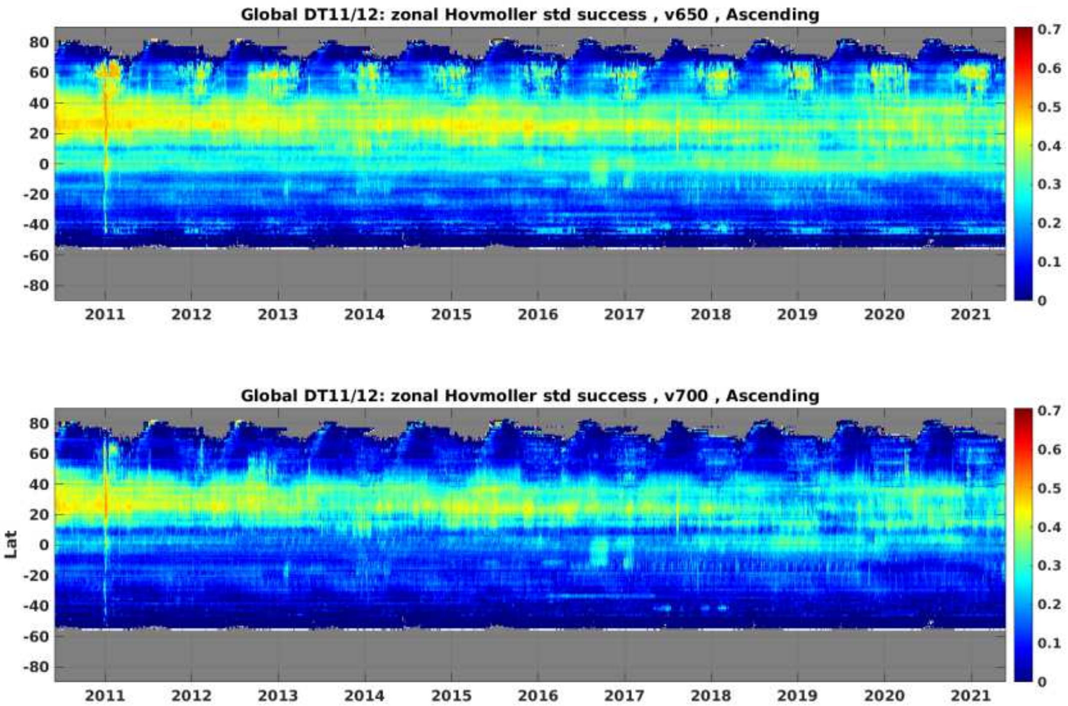

Figure 12: Global Hovmöller: std zonal NO/FO (DT 11,12) retrieval performances in time, v650 (top), v700 (bottom), ascending orbits.

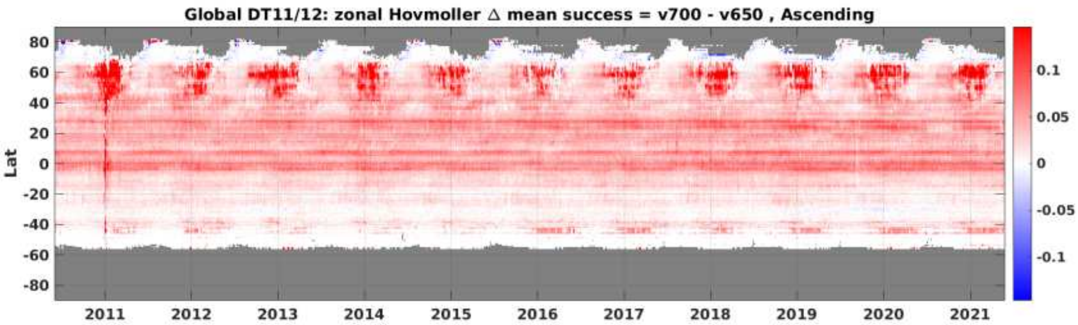

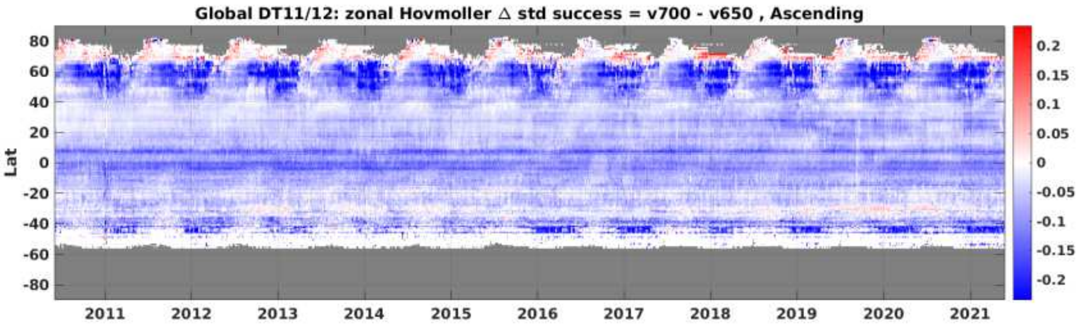

Figure 13: Global Hovmöller zonal NO/FO (DT 11,12) retrieval performances difference, v700 – v650; ∆mean (top), ∆std (bottom), ascending orbits

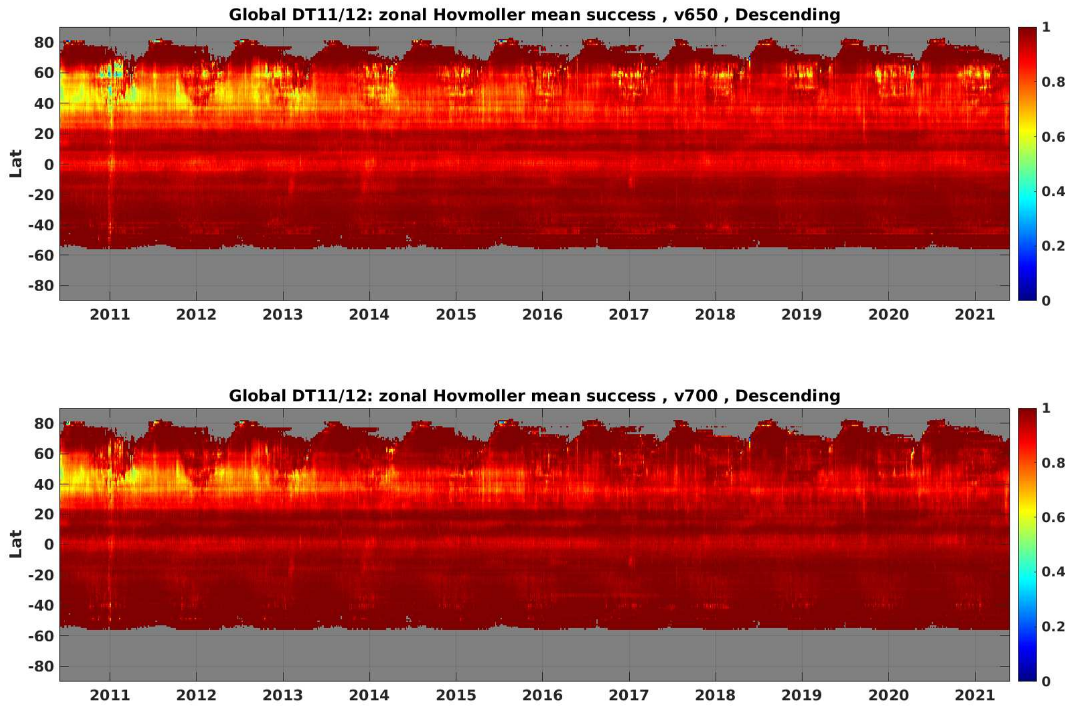

Figure 14: Global Hovmöller: mean zonal NO/FO (DT 11,12) retrieval performances in time, v650 (top), v700 (bottom), descending orbits.

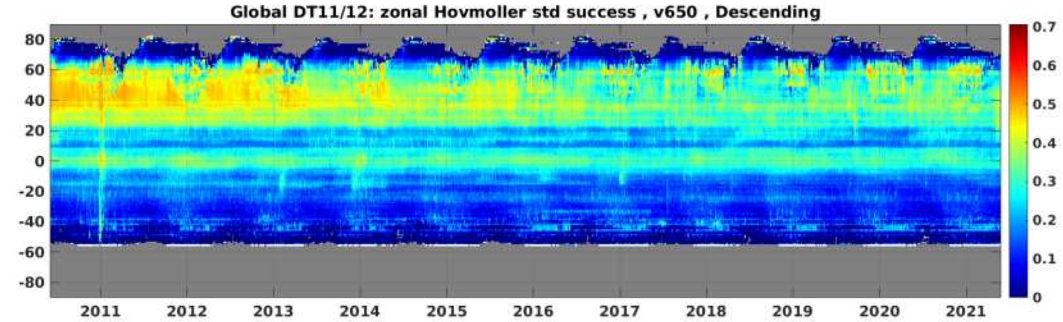

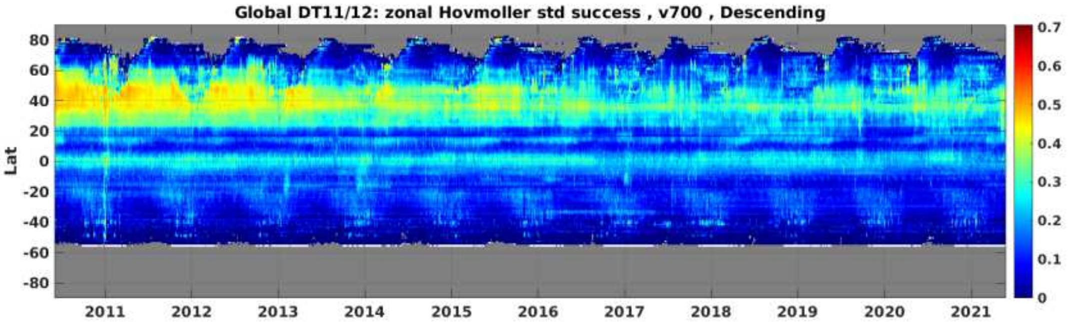

Figure 15: Global Hovmöller: std zonal NO/FO (DT 11,12) retrieval performances in time, v650 (top), v700 (bottom), descending orbits.

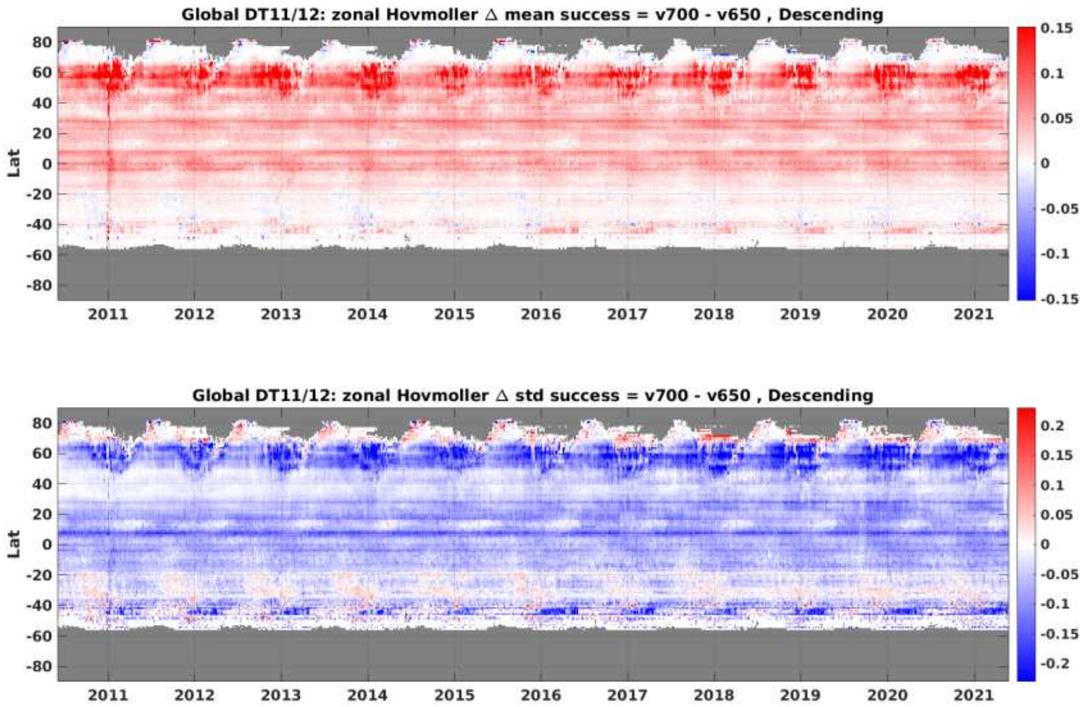

Figure 16: Global Hovmöller zonal NO/FO (DT 11,12) retrieval performances difference, v700 – v650; ∆mean (top), ∆std (bottom), descending orbits

4.2.2 ACARD/TAUNADIR RETRIEVALS (DT 2-10, 13-17)

This subsection focuses on retrieval success/failure performances for ACard/TauNadir retrievals, so for decision tree branches other than DT11 (FO), DT12 (NO) and DT1 (WO) surfaces. Numerical figure, Global maps & stats and space-time Hovmöller zonal are provided.

4.2.2.1 NUMERICAL

- Not yet available.

4.2.2.2 MAPS OVERALL REPR PERIOD 2010 – 2021

Apart over RFI areas the v700 retrievals performances for ACard is high, though less than NO/FO and also more heterogeneous.

However, it is remarkably high and stable over permanent ice (Antarctica, Greenland)

Performances v700 vs. v650 is half/half, at the most Northern latitude v700 retrievals succeed significantly less than v650: effects of integrated 11 years with all seasons? i.e.

we know CCI water fractions are higher in these areas, NPE rules converting water body to ice water body may have not appropriate temperatures thresholds indeed in Hovmöller ACard ∆performances some seasonal variations exist around winter season.

For all non FO,NO,FWO retrieval a joint MD ACard retrieval packing FRZ, FSW, FSM, FTI into a single retrieved fraction for retrieval would be an option for the future.

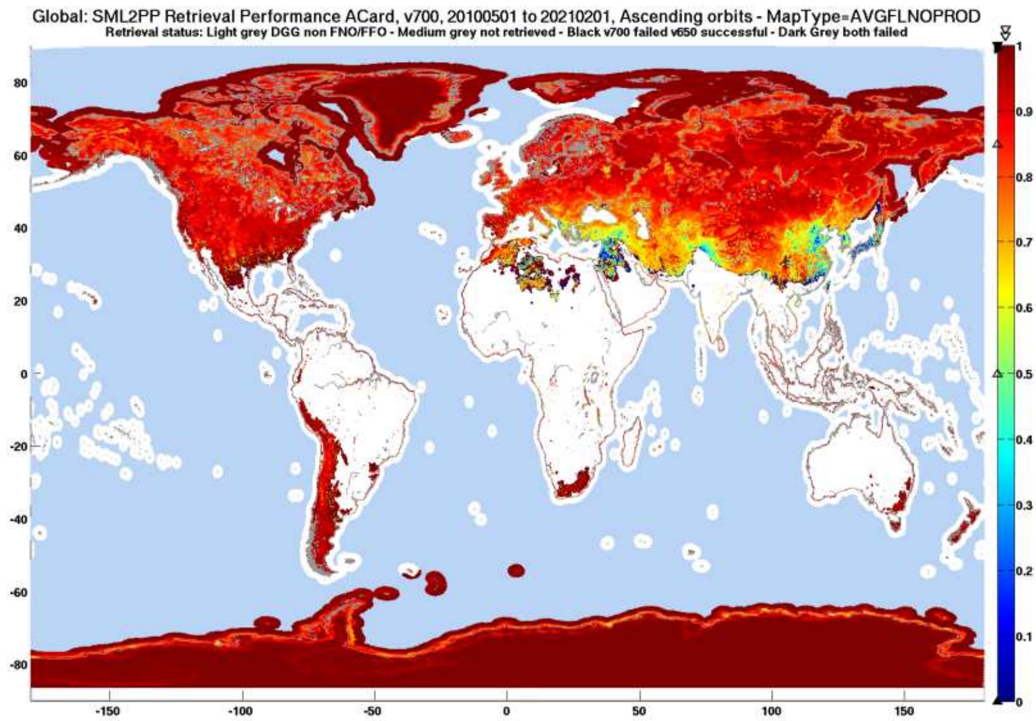

Figure 17: Map of v700 ACard (DT 2-10, 13-17) retrieval performance for the overall reprocessing campaign, 20100501- 20210131, ascending orbits

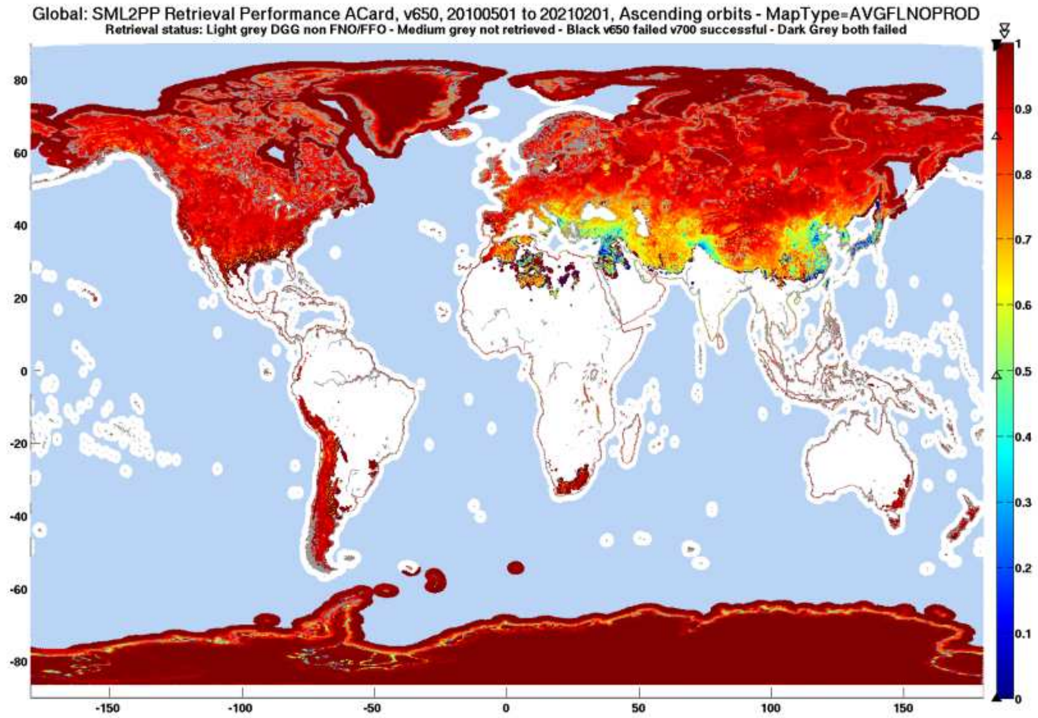

Figure 18: Map of v650 ACard (DT 2-10, 13-17) retrieval performance for the overall reprocessing campaign, 20100501- 20210131, ascending orbits

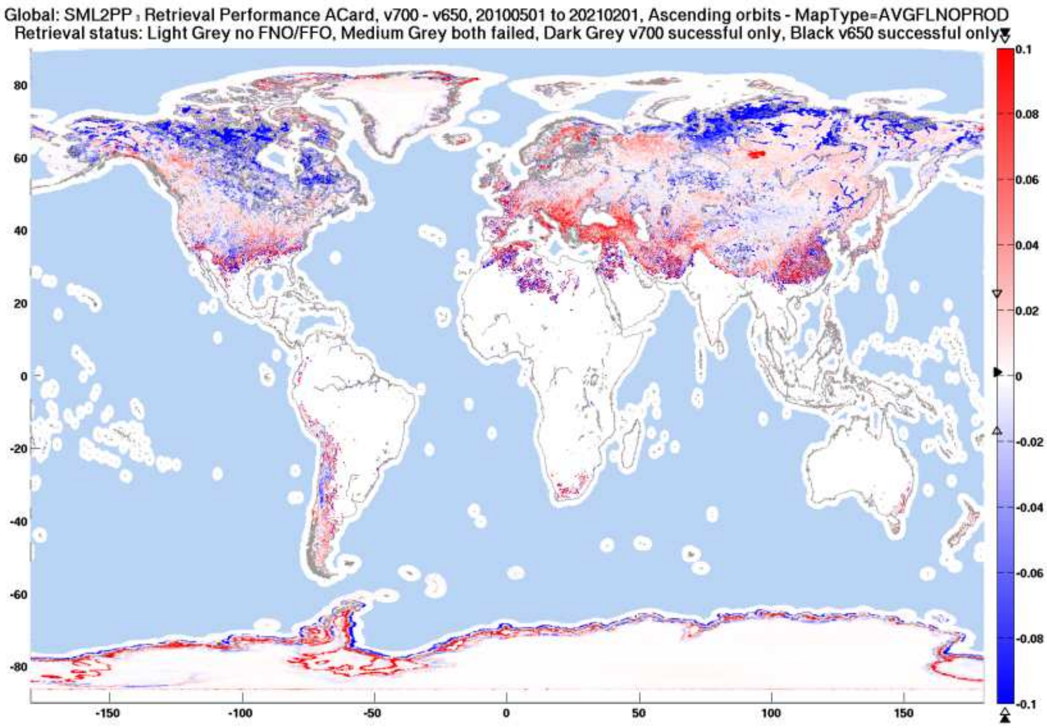

Figure 19: Map of ACard (DT 2-10, 13-17) retrieval performance difference, v700 – v650, for the overall reprocessing campaign, 20100501- 20210131, ascending orbits.

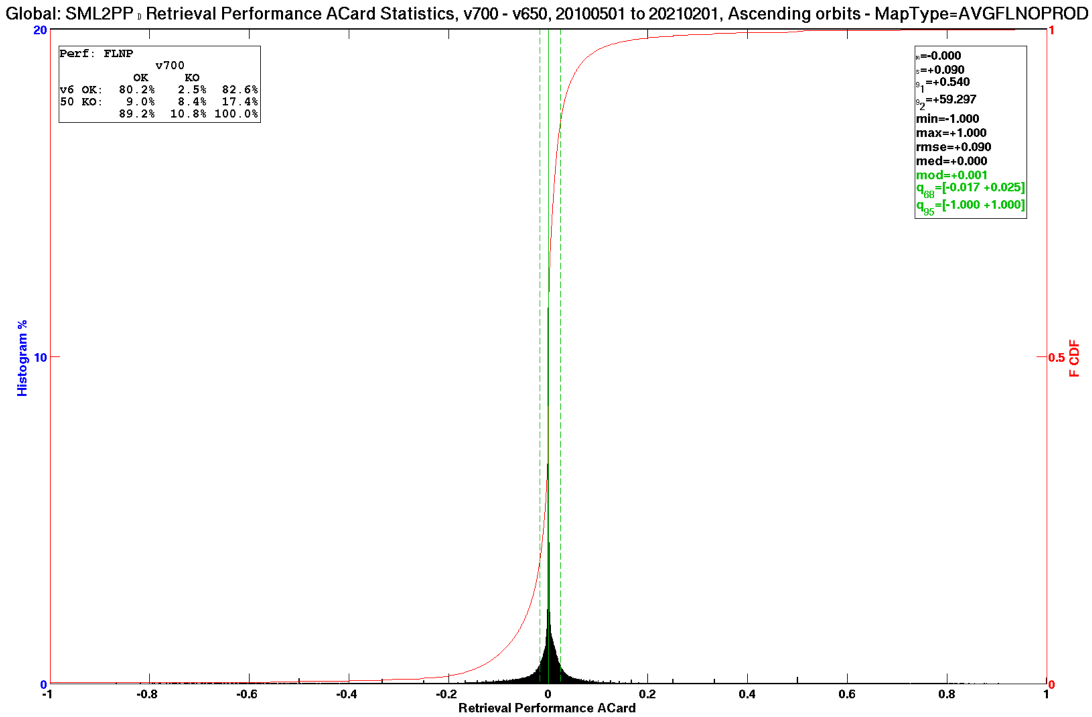

Figure 20: Histogram of ACard (DT 2-10, 13-17) retrieval performance difference, v700 – v650, for the overall reprocessing campaign, 20100501- 20210131, ascending orbits.

4.2.2.3 SPACE TIME ZONAL HOVMÖLLER

Like NO/FO, ACard retrievals performance is quite high and stable in time putting aside the active RFI band of latitude. It is particularly true over the highest latitude with permanent Snow/Ice.

However, unlike NO/FO retrievals, differences where v700 ACard has lower performances than v650 exist though with much lower magnitude. They are quite perceptible on Δmean maps (Figure 23, Figure 26) under the form of seasonal or specific steady in time blue patterns. Even of small magnitudes, they would deserve further investigations:

- blue oscillations of decreased performances (on Δmean) between N50° – N70°, perhaps stronger for descending orbits reaching maxima at summer time along with increased spatial performances variability (reddish band on Δstd).
- Close to Equator, seasonal increase of v700 failures compared to v650, this time around December.
- well visible around N25° continuous decreased v700 performances (blue thin band on Δmean).

The very visible Antarctica anomaly is due to binding list issue for ISTL1. It is present for v650 and fixed for June 2019 AUX_ECMWF onward. In REPR v700 it is no more present as the AUX_ECMWF were also reprocessed fixing the issue per se for the whole period. One of the impacts was extra failures that disappear in v700 (show in red). Both v700 & v650 become completely equivalent after June 2019 given or taken the L1C 724 impact.

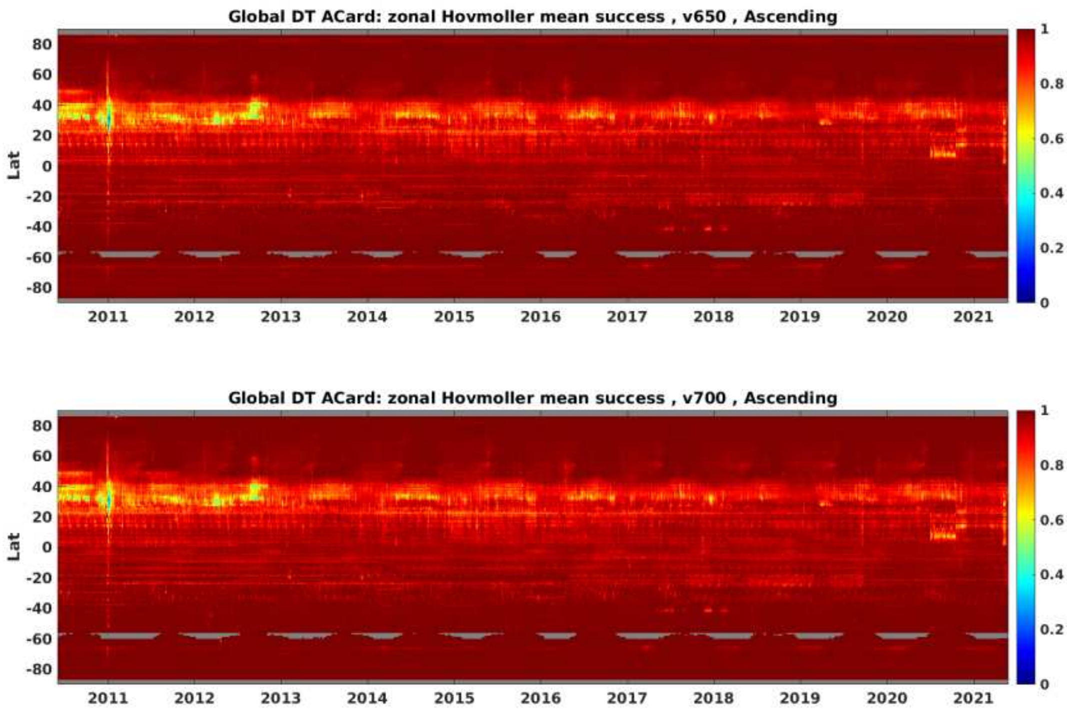

Figure 21: Global Hovmöller: mean zonal ACard (DT 2-10, 13-17) retrieval performances in time, v650 (top), v700 (bottom), ascending orbits.

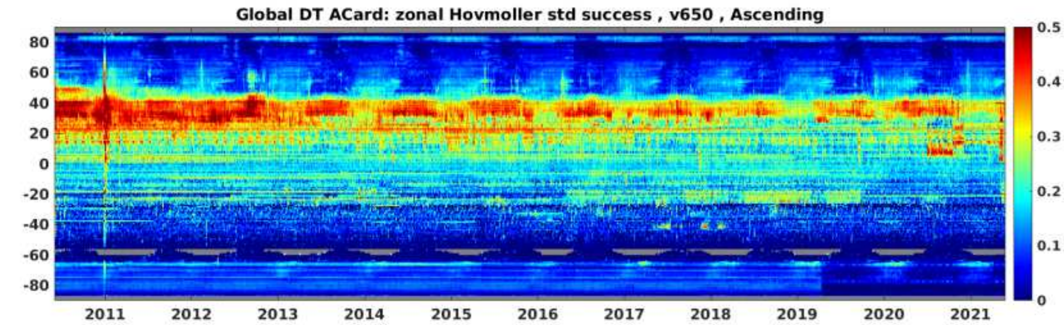

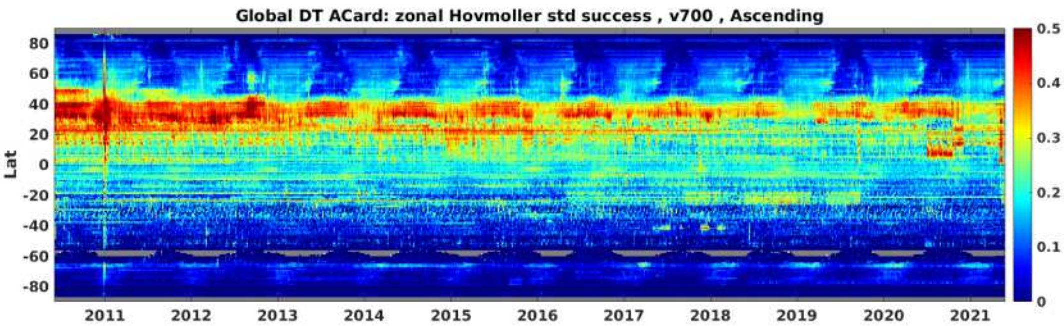

Figure 22: Global Hovmöller: std zonal ACard (DT 2-10, 13-17) retrieval performances in time, v650 (top), v700 (bottom), ascending orbits.

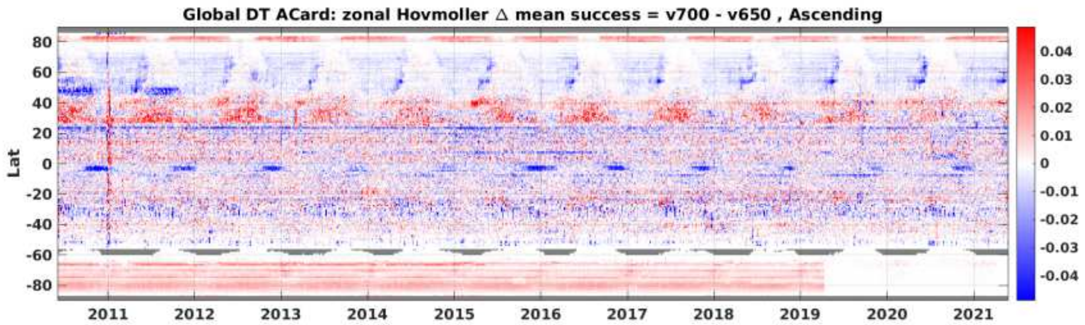

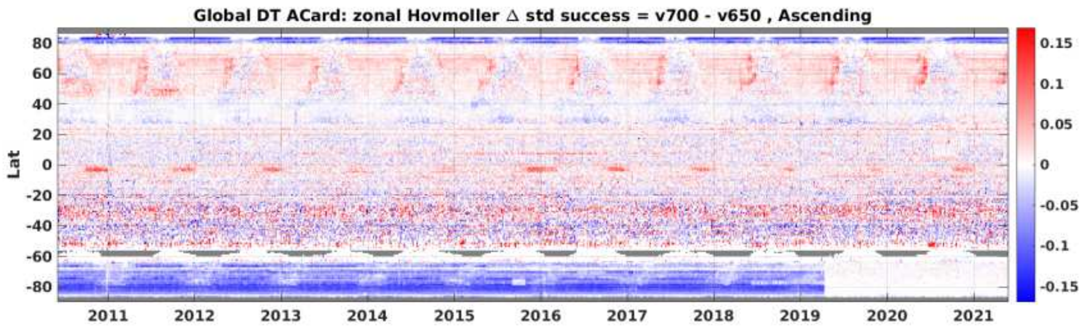

Figure 23: Global Hovmöller zonal ACard (DT 2-10, 13-17) retrieval performances difference, v700 – v650; ∆mean (top), ∆std (bottom), ascending orbits

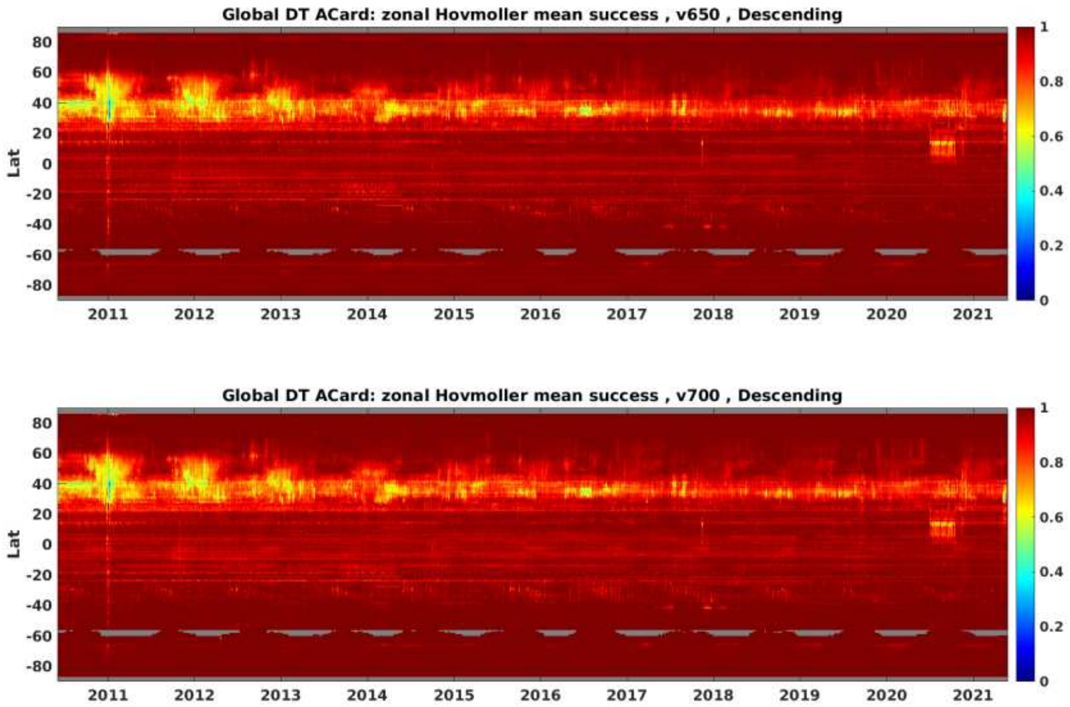

Figure 24: Global Hovmöller: mean zonal ACard (DT 2-10, 13-17) retrieval performances in time, v650 (top), v700 (bottom), descending orbits.

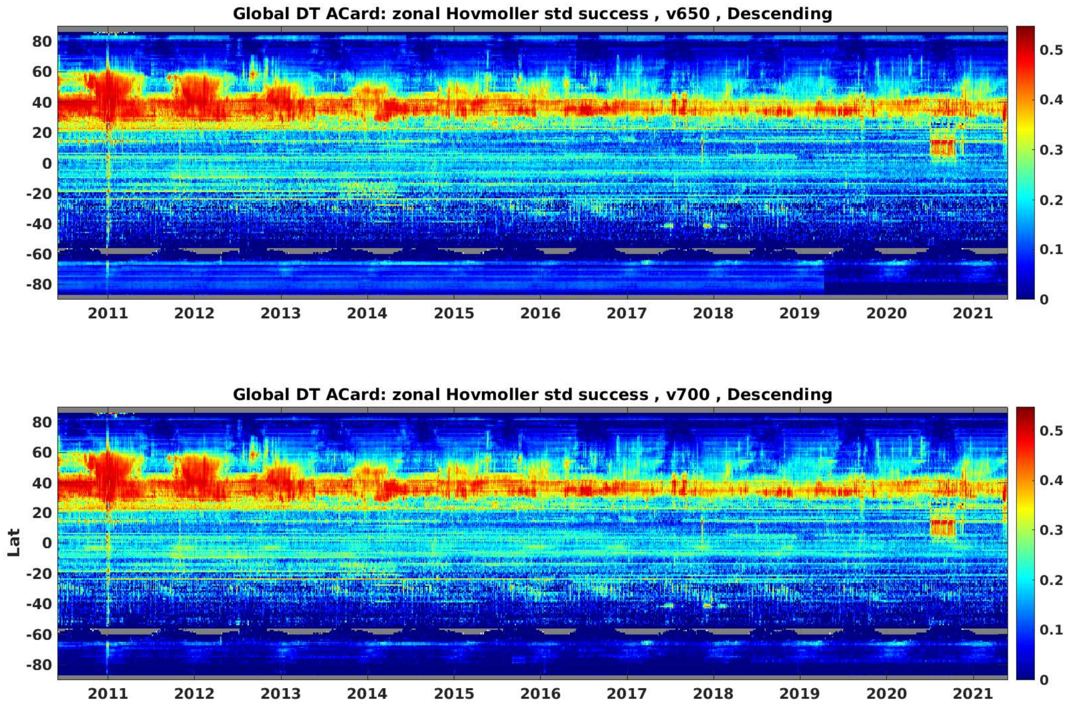

Figure 25: Global Hovmöller: std zonal ACard (DT 2-10, 13-17) retrieval performances in time, v650 (top), v700 (bottom), descending orbits.

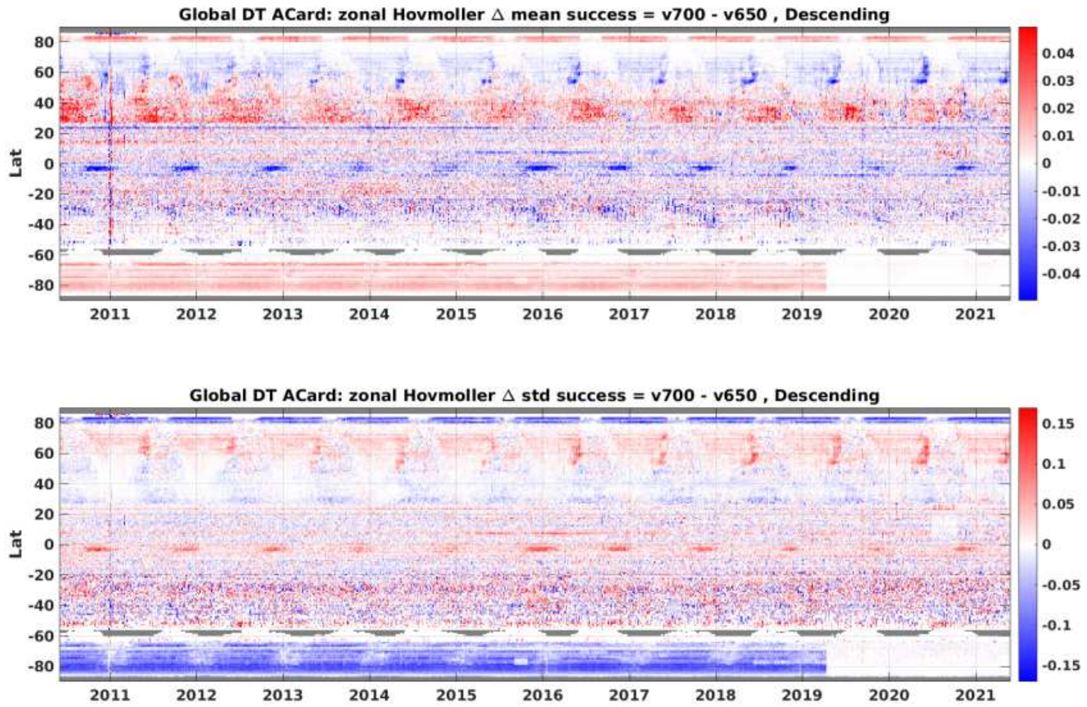

Figure 26: Global Hovmöller zonal ACard (DT 2-10, 13-17) retrieval performances difference, v700 – v650; Δmean (top), Δstd (bottom), descending orbits

4.3 RETRIEVALS FOR NOMINAL (DT12) AND FOREST (DT11) CASES

This section focuses on retrieved parameters for decision tree branches DT11 (FO) and DT12 (NO) surface so namely on retrieved SM/TauNadir and associated Chi2, RFI probability.

The three following perspectives are considered:

- Temporal: Retrieved SM time series versus network of in-situ SM time series
- Spatial: Global map & stats, summarized boxplot stats for continental areas.
- Spatiotemporal: Hovmöller plots zonal mean and std.

4.3.1 RETRIEVED SOIL MOISTURE TIME SERIES AGAINST IN-SITU SOIL MOISTURE TIME SERIES

The retrieved SM time series are co-located with in-situ time series in a pure one-to-one in-situ driven perspective:

- In space: DGGID the closest to specific station location. Different in-situ stations associated to the same SMOS retrieved DGG will have their own stats, so no averaged different stations measurements.
- Time: in-situ measurements the closest to L2SM DGGID ACQT if not larger than +/- 25'. So no averaged in-situ within that box if more than one exists.

We consider here our usual set of 487 sites (Figure 27) that generates a large amount of stats and associated figures worth detailed analysis, network by network, stations by stations but not convenient for a report.

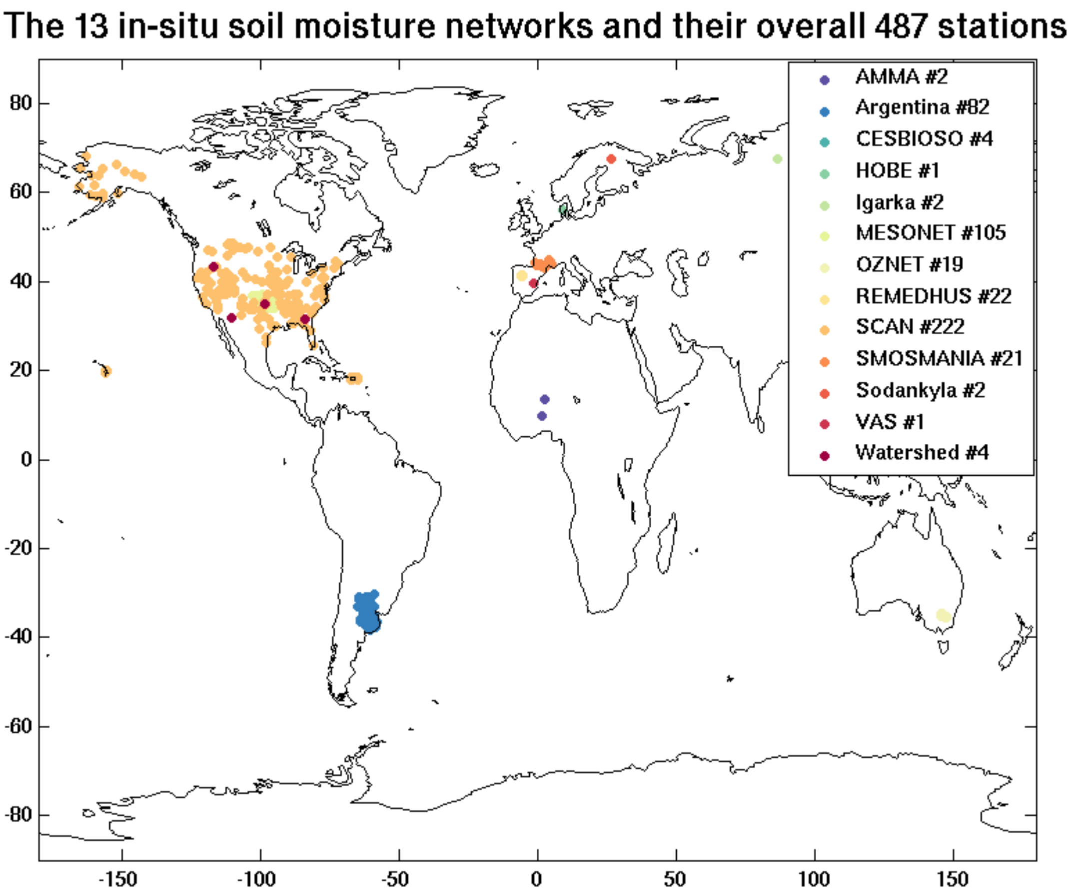

Figure 27: The 13 in-situ soil moisture network and their overall 487 stations spanning over 442 distinct DGGs.

As usual, an overall concatenated collocated (L2SM, in-situ) time series as a single big overall time series is made for the all networks and all stations they hold. It is also complemented for the 13 networks overall times series limited to the stations they hold.

Just a few words about the concatenation procedure (documented in [AD2]) as some care are required:

- Taylor Diagrams are variational diagrams i.e. a dot reports ($\rho_{SM,SMref}$, σ_{SM}), correlation, ρ, and standard deviation, σ, are by definition debiased quantity.
- The concatenation is made on piece-wise debiased individual SM station time series and associated retrieved SM time series i.e. with their mean subtracted to avoid introducing artifacts in the above bullet.
  However, all the individual station time series retrieved SM – in-situ SM biases are kept and restituted by taking the weight average of these biases weighted by the number of samples of each collocated time series segment in order to produce correct overall SM biases values displayed on the colorbar of so called 3D Taylor diagrams.
- As we are comparing two versions, v700 vs. v650, it is not adequate to keep in-situ stations for which both L2SM versions compare badly with poor time correlation or because of non-significant statistics. It will just add noise to the overall metric, just decreasing the separability of the two versions. A pre-selection is thus made before the concatenation.
  All (L2, sites/stations) co-located time series segments fulfilling the following conditions are rejected:
  - Significance of R: if not enough data or too high R p-values exist for any of the challenger, v700 or v650, the data is not kept. In such condition, the risk that the numerical, bad or good, correlations are just coming from peculiar draw and not from strong features of retrieved SM against in si-situ SM is too high.
    - Number of co-located data is < 20.
    - R p-values > 0.05.
  - Avoid blurring the overall statistics with too low L2SM/in-situ performances for both challengers. Whatever the reasons:
    - bad L2 modeling
    - bad L1C quality (RFI)
    - bad in-situ data
    - representativeness issues between SMOS SM and in-situ SM

    If both challengers, v700 and v650, are reporting R < 0.5, the SMOS SM/in-situ data for the site/station are excluded from the concatenation.

    Note: if one of the challengers has good enough performance to consider keeping the site/station and not the other, too bad for the other, the site/station is kept for both of them: fair game.

This overall concatenation perspective is respectful of the relative performance; if one challenger outperforms more often the other it will be visible. It is also respectful of the sources; long co-located segments (less gaps in in-situ or retrievals failures) have more weights in these overall metrics.

Certain tables given in following subsections provide comparative v700 vs. v650 statistics. For a given statistics, *s*, among , then , – . The following specific colours and font styles are used to emphasize the interpretation of the significance of :

- **Green** far better, **Red** far worse; statistically significant with .
- **Green** better, **Red** worse; statistically significant with .
- *Green* better, *Red* worse; yet not statistically significant .
- *Black* not really any difference

4.3.1.1 OVERALL ALL IN-SITU NETWORKS/SITES

- Ascending v700: correlation +0.14, STDD -0.016, bias -0.032, RMSD~
- Descending v700: correlation +0.13, STDD -0.012, bias -0.022, RMSD~
- To add the contingency matrix of site rejection/selection: i.e common v700/v650 rejection, v700 accepted/v650 rejected, v700 rejected/v650 accepted; common v700/v650 accepted. It is relevant information though based on correlation we know v700 has better.

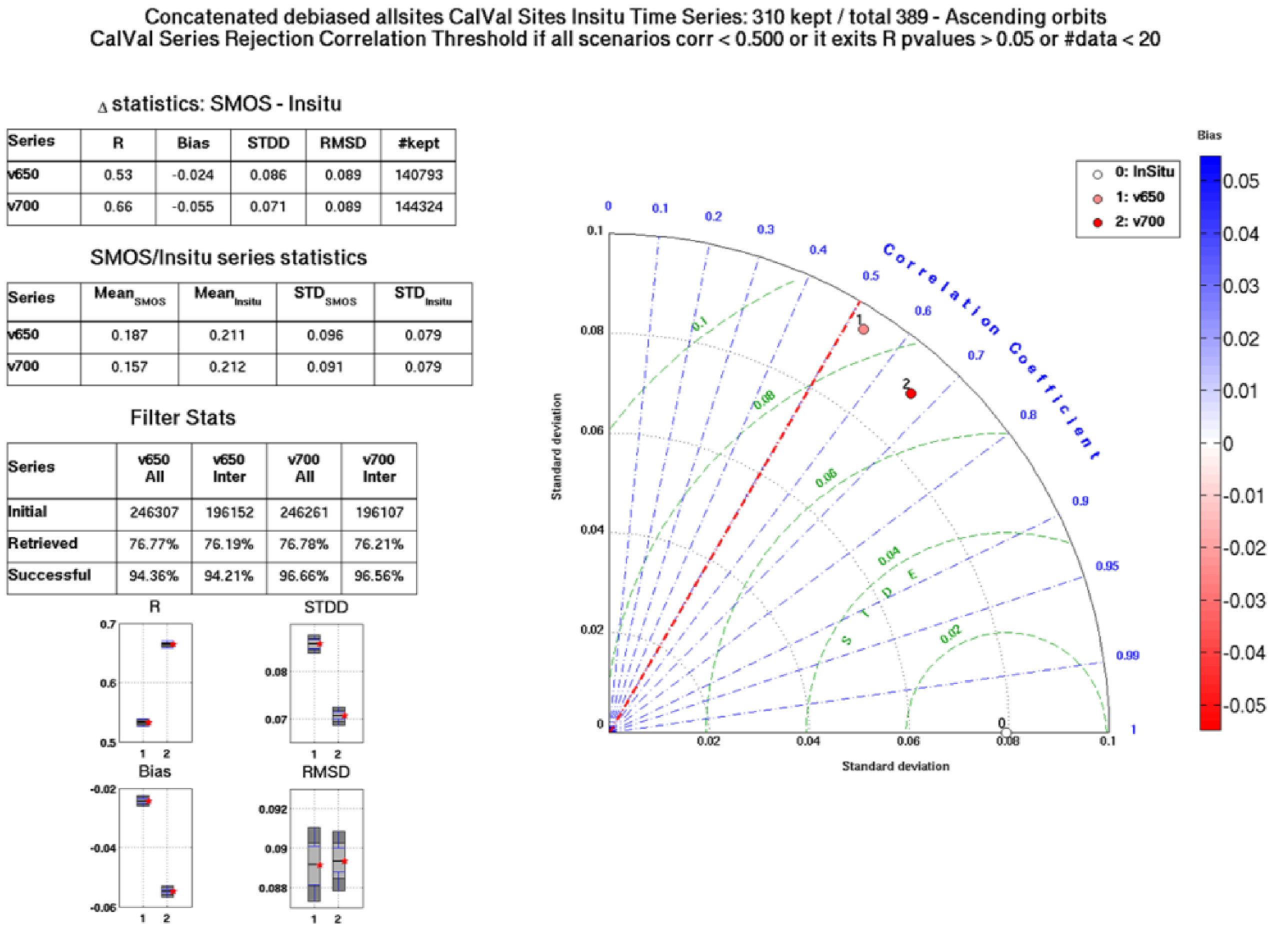

Series	R	Bias	STDD	RMSD	#kept
v650	0.53	-0.024	0.086	0.089	140793
v700	0.66	-0.055	0.071	0.089	144324

Series	$Mean_{SMOS}$	$Mean_{Insitu}$	STD_{SMOS}	STD_{Insitu}
v650	0.187	0.211	0.096	0.079
v700	0.157	0.212	0.091	0.079

Series	v650 All	v650 Inter	v700 All	v700 Inter
Initial	246307	196152	246261	196107
Retrieved	76.77%	76.19%	76.78%	76.21%
Successful	94.36%	94.21%	96.66%	96.56%

Figure 28: overall concatenated all network/sites Taylor Diagram, statistics and confidence interval v700 SM, v650 SM against in-situ SM for ascending orbits.

Concatenated debiased allsites CalVal Sites Insitu Time Series: 306 kept / total 388 - Descending orbits
CalVal Series Rejection Correlation Threshold if all scenarios corr < 0.500 or it exits R pvalues > 0.05 or #data < 20

Δ statistics: SMOS - Insitu

Series	R	Bias	STDD	RMSD	#kept
v650	0.55	-0.025	0.084	0.088	140353
v700	0.67	-0.046	0.072	0.085	143464

SMOS/Insitu series statistics

Series	$Mean_{SMOS}$	$Mean_{Insitu}$	STD_{SMOS}	STD_{Insitu}
v650	0.186	0.211	0.095	0.080
v700	0.167	0.212	0.094	0.080

Filter Stats

Series	v650 All	v650 Inter	v700 All	v700 Inter
Initial	247425	192539	247348	192509
Retrieved	77.26%	76.99%	77.29%	77.02%
Successful	94.98%	94.68%	96.94%	96.76%

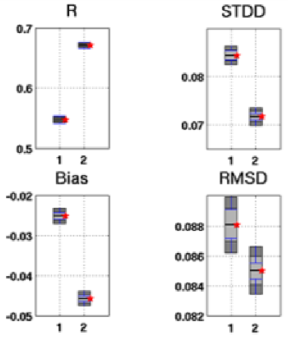

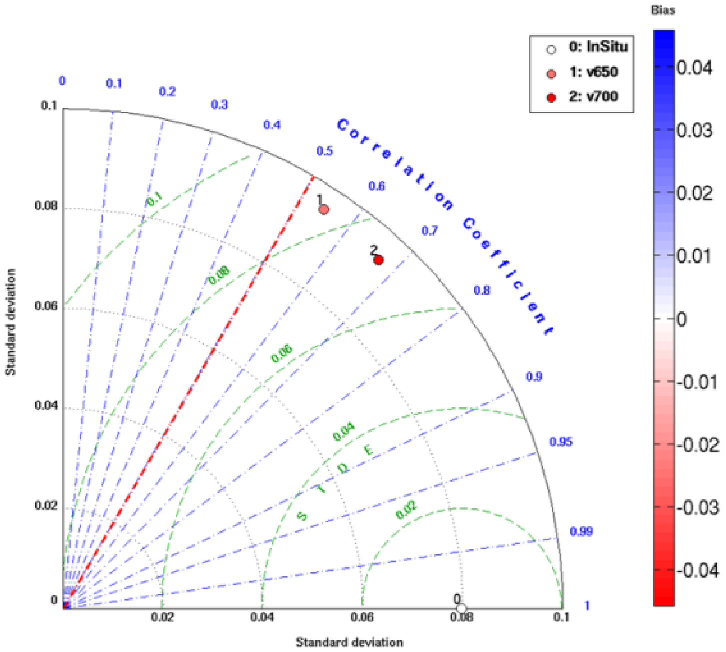

Figure 29: overall concatenated all network/sites Taylor Diagram, statistics and confidence interval v700 SM, v650 SM against in-situ SM for descending orbits.

- Working with long time series of SMOS retrieved data but for limited number of DGGs allows (technically) focusing at the decision tree branches occurrence (Table 5) along the whole concatenated time series as well as the retrievals performances per decision tree branches (**Green** far better / **Red** far worse and significant

- **Green** better / **Red** worse and significant
- *Green* better / *Red* worse but not significantly
- *black* mostly equivalent with

v700 has far better (Forest) to better (Nominal and All Wet Snow) retrievals success/failures performances while v650 have better ones for All Mixed Snow. For the other DT branches performances are more or less equivalent.

The fact that the performances gain is higher for FO than for NO is interesting. It is a signature of the v700 joint FO+NO retrieval that helps actually more FO retrievals than NO retrievals.

For FO retrievals, typically those of v650, any FNO fraction is considered as a fixed contribution. Any issues on fixed soil moisture for the BT model of the FNO fraction will have a strong impact not much attenuated by the vegetation as the FNO fixed TauNadir is low by definition.

In the opposite case, NO retrievals, FFO is a fixed contribution. Wrong soil moisture has limited impact on the FO modelled BT as the soil emission anomaly is strongly attenuated by the FFO fixed TauNadir wich is high by definition.

We also get again that v700 retrieval performances degradation is more on the ACard retrieval side, here for mixed snow surface.

Table 6).

For these validations sites, DT branches 1,2,3,4,13,14,15 and 16 are not present i.e. their frequency of occurrence is 0 and thus not reported.

Decision tree branches number, short acronyms and full name, in blue those that are observed for the sites.

1. AOW: All Open Water
2. HOW: Heterogenous Open Water
3. STP: Strong Topography Pollution
4. MTP: Medium Topography Pollution
5. **AWS: All Wet Snow**
6. **AMS: All Mixed Snow**
7. **WSP: Wet Snow Pollution**
8. **MSP: Mixed Snow Pollution**
9. **AFR: All FRost**
10. **FRP: FRost Pollution**
11. **AFO: All FOrest**
12. **ANO: All NOminal**
13. AWL: All WetLand
14. ABA: All BArren
15. AIC: All ICe
16. AUR: All Urban
17. **HET: HETerogeneous**

In **Erreur ! Référence non valide pour un signet.** the differences of frequency of decision tree branches between v700 and v650 come from the reallocation of fractions introduced by the change of FWO, CCI RADAR for the v700 and original IGBP for the v650 modulated by possible NPEs (frost,snow,…).

Actually, for these validation sites the effects of FWO change appears not strong so would be its impacts (lower SM) on retrieved SM between v700 and v650.

Table 5: F700 vs. F650 overall decision tree branches frequency

DTB	5 AWS	6 AMS	7 WSP.	8 MSP	9 AFR	10 FRP	11 AFO	12 ANO	17 HET
	ASC – Total 1191213 - 18.8 % non attempted (Swath edges, RFI)								
%F700	0.54	2.38	1.54	3.84	0.68	2.34	22.98	64.34	1.36
%F650	0.55	2.44	1.57	3.95	0.95	2.15	23.28	64.39	0.72
	DSC – Total 1193078- 18.6 % non attempted (Swath edges, RFI)								
%F700	1.06	2.76	2.64	3.58	0.40	1.42	22.81	63.98	1.34
%F650	1.13	2.82	2.76	3.60	0.59	1.30	23.08	64.01	0.71

- Retrieval performances given **Green** far better / **Red** far worse and significant

- **Green** better / **Red** worse and significant
- *Green* better / *Red* worse but not significantly
- *black* mostly equivalent with

v700 has far better (Forest) to better (Nominal and All Wet Snow) retrievals success/failures performances while v650 have better ones for All Mixed Snow. For the other DT branches performances are more or less equivalent.

The fact that the performances gain is higher for FO than for NO is interesting. It is a signature of the v700 joint FO+NO retrieval that helps actually more FO retrievals than NO retrievals.

For FO retrievals, typically those of v650, any FNO fraction is considered as a fixed contribution. Any issues on fixed soil moisture for the BT model of the FNO fraction will have a strong impact not much attenuated by the vegetation as the FNO fixed TauNadir is low by definition.

In the opposite case, NO retrievals, FFO is a fixed contribution. Wrong soil moisture has limited impact on the FO modelled BT as the soil emission anomaly is strongly attenuated by the FFO fixed TauNadir wich is high by definition.

We also get again that v700 retrieval performances degradation is more on the ACard retrieval side, here for mixed snow surface.

Table 6 are categorized per font colours and style. Green means better, red worse. Font style gives the range of performances differences in term of significance though with no accurate definition in this case:

- **Green** far better / **Red** far worse and significant
- **Green** better / **Red** worse and significant
- *Green* better / *Red* worse but not significantly
- *black* mostly equivalent with

v700 has far better (Forest) to better (Nominal and All Wet Snow) retrievals success/failures performances while v650 have better ones for All Mixed Snow. For the other DT branches performances are more or less equivalent.

The fact that the performances gain is higher for FO than for NO is interesting. It is a signature of the v700 joint FO+NO retrieval that helps actually more FO retrievals than NO retrievals.

For FO retrievals, typically those of v650, any FNO fraction is considered as a fixed contribution. Any issues on fixed soil moisture for the BT model of the FNO fraction will have a strong impact not much attenuated by the vegetation as the FNO fixed TauNadir is low by definition.

In the opposite case, NO retrievals, FFO is a fixed contribution. Wrong soil moisture has limited impact on the FO modelled BT as the soil emission anomaly is strongly attenuated by the FFO fixed TauNadir wich is high by definition.

We also get again that v700 retrieval performances degradation is more on the ACard retrieval side, here for mixed snow surface.

Table 6: P700 vs. P650 overall success/failure performances

DTB	5 AWS	6 AMS	7 WSP.	8 MSP	9 AFR	10 FRP	11 AFO	12 ANO	17 HET
	ASC – Total 1191213 - 18.8 % non attempted (Swath edges, RFI)								
%P700	**93.95**	**76.65**	*90.72*	*88.19*	*98.74*	*82.93*	**96.84**	**97.74**	*95.14*
%P650	**90.48**	**78.28**	*90.65*	*88.02*	*98.54*	*83.03*	**86.70**	**96.53**	*95.14*
	DSC – Total 1193078- 18.6 % non attempted (Swath edges, RFI)								
%P700	**93.27**	**76.29**	*91.34*	*88.46*	*99.20*	*83.16*	**96.87**	**96.92**	*95.36*
%P650	**90.24**	**78.42**	*91.52*	*87.84*	*99.12*	*82.91*	**89.22**	**95.53**	*95.66*

4.3.1.2 PER IN-SITU NETWORK

The series of figures (Figure 30 to Figure 50) report compounding Taylor diagram, confidence intervals plots and usual numerical metrics statistics R, bias, STDD and RMSD and other numerical information of SMOS v700 and v650 retrieved soil moisture against concatenated in-situ soil moisture stations per network.

The two following tables provide a comparative synthesis of R, bias, STDD and RMSD extracted from these figures for v700 vs. v650. For a given statistics, , , – , the following colours and font styles are used to emphasize the interpretation of the significance of .

- **Green** far better, **Red** far worse; statistically significant with .
- **Green** better, **Red** worse; statistically significant with .
- *Green* better, *Red* worse; yet not statistically significant .
- *Black* not really any difference

v700 dominates the correlation R and STDD corner by far while v650 the bias corner by far. The RMSD is more balanced with v700 and v650 alternatively better or worse, but also to a less significant level.

So the overall compounded errors are not that different. What is different between v700 and v650 is how these errors are partitioned in term of random/variational versus fixed.

v700 decreases the random, variational (R,STDD) contribution at the expense of the fixed contribution (bias), while for v650 it is the opposite.

Ascending versus descending orbits does no change much this two different relative behaviours of the two L2SM versions.

Table 7: Metric statistics synthesis per in-situ network for ascending orbits

Networks	R_{700}	R_{650}	$Bias_{700}$	$Bias_{650}$	$STDD_{700}$	$STDD_{650}$	$RMSD_{700}$	$RMSD_{650}$	N_{700}	N_{650}
AMMA	**0.82**	**0.77**	**0.011**	**0.030**	**0.053**	**0.064**	**0.054**	**0.070**	1317	1348
Argentina	**0.67**	**0.65**	**-0.056**	**-0.042**	*0.068*	*0.072*	*0.088*	*0.084*	6911	6730
CESBIOSO	**0.69**	**0.52**	**-0.121**	**-0.080**	**0.057**	**0.076**	**0.134**	**0.110**	2876	2866
HOBE	**0.52**	**0.36**	**-0.045**	**-0.052**	**0.073**	**0.084**	**0.086**	**0.099**	2101	2035
OZNET	**0.79**	**0.77**	**0.011**	**0.025**	*0.064*	*0.065*	**0.065**	**0.070**	11581	11548
MESONET	**0.71**	**0.56**	**-0.086**	**-0.055**	**0.064**	**0.080**	**0.107**	**0.097**	45297	44551
REMEDHUS	**0.56**	**0.52**	**-0.031**	**-0.024**	*0.072*	*0.075*	*0.079*	*0.079*	6572	6594
SCAN	**0.62**	**0.47**	**-0.040**	**-0.003**	**0.078**	**0.095**	**0.087**	**0.095**	50395	49463
SMOSMANIA	**0.64**	**0.42**	**-0.100**	**-0.053**	**0.072**	**0.106**	**0.123**	**0.118**	11948	10402
Sodankylä	**0.74**	**0.65**	*0.078*	*0.074*	**0.099**	**0.090**	**0.126**	**0.117**	1866	1808

VAS	*0.55*	*0.41*	**-0.067**	**-0.011**	*0.094*	*0.124*	*0.116*	*0.124*	622	608
Watersheds	**0.69**	**0.57**	**-0.002**	**0.021**	**0.048**	**0.058**	**0.049**	**0.061**	2838	2840

Table 8: Metric statistics synthesis per in-situ network for descending orbits

Networks	R_{700}	R_{650}	$Bias_{700}$	$Bias_{650}$	$STDD_{700}$	$STDD_{650}$	$RMSD_{700}$	$RMSD_{650}$	N_{700}	N_{650}
AMMA	**0.83**	**0.70**	**0.004**	**0.024**	**0.048**	**0.066**	**0.048**	**0.070**	1468	1490
Argentina	**0.63**	**0.59**	**-0.051**	**-0.045**	*0.070*	*0.075*	*0.087*	*0.088*	7978	7884
CESBIOSO	**0.71**	**0.50**	**-0.102**	**-0.068**	**0.057**	**0.077**	**0.117**	**0.103**	3020	2964
HOBE	**0.51**	**0.33**	**-0.073**	**-0.081**	**0.073**	**0.087**	**0.103**	**0.119**	1245	1024
OZNET	**0.78**	**0.69**	**0.014**	**0.022**	**0.070**	**0.086**	**0.071**	**0.089**	11585	11553
MESONET	**0.71**	**0.59**	**-0.069**	**-0.048**	**0.067**	**0.079**	**0.096**	**0.093**	46494	45817
REMEDHUS	**0.54**	**0.50**	**-0.032**	**-0.027**	*0.075*	*0.076*	*0.082*	*0.081*	7144	7025
SCAN	**0.62**	**0.50**	**-0.024**	**-0.001**	**0.079**	**0.090**	**0.083**	**0.090**	48599	47676
SMOSMANIA	**0.69**	**0.43**	**-0.102**	**-0.067**	**0.066**	**0.098**	*0.121*	*0.119*	12467	11477
Sodankylä	**0.55**	**0.41**	**-0.067**	**-0.011**	**0.094**	**0.124**	*0.116*	*0.124*	622	608
VAS	**0.62**	**0.58**	**-0.046**	**-0.011**	**0.090**	**0.092**	**0.101**	**0.093**	686	664
Watersheds	**0.70**	**0.57**	**-0.000**	**0.016**	**0.048**	**0.054**	**0.048**	**0.056**	2778	2779

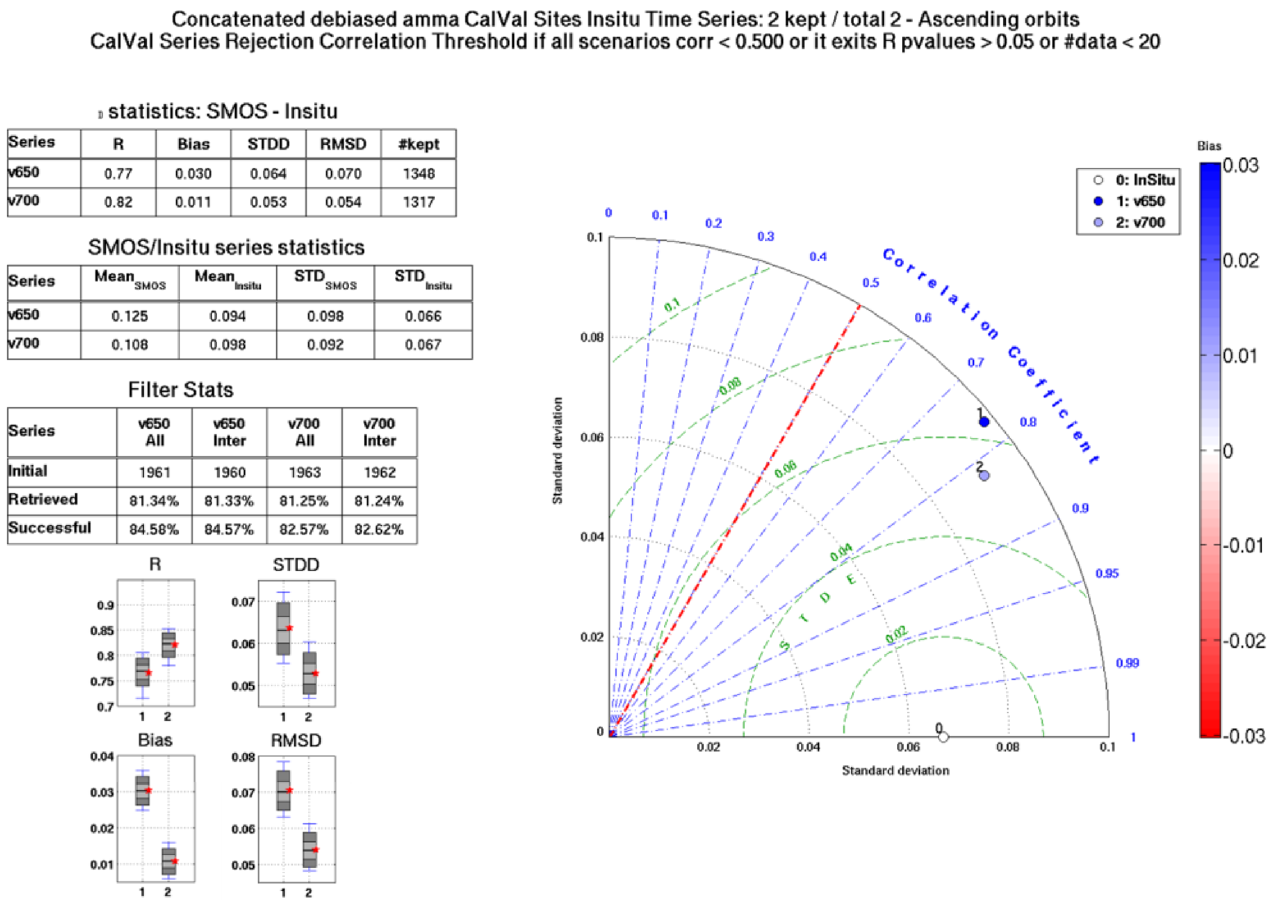

statistics: SMOS - Insitu

Series	R	Bias	STDD	RMSD	#kept
v650	0.77	0.030	0.064	0.070	1348
v700	0.82	0.011	0.053	0.054	1317

SMOS/Insitu series statistics

Series	$Mean_{SMOS}$	$Mean_{Insitu}$	STD_{SMOS}	STD_{Insitu}
v650	0.125	0.094	0.098	0.066
v700	0.108	0.098	0.092	0.067

Filter Stats

Series	v650 All	v650 Inter	v700 All	v700 Inter
Initial	1961	1960	1963	1962
Retrieved	81.34%	81.33%	81.25%	81.24%
Successful	84.58%	84.57%	82.57%	82.62%

Figure 30: overall concatenated all AMMA network sites Taylor Diagram, statistics and confidence interval v700 SM, v650 SM against in-situ SM for ascending orbits.

Concatenated debiased amma CalVal Sites Insitu Time Series: 2 kept / total 2 - Descending orbits
CalVal Series Rejection Correlation Threshold if all scenarios corr < 0.500 or it exits R pvalues > 0.05 or #data < 20

statistics: SMOS - Insitu

Series	R	Bias	STDD	RMSD	#kept
v650	0.70	0.024	0.066	0.070	1490
v700	0.83	0.004	0.048	0.048	1468

SMOS/Insitu series statistics

Series	$Mean_{SMOS}$	$Mean_{Insitu}$	STD_{SMOS}	STD_{Insitu}
v650	0.116	0.092	0.093	0.063
v700	0.098	0.094	0.086	0.064

Filter Stats

Series	v650 All	v650 Inter	v700 All	v700 Inter
Initial	1960	1959	1961	1960
Retrieved	82.35%	82.34%	82.25%	82.24%
Successful	92.32%	92.37%	91.07%	91.07%

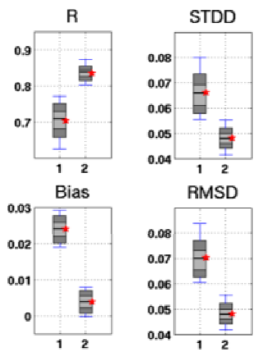

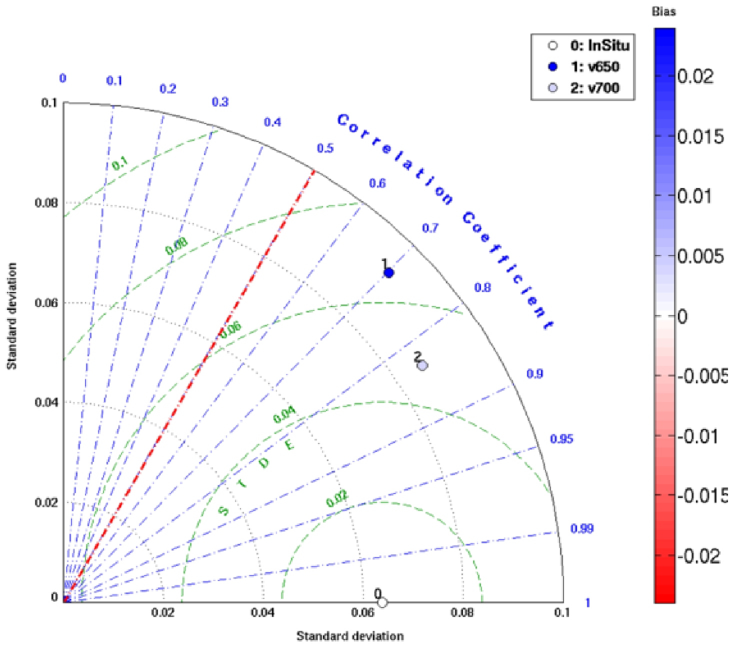

Figure 31: overall concatenated all AMMA network sites Taylor Diagram, statistics and confidence interval v700 SM, v650 SM against in-situ SM for descending orbits.

Concatenated debiased Argentina CalVal Sites Insitu Time Series: 37 kept / total 52 - Ascending orbits
CalVal Series Rejection Correlation Threshold if all scenarios corr < 0.500 or it exits R pvalues > 0.05 or #data < 20

statistics: SMOS - Insitu

Series	R	Bias	STDD	RMSD	#kept
v650	0.65	-0.042	0.072	0.084	6730
v700	0.67	-0.056	0.068	0.088	6911

SMOS/Insitu series statistics

Series	$Mean_{SMOS}$	$Mean_{Insitu}$	STD_{SMOS}	STD_{Insitu}
v650	0.205	0.247	0.094	0.071
v700	0.192	0.248	0.091	0.071

Filter Stats

Series	v650 All	v650 Inter	v700 All	v700 Inter
Initial	22723	8957	22710	8954
Retrieved	80.61%	80.22%	80.55%	80.14%
Successful	94.94%	93.67%	97.06%	96.31%

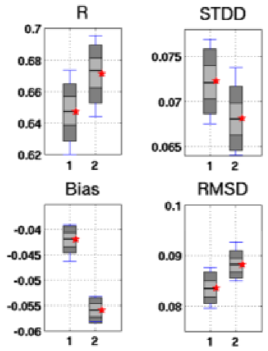

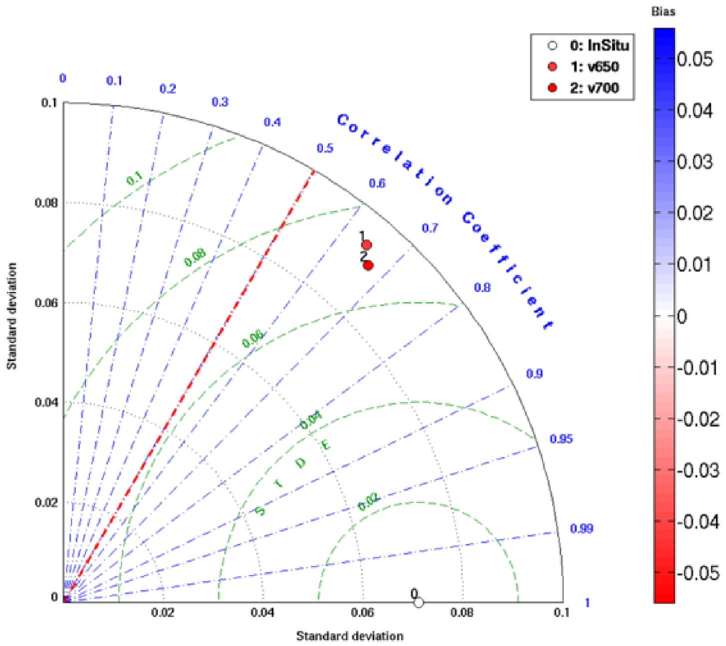

Figure 32: overall concatenated all Argentina network sites Taylor Diagram, statistics and confidence interval v700 SM, v650 SM against in-situ SM for ascending orbits.

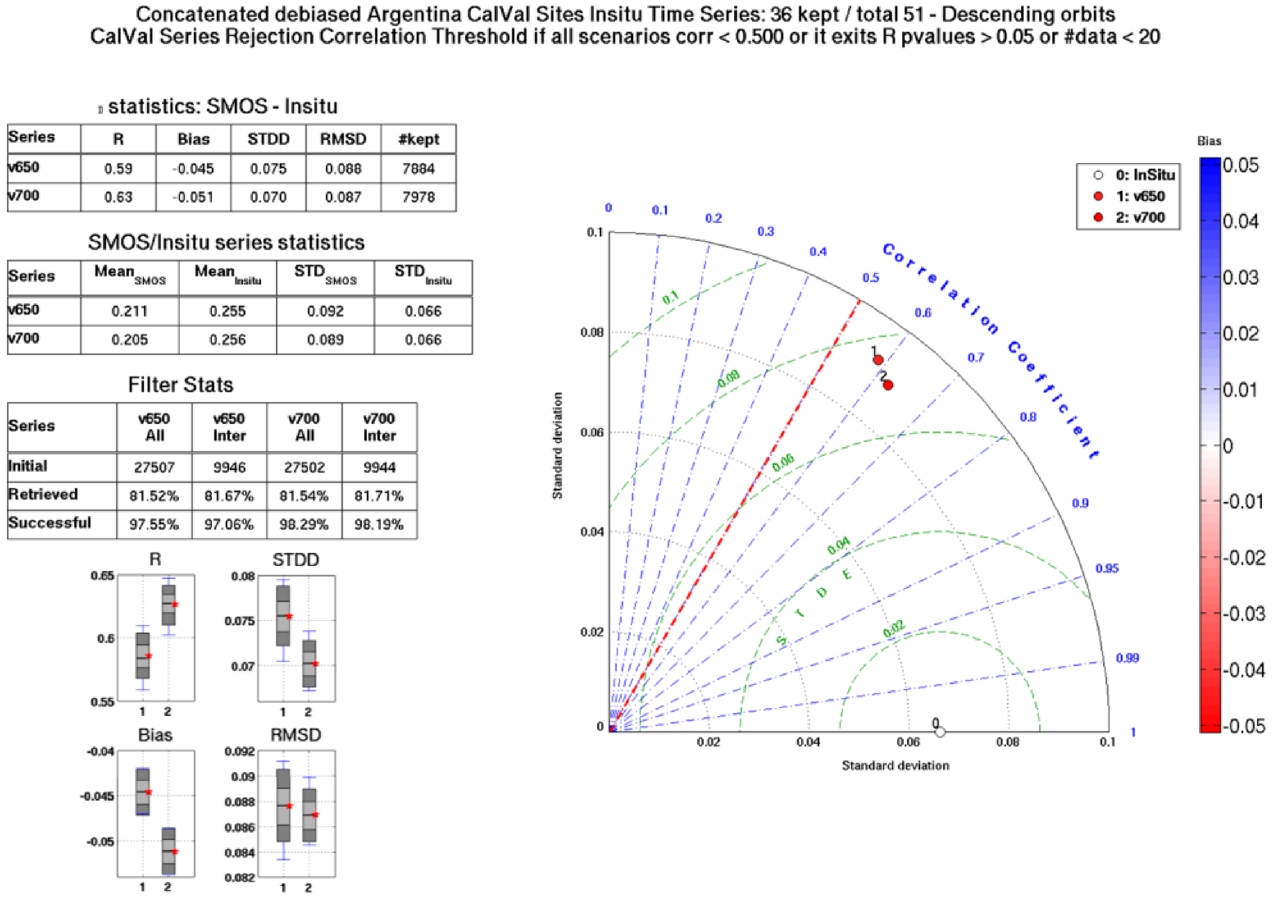

statistics: SMOS - Insitu

Series	R	Bias	STDD	RMSD	#kept
v650	0.59	-0.045	0.075	0.088	7884
v700	0.63	-0.051	0.070	0.087	7978

SMOS/Insitu series statistics

Series	$Mean_{SMOS}$	$Mean_{Insitu}$	STD_{SMOS}	STD_{Insitu}
v650	0.211	0.255	0.092	0.066
v700	0.205	0.256	0.089	0.066

Filter Stats

Series	v650 All	v650 Inter	v700 All	v700 Inter
Initial	27507	9946	27502	9944
Retrieved	81.52%	81.67%	81.54%	81.71%
Successful	97.55%	97.06%	98.29%	98.19%

Figure 33: overall concatenated all Argentina network sites Taylor Diagram, statistics and confidence interval v700 SM, v650 SM against in-situ SM for descending orbits.

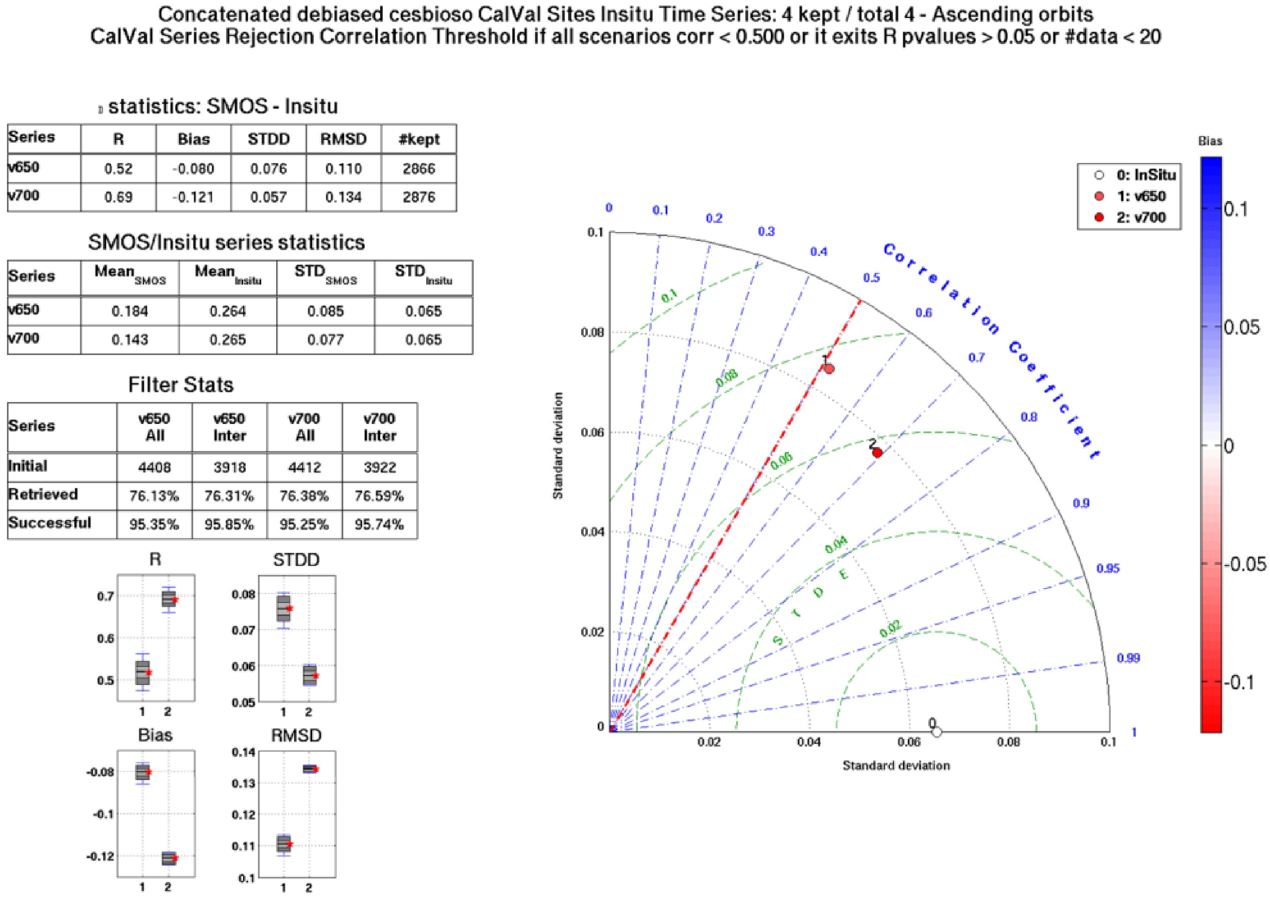

statistics: SMOS - Insitu

Series	R	Bias	STDD	RMSD	#kept
v650	0.52	-0.080	0.076	0.110	2866
v700	0.69	-0.121	0.057	0.134	2876

SMOS/Insitu series statistics

Series	$Mean_{SMOS}$	$Mean_{Insitu}$	STD_{SMOS}	STD_{Insitu}
v650	0.184	0.264	0.085	0.065
v700	0.143	0.265	0.077	0.065

Filter Stats

Series	v650 All	v650 Inter	v700 All	v700 Inter
Initial	4408	3918	4412	3922
Retrieved	76.13%	76.31%	76.38%	76.59%
Successful	95.35%	95.85%	95.25%	95.74%

Figure 34: overall concatenated all CESBIOSO network sites Taylor Diagram, statistics and confidence interval v700 SM, v650 SM against in-situ SM for ascending orbits.

Concatenated debiased cesbioso CalVal Sites Insitu Time Series: 4 kept / total 4 - Descending orbits
CalVal Series Rejection Correlation Threshold if all scenarios corr < 0.500 or it exits R pvalues > 0.05 or #data < 20

statistics: SMOS - Insitu

Series	R	Bias	STDD	RMSD	#kept
v650	0.50	-0.068	0.077	0.103	2964
v700	0.71	-0.102	0.057	0.117	3020

SMOS/Insitu series statistics

Series	$Mean_{SMOS}$	$Mean_{Insitu}$	STD_{SMOS}	STD_{Insitu}
v650	0.193	0.261	0.085	0.066
v700	0.159	0.261	0.080	0.065

Filter Stats

Series	v650 All	v650 Inter	v700 All	v700 Inter
Initial	4406	3924	4406	3924
Retrieved	80.39%	80.12%	80.53%	80.22%
Successful	94.47%	94.27%	95.83%	95.93%

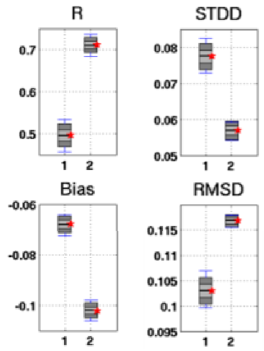

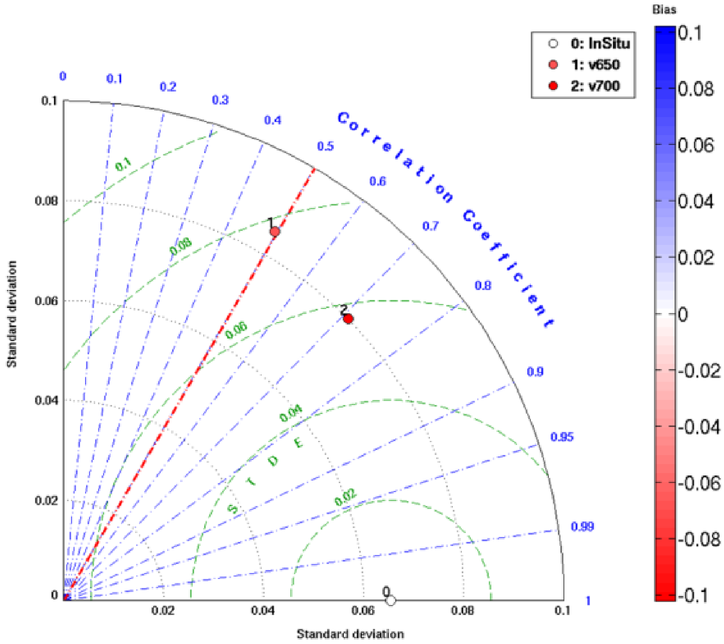

Figure 35: overall concatenated all CESBIOSO network sites Taylor Diagram, statistics and confidence interval v700 SM, v650 SM against in-situ SM for descending orbits.

Concatenated debiased hobe CalVal Sites Insitu Time Series: 1 kept / total 1 - Ascending orbits
CalVal Series Rejection Correlation Threshold if all scenarios corr < 0.500 or it exits R pvalues > 0.05 or #data < 20

statistics: SMOS - Insitu

Series	R	Bias	STDD	RMSD	#kept
v650	0.36	-0.052	0.084	0.099	2035
v700	0.52	-0.045	0.073	0.086	2101

SMOS/Insitu series statistics

Series	$Mean_{SMOS}$	$Mean_{Insitu}$	STD_{SMOS}	STD_{Insitu}
v650	0.189	0.241	0.085	0.059
v700	0.197	0.242	0.083	0.060

Filter Stats

Series	v650 All	v650 Inter	v700 All	v700 Inter
Initial	3049	3049	3047	3047
Retrieved	70.65%	70.65%	70.73%	70.73%
Successful	94.48%	94.48%	97.49%	97.49%

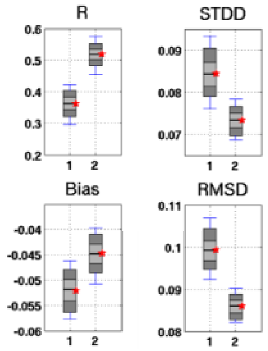

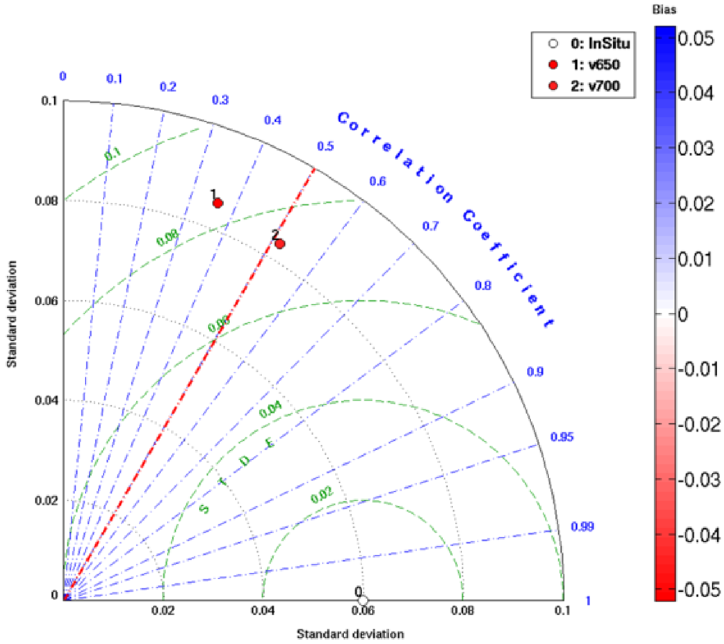

Figure 36: overall concatenated all HOBE network sites Taylor Diagram, statistics and confidence interval v700 SM, v650 SM against in-situ SM for ascending orbits.

Concatenated debiased hobe CalVal Sites Insitu Time Series: 1 kept / total 1 - Descending orbits
CalVal Series Rejection Correlation Threshold if all scenarios corr < 0.500 or it exits R pvalues > 0.05 or #data < 20

statistics: SMOS - Insitu

Series	R	Bias	STDD	RMSD	#kept
v650	0.33	-0.081	0.087	0.119	1024
v700	0.51	-0.073	0.073	0.103	1245

SMOS/Insitu series statistics

Series	$Mean_{SMOS}$	$Mean_{Insitu}$	STD_{SMOS}	STD_{Insitu}
v650	0.167	0.248	0.085	0.063
v700	0.174	0.247	0.081	0.062

Filter Stats

Series	v650 All	v650 Inter	v700 All	v700 Inter
Initial	2965	2965	2966	2966
Retrieved	65.43%	65.43%	65.31%	65.31%
Successful	52.78%	52.78%	64.27%	64.27%

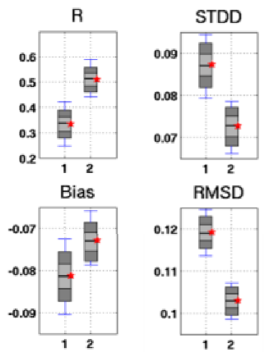

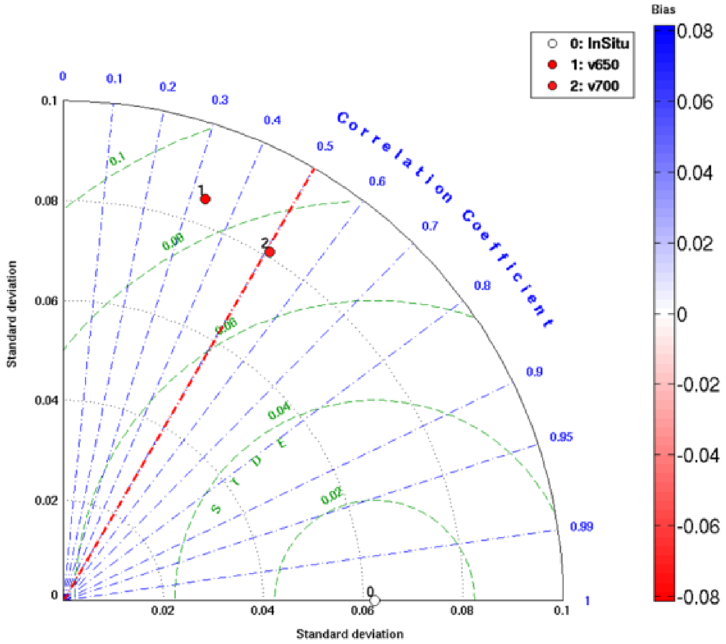

Figure 37: overall concatenated all HOBE network sites Taylor Diagram, statistics and confidence interval v700 SM, v650 SM against in-situ SM for descending orbits.

Concatenated debiased mesonet CalVal Sites Insitu Time Series: 97 kept / total 103 - Ascending orbits
CalVal Series Rejection Correlation Threshold if all scenarios corr < 0.500 or it exits R pvalues > 0.05 or #data < 20

statistics: SMOS - Insitu

Series	R	Bias	STDD	RMSD	#kept
v650	0.56	-0.055	0.080	0.097	44551
v700	0.71	-0.086	0.064	0.107	45297

SMOS/Insitu series statistics

Series	$Mean_{SMOS}$	$Mean_{Insitu}$	STD_{SMOS}	STD_{Insitu}
v650	0.177	0.233	0.089	0.080
v700	0.147	0.233	0.086	0.080

Filter Stats

Series	v650 All	v650 Inter	v700 All	v700 Inter
Initial	60212	57157	60081	57043
Retrieved	80.15%	80.44%	80.21%	80.50%
Successful	96.82%	96.90%	98.62%	98.65%

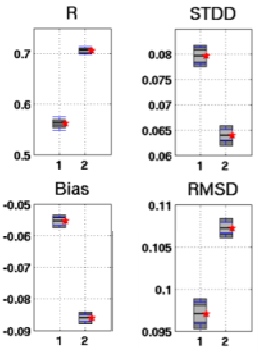

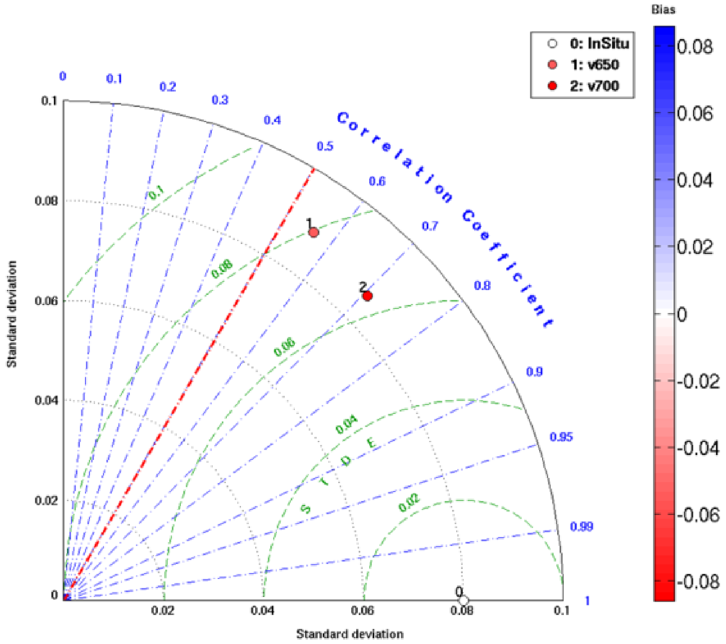

Figure 38: overall concatenated all MESONET network sites Taylor Diagram, statistics and confidence interval v700 SM, v650 SM against in-situ SM for ascending orbits.

Concatenated debiased mesonet CalVal Sites Insitu Time Series: 100 kept / total 103 - Descending orbits
CalVal Series Rejection Correlation Threshold if all scenarios corr < 0.500 or it exits R pvalues > 0.05 or #data < 20

statistics: SMOS - Insitu

Series	R	Bias	STDD	RMSD	#kept
v650	0.59	-0.048	0.079	0.093	45817
v700	0.71	-0.069	0.067	0.096	46494

SMOS/Insitu series statistics

Series	$Mean_{SMOS}$	$Mean_{Insitu}$	STD_{SMOS}	STD_{Insitu}
v650	0.181	0.229	0.094	0.079
v700	0.161	0.230	0.094	0.079

Filter Stats

Series	v650 All	v650 Inter	v700 All	v700 Inter
Initial	63466	58803	63388	58769
Retrieved	79.41%	81.07%	79.46%	81.11%
Successful	96.04%	96.11%	97.49%	97.54%

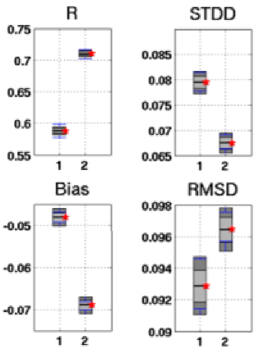

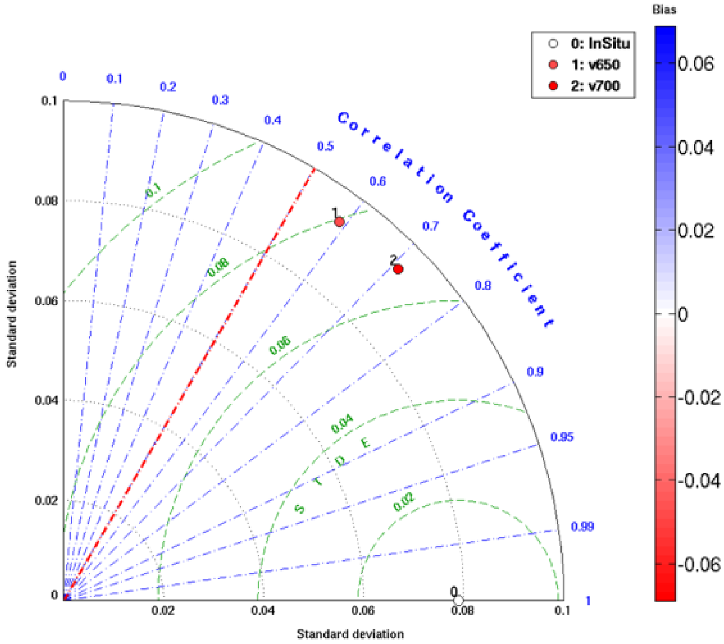

Figure 39: overall concatenated all MESONET network sites Taylor Diagram, statistics and confidence interval v700 SM, v650 SM against in-situ SM for descending orbits.

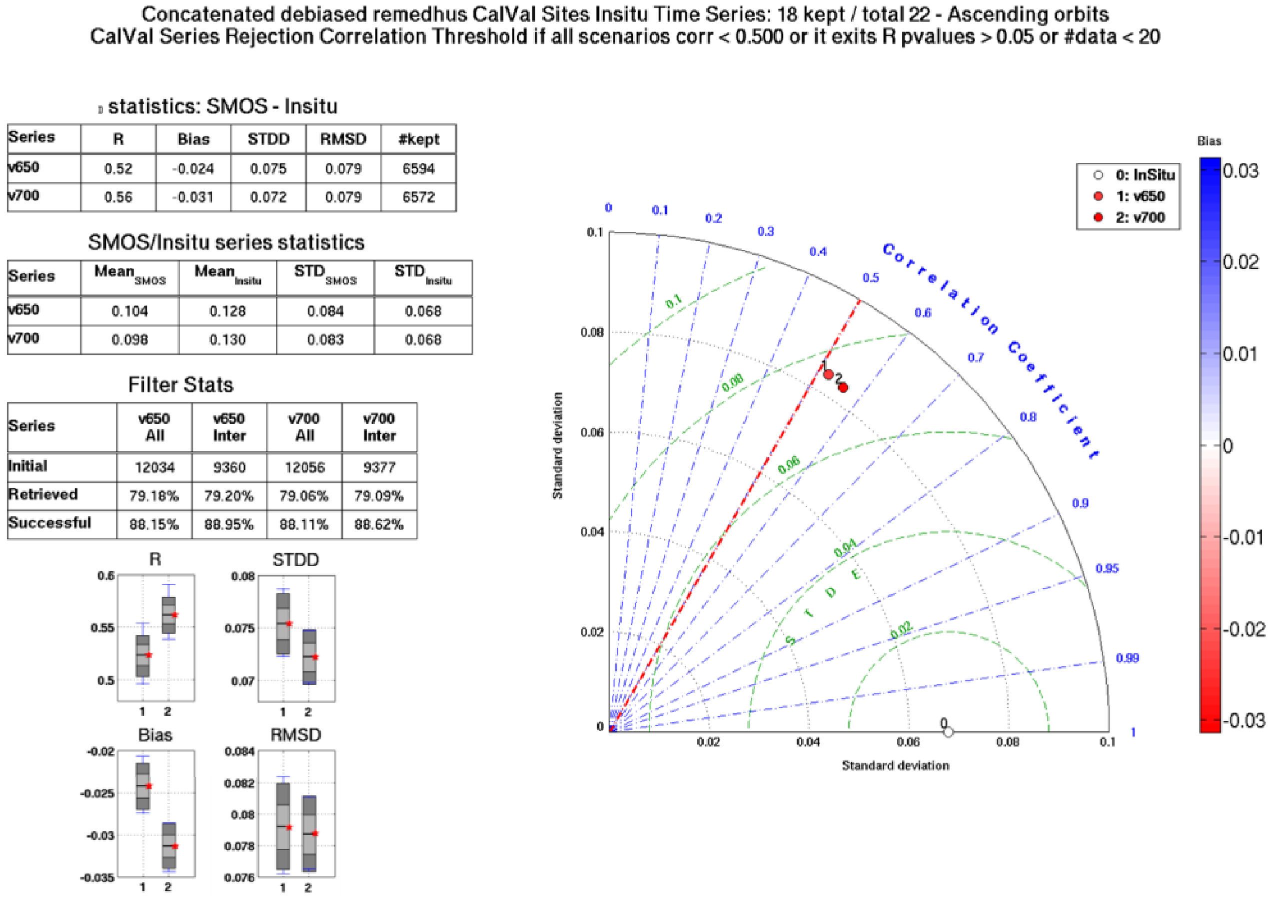

Figure 40: overall concatenated all REMEDHUS network sites Taylor Diagram, statistics and confidence interval v700 SM, v650 SM against in-situ SM for ascending orbits.

Concatenated debiased remedhus CalVal Sites Insitu Time Series: 18 kept / total 22 - Descending orbits
CalVal Series Rejection Correlation Threshold if all scenarios corr < 0.500 or it exits R pvalues > 0.05 or #data < 20

statistics: SMOS - Insitu

Series	R	Bias	STDD	RMSD	#kept
v650	0.50	-0.027	0.076	0.081	7025
v700	0.54	-0.032	0.075	0.082	7144

SMOS/Insitu series statistics

Series	$Mean_{SMOS}$	$Mean_{Insitu}$	STD_{SMOS}	STD_{Insitu}
v650	0.108	0.135	0.083	0.068
v700	0.103	0.135	0.085	0.068

Filter Stats

Series	v650 All	v650 Inter	v700 All	v700 Inter
Initial	12127	9623	12127	9623
Retrieved	80.98%	80.87%	80.91%	80.82%
Successful	89.10%	90.27%	91.42%	91.86%

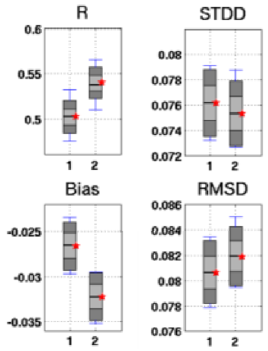

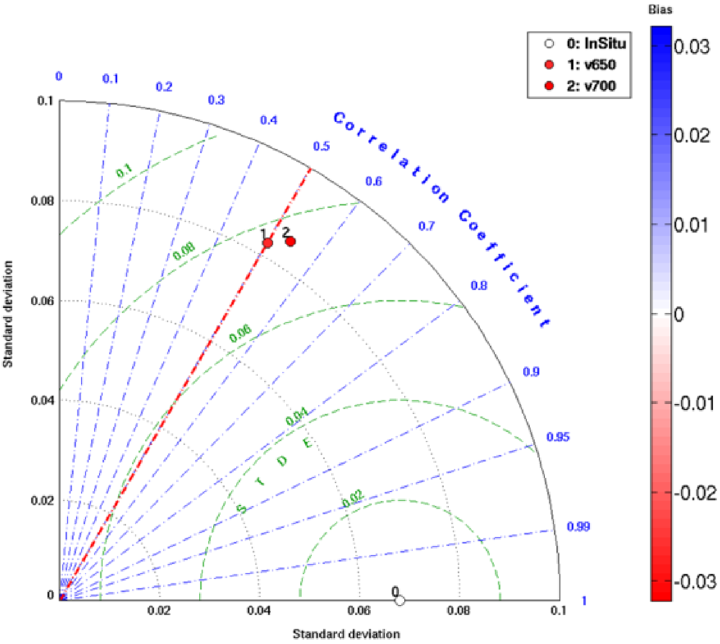

Figure 41: overall concatenated all REMEDHUS network sites Taylor Diagram, statistics and confidence interval v700 SM, v650 SM against in-situ SM for descending orbits.

Concatenated debiased scan CalVal Sites Insitu Time Series: 106 kept / total 156 - Ascending orbits
CalVal Series Rejection Correlation Threshold if all scenarios corr < 0.500 or it exits R pvalues > 0.05 or #data < 20

statistics: SMOS - Insitu

Series	R	Bias	STDD	RMSD	#kept
v650	0.47	-0.003	0.095	0.095	49463
v700	0.62	-0.040	0.078	0.087	50395

SMOS/Insitu series statistics

Series	$Mean_{SMOS}$	$Mean_{Insitu}$	STD_{SMOS}	STD_{Insitu}
v650	0.210	0.213	0.100	0.081
v700	0.174	0.214	0.095	0.081

Filter Stats

Series	v650 All	v650 Inter	v700 All	v700 Inter
Initial	85185	68803	85220	68828
Retrieved	75.47%	74.91%	75.52%	74.98%
Successful	95.59%	95.97%	97.55%	97.65%

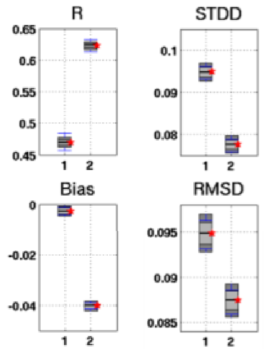

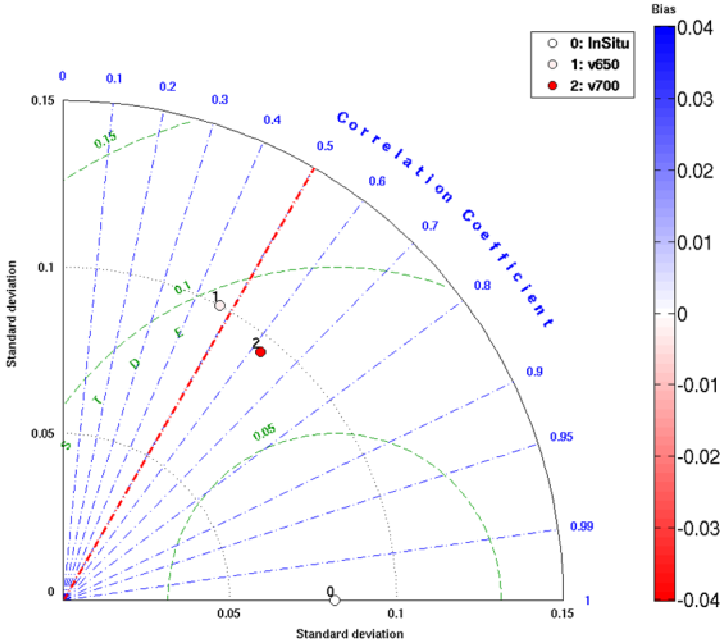

Figure 42: overall concatenated all SCAN network sites Taylor Diagram, statistics and confidence interval v700 SM, v650 SM against in-situ SM for ascending orbits.

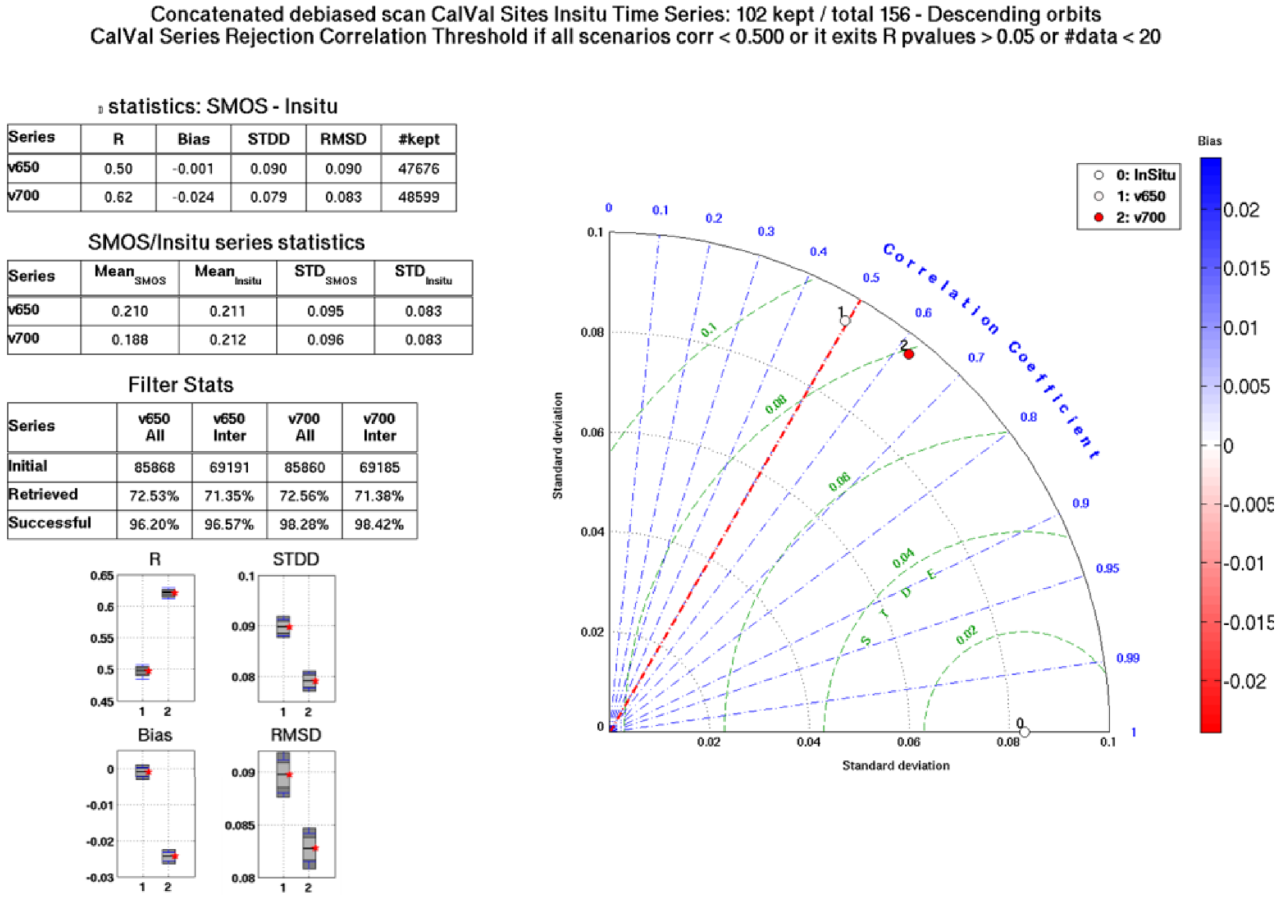

Figure 43: overall concatenated all SCAN network sites Taylor Diagram, statistics and confidence interval v700 SM, v650 SM against in-situ SM for descending orbits.

Concatenated debiased smosmania CalVal Sites Insitu Time Series: 19 kept / total 21 - Ascending orbits
CalVal Series Rejection Correlation Threshold if all scenarios corr < 0.500 or it exits R pvalues > 0.05 or #data < 20

statistics: SMOS - Insitu

Series	R	Bias	STDD	RMSD	#kept
v650	0.42	-0.053	0.106	0.118	10402
v700	0.64	-0.100	0.072	0.123	11948

SMOS/Insitu series statistics

Series	$Mean_{SMOS}$	$Mean_{Insitu}$	STD_{SMOS}	STD_{Insitu}
v650	0.167	0.220	0.111	0.081
v700	0.119	0.218	0.088	0.081

Filter Stats

Series	v650 All	v650 Inter	v700 All	v700 Inter
Initial	20396	18771	20392	18766
Retrieved	72.09%	72.13%	71.97%	72.01%
Successful	76.84%	76.82%	88.37%	88.41%

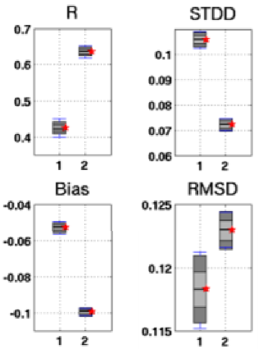

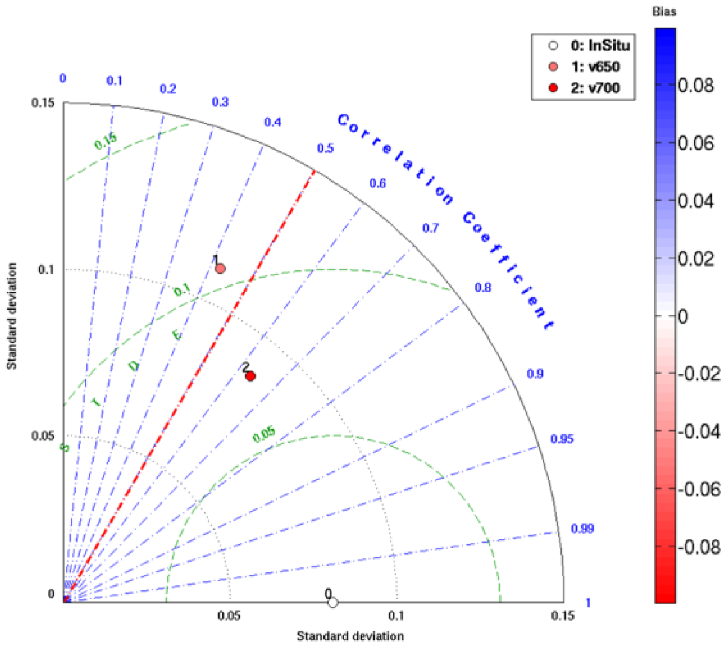

Figure 44: overall concatenated all SMOSMANIA network sites Taylor Diagram, statistics and confidence interval v700 SM, v650 SM against in-situ SM for ascending orbits.

Concatenated debiased smosmania CalVal Sites Insitu Time Series: 18 kept / total 21 - Descending orbits
CalVal Series Rejection Correlation Threshold if all scenarios corr < 0.500 or it exits R pvalues > 0.05 or #data < 20

statistics: SMOS - Insitu

Series	R	Bias	STDD	RMSD	#kept
v650	0.43	-0.067	0.098	0.119	11477
v700	0.69	-0.102	0.066	0.121	12467

SMOS/Insitu series statistics

Series	$Mean_{SMOS}$	$Mean_{Insitu}$	STD_{SMOS}	STD_{Insitu}
v650	0.174	0.241	0.100	0.082
v700	0.139	0.241	0.085	0.083

Filter Stats

Series	v650 All	v650 Inter	v700 All	v700 Inter
Initial	18185	17108	18199	17120
Retrieved	78.14%	78.07%	78.20%	78.13%
Successful	86.07%	85.93%	93.22%	93.20%

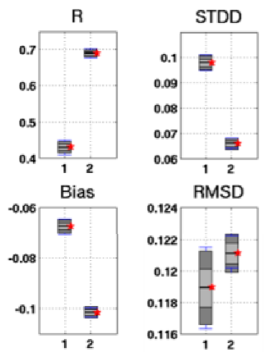

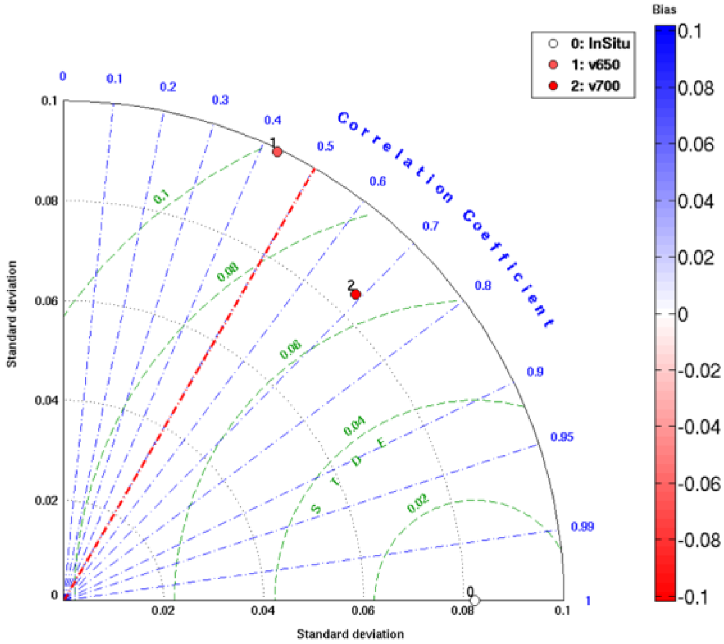

Figure 45: overall concatenated all SMOSMANIA network sites Taylor Diagram, statistics and confidence interval v700 SM, v650 SM against in-situ SM for descending orbits.

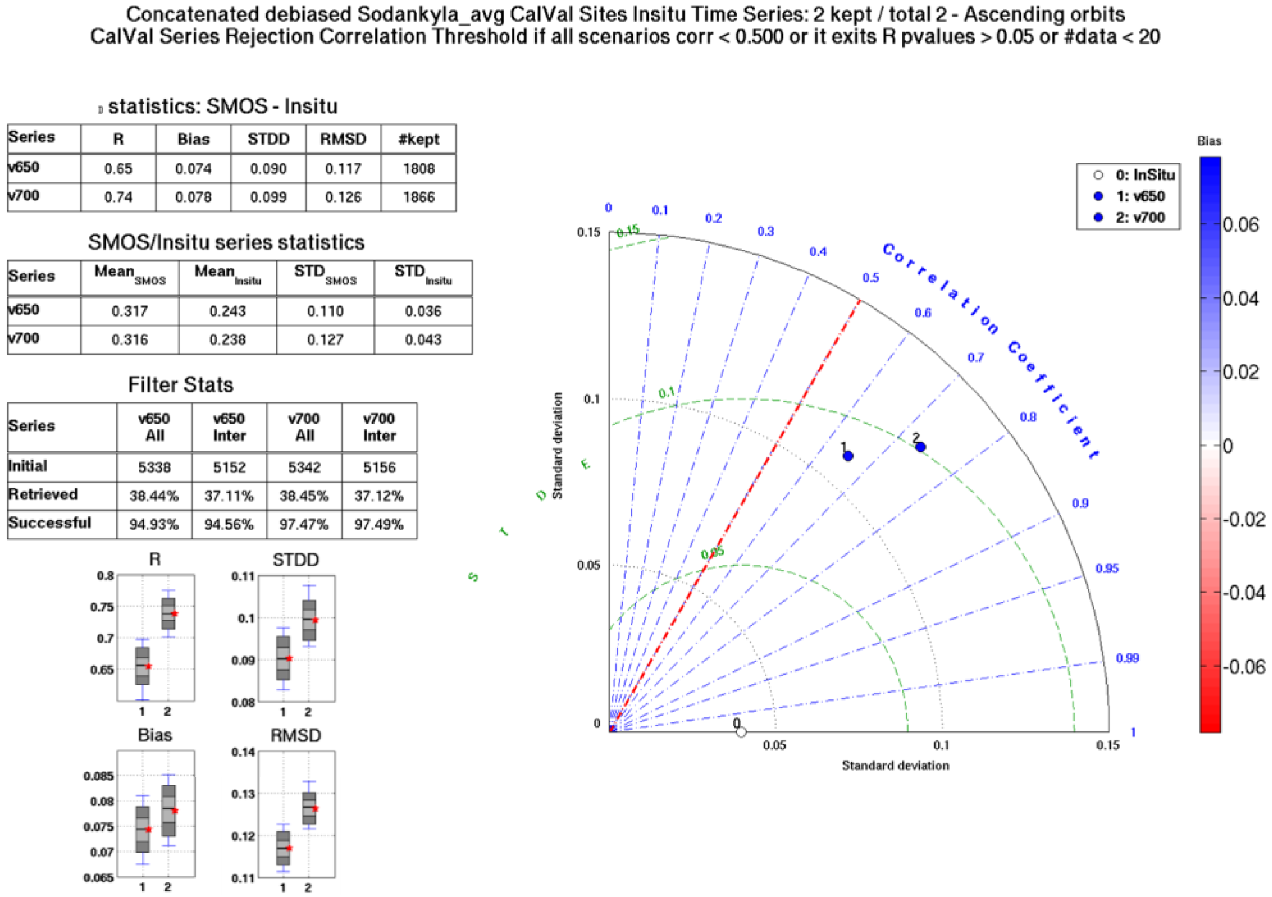

Figure 46: overall concatenated all Sodankylä network sites Taylor Diagram, statistics and confidence interval v700 SM, v650 SM against in-situ SM for descending orbits.

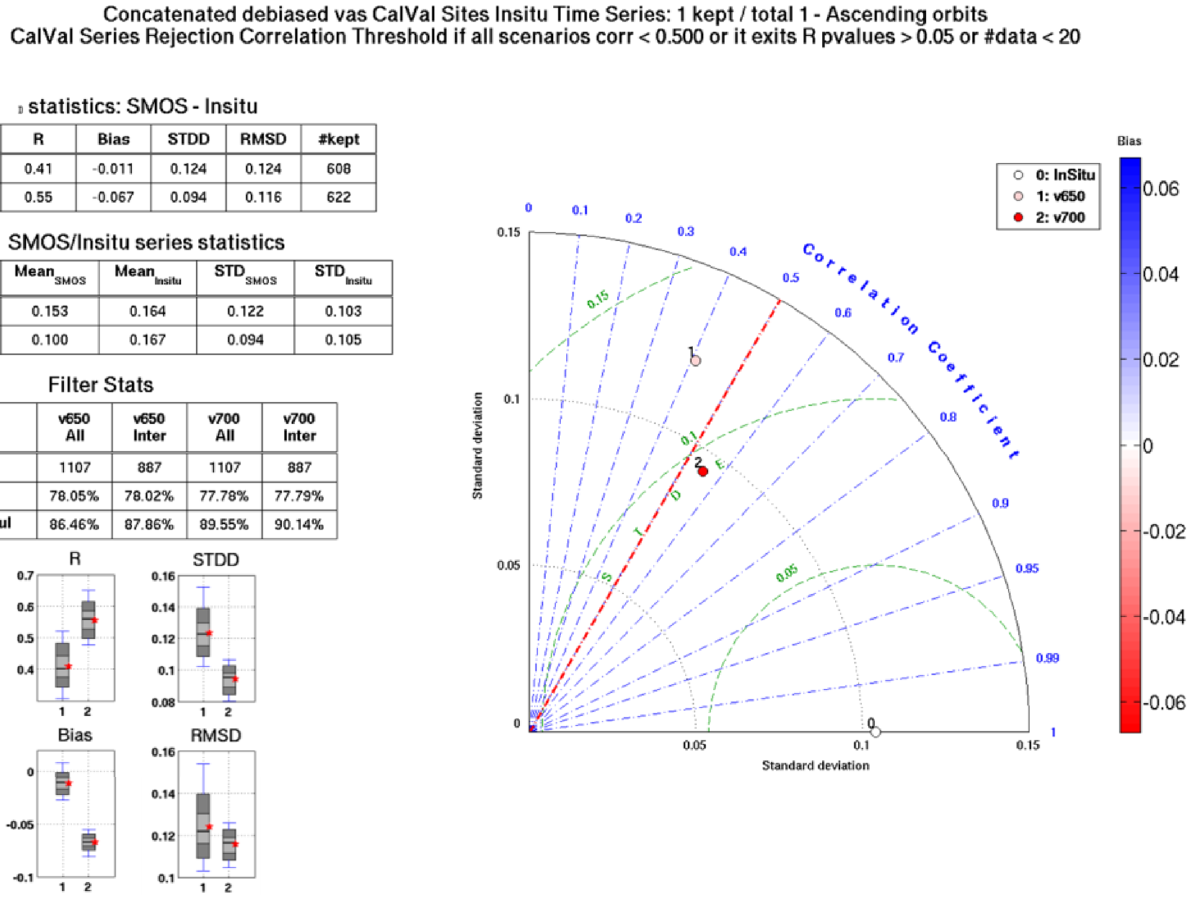

Figure 47: overall concatenated all VAS network sites Taylor Diagram, statistics and confidence interval v700 SM, v650 SM against in-situ SM for ascending orbits.

Concatenated debiased vas CalVal Sites Insitu Time Series: 1 kept / total 1 - Descending orbits
CalVal Series Rejection Correlation Threshold if all scenarios corr < 0.500 or it exits R pvalues > 0.05 or #data < 20

statistics: SMOS - Insitu

Series	R	Bias	STDD	RMSD	#kept
v650	0.58	-0.011	0.092	0.093	664
v700	0.62	-0.046	0.090	0.101	686

SMOS/Insitu series statistics

Series	$Mean_{SMOS}$	$Mean_{Insitu}$	STD_{SMOS}	STD_{Insitu}
v650	0.136	0.147	0.081	0.111
v700	0.103	0.149	0.083	0.113

Filter Stats

Series	v650 All	v650 Inter	v700 All	v700 Inter
Initial	1120	872	1121	873
Retrieved	81.16%	81.42%	81.36%	81.56%
Successful	93.18%	93.52%	96.82%	96.35%

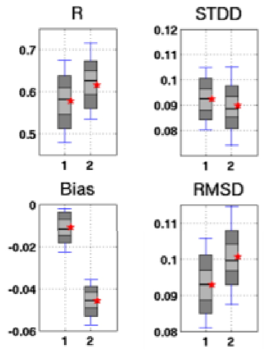

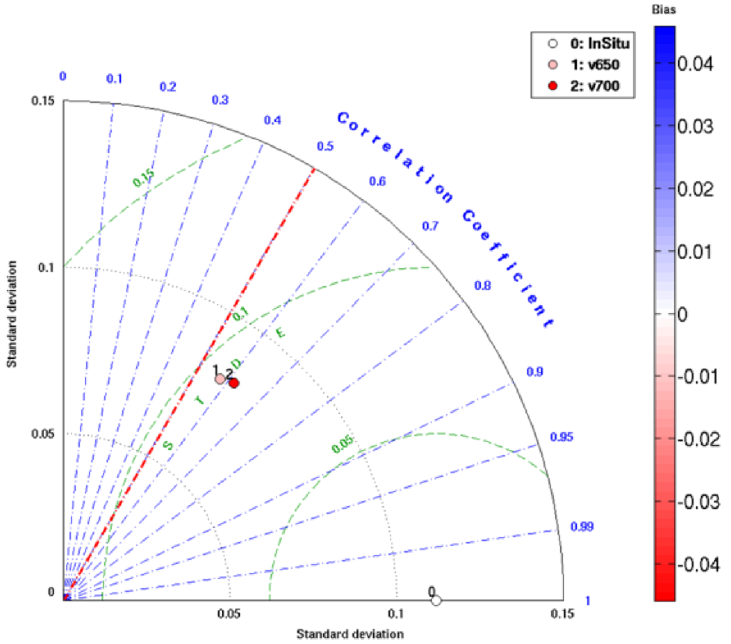

Figure 48: overall concatenated all VAS network sites Taylor Diagram, statistics and confidence interval v700 SM, v650 SM against in-situ SM for descending orbits.

Concatenated debiased watersheds CalVal Sites Insitu Time Series: 4 kept / total 4 - Ascending orbits
CalVal Series Rejection Correlation Threshold if all scenarios corr < 0.500 or it exits R pvalues > 0.05 or #data < 20

statistics: SMOS - Insitu

Series	R	Bias	STDD	RMSD	#kept
v650	0.57	0.021	0.058	0.061	2840
v700	0.69	-0.002	0.048	0.049	2838

SMOS/Insitu series statistics

Series	$Mean_{SMOS}$	$Mean_{Insitu}$	STD_{SMOS}	STD_{Insitu}
v650	0.123	0.102	0.068	0.054
v700	0.100	0.102	0.066	0.054

Filter Stats

Series	v650 All	v650 Inter	v700 All	v700 Inter
Initial	3886	3882	3888	3884
Retrieved	74.19%	74.19%	74.20%	74.20%
Successful	98.61%	98.61%	98.47%	98.47%

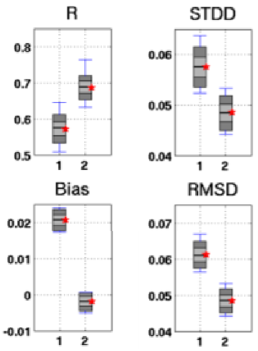

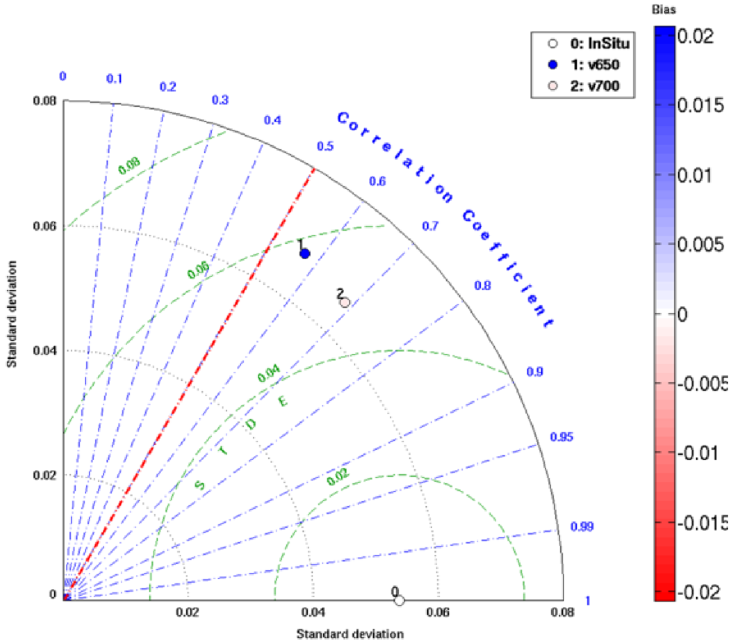

Figure 49: overall concatenated all WATERSHEDS network sites Taylor Diagram, statistics and confidence interval v700 SM, v650 SM against in-situ SM for ascending orbits.

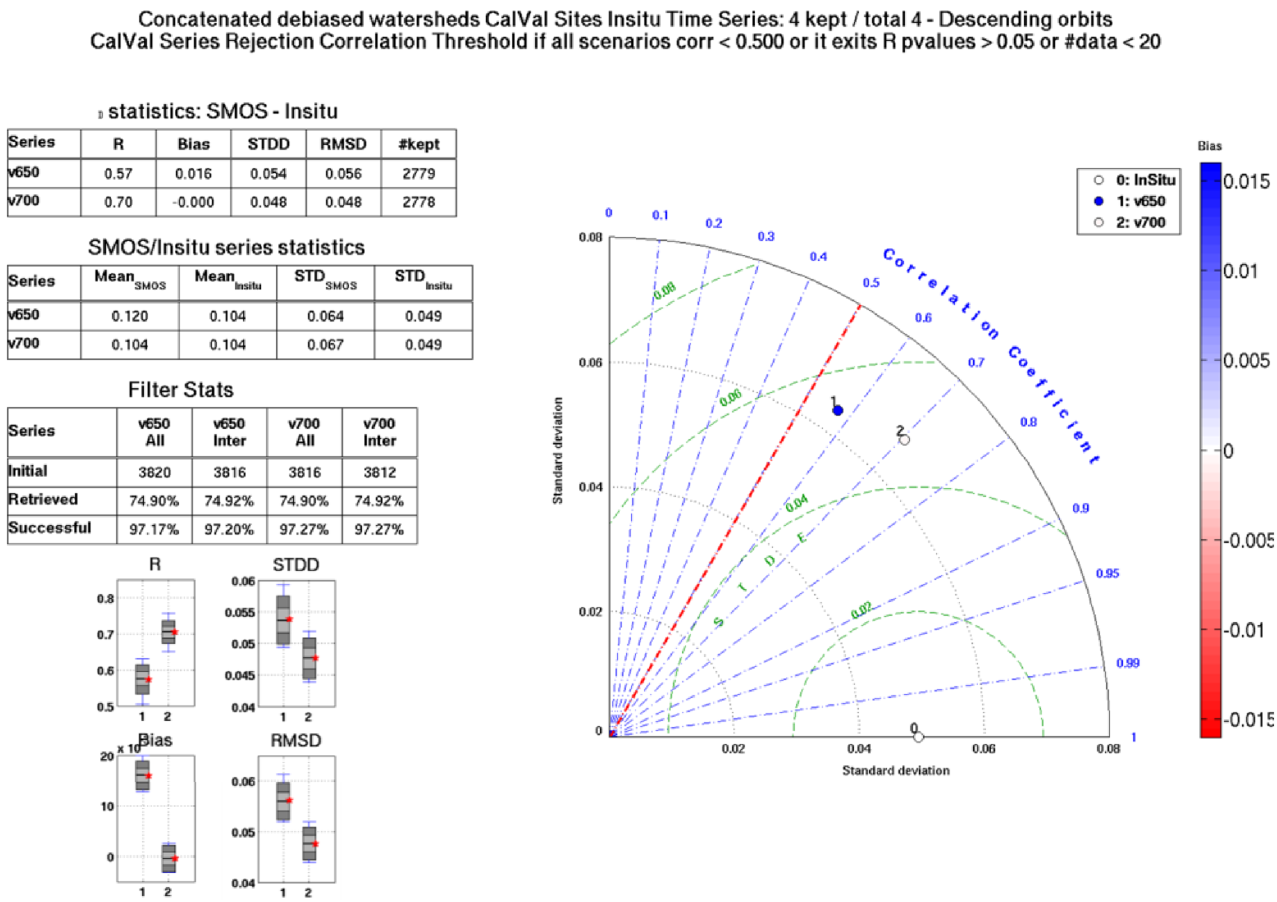

Series	R	Bias	STDD	RMSD	#kept
v650	0.57	0.016	0.054	0.056	2779
v700	0.70	-0.000	0.048	0.048	2778

Series	$Mean_{SMOS}$	$Mean_{Insitu}$	STD_{SMOS}	STD_{Insitu}
v650	0.120	0.104	0.064	0.049
v700	0.104	0.104	0.067	0.049

Series	v650 All	v650 Inter	v700 All	v700 Inter
Initial	3820	3816	3816	3812
Retrieved	74.90%	74.92%	74.90%	74.92%
Successful	97.17%	97.20%	97.27%	97.27%

Figure 50: overall concatenated all Watershed network sites Taylor Diagram, statistics and confidence interval v700 SM, v650 SM against in-situ SM for descending orbits.

4.3.1.3 INSIGHT ON SOME SPECIFIC IN-SITU SITES

This section is no yet populated. The purpose is to add TP/stats for specific sites with contrasted metrics SMOS SM vs. in-situ SM: for v700 and for v650:

- The highest/lowest R
- The highest/lowest STDD
- The highest/lowest |bias|
- The highest/lowest RMSD

4.3.2 SPATIAL MAPS

The following section present global maps made from ascending orbits of retrieved SM, TauNadir, Chi2 and PRFI12 for the whole reprocessing period 20100501 – 20210131 and for different segment of time from the three reprocessing instances. Retrieved values maps for v700 and v650, their maps of differences or maps of ratios and stats are provided.

Parameters maps are average in time of parameters values over the period per DGG, difference/ratio maps are average in time of orbit-wise differences (common successful orbits) per DGG.

For a given vxxx map, black markers indicate systematically failing retrievals over the considered period while the other version vyyy report at least 1 non failing retrievals. Dark grey markers indicated that both vxxx and the other vyyy version are systematically failing together. Light grey areas indicate other retrieval case than the maps focuses on e.g. ACard/TauNadir, Tsurf systematic retrieved areas for SM/TauNadir maps and vice-versa.

Color-bar: the ► marker indicates the distribution mode, the two inner v^ markers its 68.3% potentially asymmetrical percentile (1σ equivalent Gaussian), the two outer its 95.4% potentially asymmetrical percentile (2 σ equivalent Gaussian), the ▲▼ the min/max values.

4.3.2.1 RETRIEVED SOIL MOISTURE

The section 4.3.2.1.1 shows the maps for the whole 10+ years of average in time soil moisture. These maps give the big picture but also include the entire past story especially the RFI situation that changed in time. v700 has lower soil moisture than v650 on specific areas. It is the case around rivers networks (well visible e.g. over Amazon) and for low vegetation areas (e.g. Sahel) band. The former comes from the higher FWO (ESA CCI) for v700 and the latter from the omega increase.

On other areas, specifically at high latitudes, the organic soil is competing in the other direction limiting the decrease and sometime wining with higher retrieved v700 values than v650.

Generally speaking v700 soil moisture map appears slightly smoother than v650 due to joint NO/FO retrieval.

The sections 4.3.2.1.2, 4.3.2.1.3, 4.3.2.1.4 focusing on few months only of reprocessing segment S1, S2, S3, do not change drastically these observations though with some changes in magnitudes but also different RFI situation particularly strong for S1 (beginning of the mission). What is essentially different is the black dots appearing mostly on v650 maps and not on v700 ones. These black dots identify systematic failures over the period of a map for given version while for the other version retrievals did not fail systematically. Over 10 years it does not appear as it is sufficient for a DGG that one successful retrieval exists for one version while many exist for the other version to appear on the map. For shorter period it is less the case and the many black dots appearing on v650 maps are very localized, actually where essentially the FFO+FNO join retrieval is in action where v700 is gaining with less failures.

4.3.2.1.1 Whole REPR period 201006 – 20210131

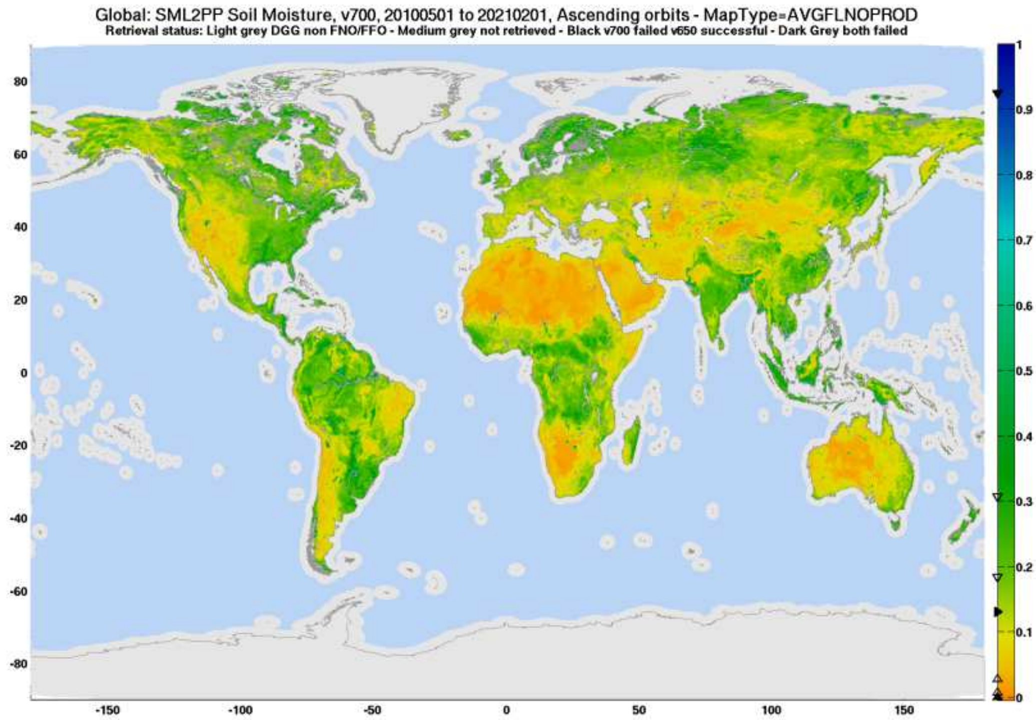

Figure 51: Whole reprocessing 20100501 - 20210231; Global map time average of retrieved v700 SM. Black dots, mean systematic v700 failures while v650 report at least one valid over the period.

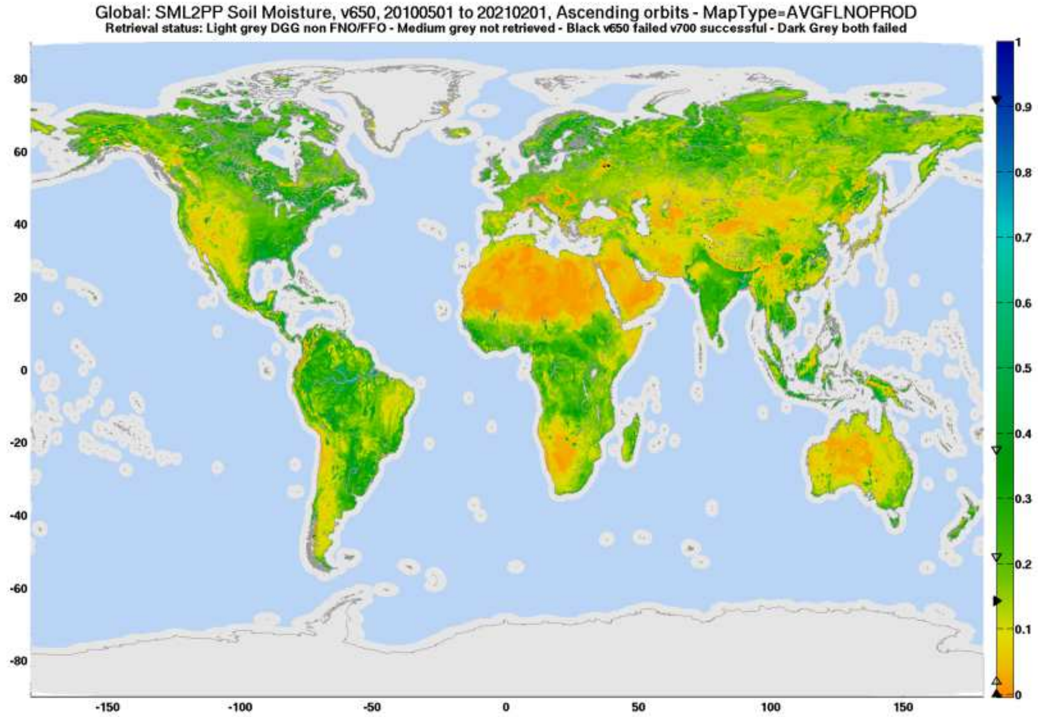

Figure 52: Whole reprocessing 20100501 - 20210231; Global map time average of retrieved v650 SM. Black dots, mean systematic v650 failures while v700 report at least one valid over the period.

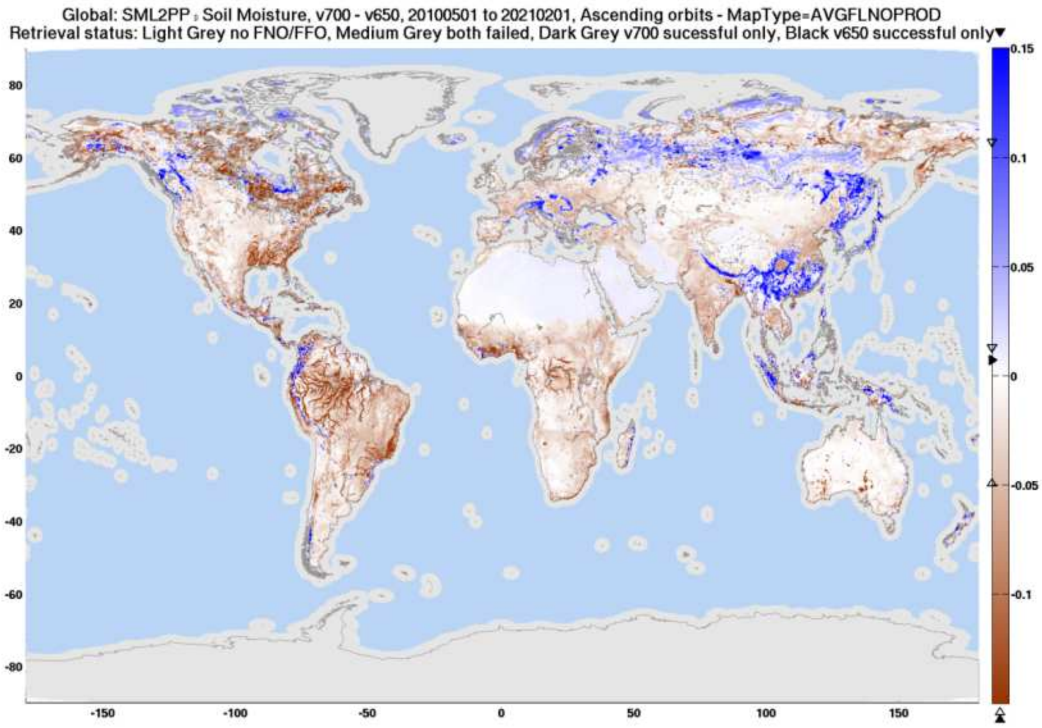

Figure 53: Whole reprocessing 20100501 - 20210231; Global map time average of differences of v700 retrieved SM minus v650 retrieved SM.

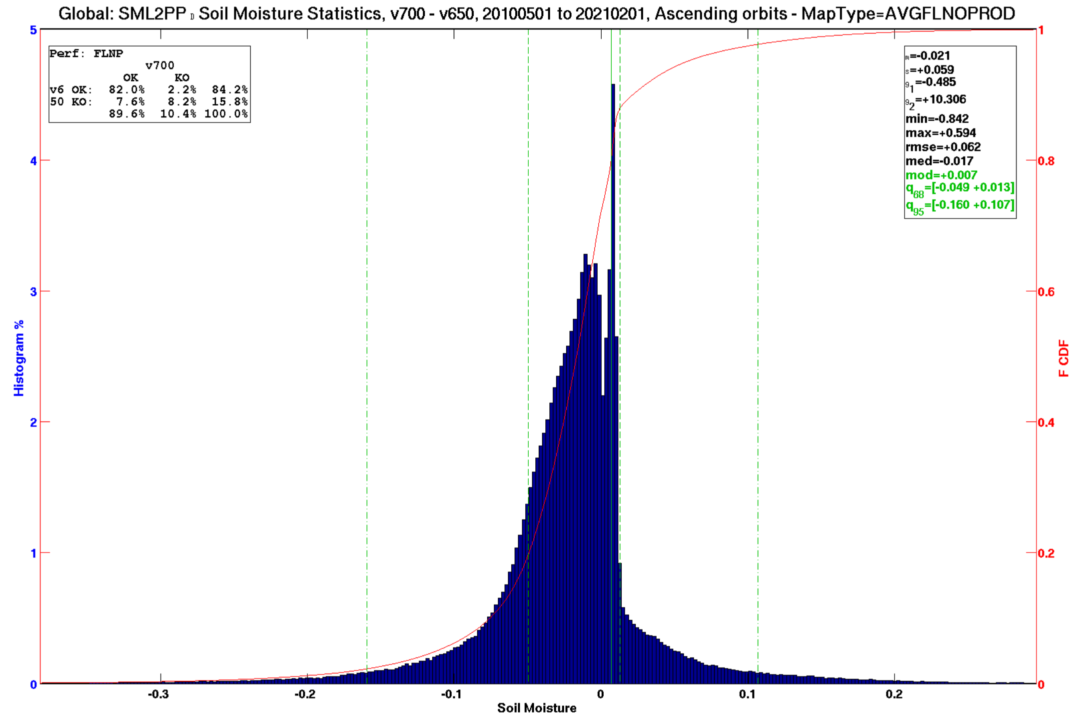

Figure 54: Whole reprocessing 20100501 - 20210231; Global histogram, cdf and stats of differences of v700 retrieved SM minus v650 retrieved SM.

4.3.2.1.2 S1: 20100601 – 20100905

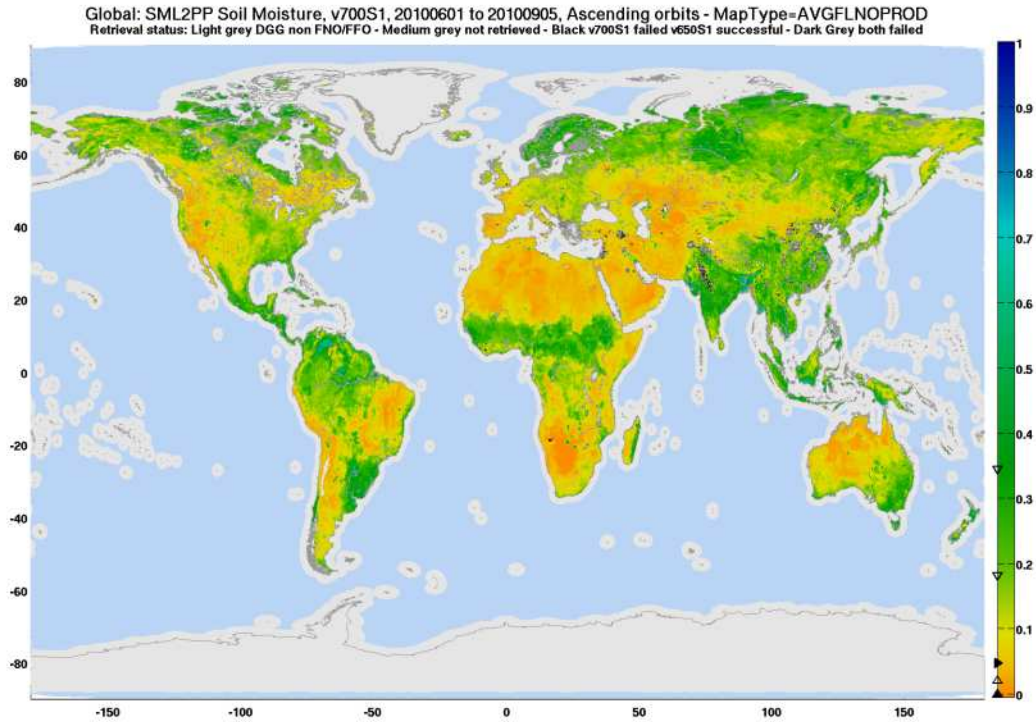

Figure 55: Reprocessing instance S1; Global map time average of retrieved v700 retrieved SM. Black dots, mean systematic v700 failures while v650 report at least one valid.

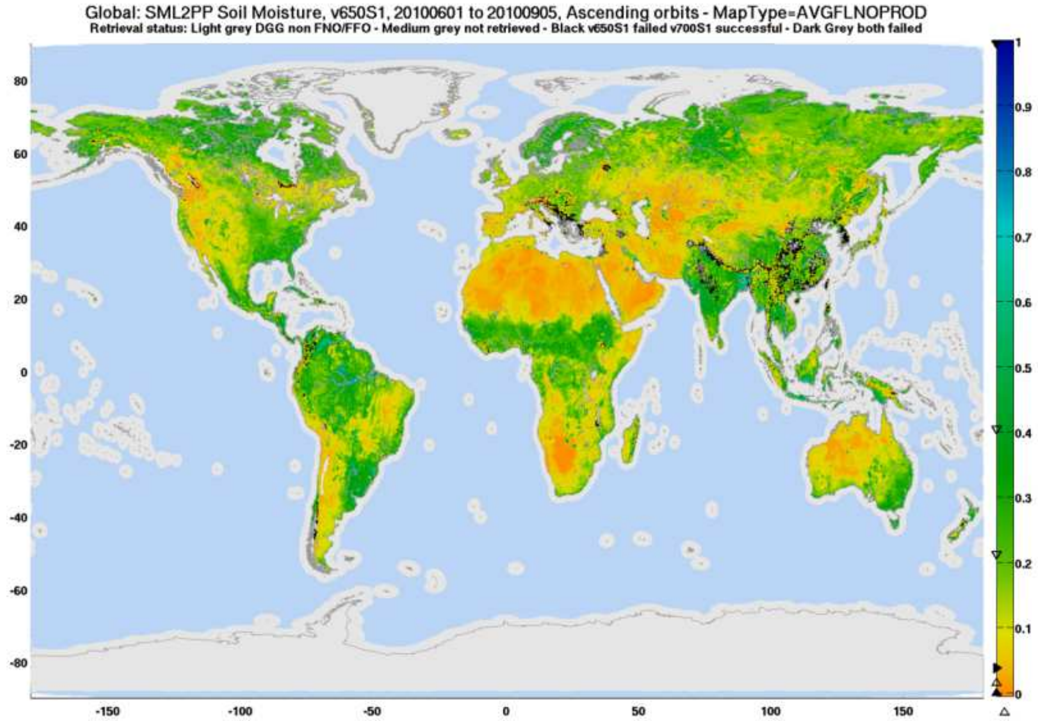

Figure 56: Reprocessing instance S1; Global map time average of retrieved v650 retrieved SM. Black dots, mean systematic v650 failures while v700 report at least one valid.

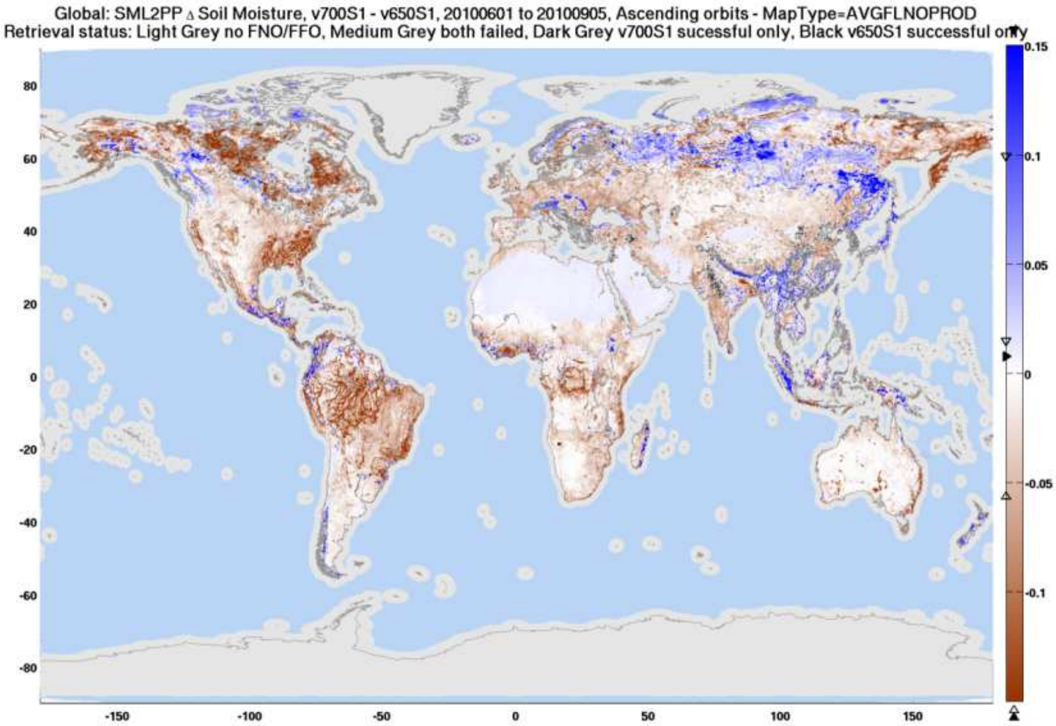

Figure 57: Reprocessing instance S1; Global map time average of differences of v700 retrieved SM minus v650 retrieved SM.

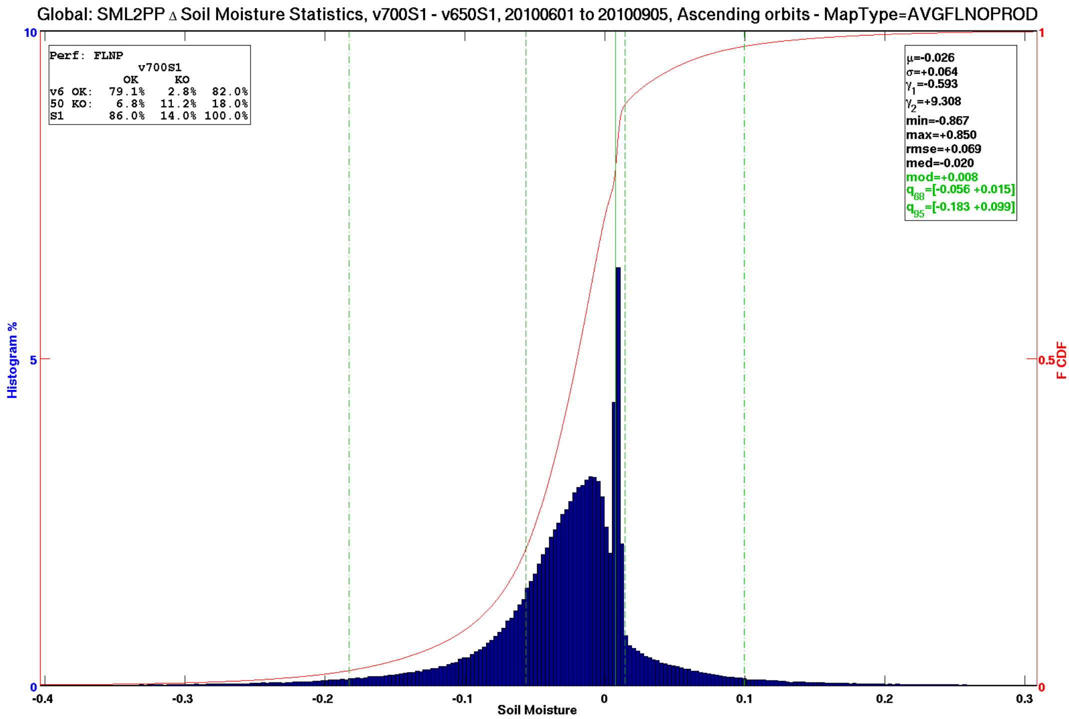

Figure 58: Reprocessing instance S1; Global histogram, cdf and stats of differences of v700 retrieved SM minus v650 retrieved SM.

4.3.2.1.3 S2: 20140201 – 20140524

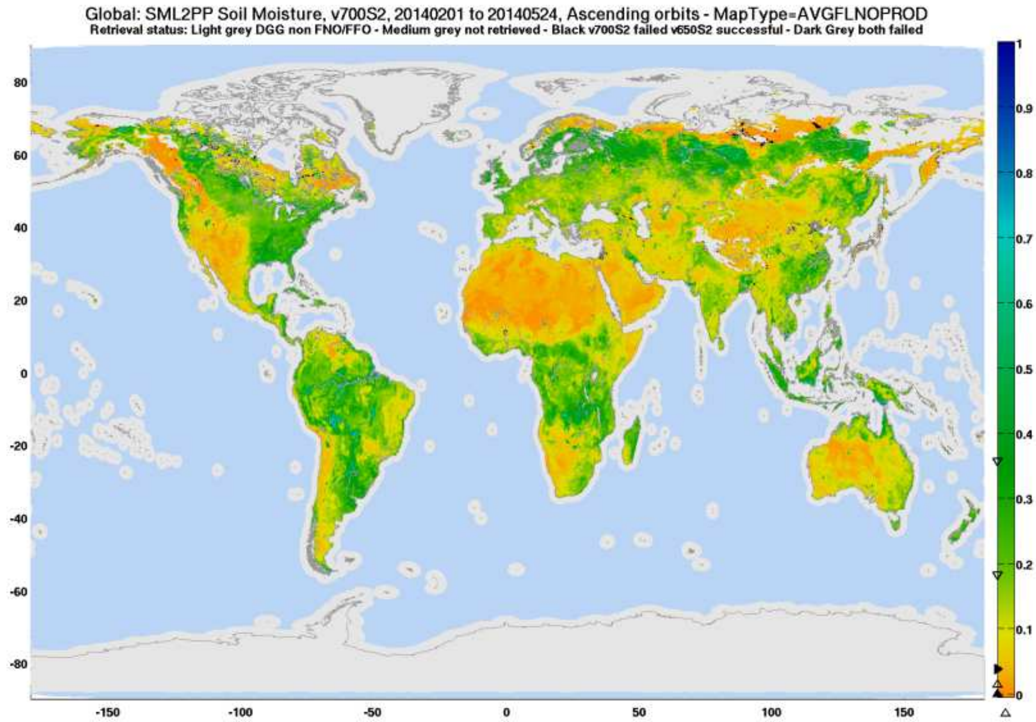

Figure 59: Reprocessing instance S2; Global map time average of retrieved v700 retrieved SM. Black dots, mean systematic v700 failures while v650 report at least one valid.

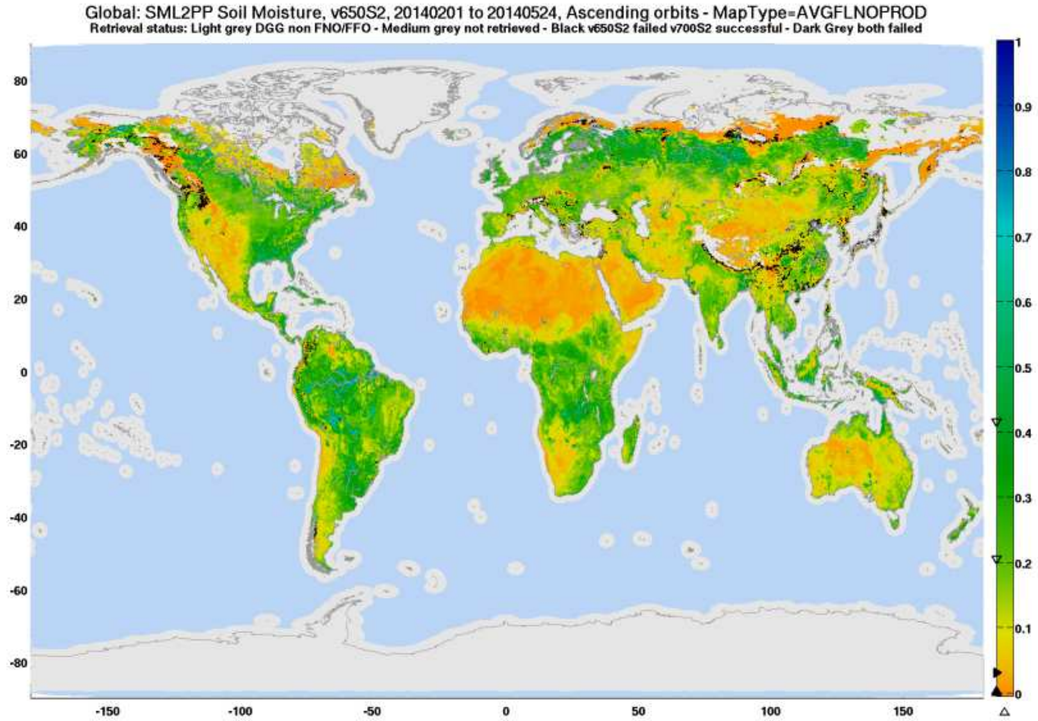

Figure 60: Reprocessing instance S2; Global map time average of retrieved v650 retrieved SM. Black dots, mean systematic v650 failures while v700 report at least one valid.

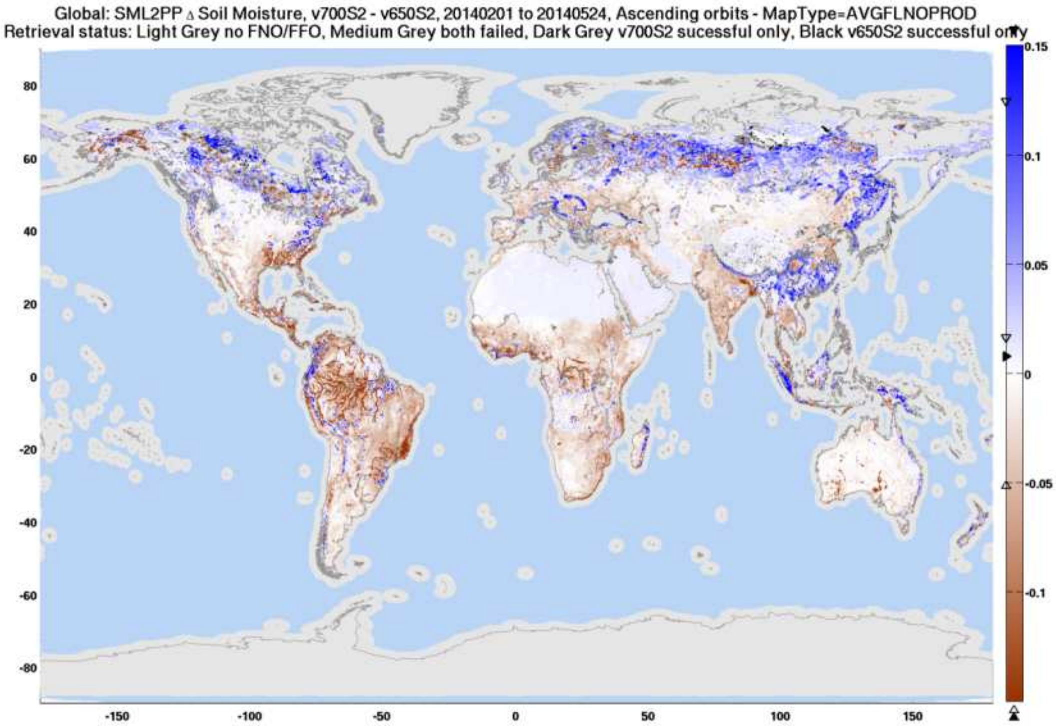

Figure 61: Reprocessing instance S2; Global map time average of differences of v700 retrieved SM minus v650 retrieved SM.

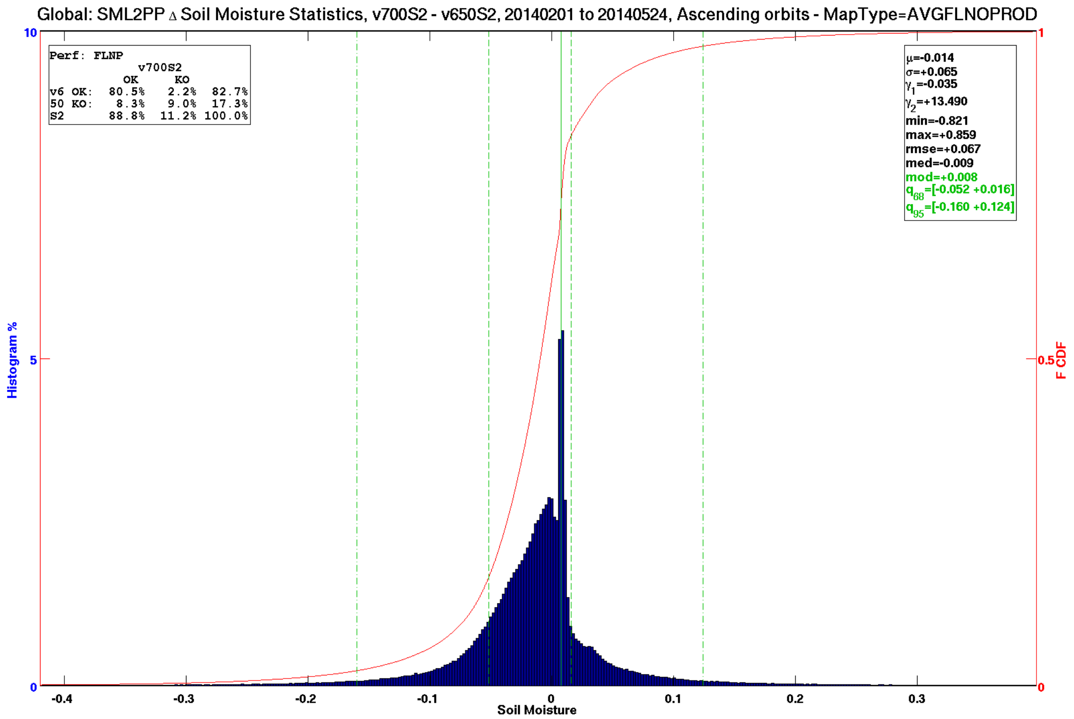

Figure 62: Reprocessing instance S2; Global histogram, cdf and stats of differences of v700 retrieved SM minus v650 retrieved SM.

4.3.2.1.4 S3: 20180201 – 20180414

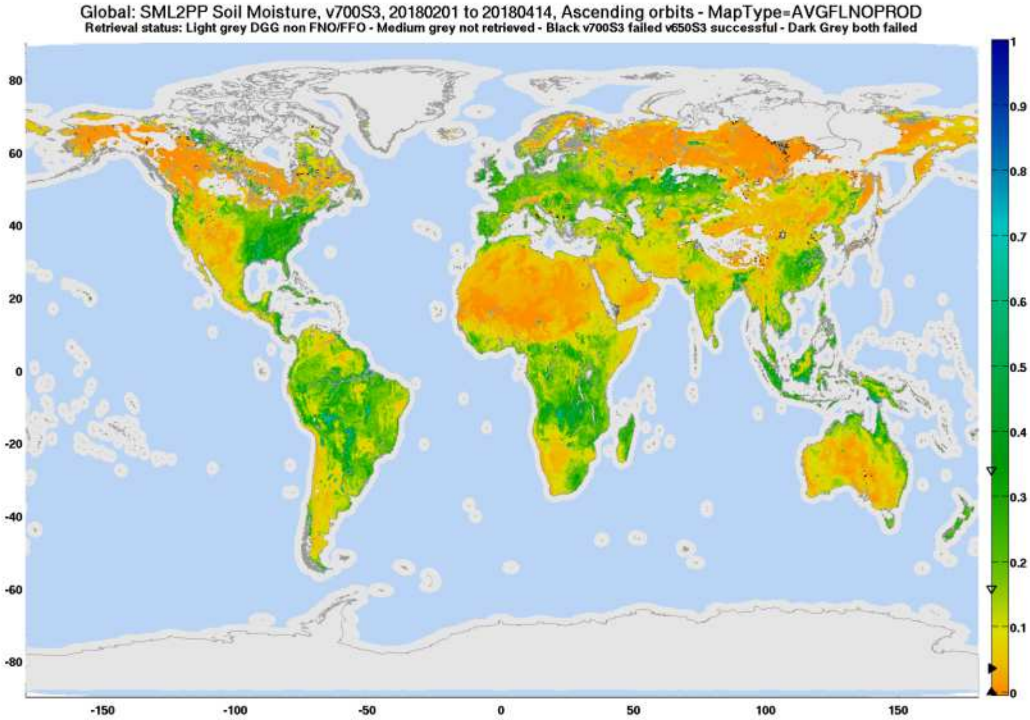

Figure 63: Reprocessing instance S3; Global map time average of retrieved v700 retrieved SM. Black dots, mean systematic v700 failures while v650 report at least one valid.

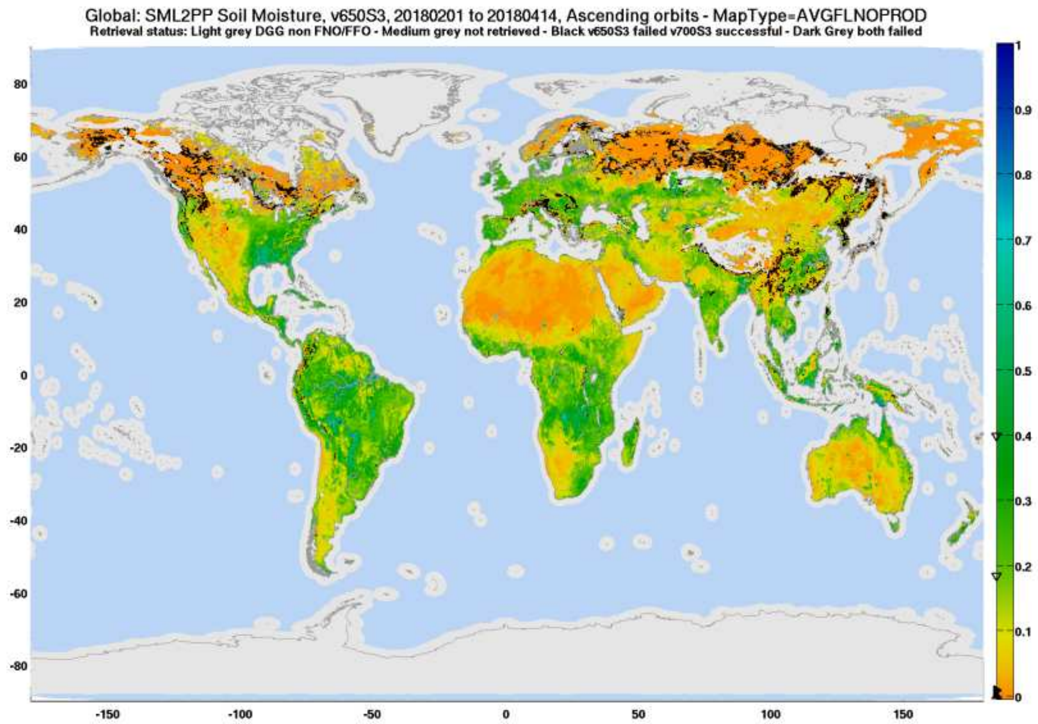

Figure 64: Reprocessing instance S3; Global map time average of retrieved v650 retrieved SM. Black dots, mean systematic v650 failures while v700 report at least one valid.

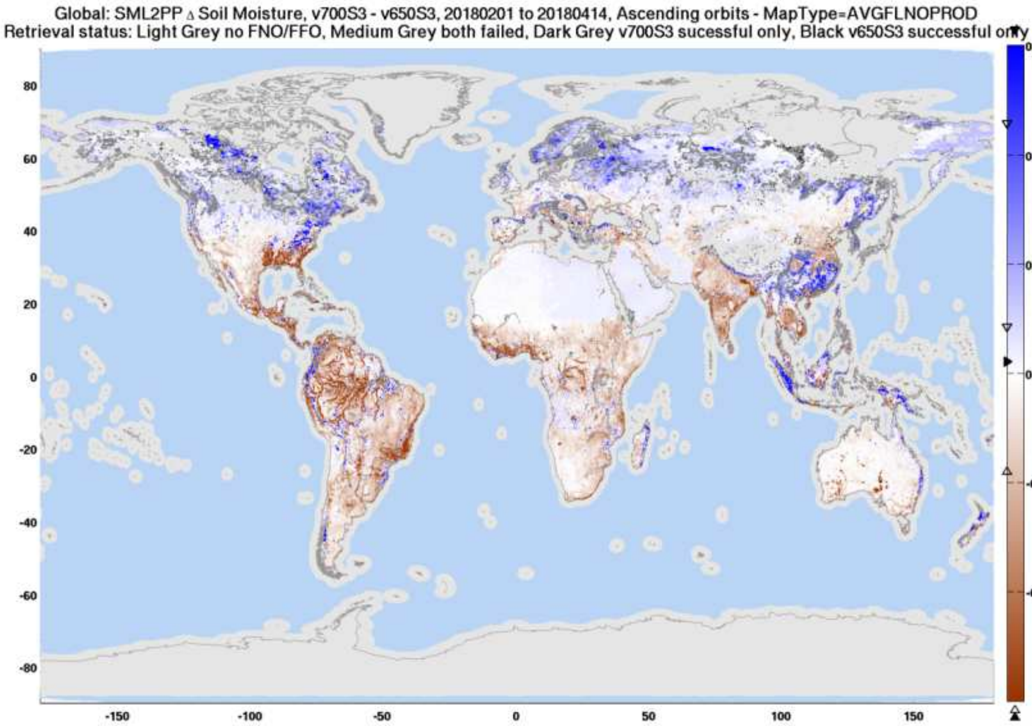

Figure 65: Reprocessing instance S3; Global map time average of differences of v700 retrieved SM minus v650 retrieved SM.

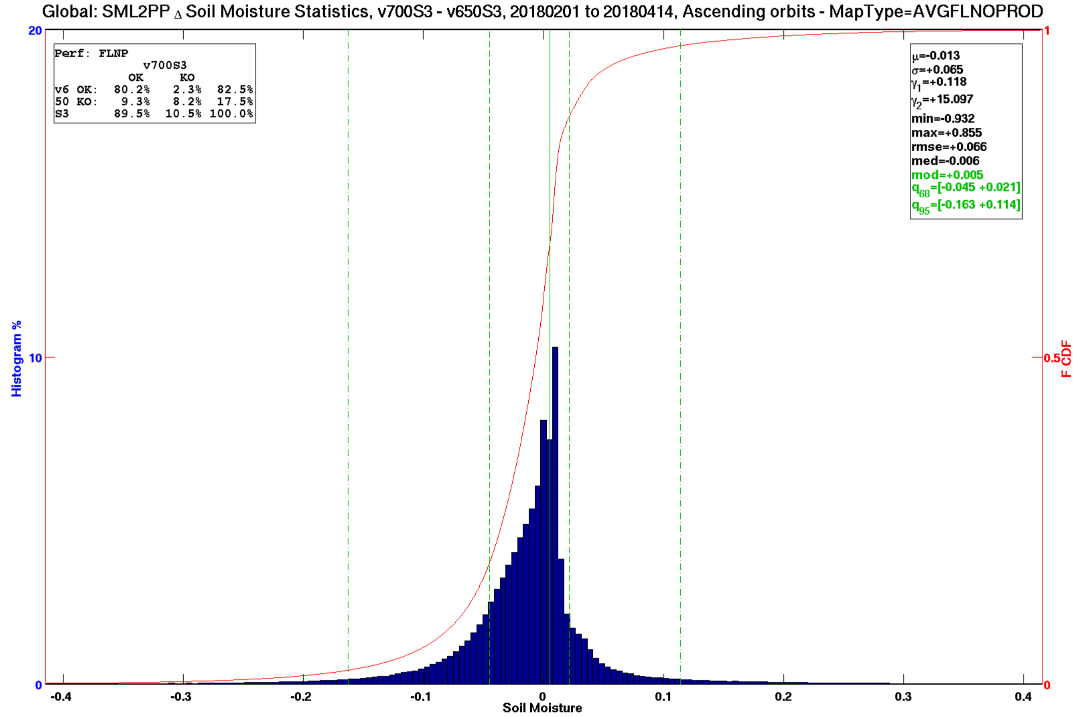

Figure 66: Reprocessing instance S3; Global histogram, cdf and stats of differences of v700 retrieved SM minus v650 retrieved SM.

4.3.2.2 RETRIEVED TAUNADIR (VOD)

Over the 10 years, the most apparent change in retrieved nadir Tau is the smoothing effect introduced by the joint NO+FO retrievals and well visible on v700 map. At the border of dense forest we have observed a gain in the number successful retrievals for v700 visible for S1, S2, S3 segments; it is also the case of course for TauNadir (maps of sections 4.3.2.2.2, 4.3.2.2.3, 4.3.2.2.4). However the impact on TauNadir is also very clear, more successful retrievals appear but usually with lower retrieved TauNadir that form a thin brown border well visible on the Δmaps. The vegetation opacity is the parameter having the strongest non linear connection with the BT in our model due to its exponential form (i.e. is very different of particularly if Tau_{FO} and Tau_{NO} are different)

Apart on these transitions FO/NO areas and an overall slightly decreased TauNadir, Northern latitudes show significant increases of v700 retrieved opacity, probably in relation both to higher v700 water fractions and organic soil.

4.3.2.2.1 Whole REPR period 201006 – 20210131

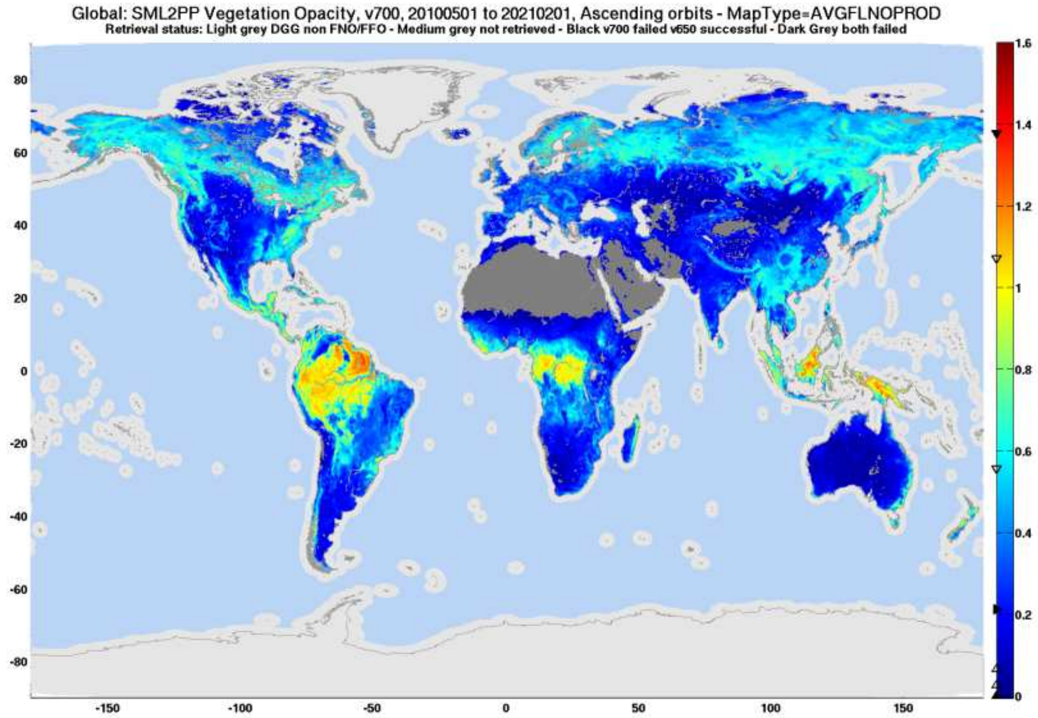

Figure 67: Global map of v700 retrieved opacity over the whole reprocessing period, 2010501 - 20210131

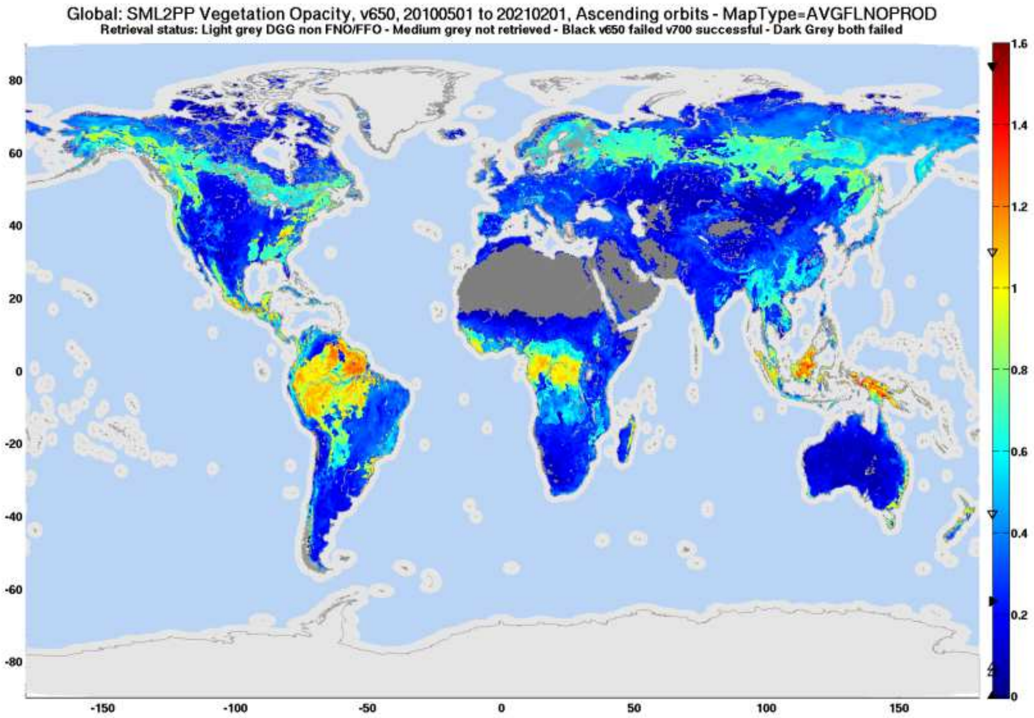

Figure 68: Global map of v650 retrieved opacity over the whole reprocessing period, 2010501 - 20210131

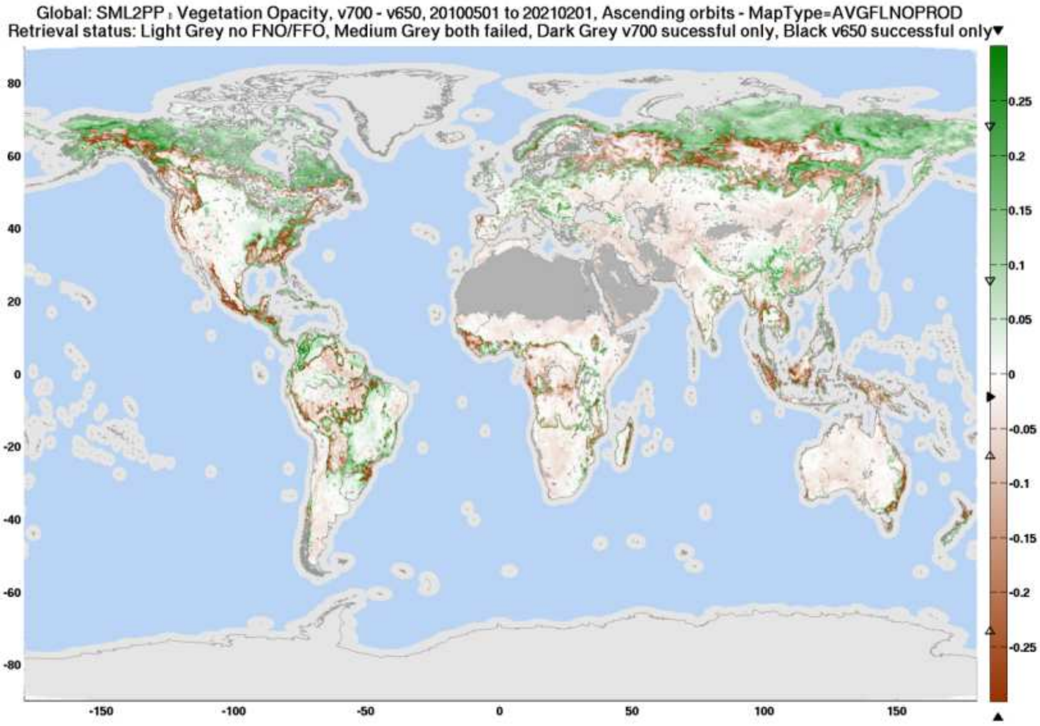

Figure 69: Global map of retrieved opacity difference, v700 – v650, over the whole reprocessing period, 2010501 - 20210131

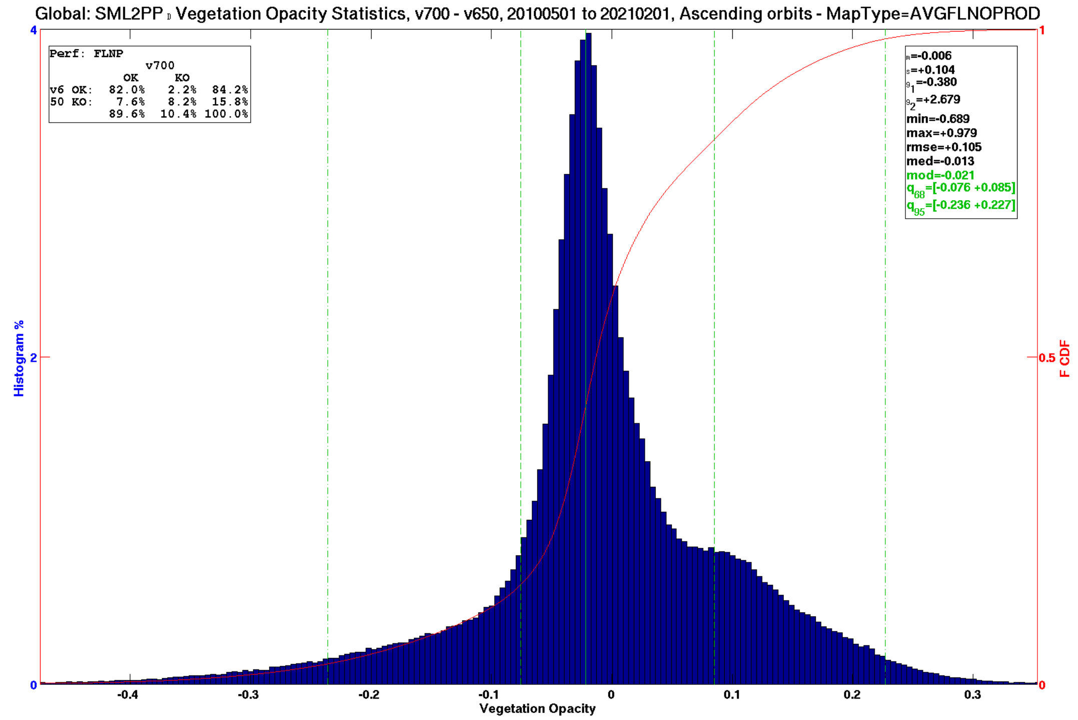

Figure 70: histogram of Global retrieved opacity difference, v700 – v650, over the whole reprocessing period, 2010501 - 20210131

4.3.2.2.2 S1: 20100601 – 20100905

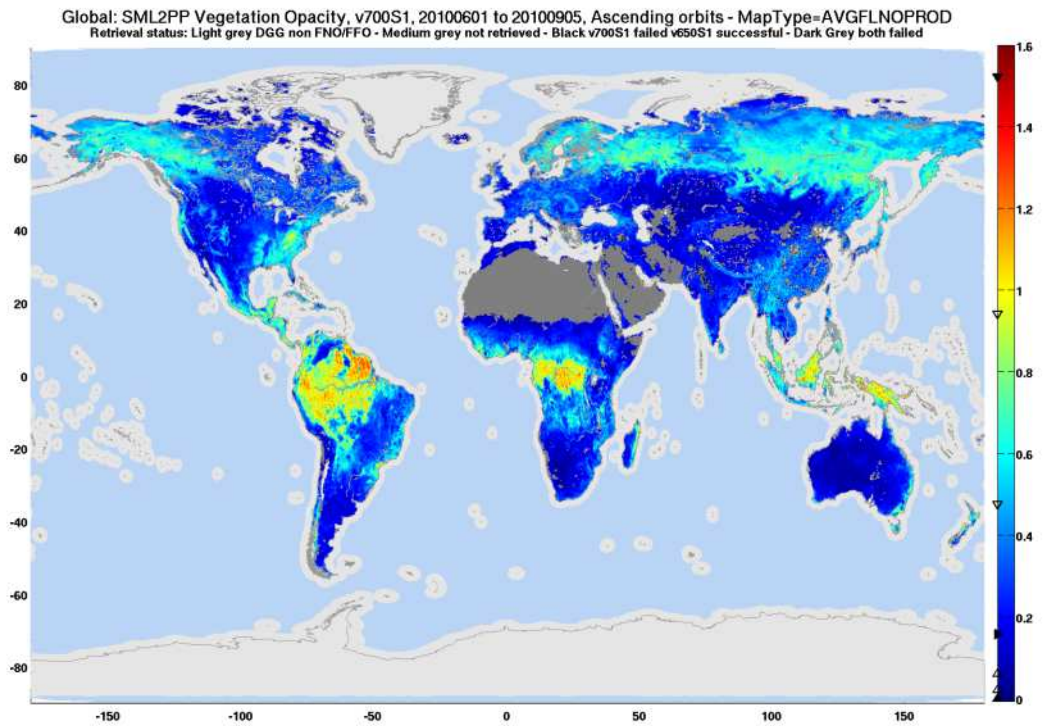

Figure 71: Reprocessing instance S1; Global map time average of retrieved v700 retrieved VOD. Black dots, mean systematic v700 failures while v650 report at least one valid.

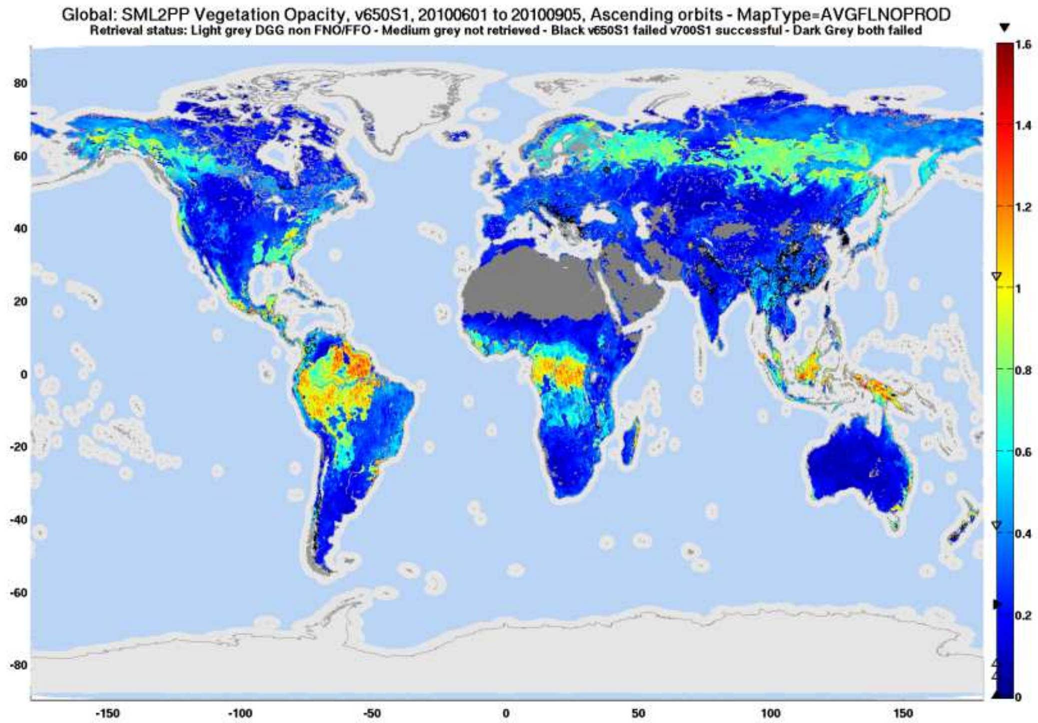

Figure 72: Reprocessing instance S1; Global map time average of retrieved v650 retrieved VOD. Black dots, mean systematic v650 failures while v700 report at least one valid.

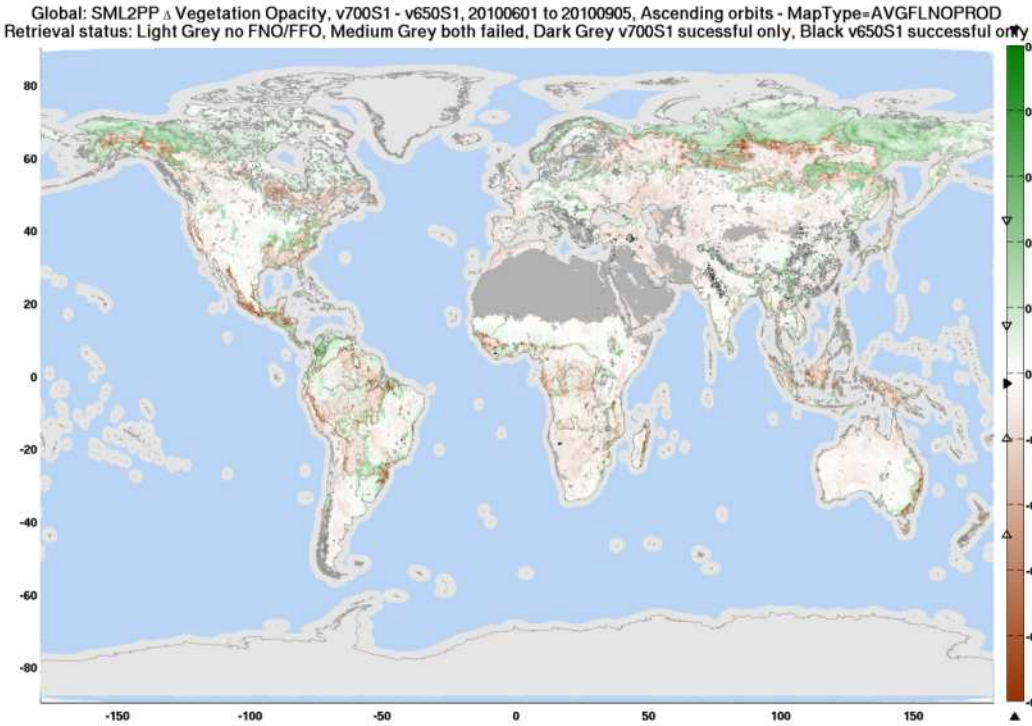

Figure 73: Reprocessing instance S1; Global map time average of differences of v700 retrieved VOD minus v650 retrieved VOD.

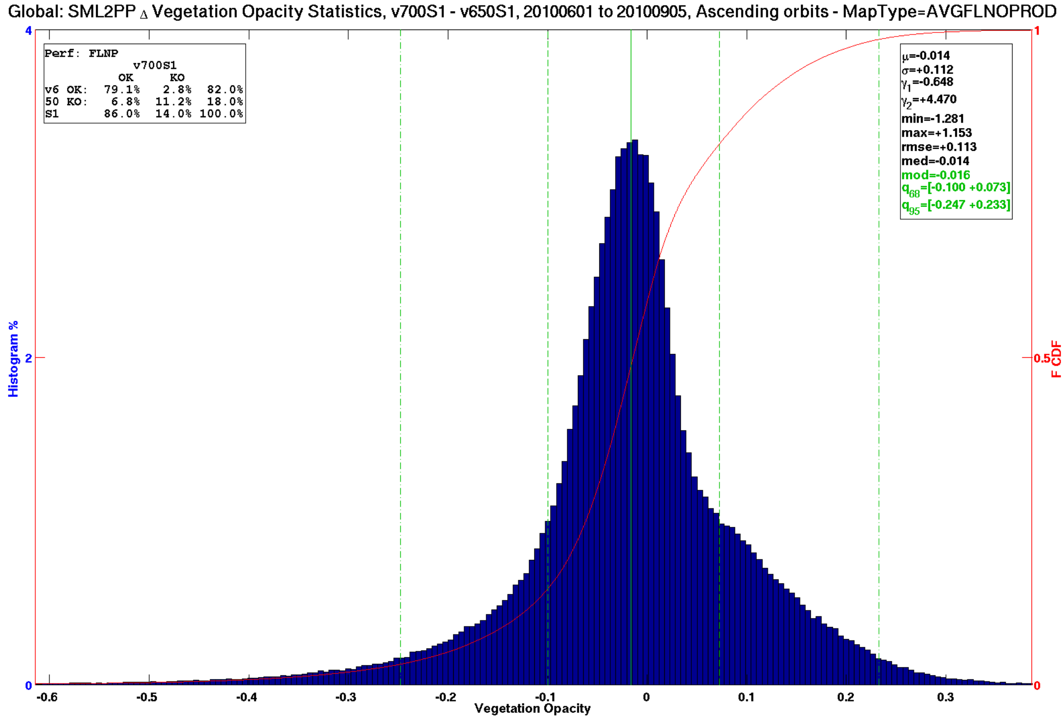

Figure 74: Reprocessing instance S1; Global histogram, cdf and stats of differences of v700 retrieved VOD minus v650 retrieved VOD.

4.3.2.2.3 S2: 20140201 – 20140524

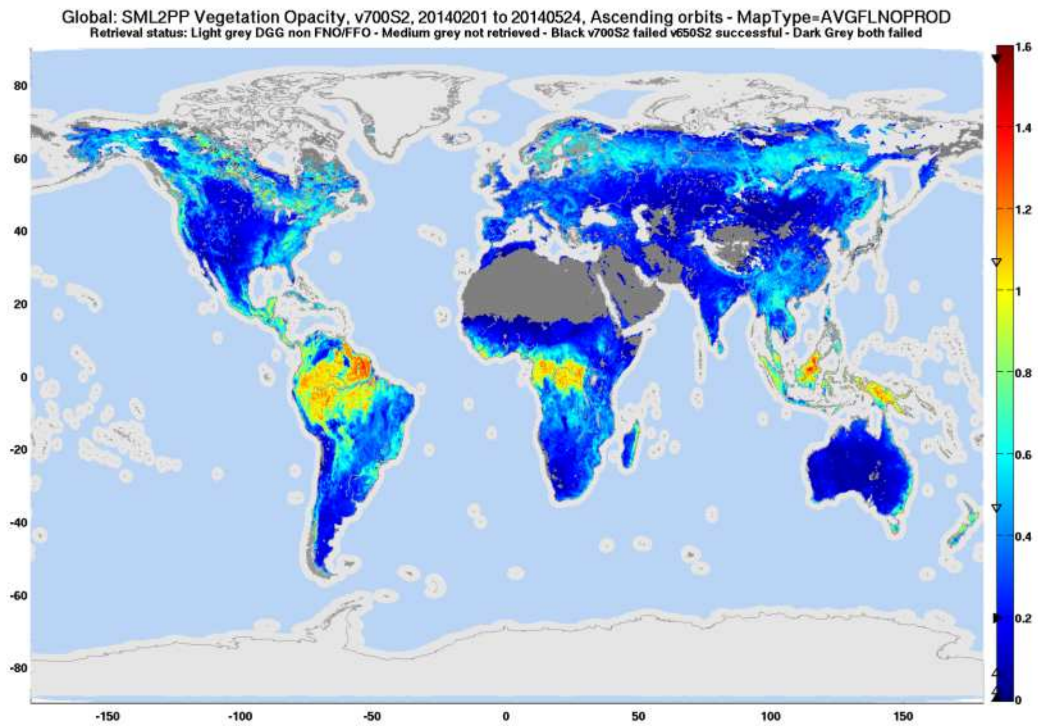

Figure 75: Reprocessing instance S2; Global map time average of retrieved v700 retrieved VOD. Black dots, mean systematic v700 failures while v650 report at least one valid.

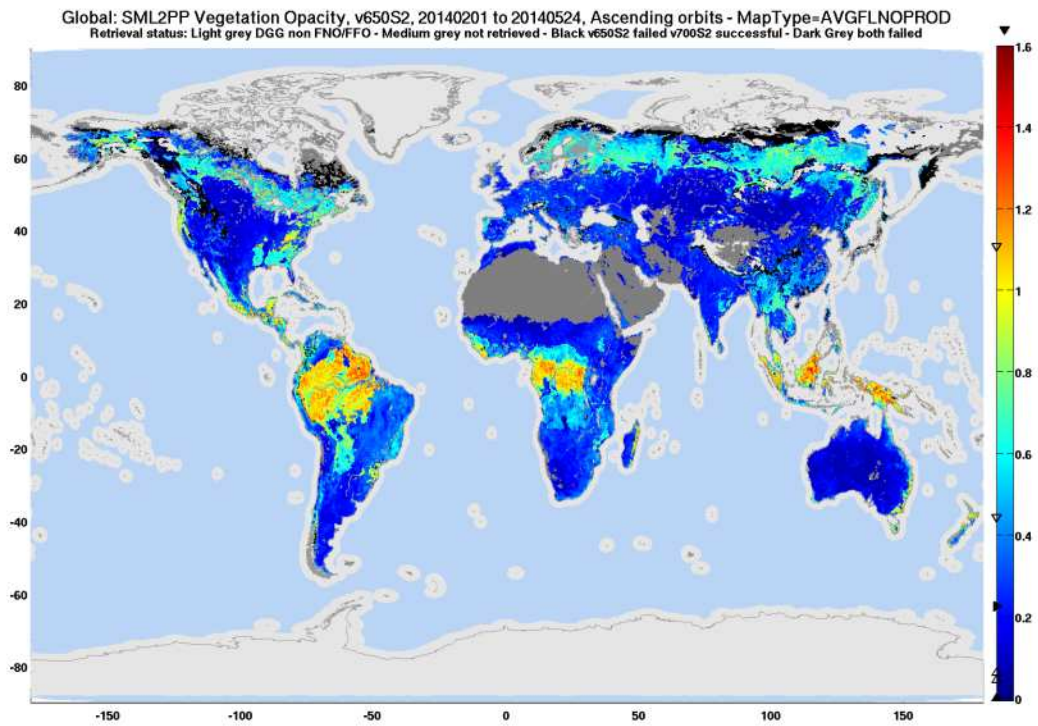

Figure 76: Reprocessing instance S2; Global map time average of retrieved v650 retrieved VOD. Black dots, mean systematic v650 failures while v700 report at least one valid.

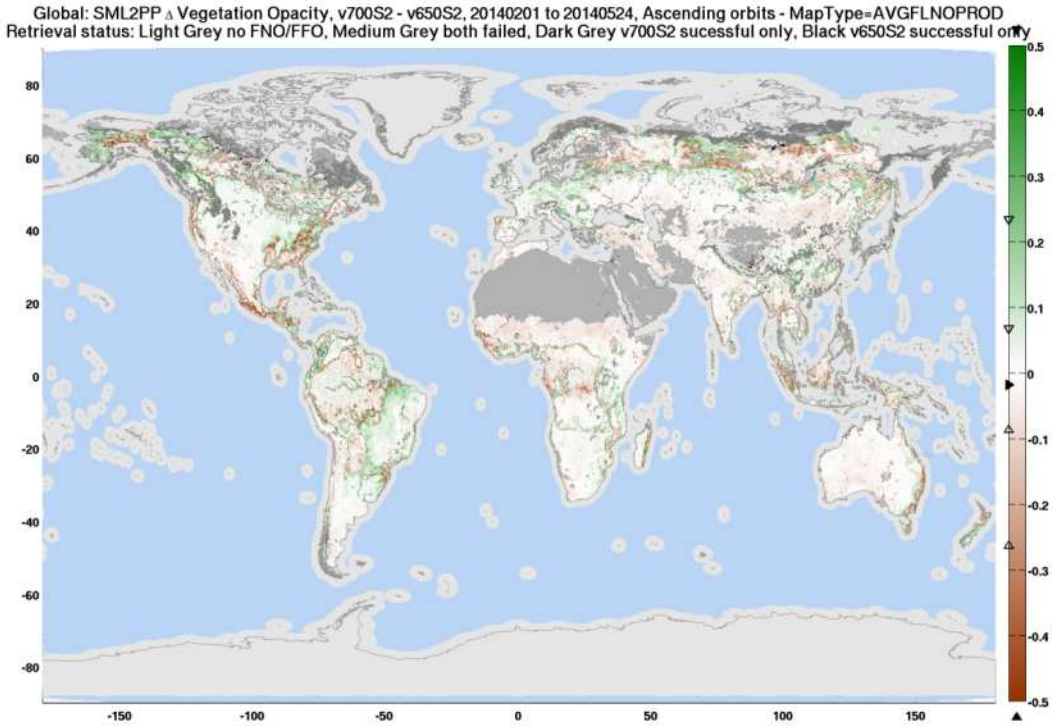

Figure 77: Reprocessing instance S2; Global map time average of differences of v700 retrieved VOD minus v650 retrieved VOD.

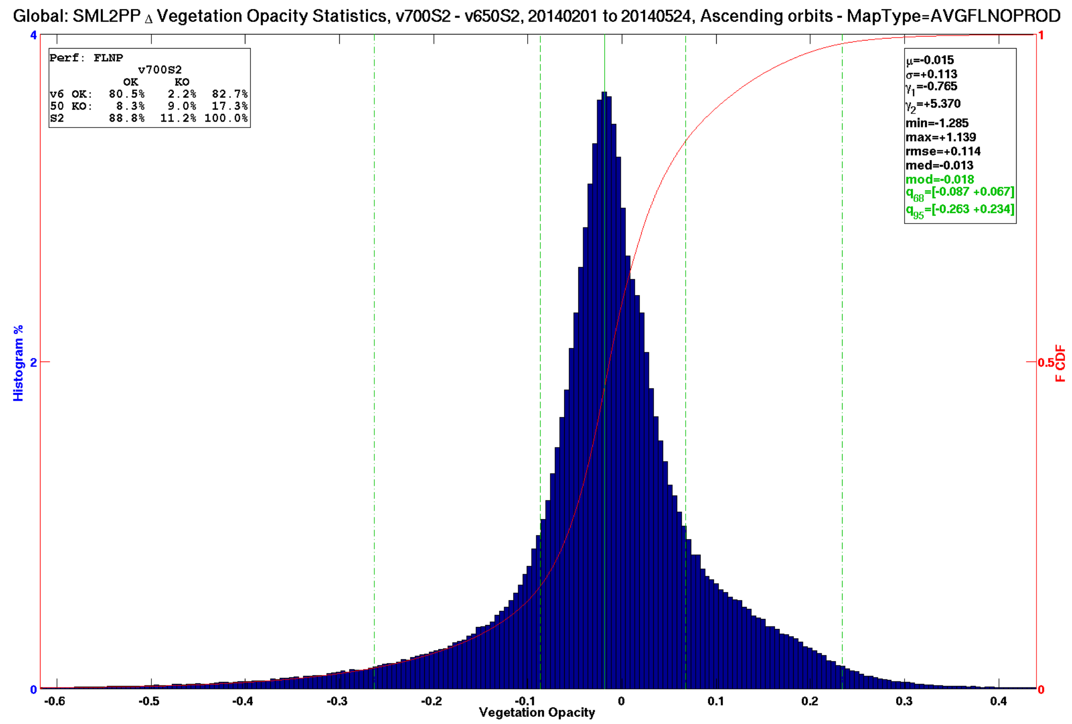

Figure 78: Reprocessing instance S2; Global histogram, cdf and stats of differences of v700 retrieved VOD minus v650 retrieved VOD.

4.3.2.2.4 S3: 20180201 – 20180414

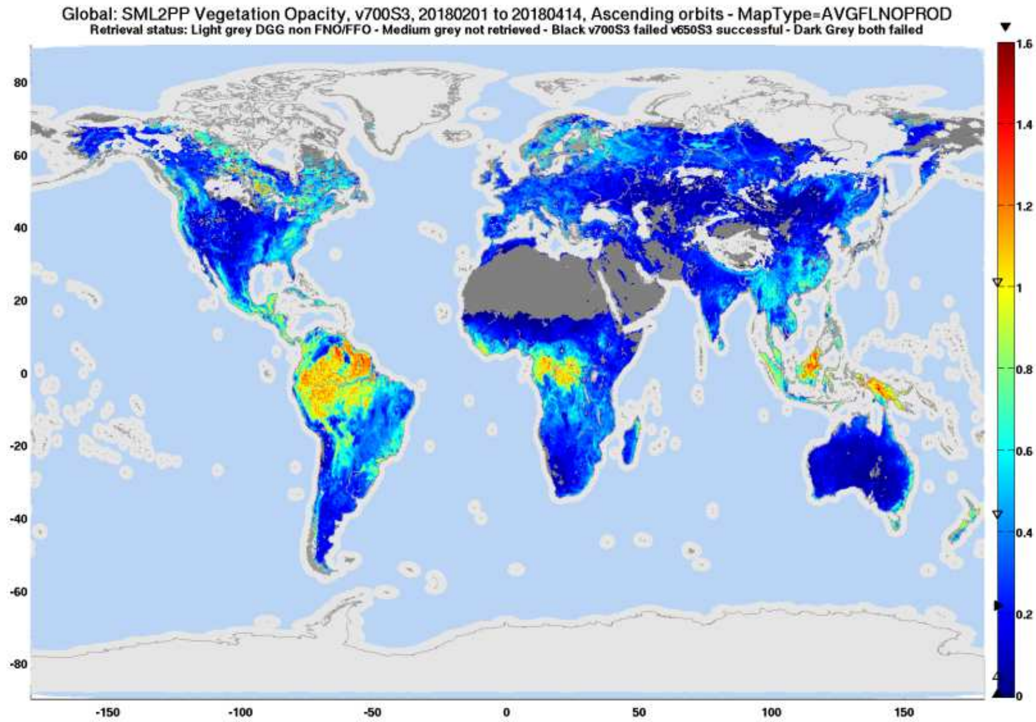

Figure 79: Reprocessing instance S3; Global map time average of retrieved v700 retrieved VOD. Black dots, mean systematic v700 failures while v650 report at least one valid.

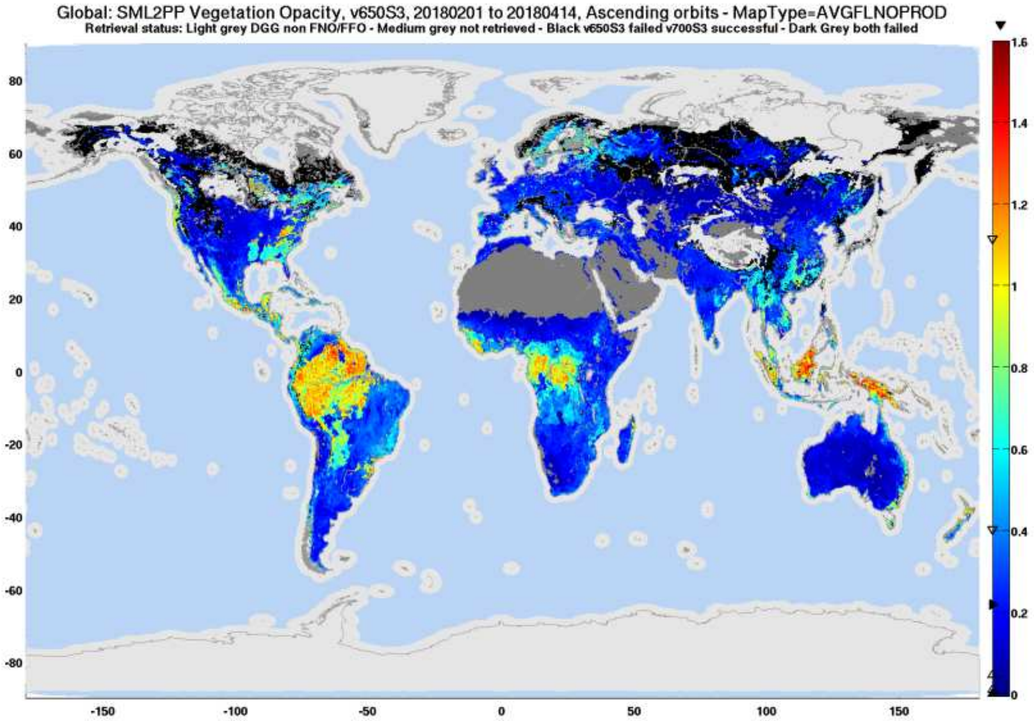

Figure 80: Reprocessing instance S3; Global map time average of retrieved v650 retrieved VOD. Black dots, mean systematic v650 failures while v700 report at least one valid.

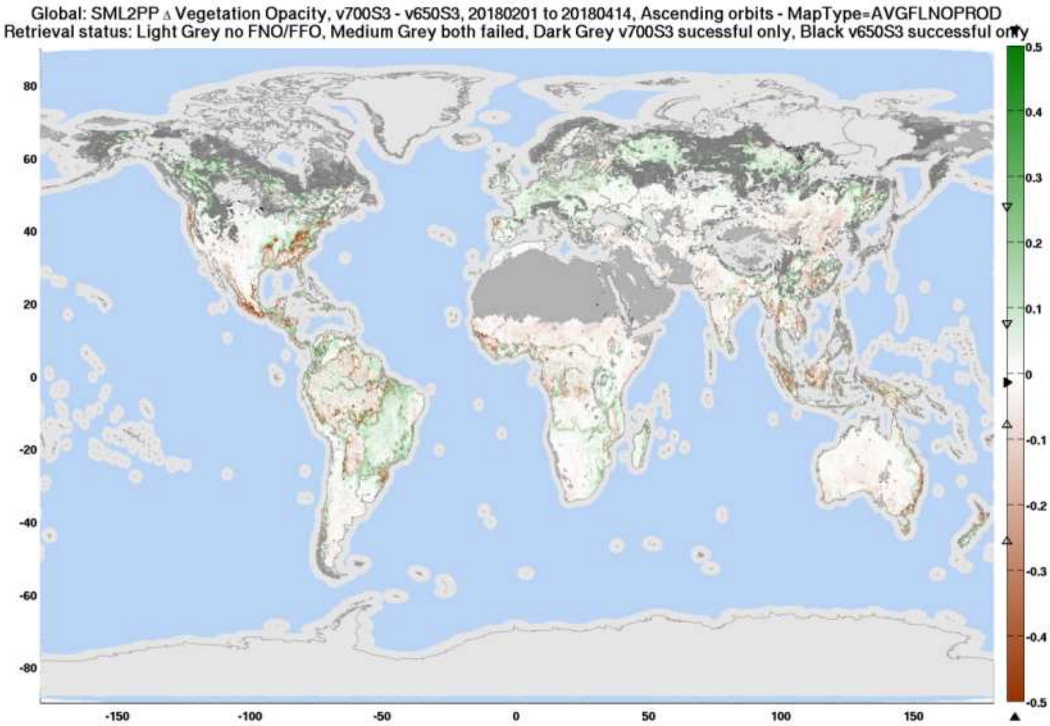

Figure 81: Reprocessing instance S3; Global map time average of differences of v700 retrieved VOD minus v650 retrieved VOD.

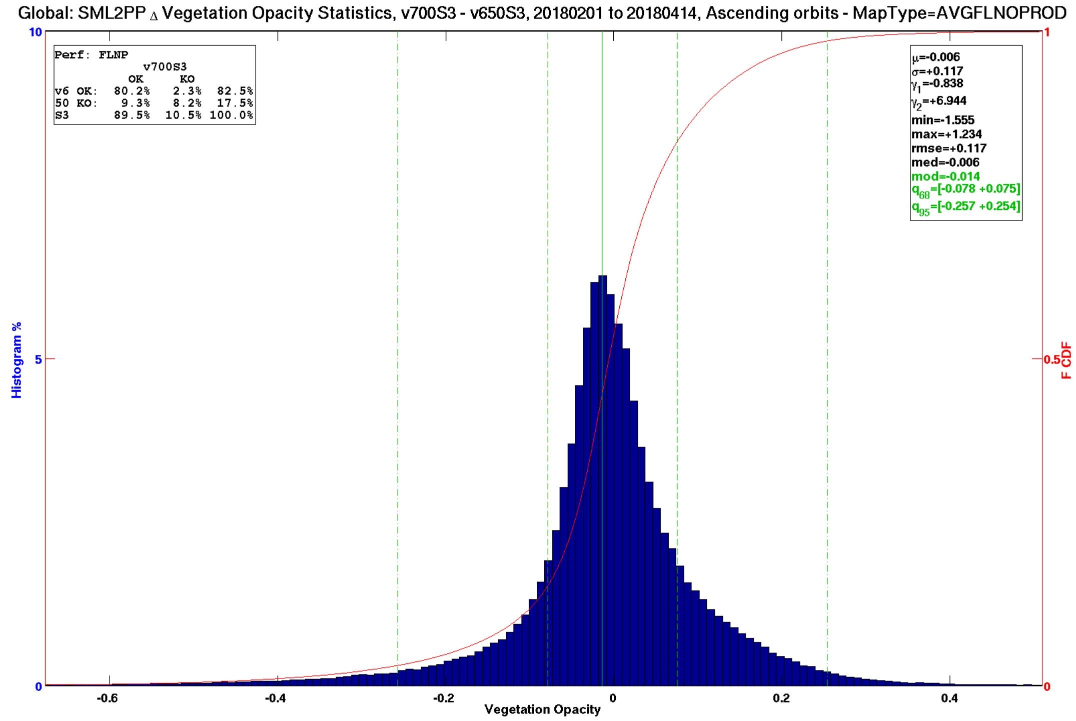

Figure 82: Reprocessing instance S3; Global histogram, cdf and stats of differences of v700 retrieved VOD minus v650 retrieved VOD.

4.3.2.3 RETRIEVED CHI2

Comparing the Chi2 between v700 and v650 is not that easy for two reasons. Despite the post retrieval Chi2 rescaling coefficient used for v650 and the optimal value obtained for σ_{IRE} appeared to be consistent, the v700 introduce a different (bigger) normalization. Secondly, the L1C 724 introduce changes particularly due to Gibbs2 (reducing the Chi2 toward the water body mass). We observe a strong signature on Chi2 ratio maps; from more neutral white inland toward blue (reduced) Chi2 approaching to water masses. It could be the Gibbs2 effect we never observed so well thanks to the 10 years of data.

The second important effect is RFI. Chi2 is very sensitive to RFI and for both versions it is the main big feature of Chi2 drop we can observe on maps. However, if mostly v700 has lower Chi2 or equivalent than v650 it is not the case over RFI areas where actually it is the opposite. All in one it is rather a good thing though it is not well understood.

4.3.2.3.1 Whole REPR period 201006 – 20210131

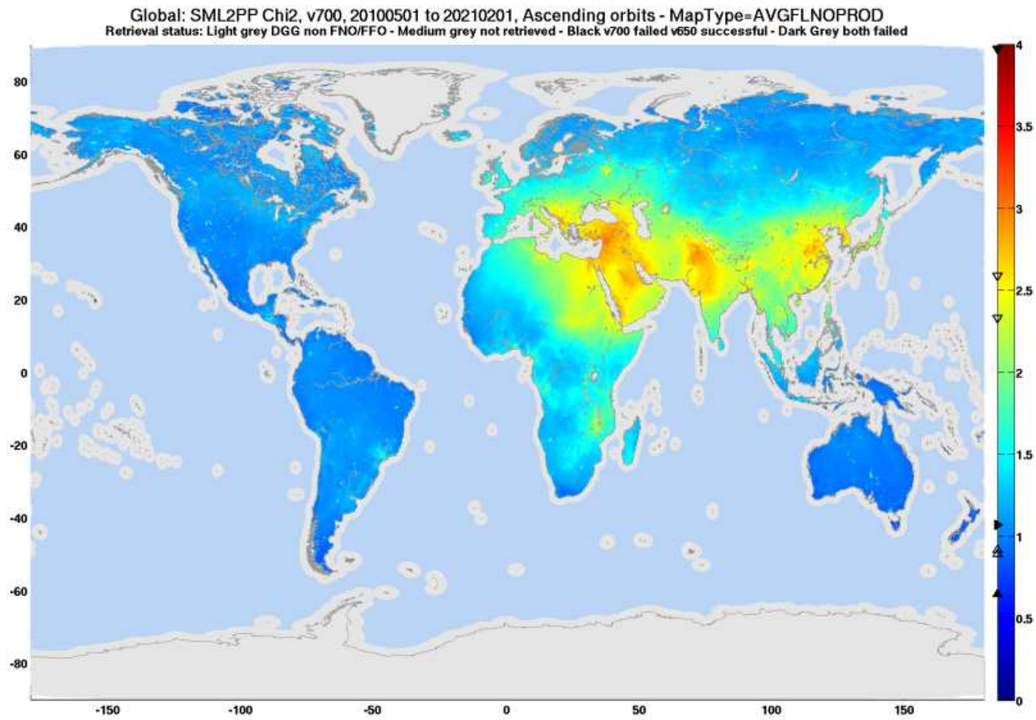

Figure 83: Whole reprocessing 20100501 - 20210231; Global map time average of retrieved v700 Chi2. Black dots, mean systematic v700 failures while v650 report at least one valid over the period.

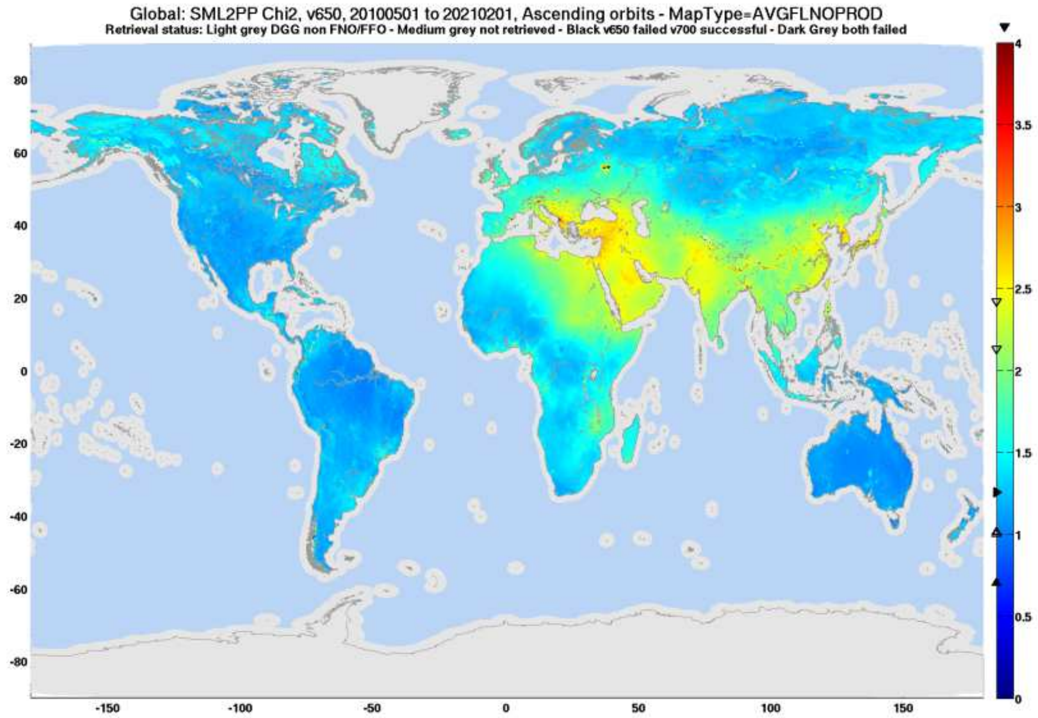

Figure 84: Whole reprocessing 20100501 - 20210231; Global map time average of retrieved v650 Chi2. Black dots, mean systematic v700 failures while v650 report at least one valid over the period.

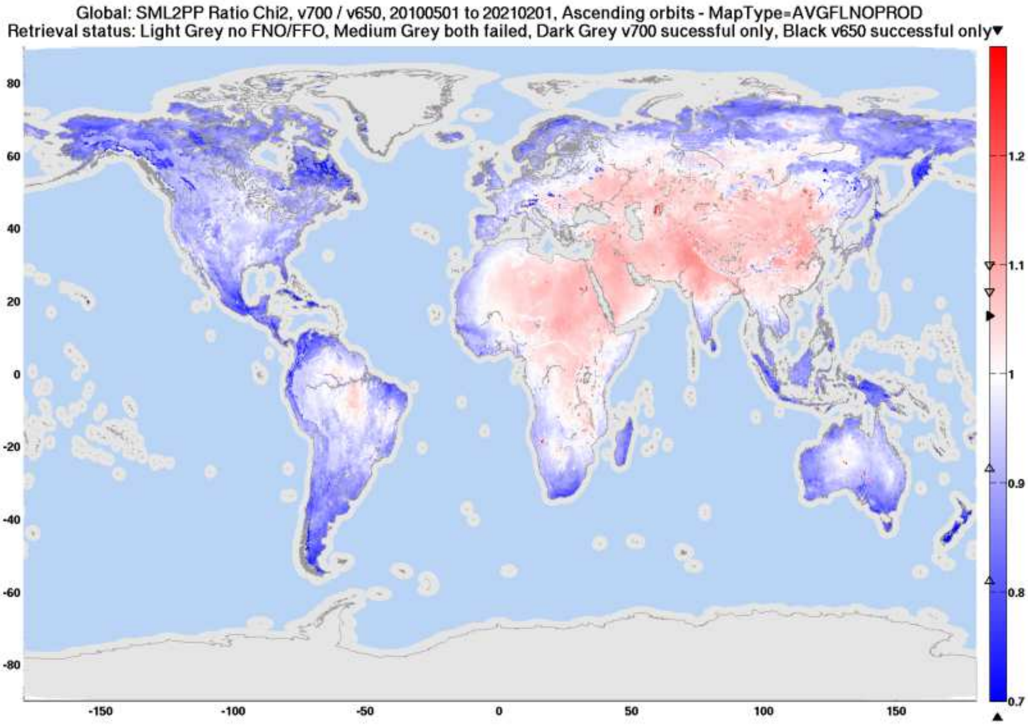

Figure 85: Whole reprocessing 20100501 - 20210231; Global map time average of retrieved Chi2 ratios ——.

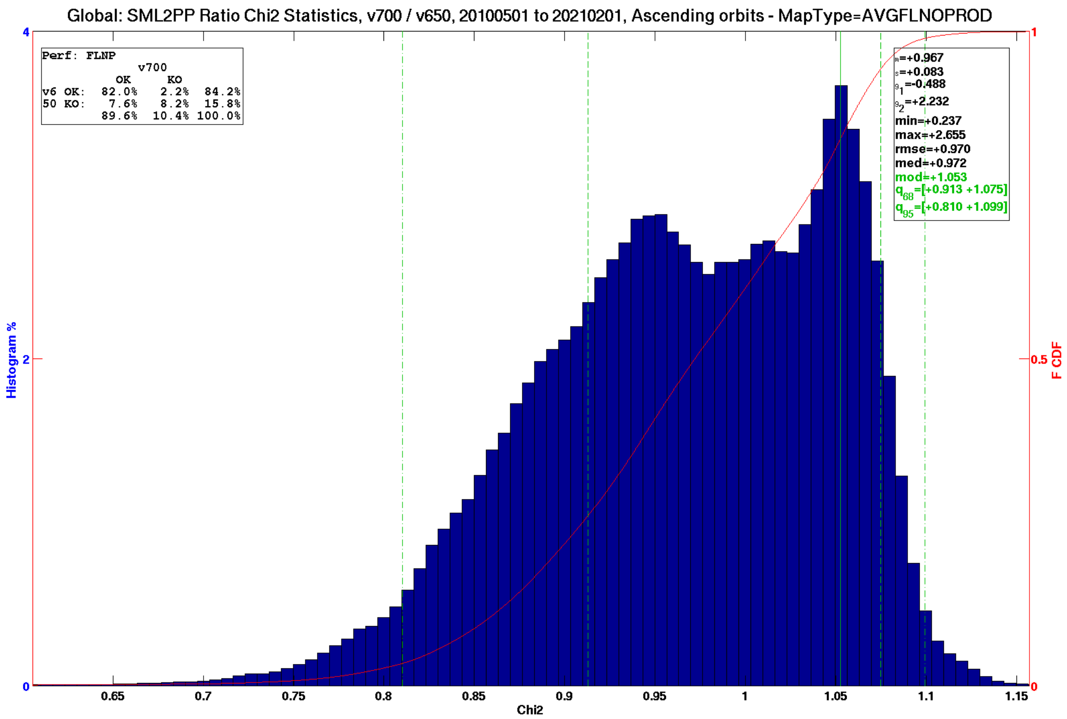

Figure 86: Whole reprocessing 20100501 - 20210231; Global histogram, cdf and stats of Chi2 ratios ——.

4.3.2.3.2 S1: 20100601 – 20100905

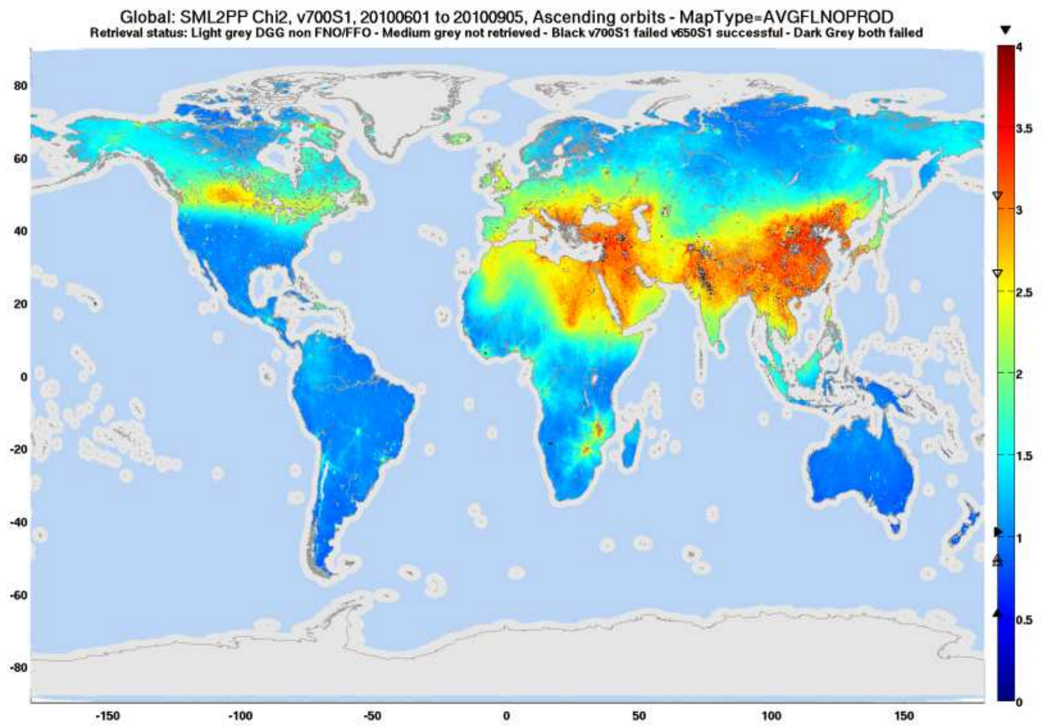

Figure 87: Reprocessing instance S1; Global map time average of retrieved v700 retrieved Chi2. Black dots, mean systematic v700 failures while v650 report at least one valid.

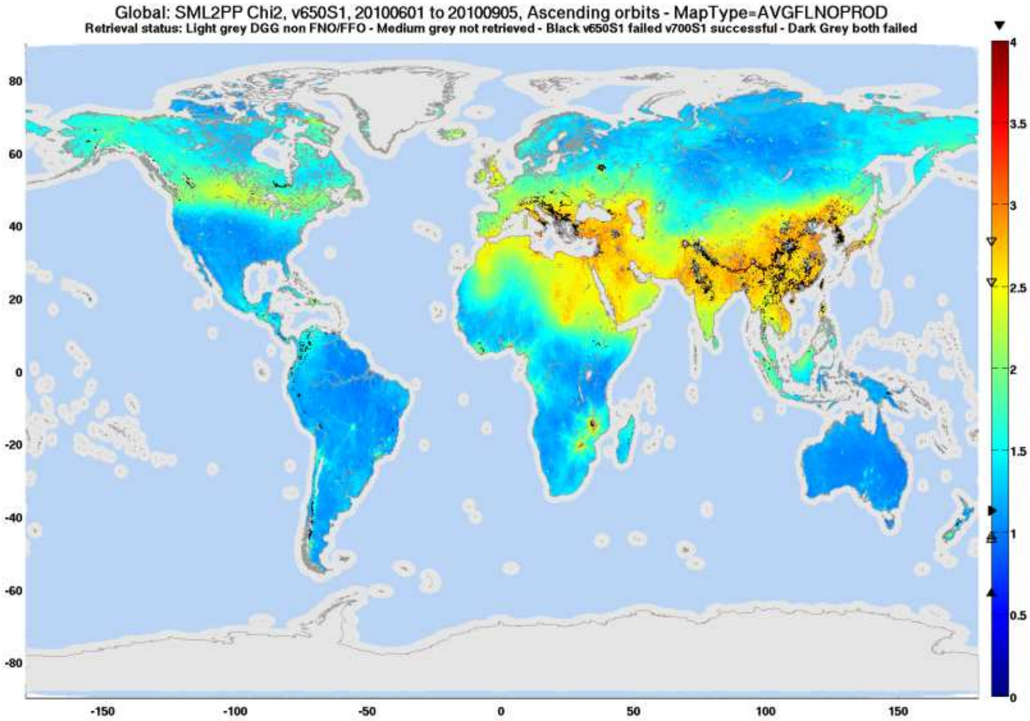

Figure 88: Reprocessing instance S1; Global map time average of retrieved v650 retrieved Chi2. Black dots, mean systematic v650 failures while v700 report at least one valid.

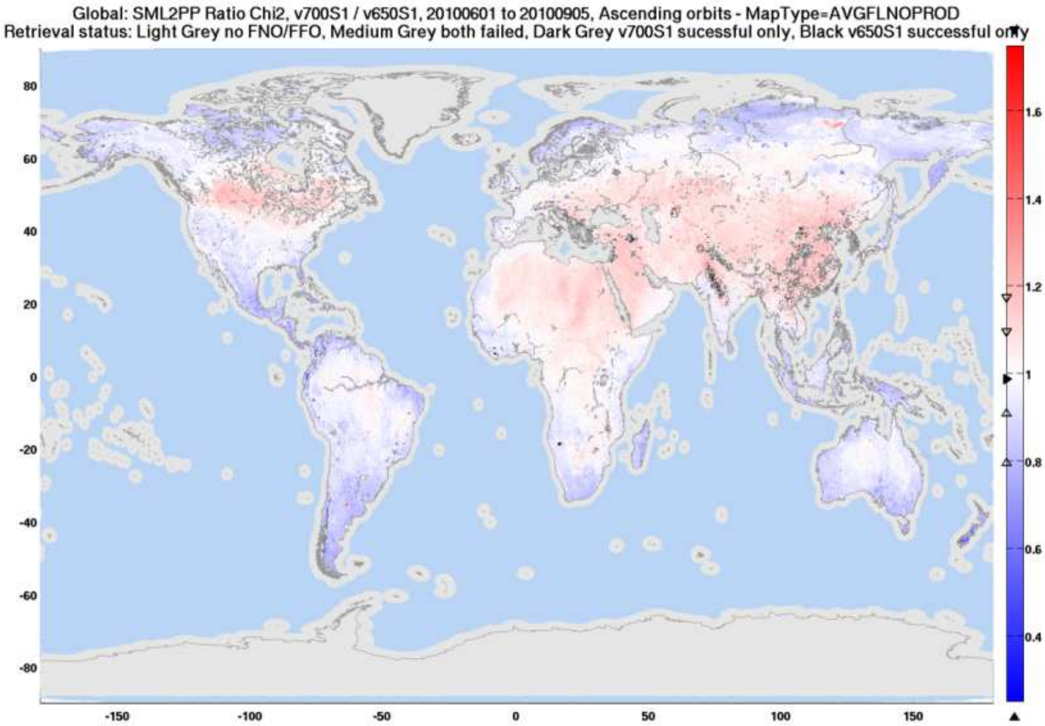

Figure 89: Reprocessing instance S1; Global map time average of retrieved Chi2 ratios ——.

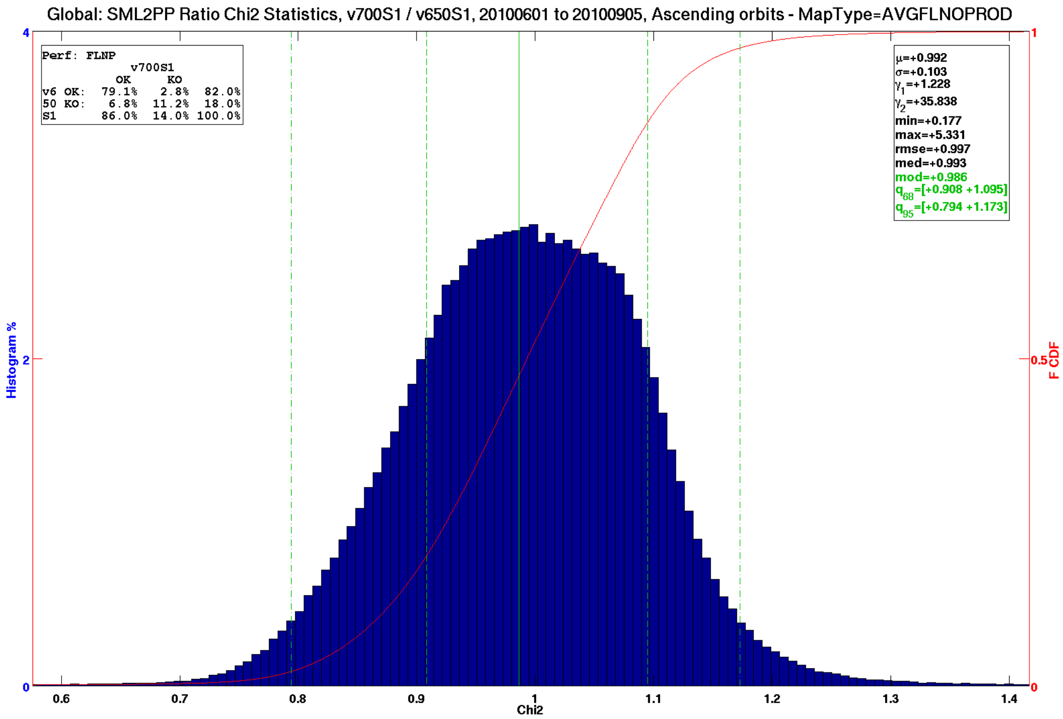

Figure 90: Reprocessing instance S1; Global histogram, cdf and stats of retrieved Chi2 ratios ——.

4.3.2.3.3 S2: 20140201 – 20140524

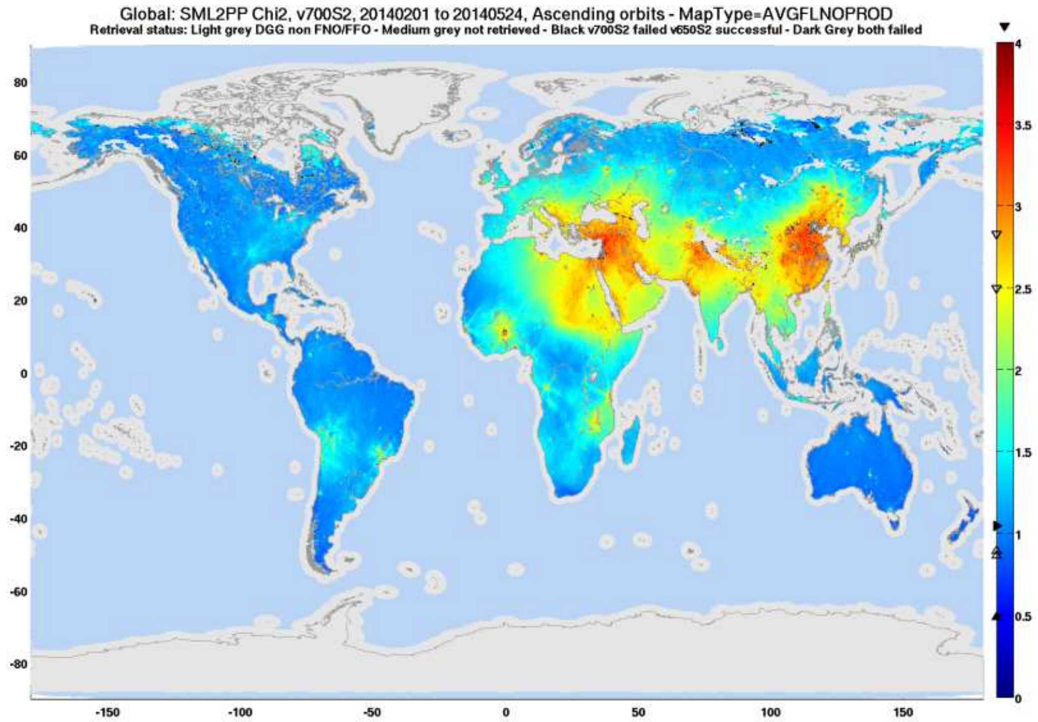

Figure 91: Reprocessing instance S2; Global map time average of retrieved v700 retrieved Chi2. Black dots, mean systematic v700 failures while v650 report at least one valid.

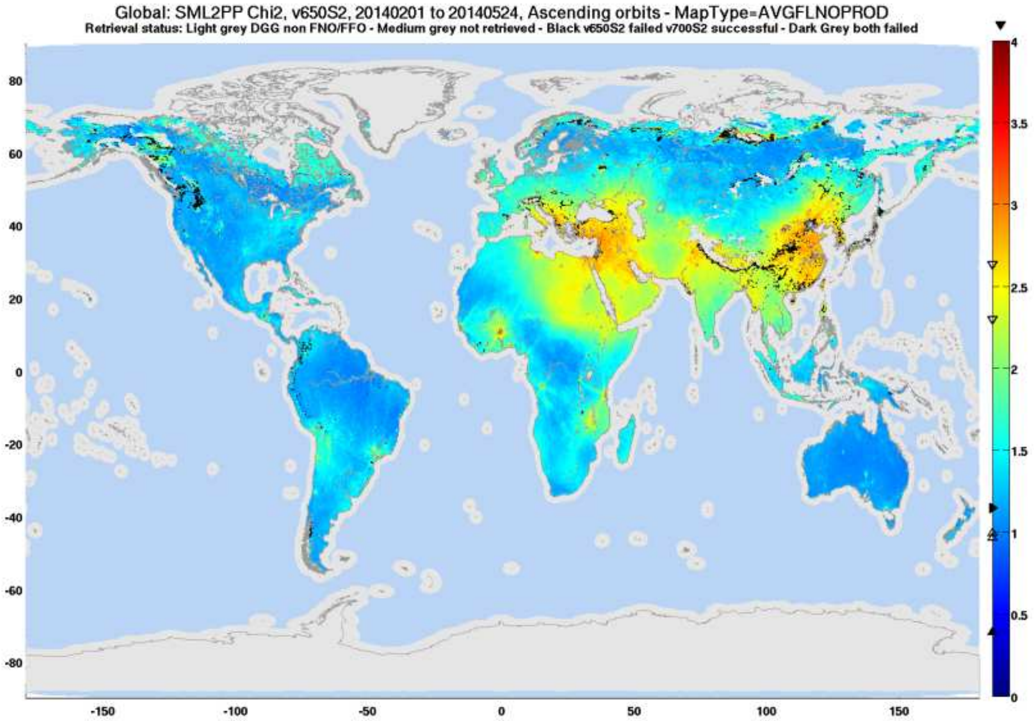

Figure 92: Reprocessing instance S2; Global map time average of retrieved v650 retrieved Chi2. Black dots, mean systematic v650 failures while v700 report at least one valid.

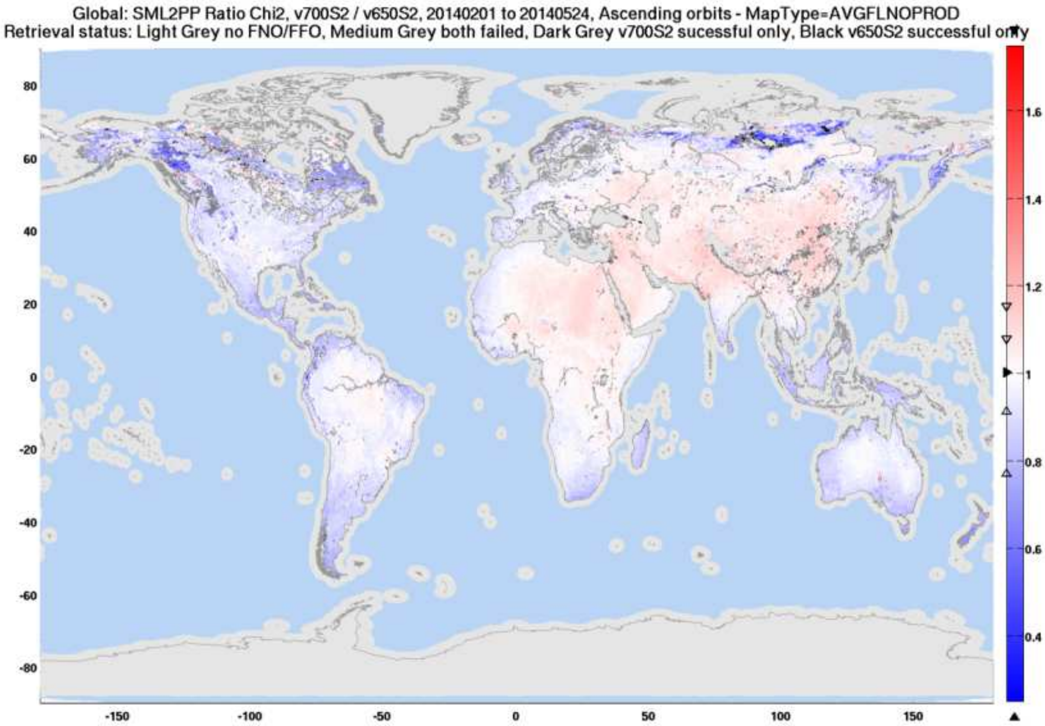

Figure 93: Reprocessing instance S2; Global map time average of retrieved Chi2 ratios ——.

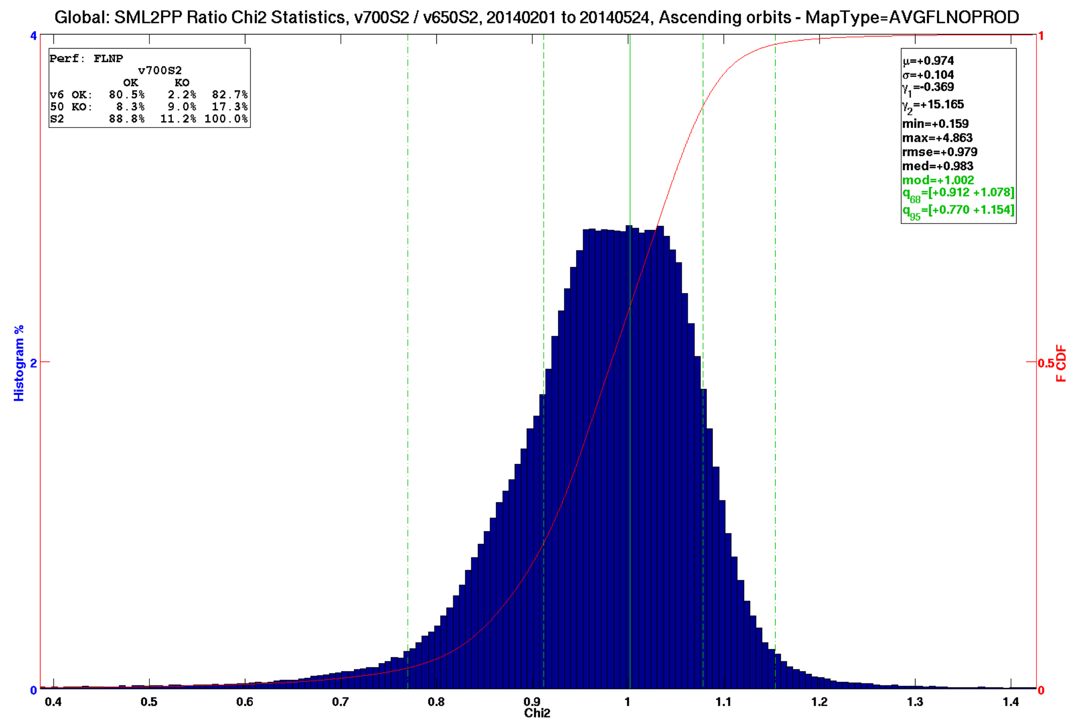

Figure 94: Reprocessing instance S2; Global histogram, cdf and stats of retrieved Chi2 ratios ____.

4.3.2.3.4 S3: 20180201 – 20180414

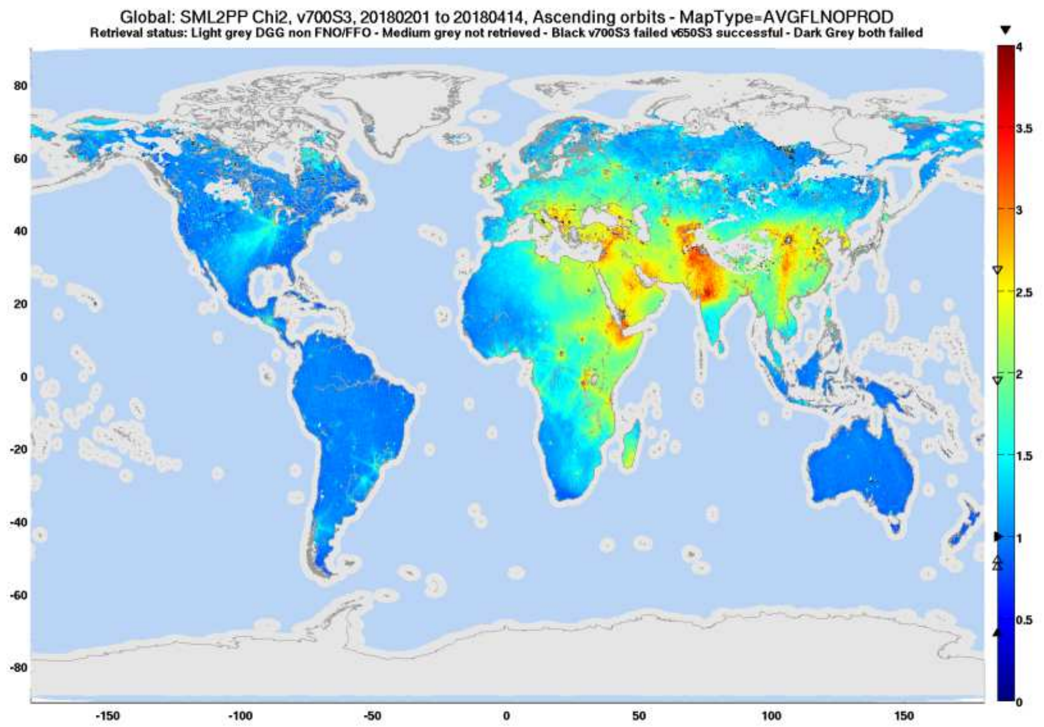

Figure 95: Reprocessing instance S3; Global map time average of retrieved v700 retrieved Chi2. Black dots, mean systematic v700 failures while v650 report at least one valid.

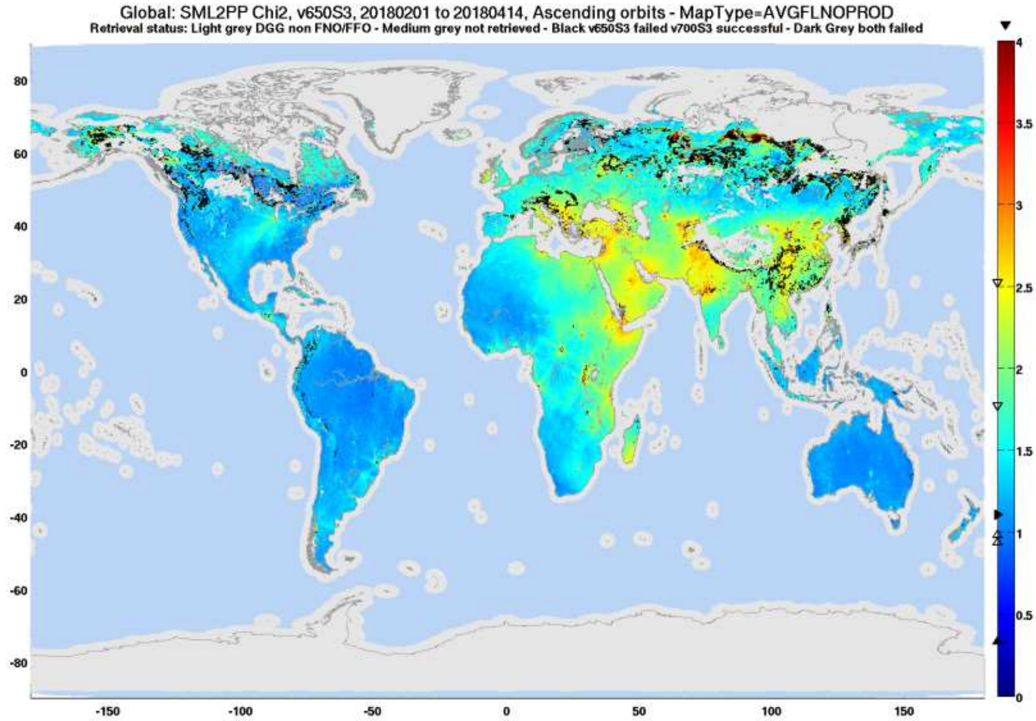

Figure 96: Reprocessing instance S3; Global map time average of retrieved v650 retrieved Chi2. Black dots, mean systematic v650 failures while v700 report at least one valid.

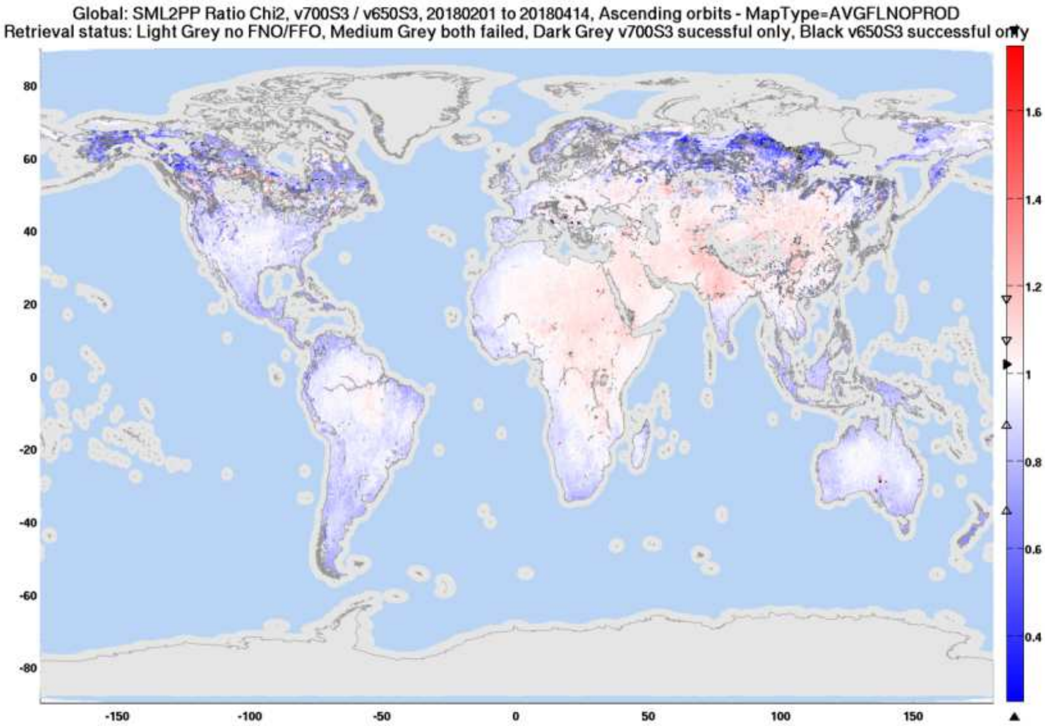

Figure 97: Reprocessing instance S3; Global map time average of retrieved Chi2 ratios ——.

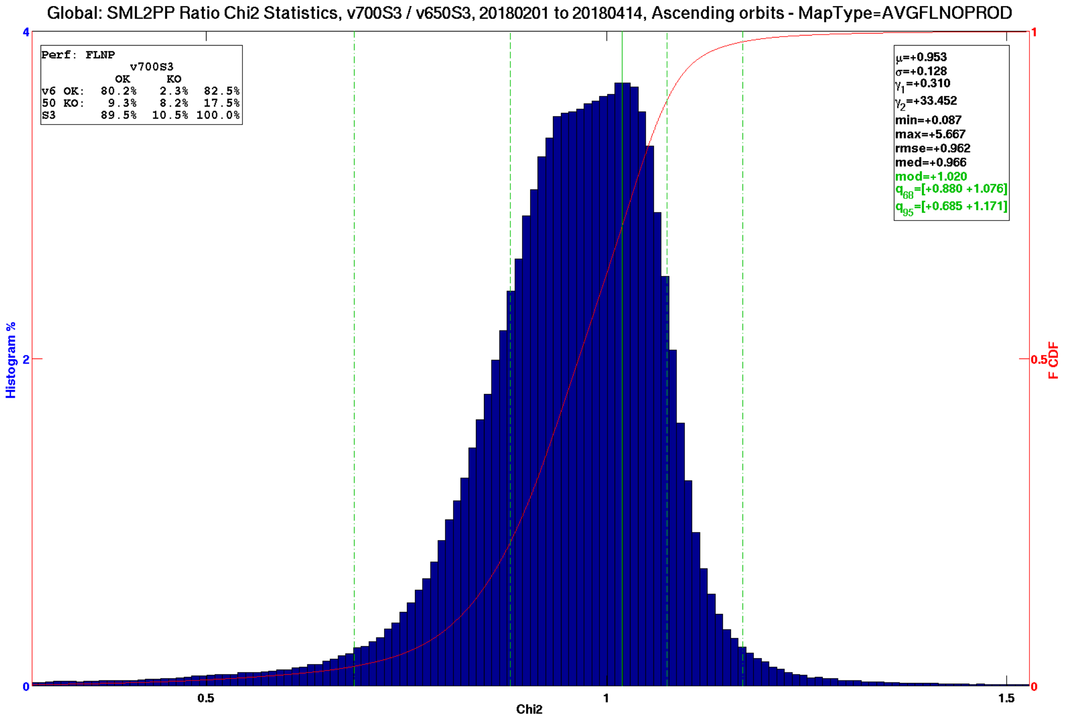

Figure 98: Reprocessing instance S3; Global histogram, cdf and stats of retrieved Chi2 ratios ——.

4.3.2.4 RFI PROBABILITY

We did not expect differences between v700 and v650 and it is mostly the case. However slight changes exist due to differences between L1C v620 and L1C v724 and potentially difference in detected outliers due to L2 changes (impacted also by L1C changes):

- L1C 724 generates on average slightly drier retrieved SM (by ~0.01 m3/m3 – 0.02 m3/m3) we could potentially expect slightly warmer BTs. Being on non RFI clean areas some BTs accepted just below threshold may become rejected using v724 => potential increase of PRFI12.
- Outliers in modeling, several changes in L2 may generates different outliers along also with L1Cs v724 BT changes – all in one it may generates less/more outliers possibly specific places (spatial patterns). Outliers in our algorithms are considered as possible low RFI impacts and are counted in the PRFI12.

4.3.2.4.1 Whole REPR period 201006 – 20210131

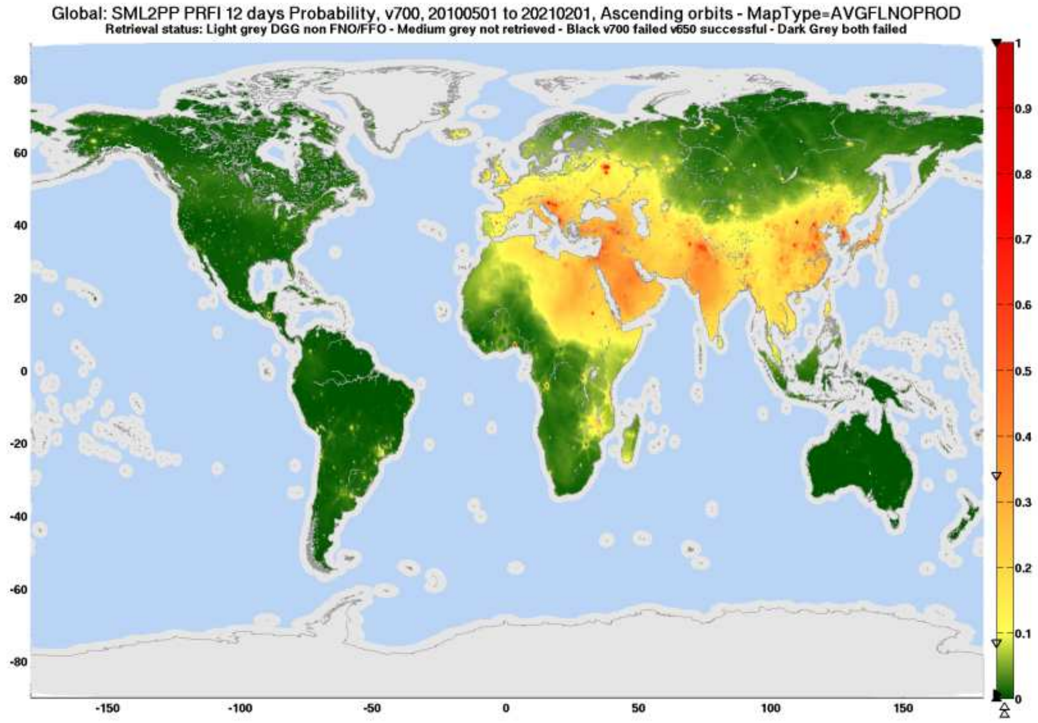

Figure 99: Whole reprocessing 20100501 - 20210231; Global map time average of v700 PRFI12.

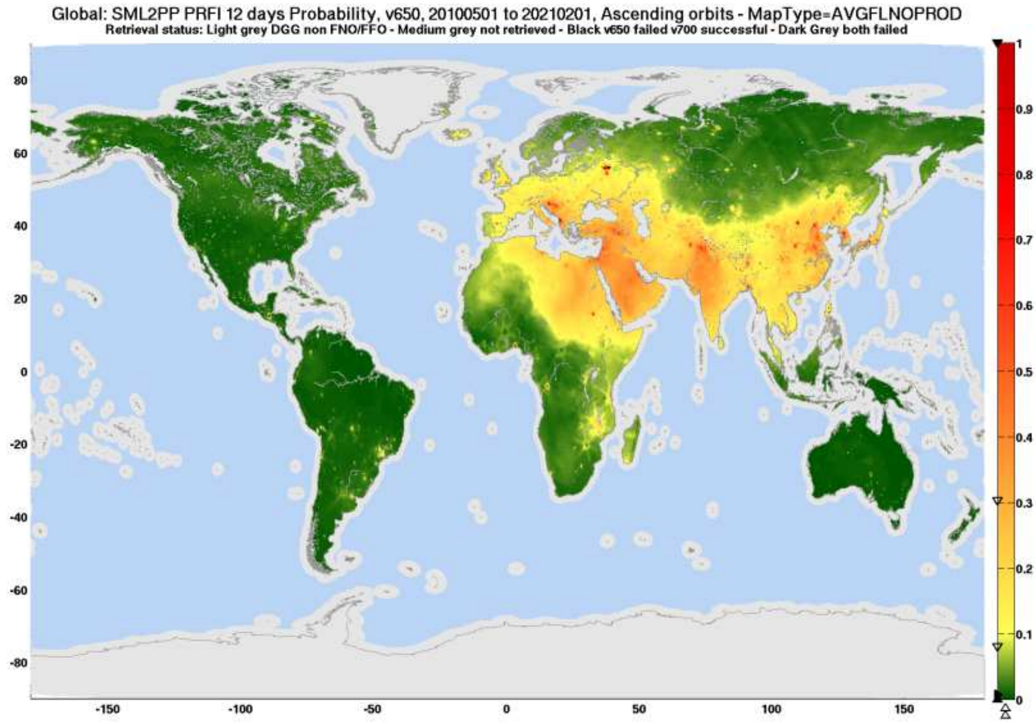

Figure 100: Whole reprocessing 20100501 - 20210231; Global map time average of v650 PRFI12.

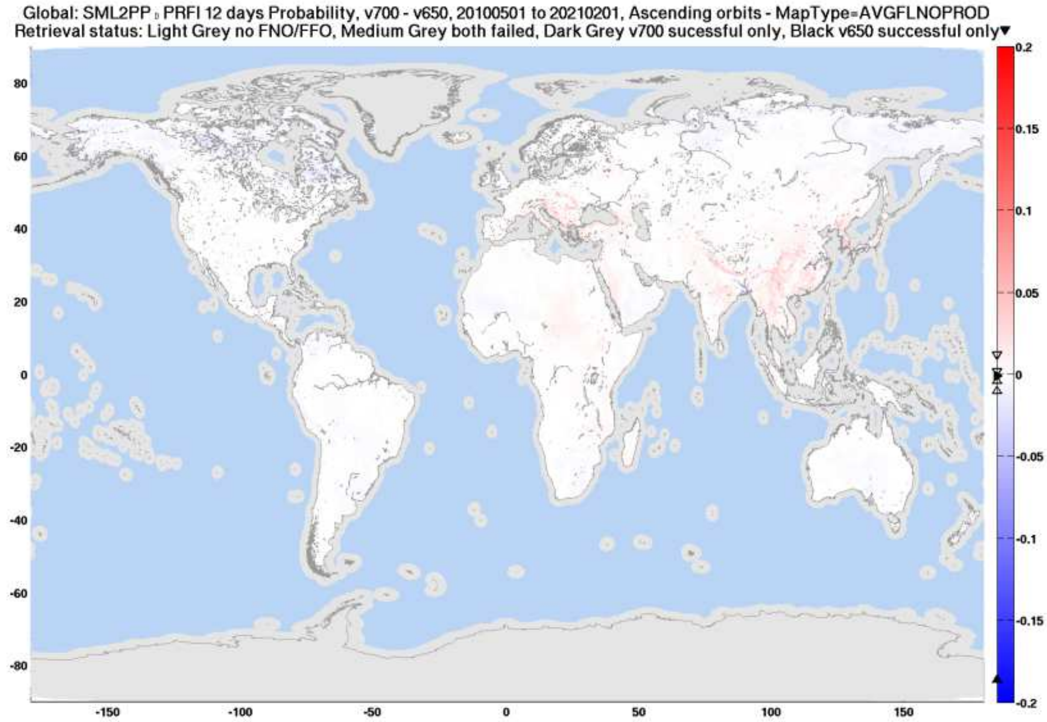

Figure 101: Whole reprocessing 20100501 - 20210231; Global map time average of difference v700 PRFI12 – v650 PRFI12.

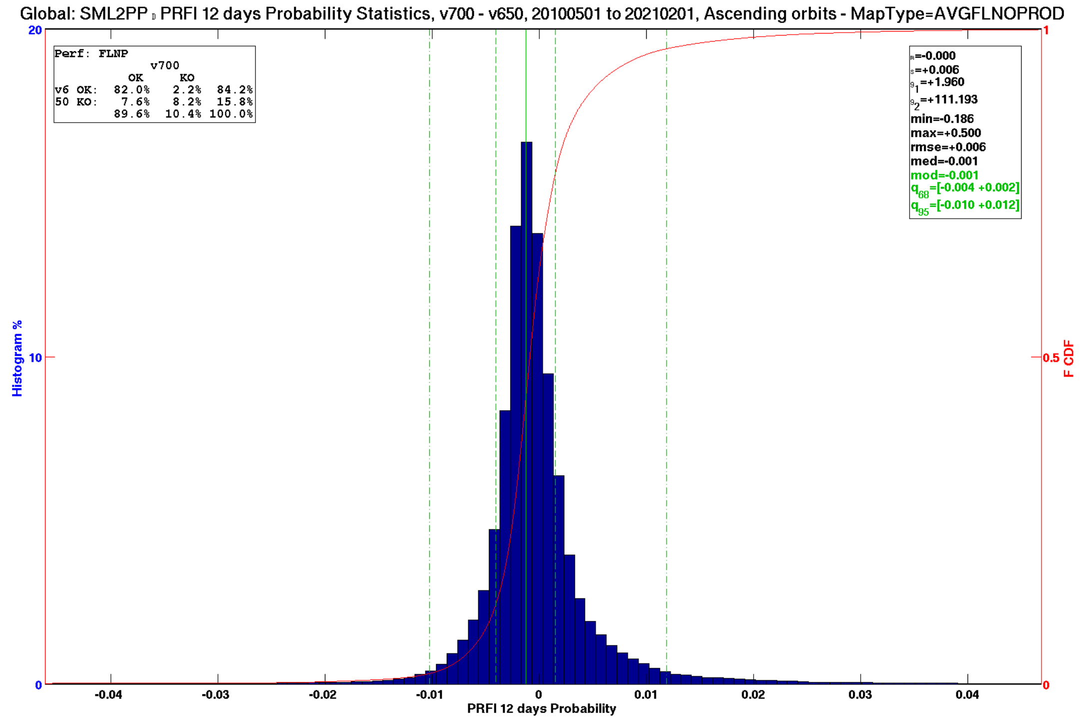

Figure 102: Whole reprocessing 20100501 - 20210231; Global histogram, cdf and stats of differences of v700 PRFI12 minus v650 PRFI12.

4.3.2.4.2 S1: 20100601 – 20100905

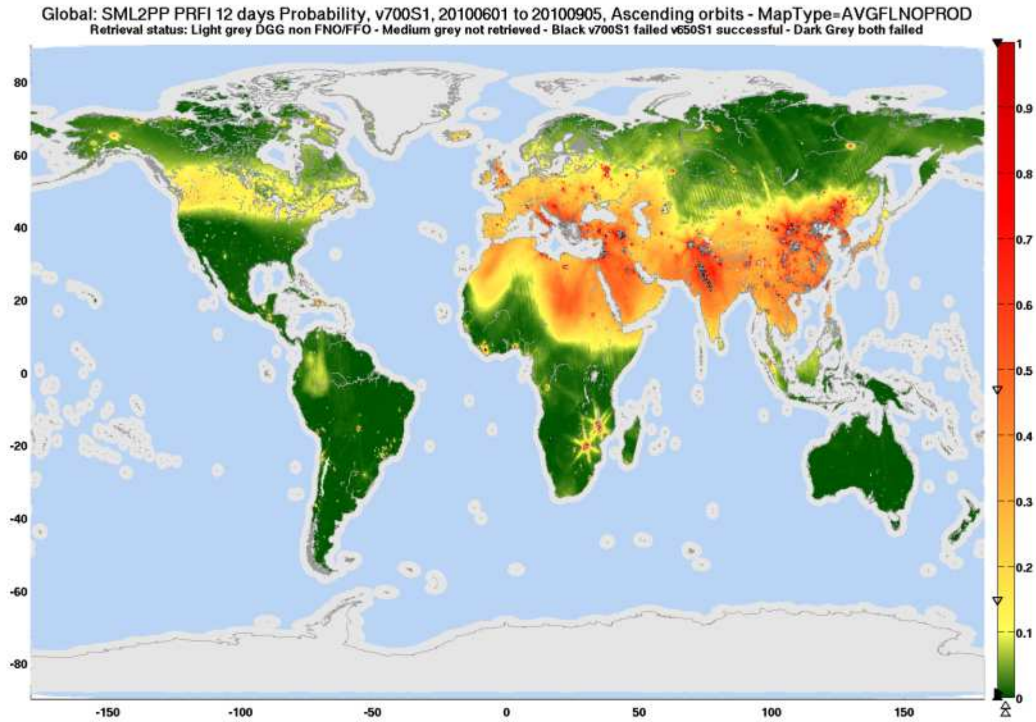

Figure 103: Reprocessing instance S1; Global map time average of v700 PRFI12.

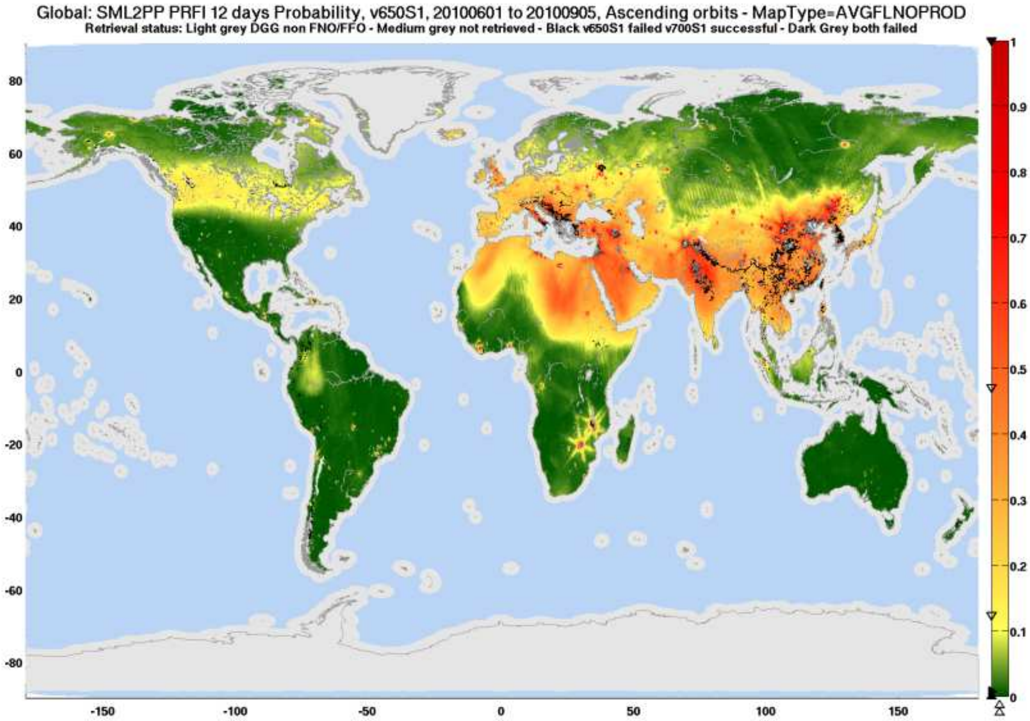

Figure 104: Reprocessing instance S1; Global map time average of v650 PRFI12.

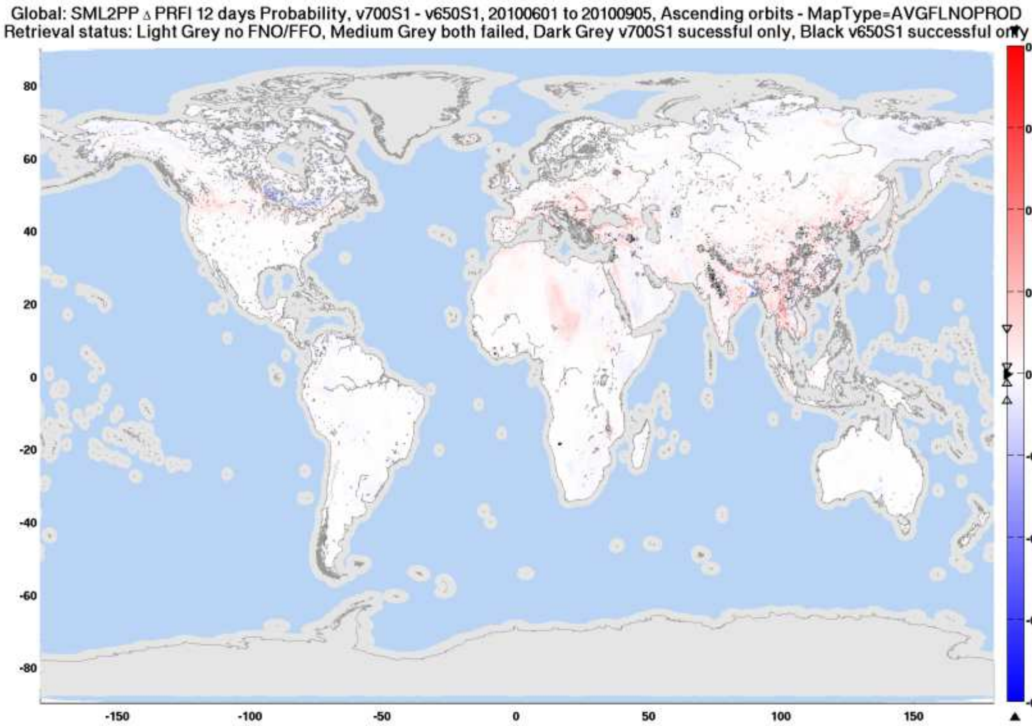

Figure 105: Reprocessing instance S1; Global map time average of v700 PRFI12 minus v650 PRFI12.

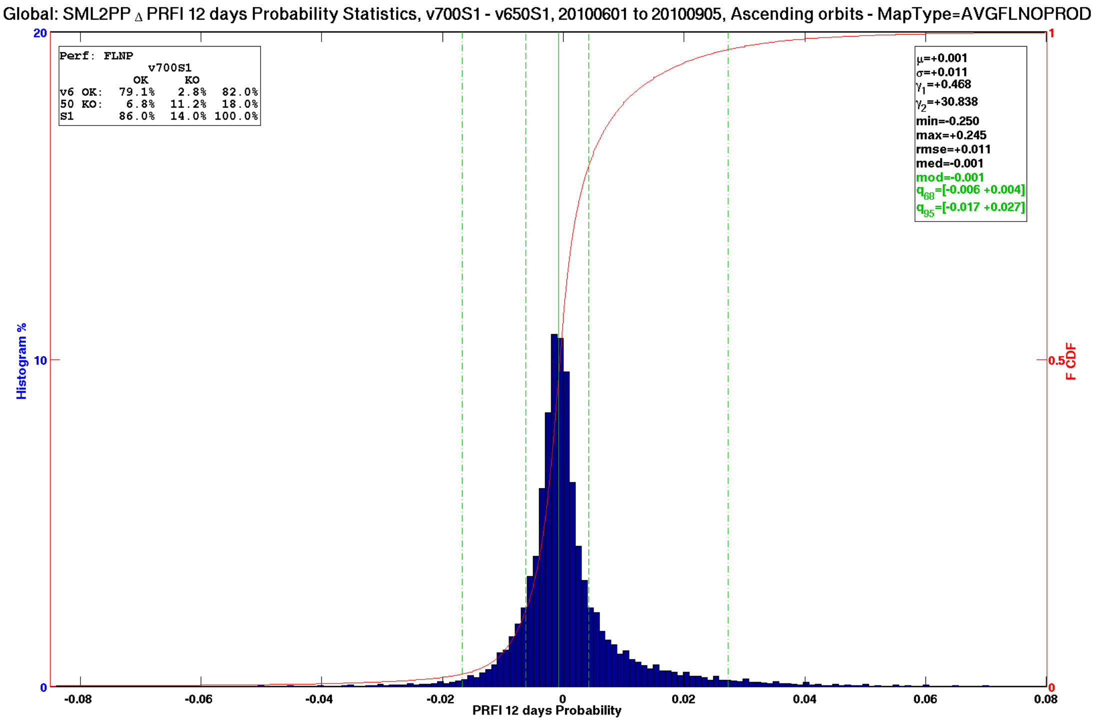

Figure 106: Reprocessing instance S1; Global histogram, cdf and stats of ratio of v700 PRFI12 minus v650 PRFI12.

4.3.2.4.3 S2: 20140201 – 20140524

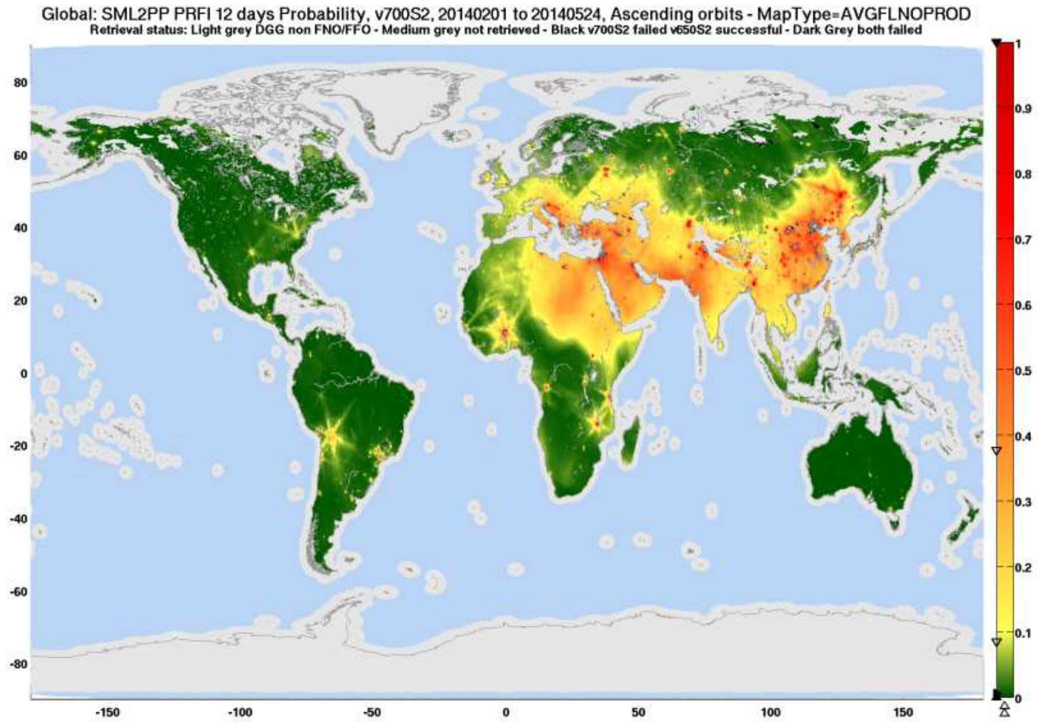

Figure 107: Reprocessing instance S2; Global map time average of v700 PRFI12.

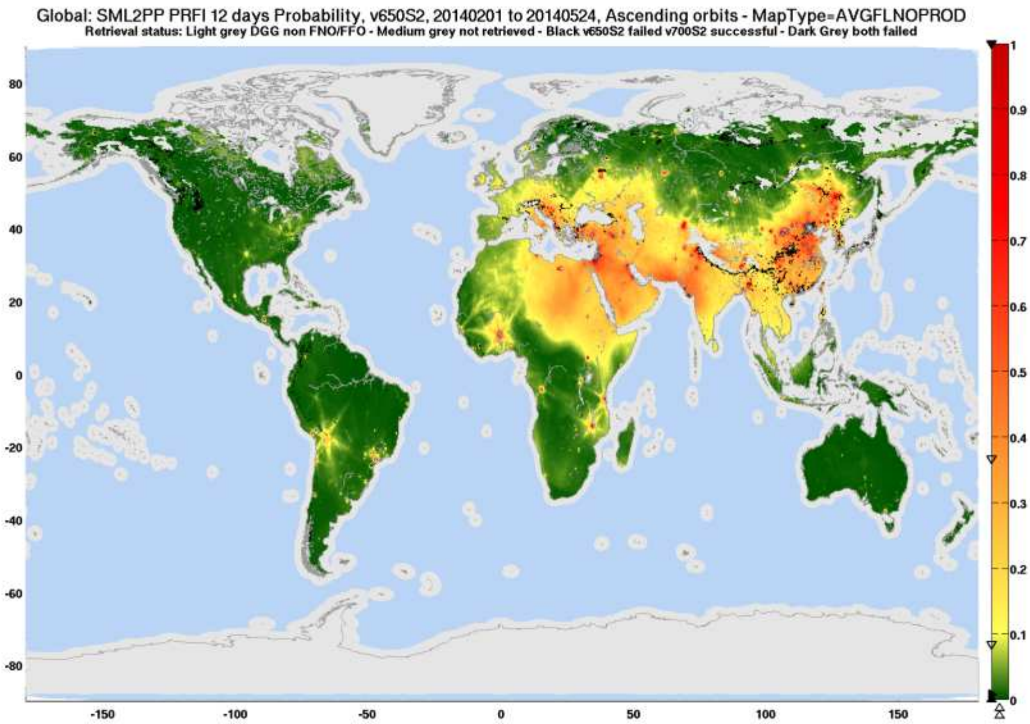

Figure 108: Reprocessing instance S2; Global map time average of v650 PRFI12.

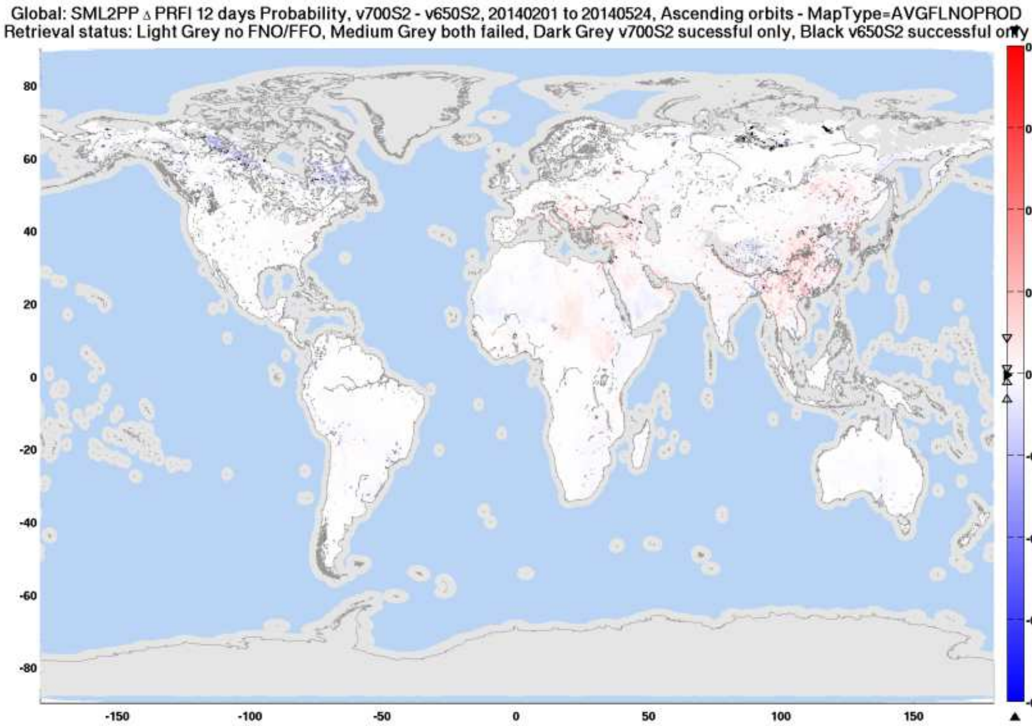

Figure 109: Reprocessing instance S2; Global map time average of v700 PRFI12 minus v650 PRFI12.

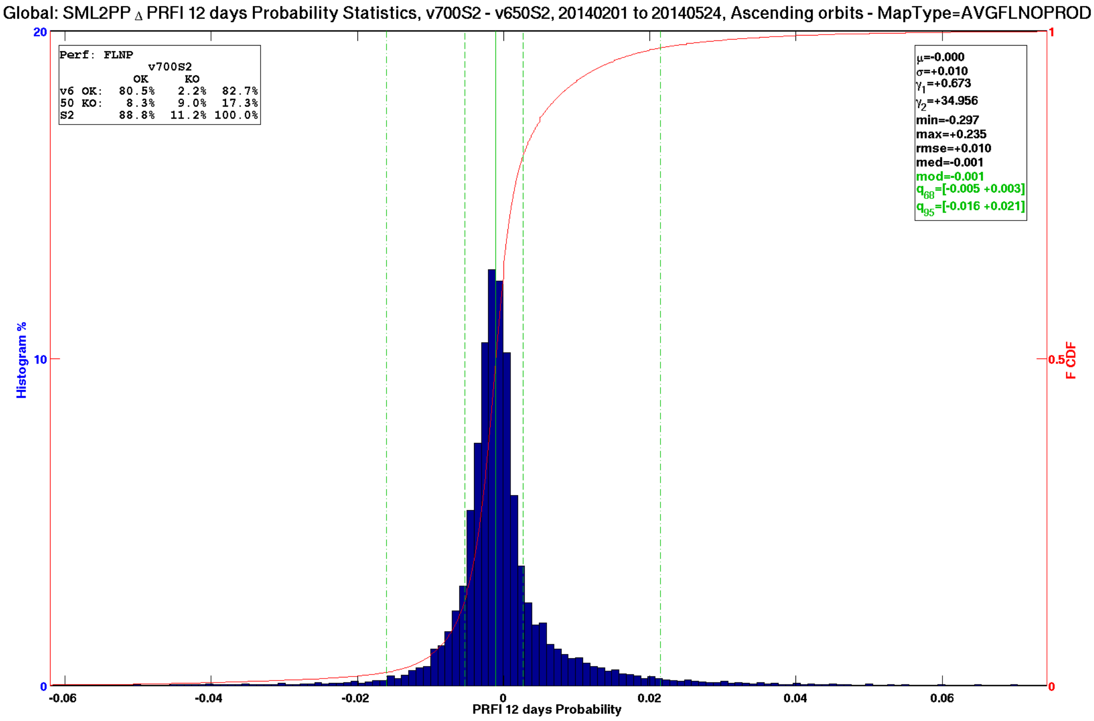

Figure 110: Reprocessing instance S2; Global histogram, cdf and stats of ratio of v700 PRFI12 minus v650 PRFI12.

4.3.2.4.4 S3: 20180201 – 20180414

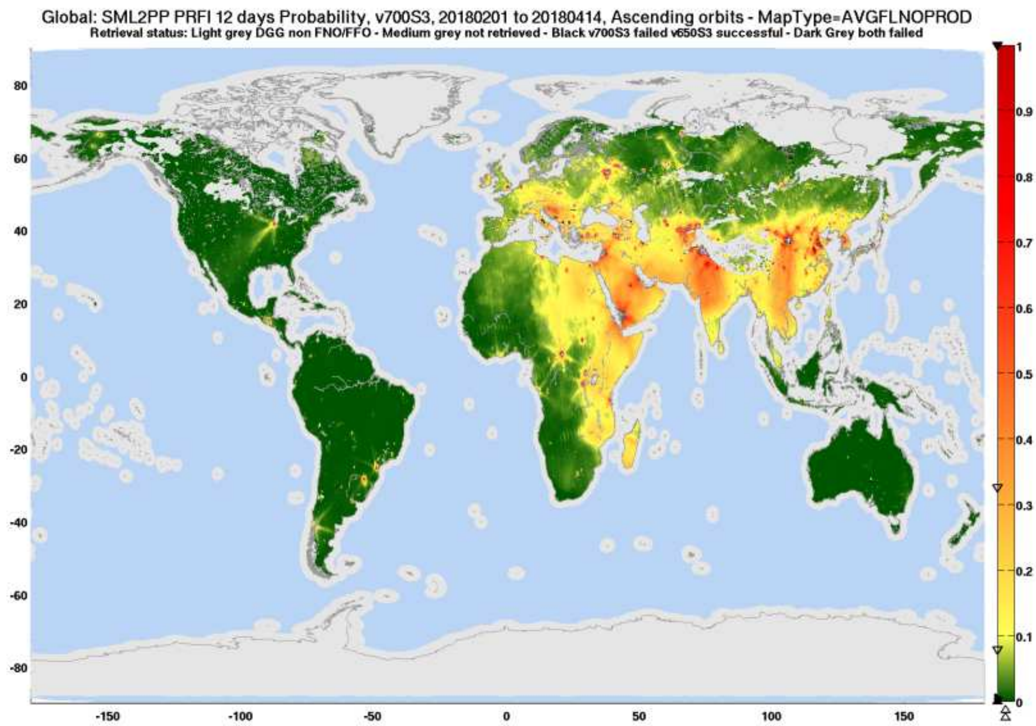

Figure 111: Reprocessing instance S3; Global map time average of v700 PRFI12.

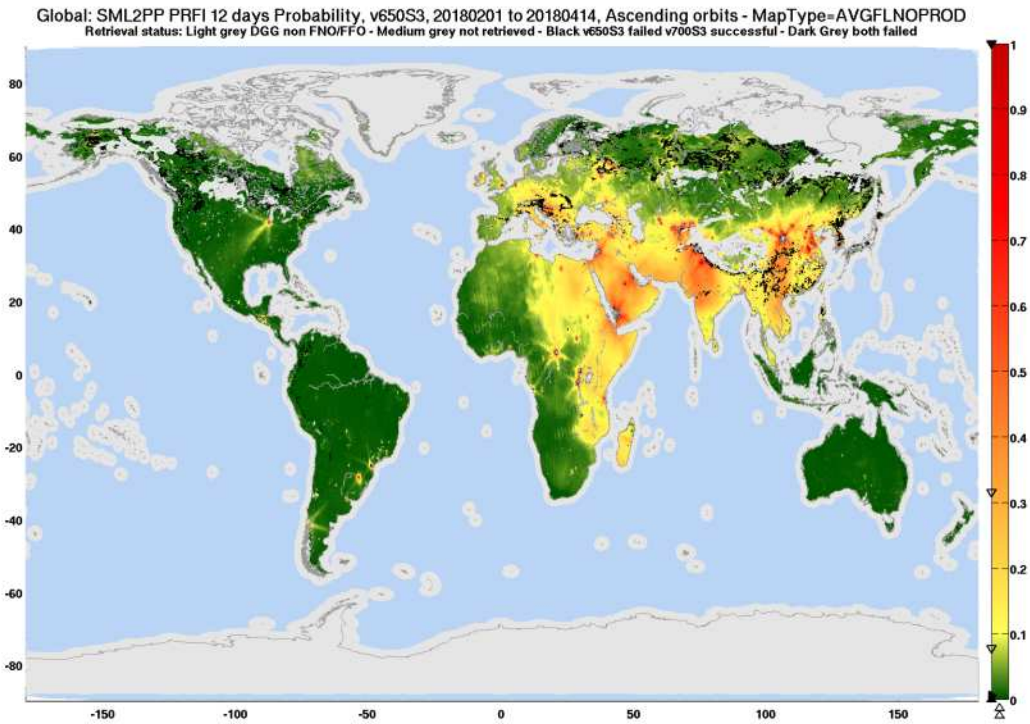

Figure 112: Reprocessing instance S3; Global map time average of v650 PRFI12.

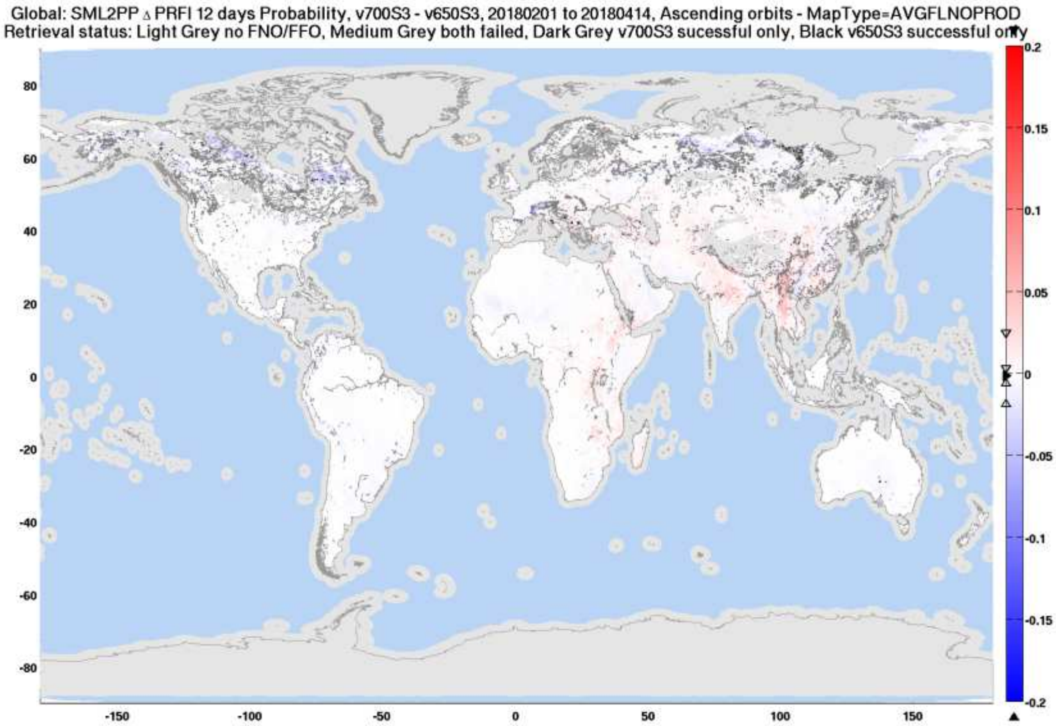

Figure 113: Reprocessing instance S3; Global map time average of v700 PRFI12 minus v650 PRFI12.

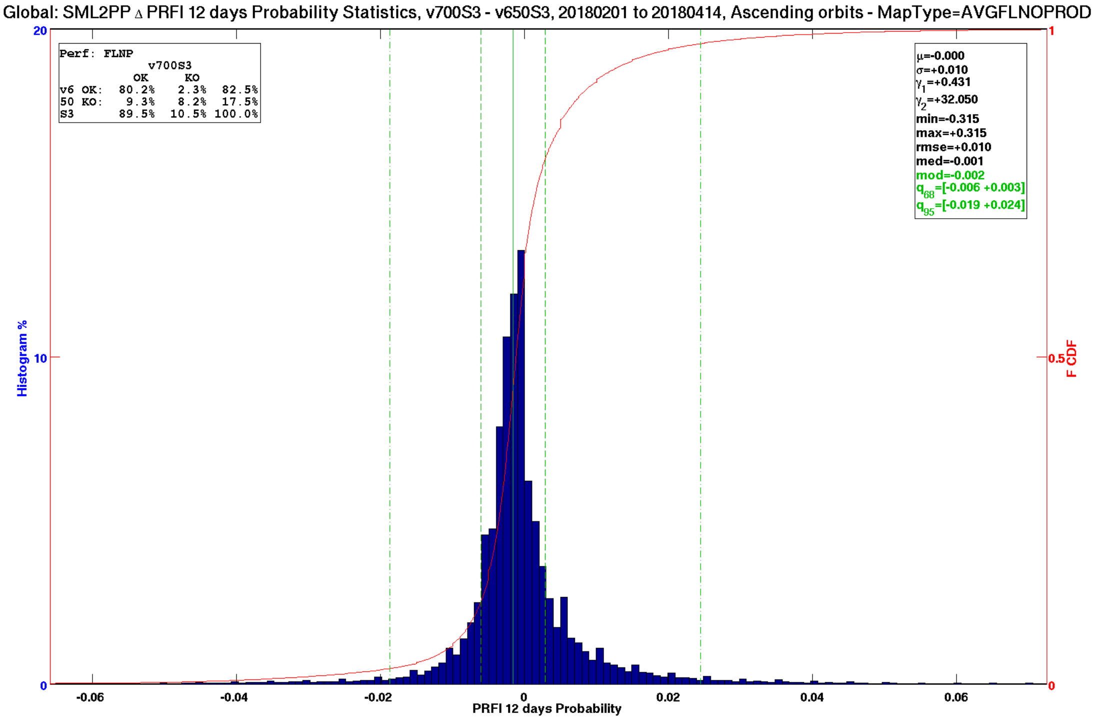

Figure 114: Reprocessing instance S3; Global histogram, cdf and stats of ratio of v700 PRFI12 minus v650 PRFI12.

4.3.2.5 SPATIAL VARIABILITY ACROSS CONTINENTS

The following box-plots summarize the ΔSM, ΔTauNadir v700 minus v650 spatial distributions and the ratio of Chi2 and Chi2P, v700 over v650 spatial distribution for the different areas of Figure 115 and at Global. They are given for each reprocessing instance. We remind that the middle bar is the distribution mode, the (possibly asymmetric) inner low/up bracket bar represent 68.3% of the distribution and outer low/up bracket bar represent 95.4% of the distribution, the bottom/top number the maxima.

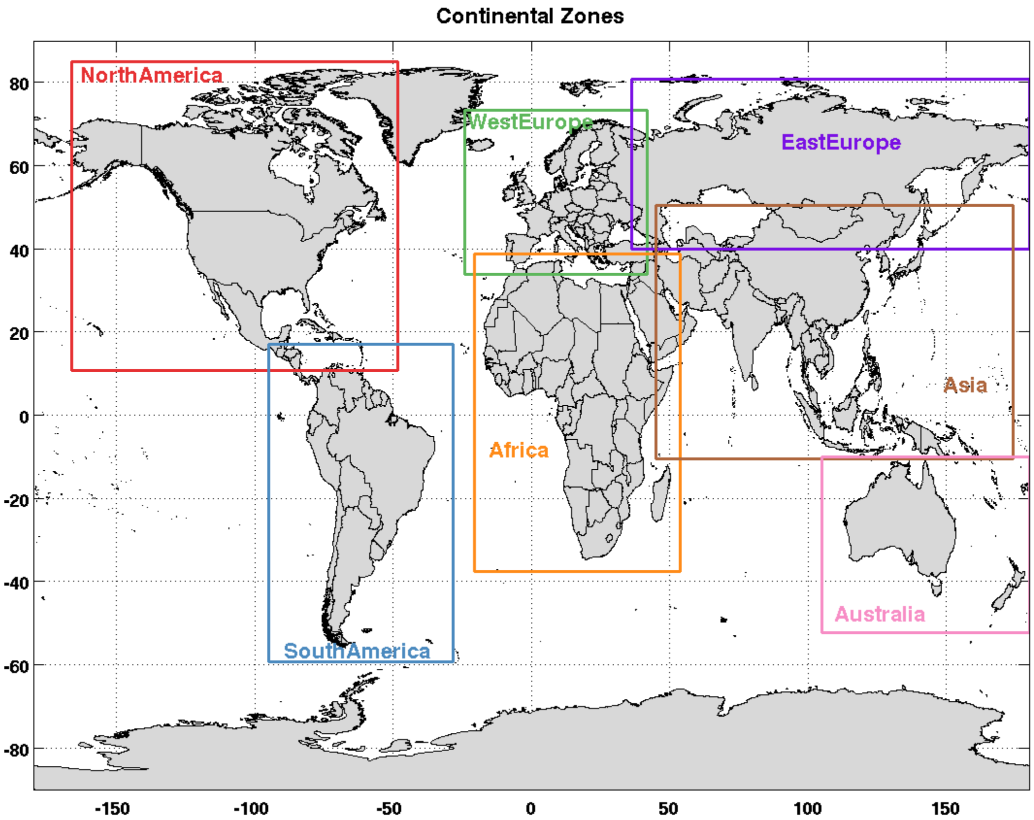

Figure 115: Continental areas boundary for spatial maps and box-plots.

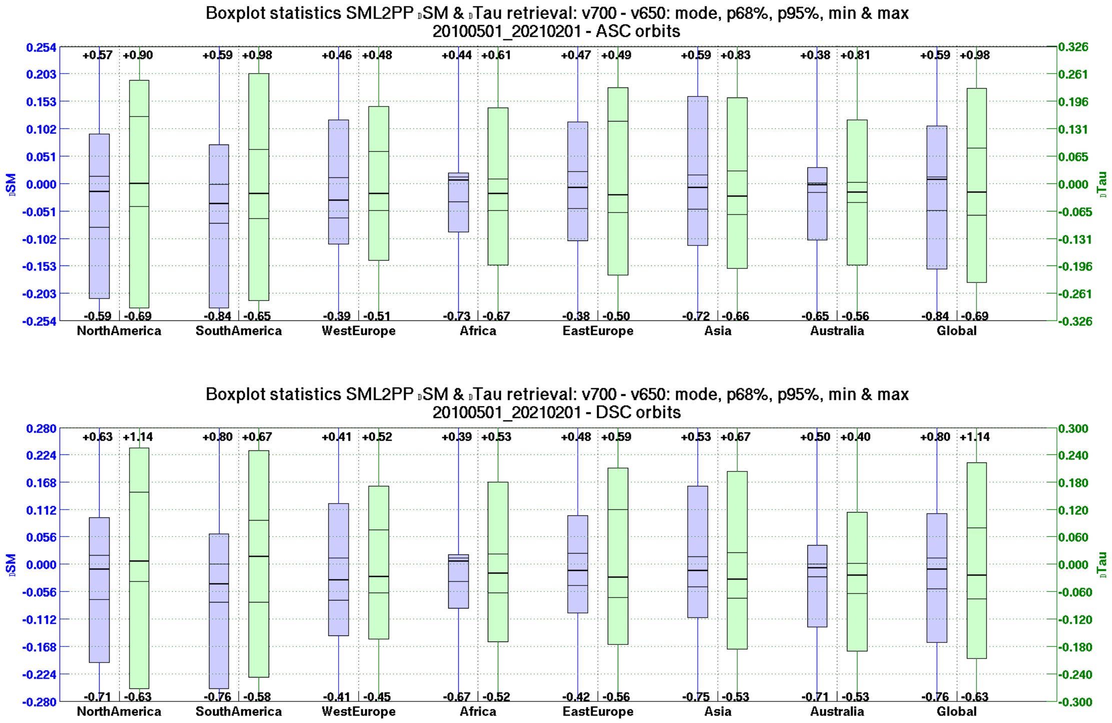

Figure 116: Whole reprocessing 20100501-20210131; box-plots per continents of differences of retrieved SM v700-v650 (blue), differences of retrieved VOD (green), top ascending orbits, bottom descending orbits.

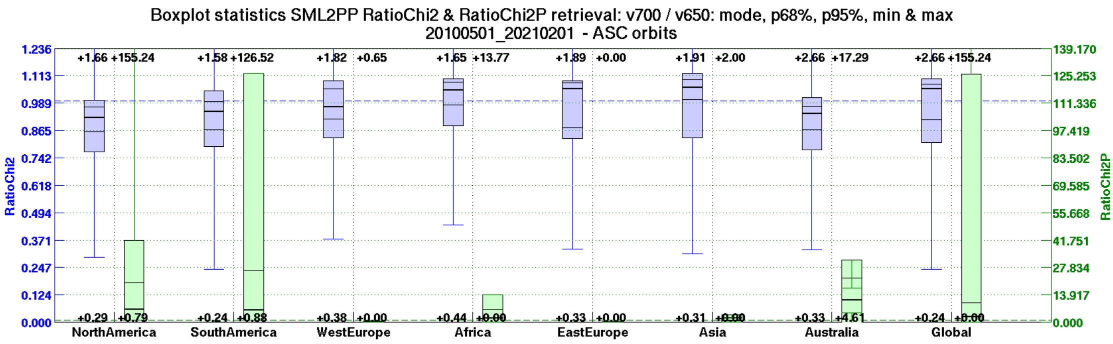

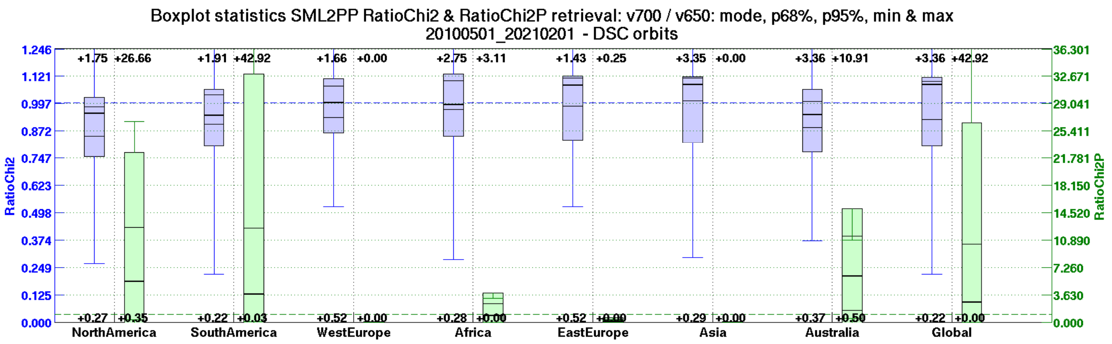

Figure 117: Whole reprocessing 20100501-20210131; box-plots per continents of differences of retrieved SM v700-v650 (blue), differences of retrieved VOD (green), top ascending orbits, bottom ascending orbits.

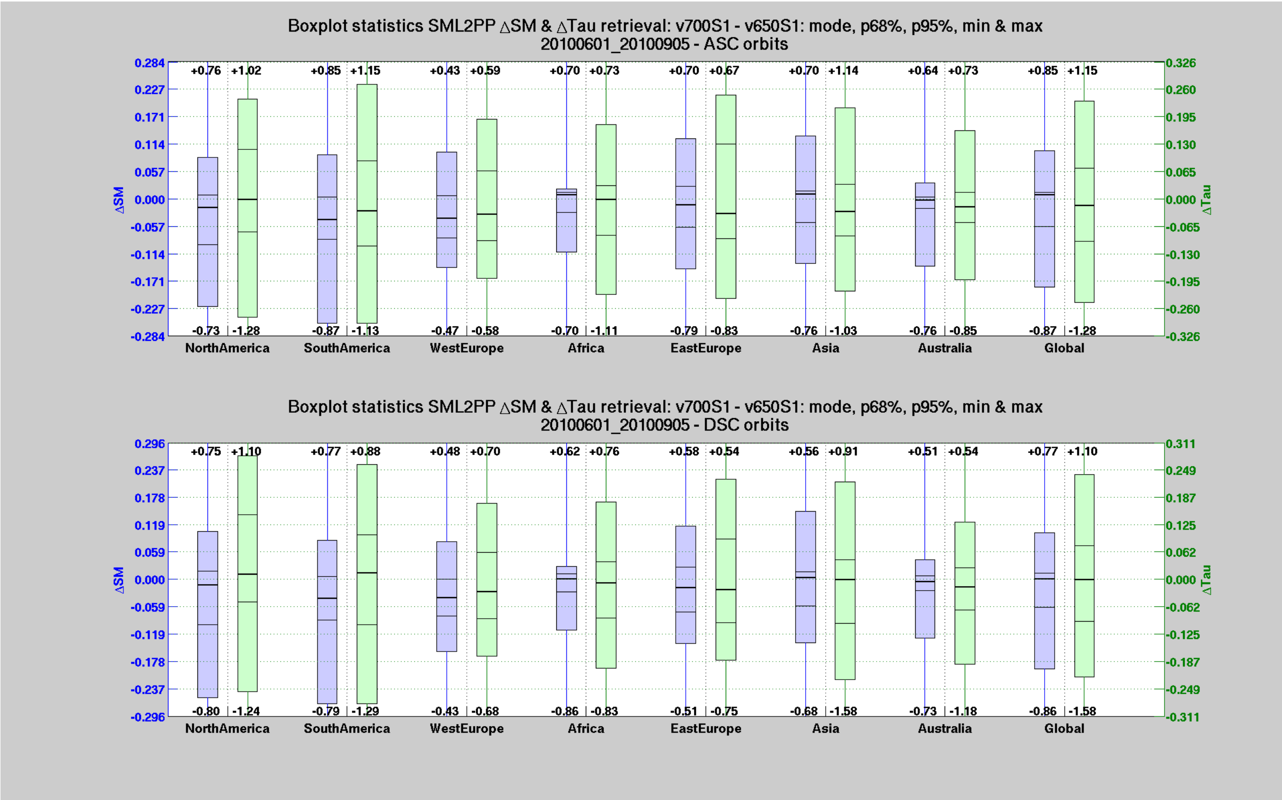

Figure 118: Reprocessing instance S1; box-plots per continents of differences of retrieved SM v700-v650 (blue), differences of retrieved VOD (green), top ascending orbits, bottom descending orbits.

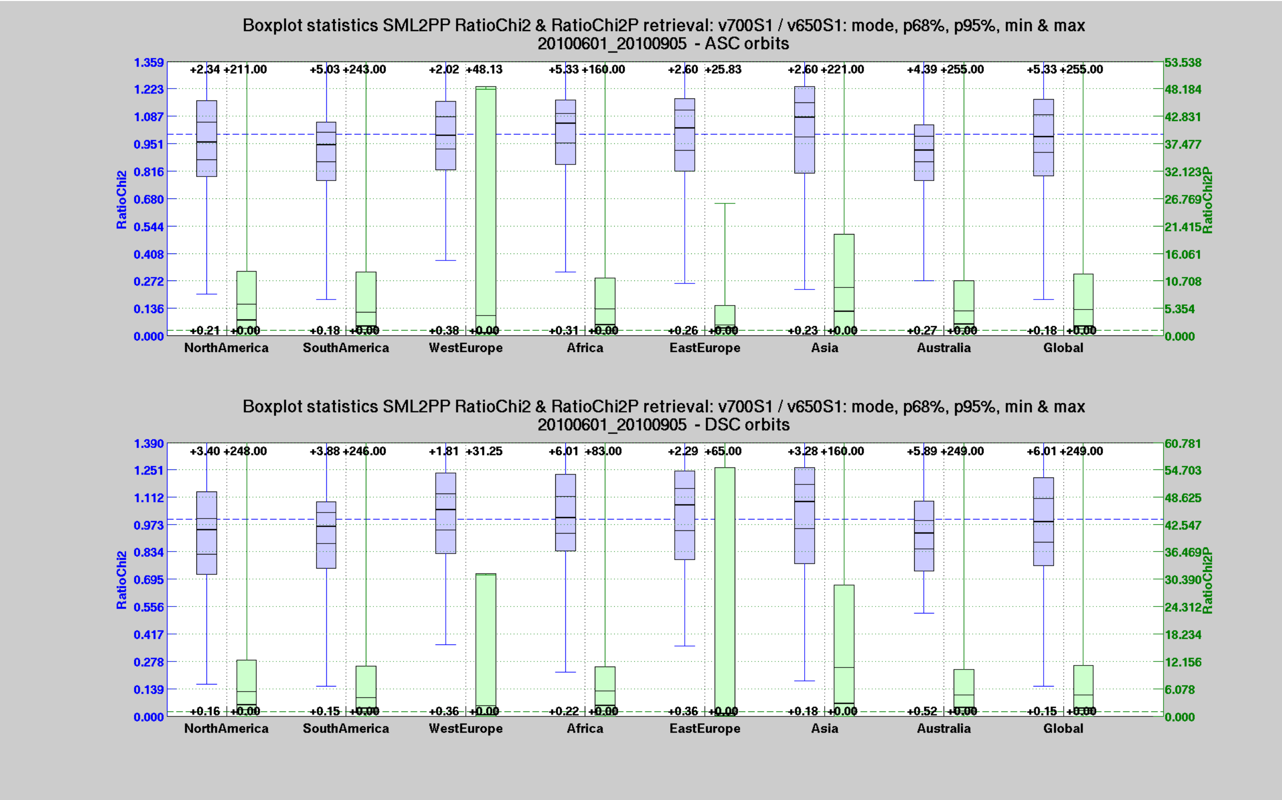

Figure 119: Reprocessing instance S1; box-plots per continents of ratios of retrieved Chi2 v700-v650 (blue), ratio of retrieved Chi2P (green), top ascending orbits, bottom descending orbits.

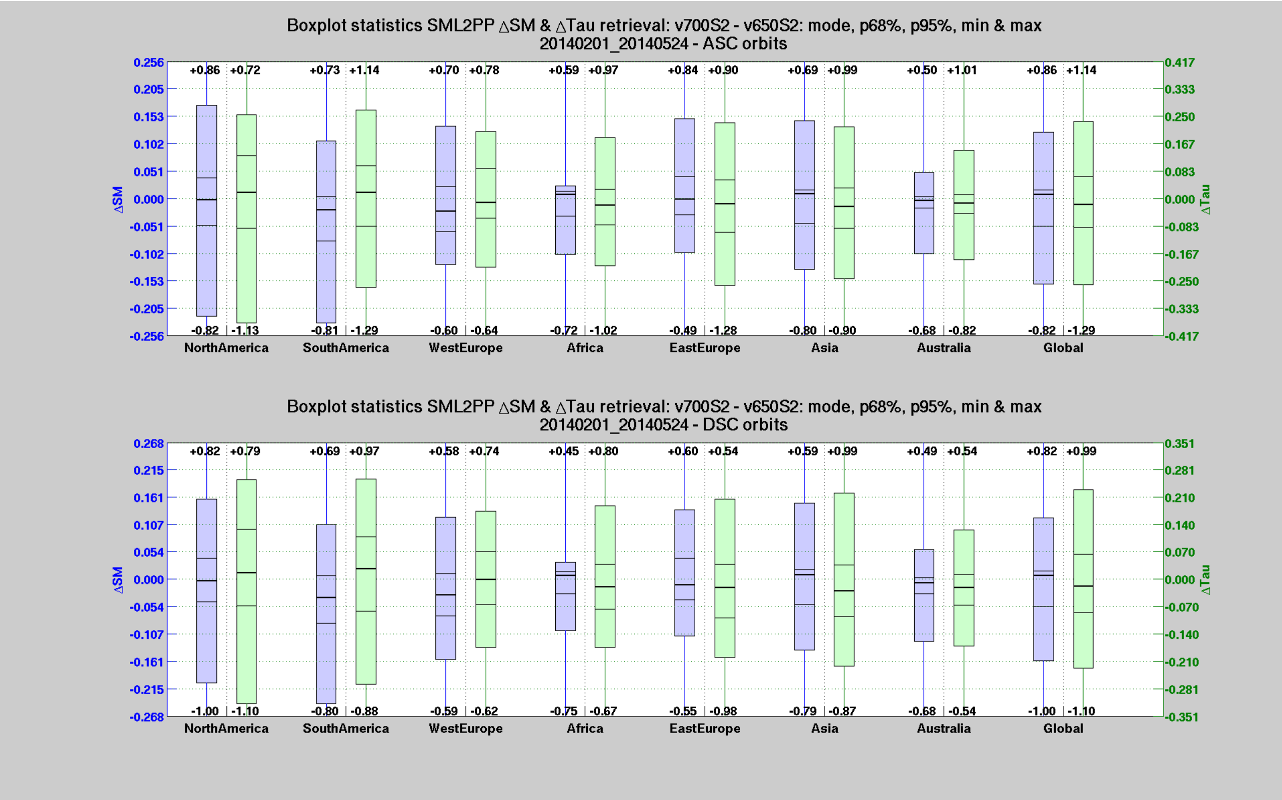

Figure 120: Reprocessing instance S2; box-plots per continents of differences of retrieved SM v700-v650 (blue), differences of retrieved VOD (green), top ascending orbits, bottom descending orbits.

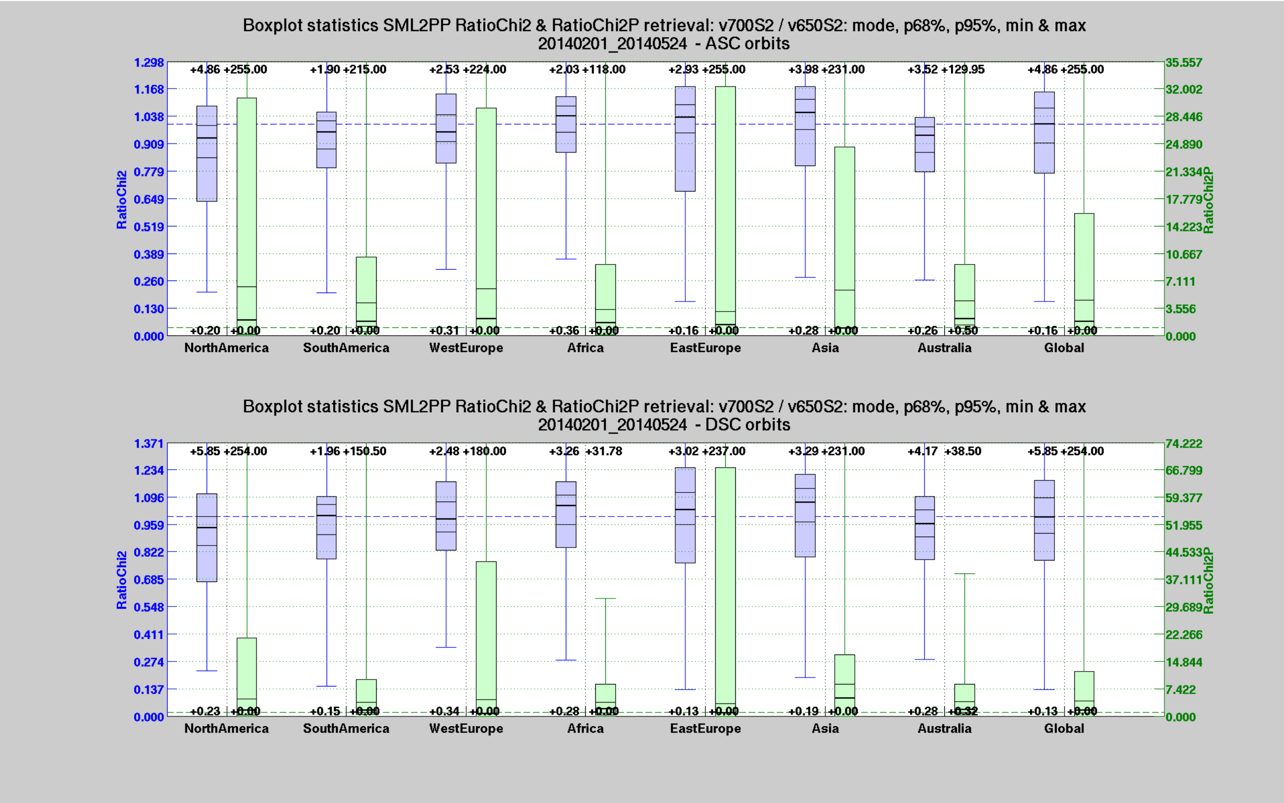

Figure 121: Reprocessing instance S2; box-plots per continents of ratios of retrieved Chi2 v700-v650 (blue), ratio of retrieved Chi2P (green), top ascending orbits, bottom descending orbits.

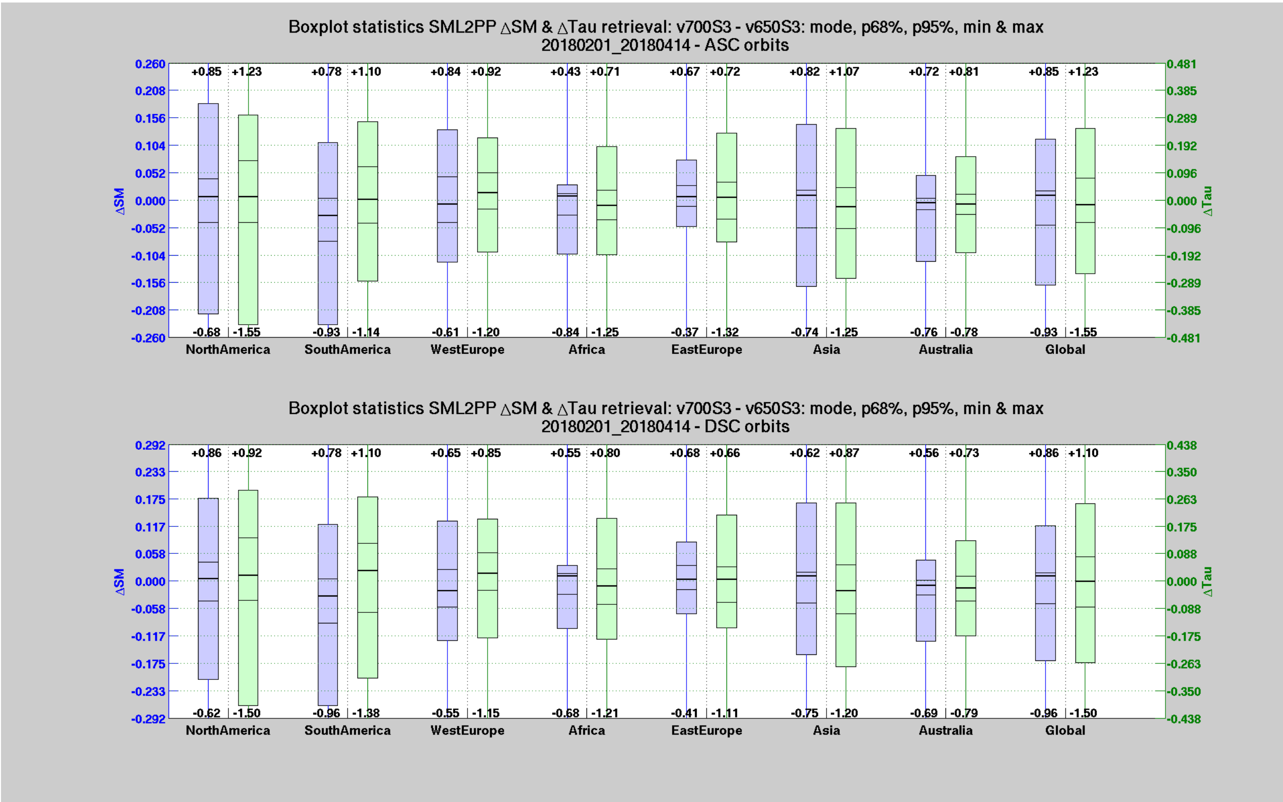

Figure 122: Reprocessing instance S3; box-plots per continents of differences of retrieved SM v700-v650 (blue), differences of retrieved VOD (green), top ascending orbits, bottom descending orbits.

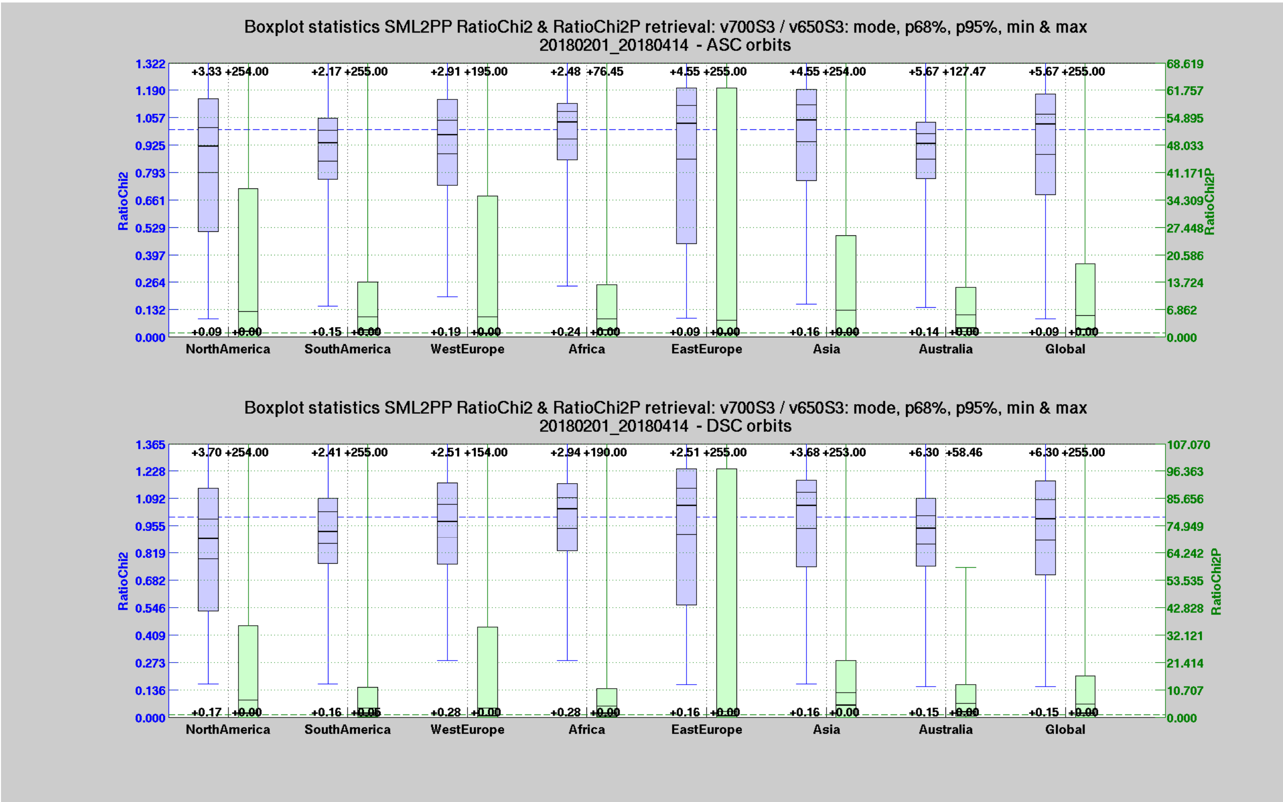

Figure 123: Reprocessing instance S3; box-plots per continents of ratios of retrieved Chi2 v700-v650 (blue), ratio of retrieved Chi2P (green), top ascending orbits, bottom descending orbits.

4.3.3 SPACETIME PERSPECTIVE: HOVMÖLLER PLOTS

The overall spatial and time dynamic is provided through Hovmöller plots considering zonal/meridional mean/standard deviation perspectives. They are split as usual per ascending/descending orbits overpasses.

The time resolution is 4 days to ensure a Global coverage when split per ascending / descending orbits. The latitude/longitude resolution is 1° to compute zonal/meridional mean/standard deviation.

All main parameters are considered globally and limited per continental areas (Figure 115).

In this document only Global zonal Hovmöller plots are presented.

4.3.3.1 RETRIEVED SOIL MOISTURE

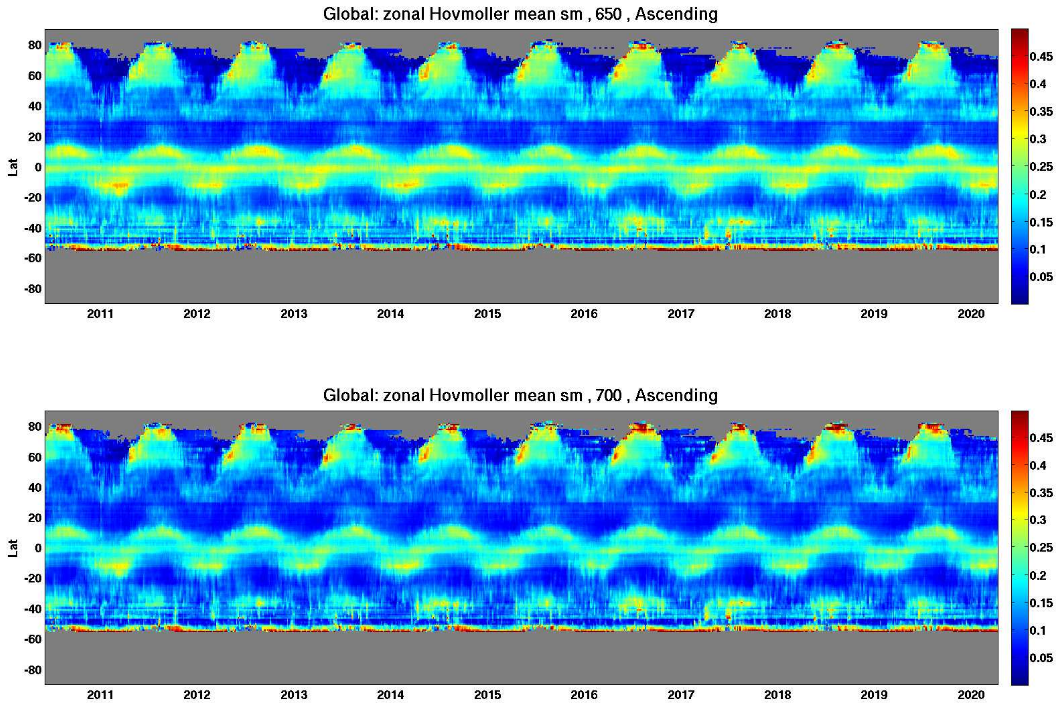

Figure 124: Global Hovmöller: mean zonal SM, v650 (top), v700 (bottom), ascending orbits

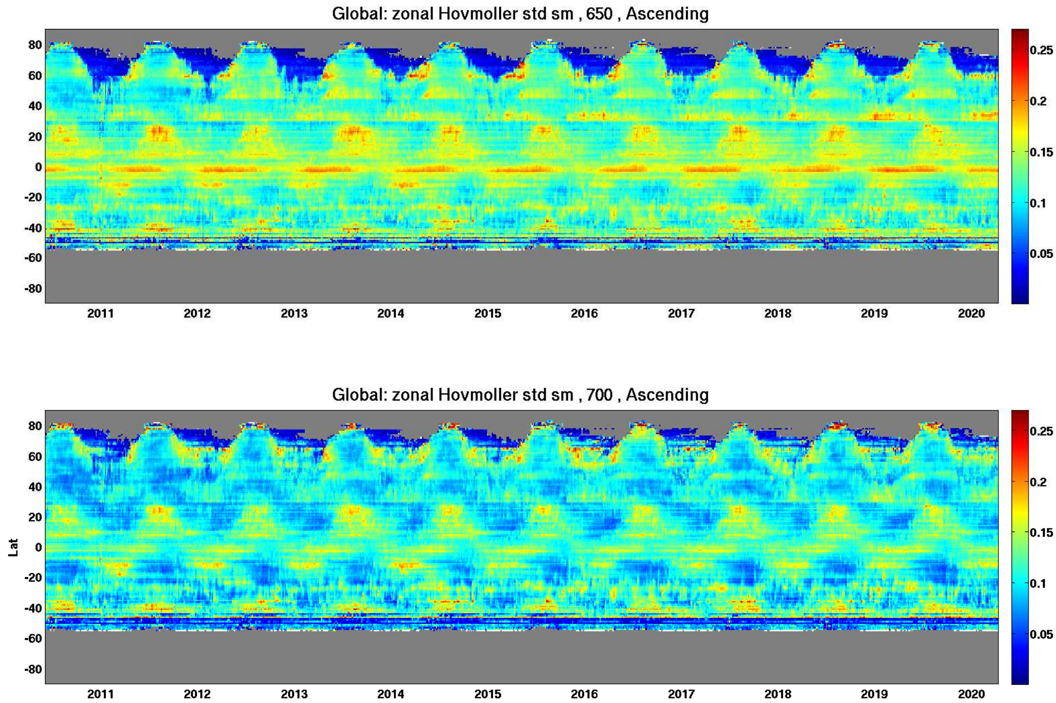

Figure 125: Global Hovmöller: std zonal SM, v650 (top), v700 (bottom), ascending orbits

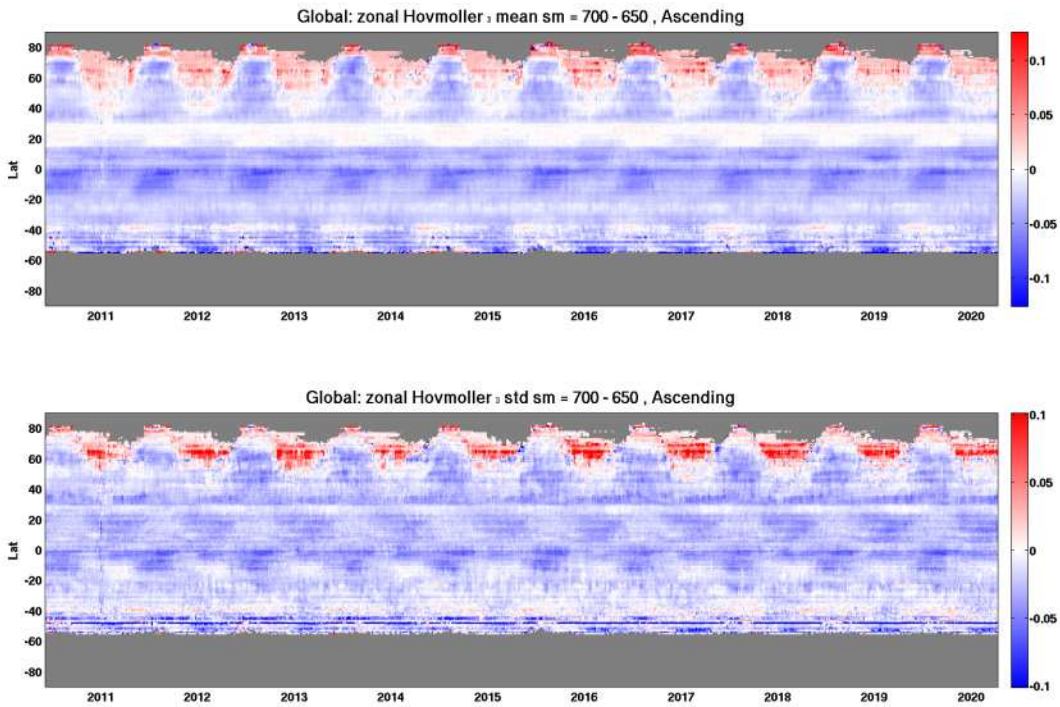

Figure 126: Global ∆Hovmöller, v700 – v650: ∆mean SM (top), ∆std SM (bottom), ascending orbits

4.3.3.2 RETRIEVED TAUNADIR (VOD)

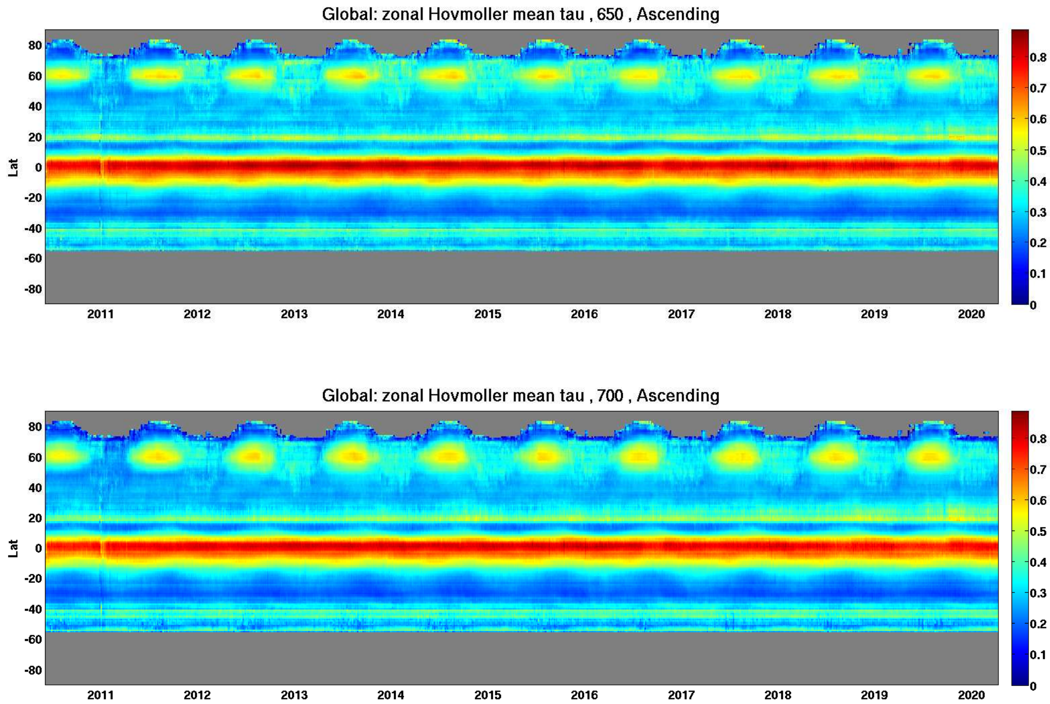

Figure 127: Global Hovmöller: mean zonal TauNadir, v650 (top), v700 (bottom), ascending orbits

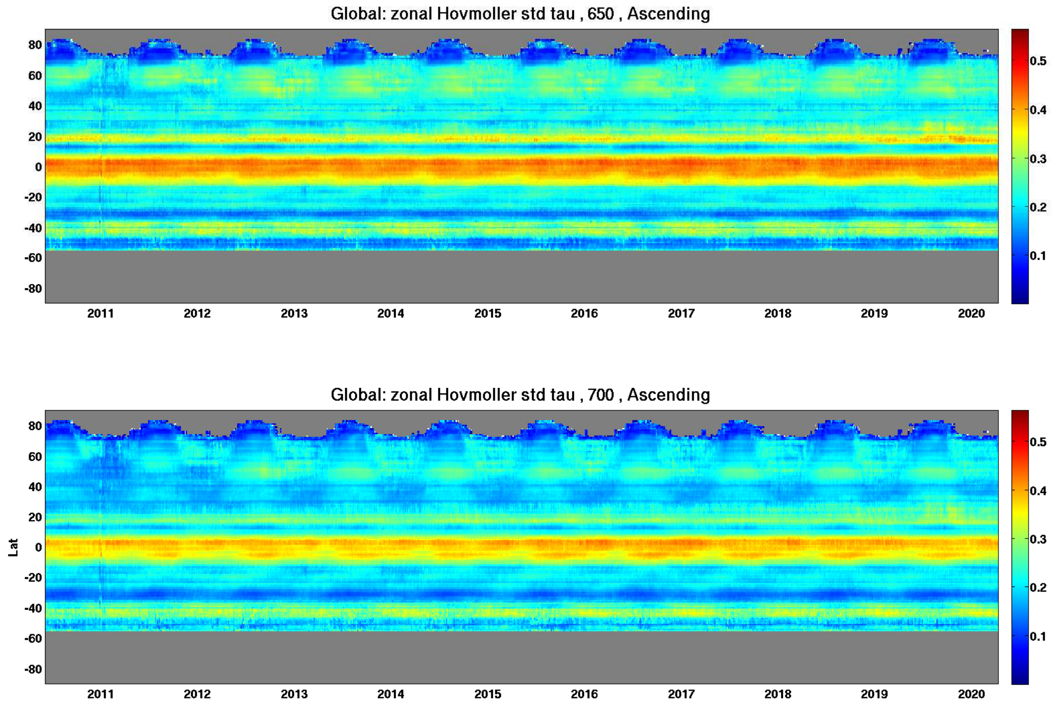

Figure 128: Global Hovmöller: std zonal TauNadir, v650 (top), v700 (bottom), ascending orbits

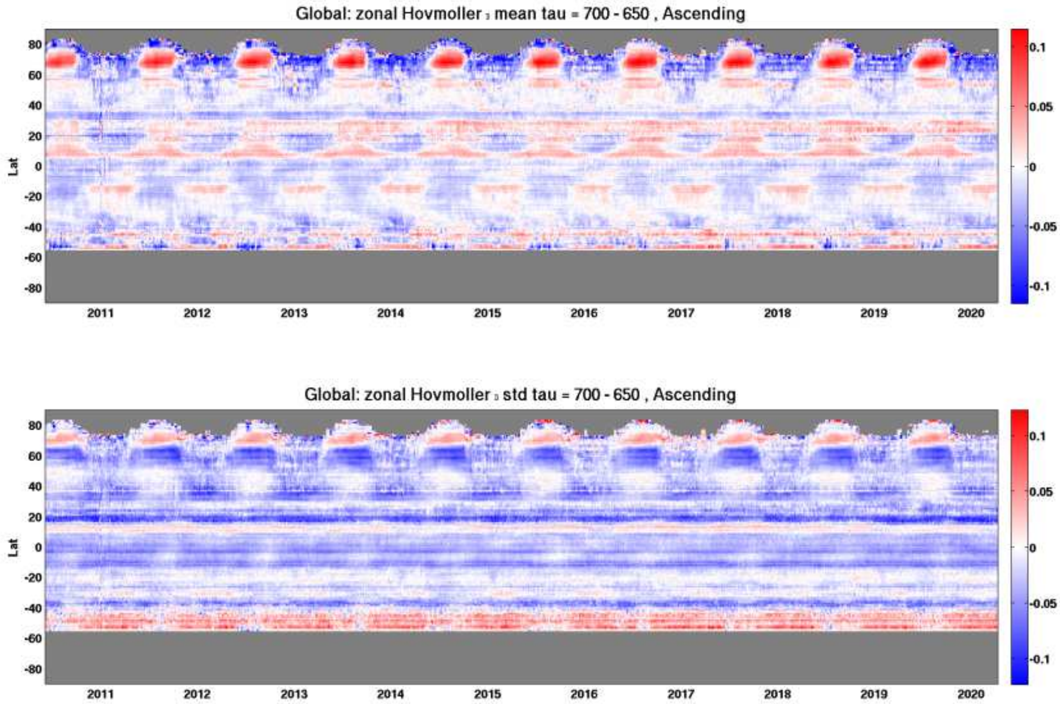

Figure 129: Global ∆Hovmöller, v700 – v650: ∆mean TauNadir (top), ∆std TauNadir (bottom), ascending orbits

4.3.3.3 RETRIEVED CHI2

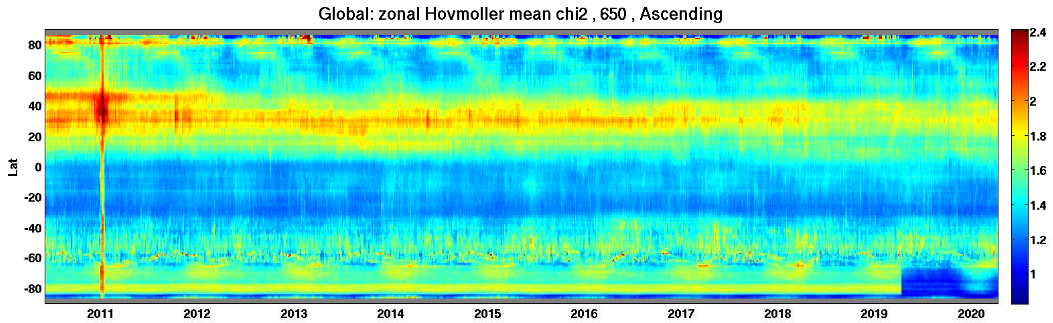

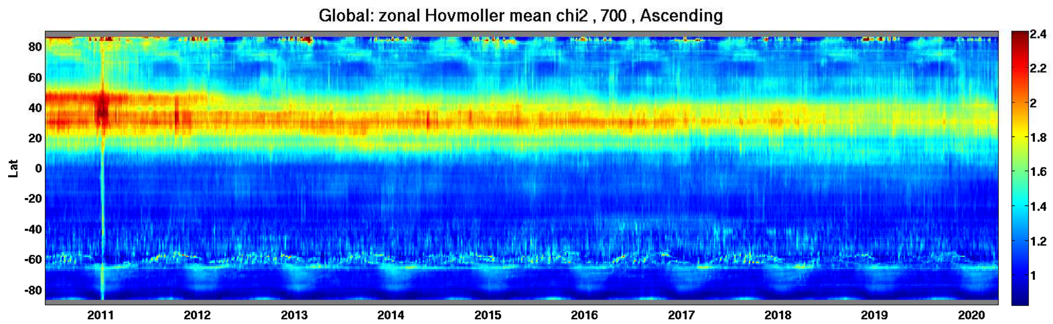

Figure 130: Global Hovmöller: mean zonal Chi2, v650 (top), v700 (bottom), ascending orbits

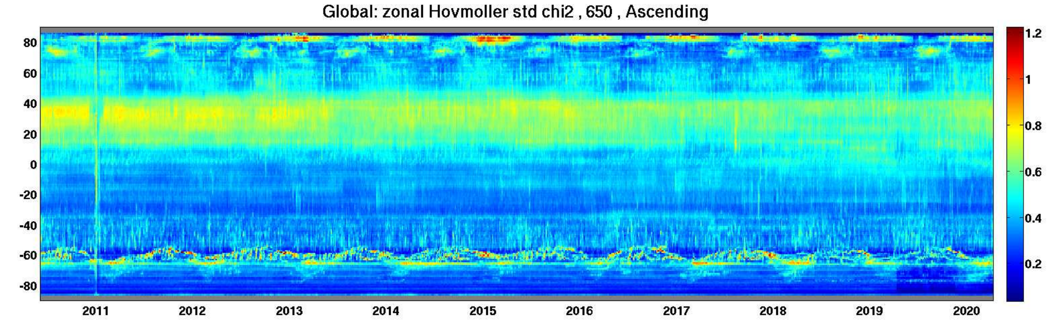

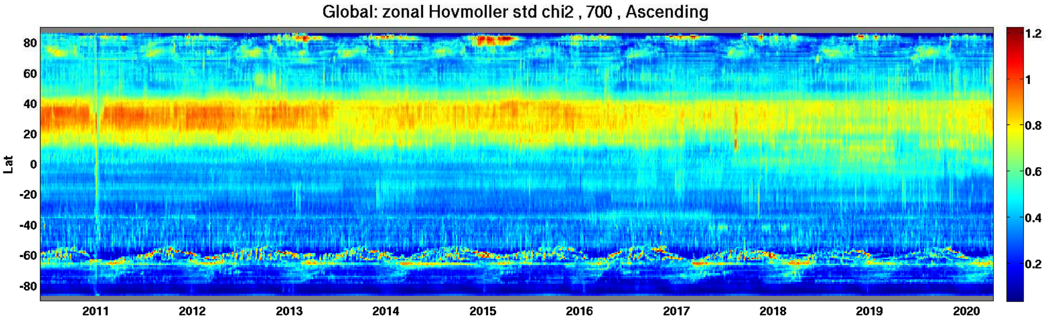

Figure 131: Global Hovmöller: std zonal Chi2, v650 (top), v700 (bottom), ascending orbits

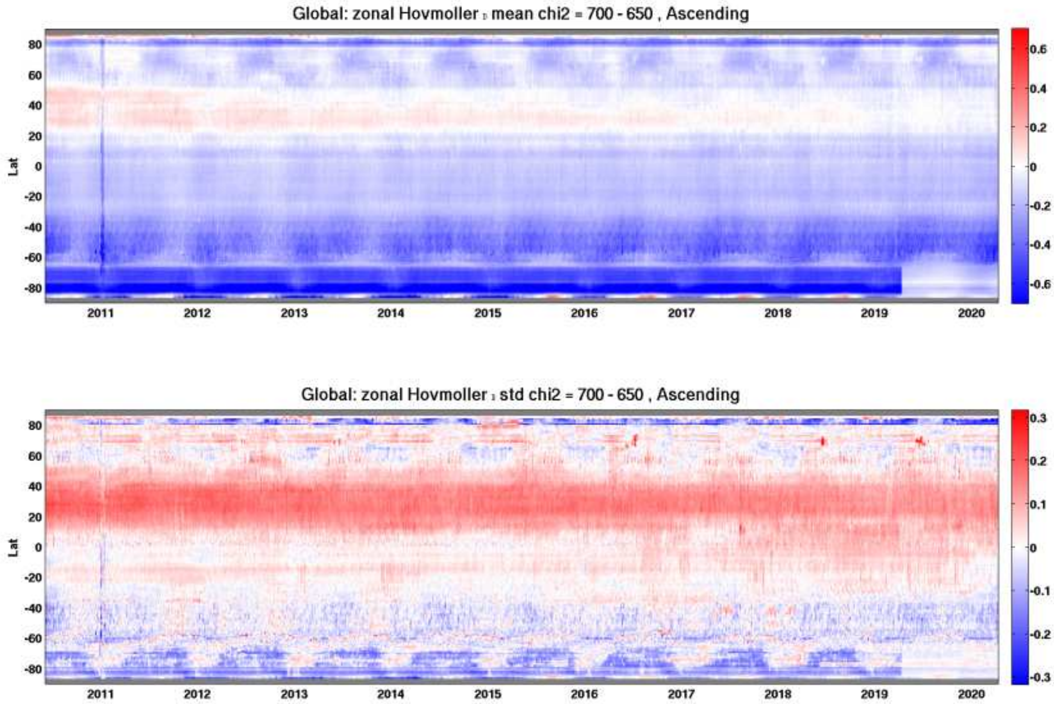

Figure 132: Global ∆Hovmöller, v700 – v650: ∆mean Chi2 (top), ∆std Chi2 (bottom), ascending orbits

4.3.3.4 RFI PROBABILITY

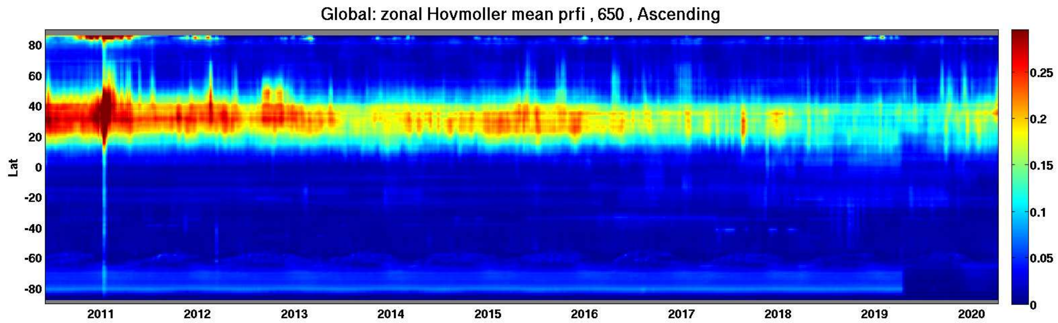

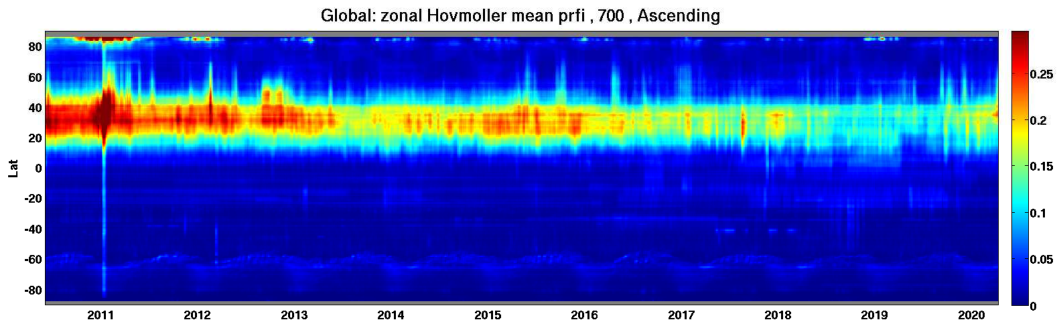

Figure 133: Global Hovmöller: mean zonal PRFI12, v650 (top), v700 (bottom), ascending orbits

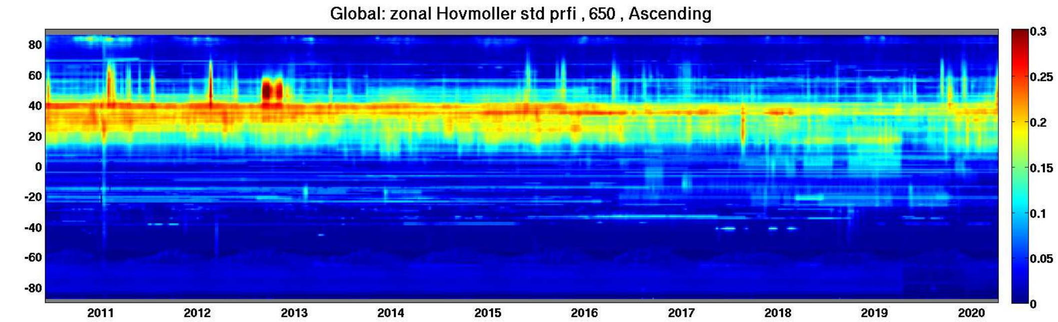

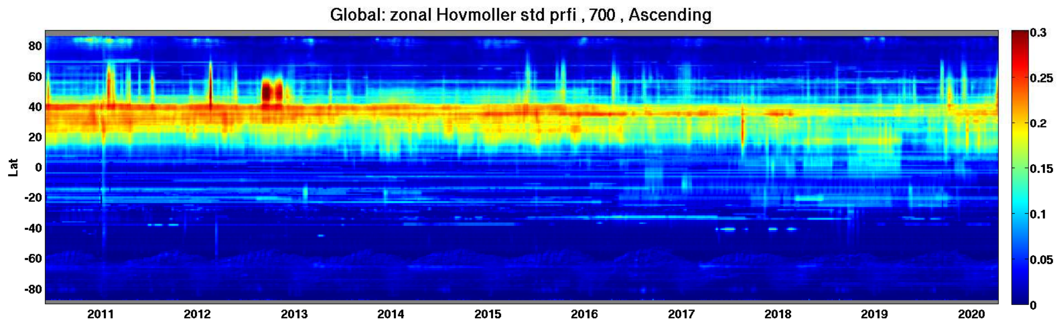

Figure 134: Global Hovmöller: std zonal PRFI12, v650 (top), v700 (bottom), ascending orbits

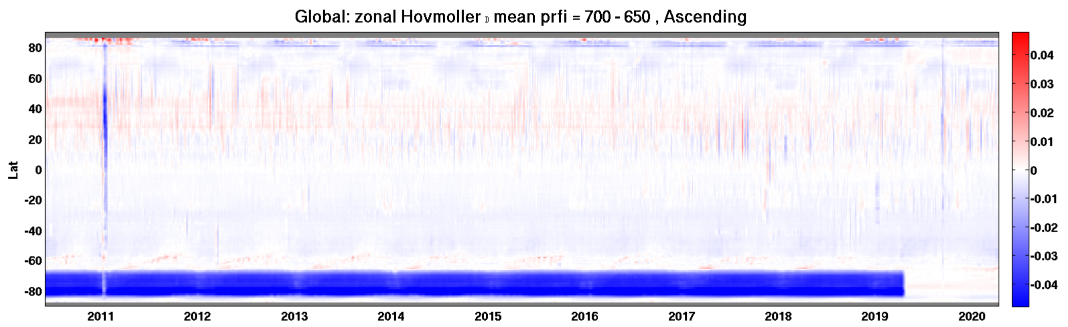

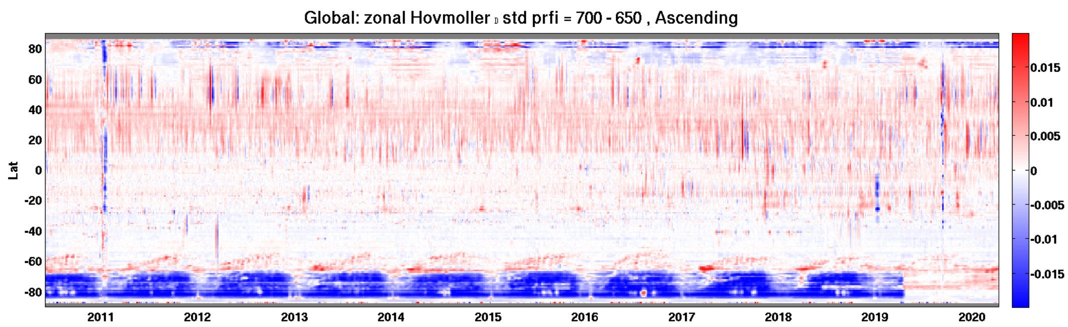

Figure 135: Global ∆Hovmöller, v700 – v650: ∆mean PRFI12 (top), ∆std PRFI12 (bottom), ascending orbits

4.4 ASCENDING VERSUS DESCENDING ORBITS

Since the beginning of the mission we observe differences in our retrievals between ascending 6am LST morning orbits and descending 6pm LST descending orbits.

Some differences may be linked to possible geophysical features if deemed to be observed at SMOS coarse resolution and with the instrument sensitivity. It could be the case for example to the retrieved soil moisture that we know can exhibit diurnal variation.

Some others may be linked external aspect affecting the observation. For example it is known that the ionosphere is more turbulent at 6pm LST than at 6am LST generating maybe noisier observation and stronger Faraday rotation effects. And it is also well known that RFI sources have asymmetrical impact; a given source impact differently the (far) neighbourhood of DGGs due to the SMOS tilted antenna plane looking ahead the flight path.

Finally such differences could also come from limitations and/or algorithms issues like ECMWF forecast temperatures morning/evening may have different error patterns. The

6am LST orbits observe a surface system closer to the thermodynamic equilibrium than 6pm LST.

4.4.1 PRFI12, SUCCESS, CHI2, CHI2P

The main factor of asymmetry between ascending the RFI impact, at least for the Northern hemisphere as show below on the Hovmöller plot Figure 136 of the PRFI12 differences Ascending – Descending. Same RFI sources define two bands of latitude depending on the orbits due to the titled SMOS antenna plane.

The N40°-N60° band is more affected by RFI for descending passes while it is the opposite for the N10°-N30 band which is more affected for ascending orbits. PRFI12 for v700 and v650 are very close, so the difference ASC-DSC is.

However, slightly more RFI is detected on the v700. This slight difference may come from slightly warmer L1C v724 than L1C v620 which makes some sense with the L2L1 metrics L1C v724 vs. L1C v620 that reported lower retrieved SM derived from v724; 0.01 m^3/m^3 lower on average.

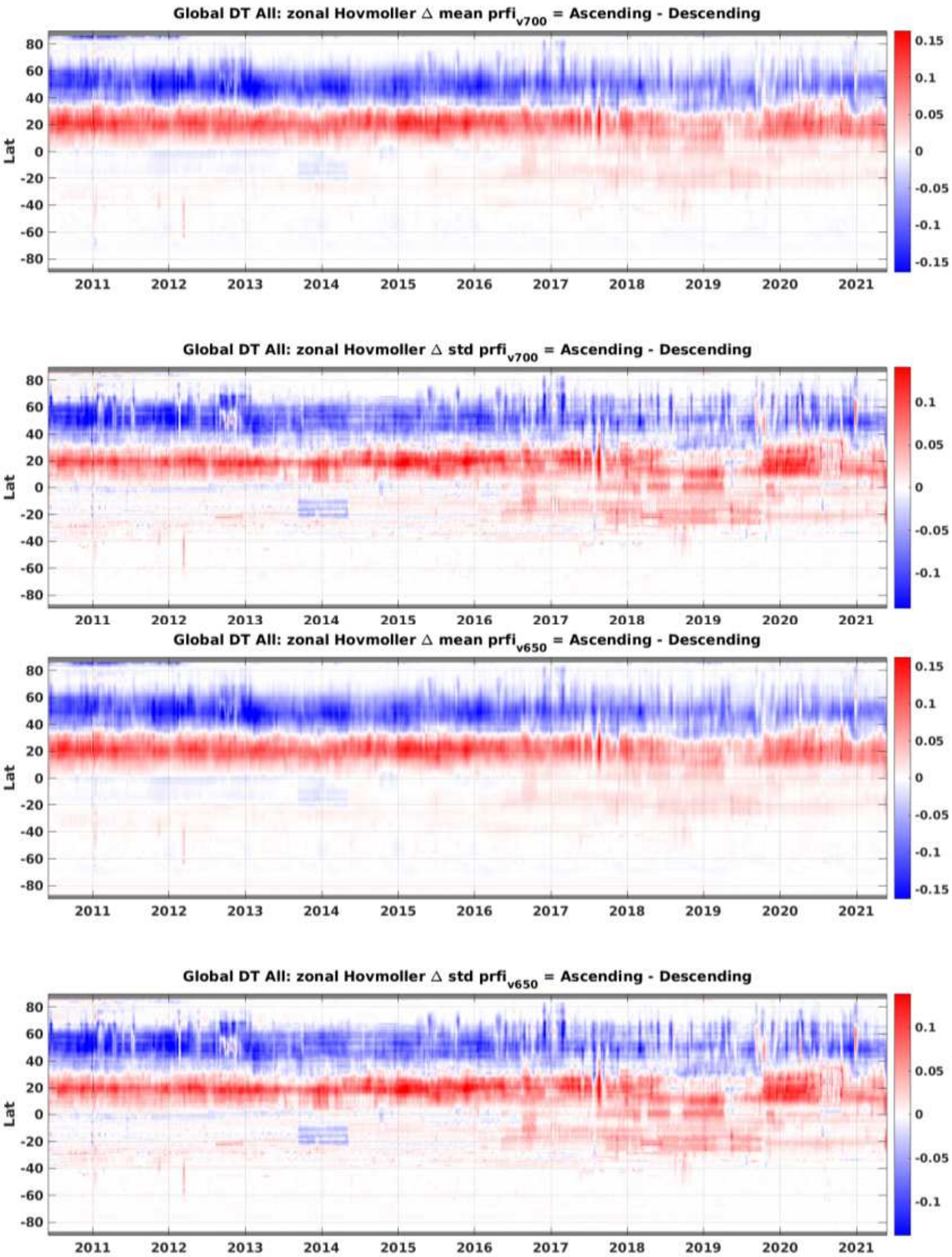

Figure 136: v700 Zonal hovmoller of differences Ascending – Descending for mean PRFI12; 1st and 2nd row v700, 3rd and 4th row v650.

The RFI asymmetrical impact will be always present in other Hovmöller ASC-DSC parameters plot, particularly for the Northern hemisphere. It is not easy, then, to detect other sources of variations like natural (geophysical) or instrumental (L1C) ones and how differently the L2SM v700 and v650 capture them.

It is for example the case for the percentage of successful retrievals, Chi2, Chi2P contains good parts that are clearly correlated with RFI in the following Figure 137 to Figure 139. However these figures display also seasonal modulations or specific features on top RFI's.

Differences between v700 and v650 seem to exist but are barely observable may require dedicated differential figures i.e. (v700ASC-v700DSC) – (v650ASC-v650ASC) to let them appear.

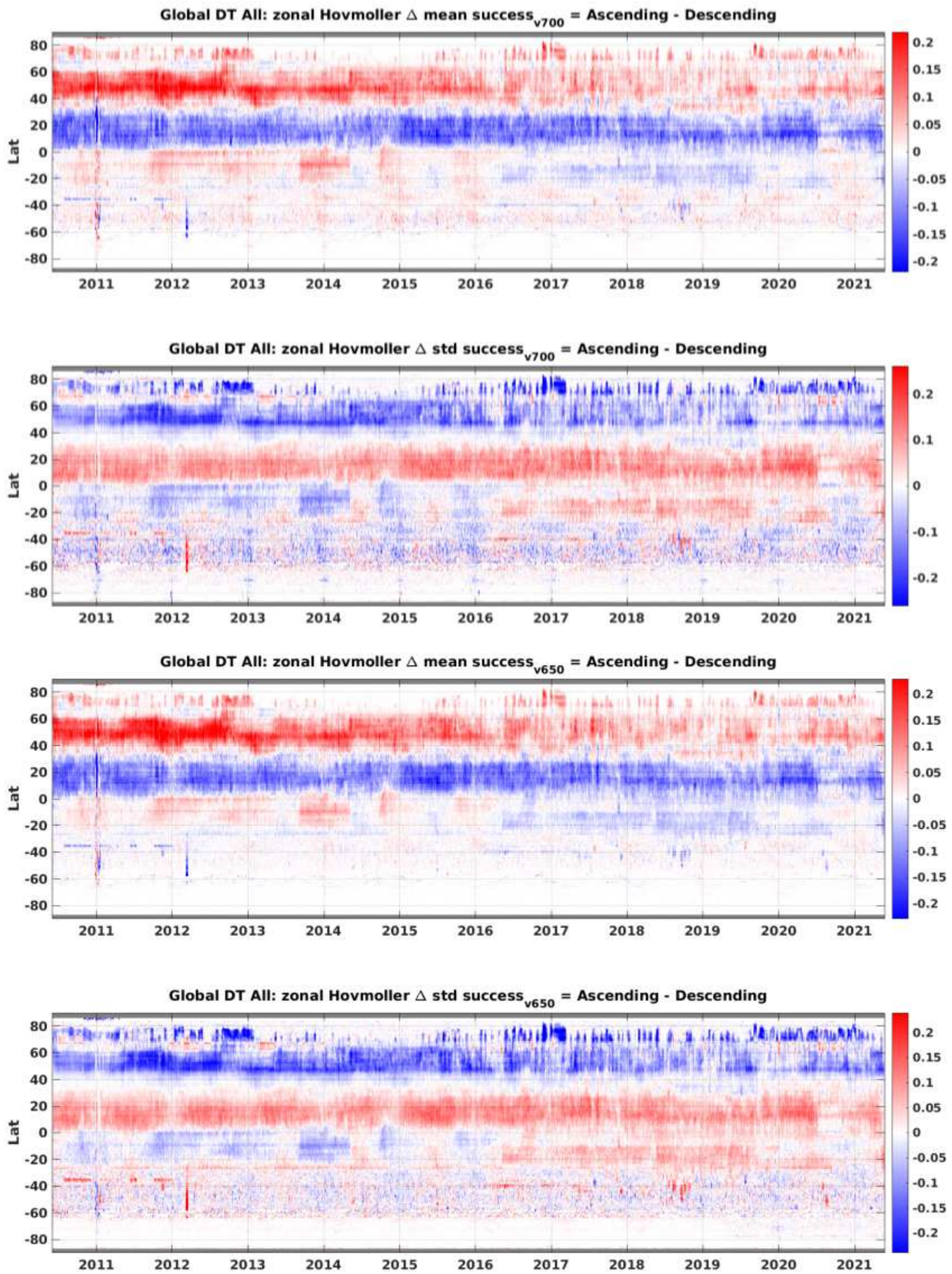

Figure 137: Zonal hovmoller of differences Ascending – Descending for mean success and std success; 1st and 2nd row v700, 3rd and 4th row v650.

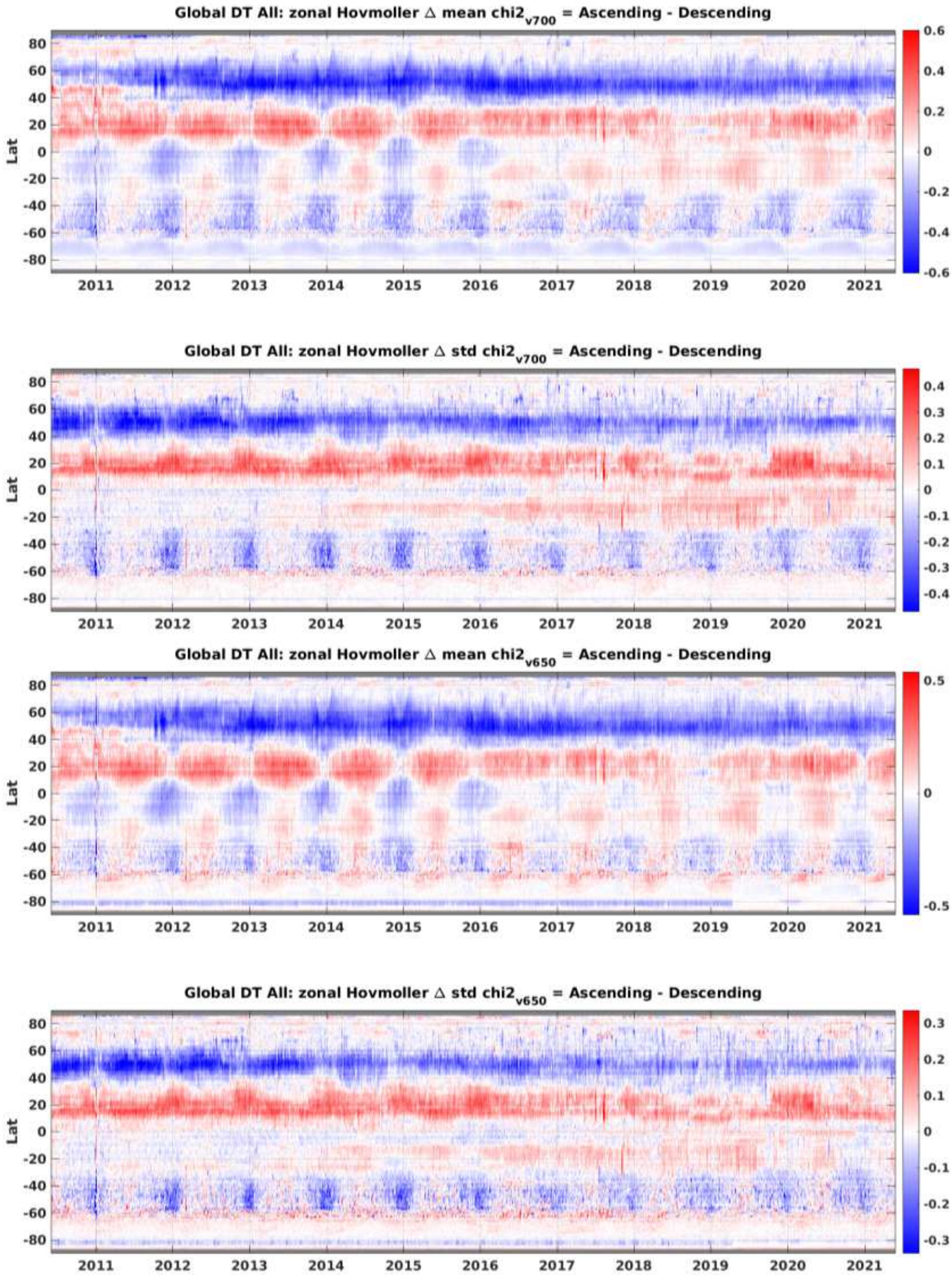

Figure 138: v700 Zonal hovmoller of differences Ascending – Descending for mean Chi2; 1st and 2nd row v700, 3rd and 4th row v650.

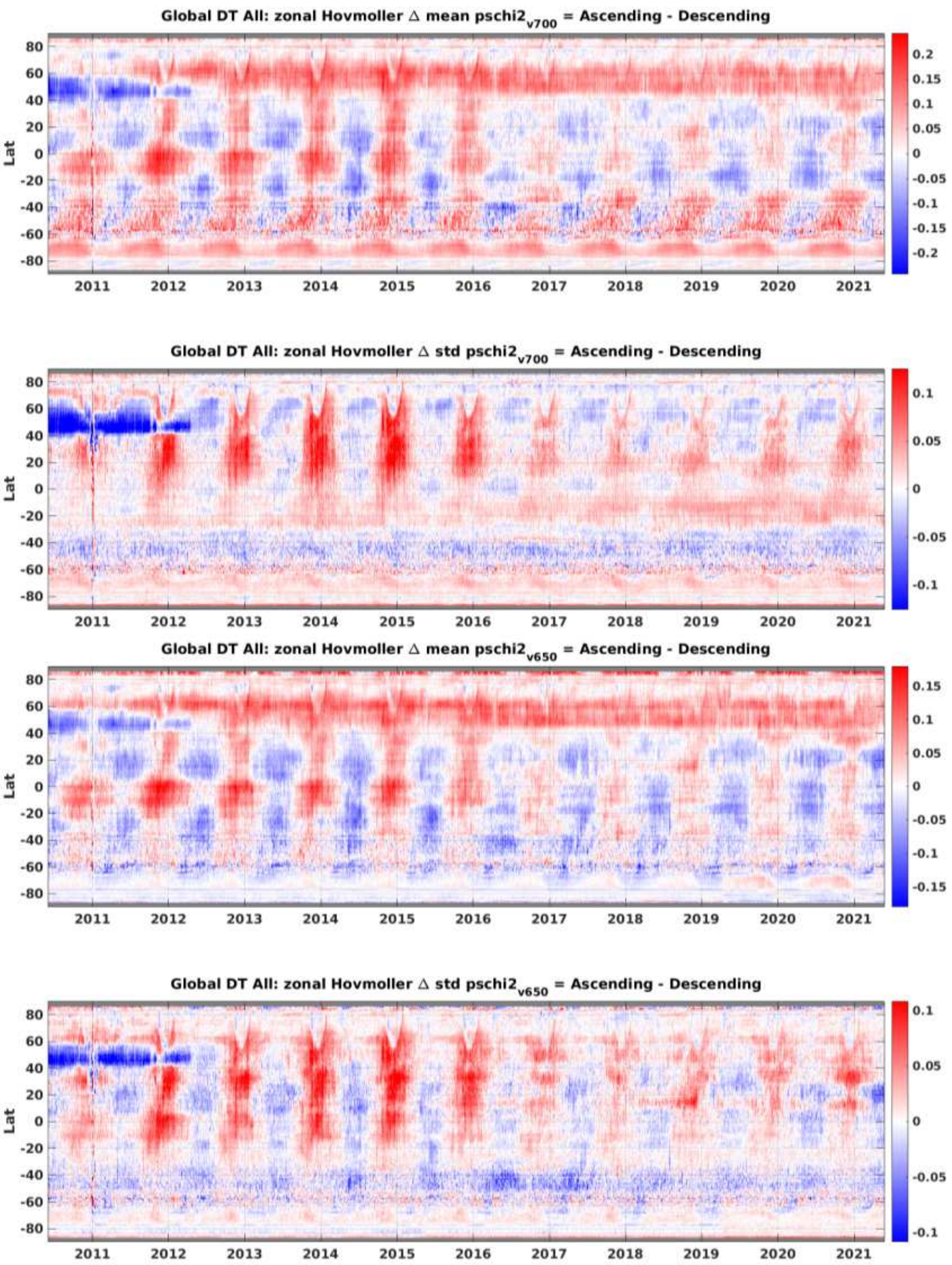

Figure 139: v700 Zonal hovmoller of differences Ascending – Descending for mean Chi2P; 1st and 2nd row v700, 3rd and 4th row v650.

4.4.2 SM, TAUNADIR, |ε|

Despite the other retrieved parameters, SM, TauNadir, are necessarily impacted by RFI (and in much unknown ways), ASC – DSC maps reveal patterns. Seasonal variations and systematic differences can be observed but with origins yet to be understood.

Further analyses are definitively required for this section. Given the large volume of data available very strict data selection could be applied e.g. not instant RFI, no PRFI12 at all. For good measure we could complement that with Chi2 rejection higher than 2 for lower RFI level passing though the filter. The thresholds for Chi2 or Chi2P are to be considered with care as the purpose is not to reject modelling error or L1C specificities. Adding focus on spatial maps would be interesting (e.g. dense forest).

One interesting aspect captured by both L2SM versions is the DEW line impact (brown band around N50°). Equipments were refurbished and ended in may 2012. As we have seen ascending passes were more impacted than descending. Assuming that 6am – 6pm soil moisture variation is dominated by RFI, we can consider the differences for years onward as a reference, then we can estimate the cost of RFI as generating 0.04 m^3/m^3 to 0.06 m^3/m^3 underestimation in our soil moisture retrievals. RFI impact on retrieved opacity is much less known compared to soil moisture; however it appears clearly in this case to generate also an underestimation of the retrieved opacity by ~0.1 if not more.

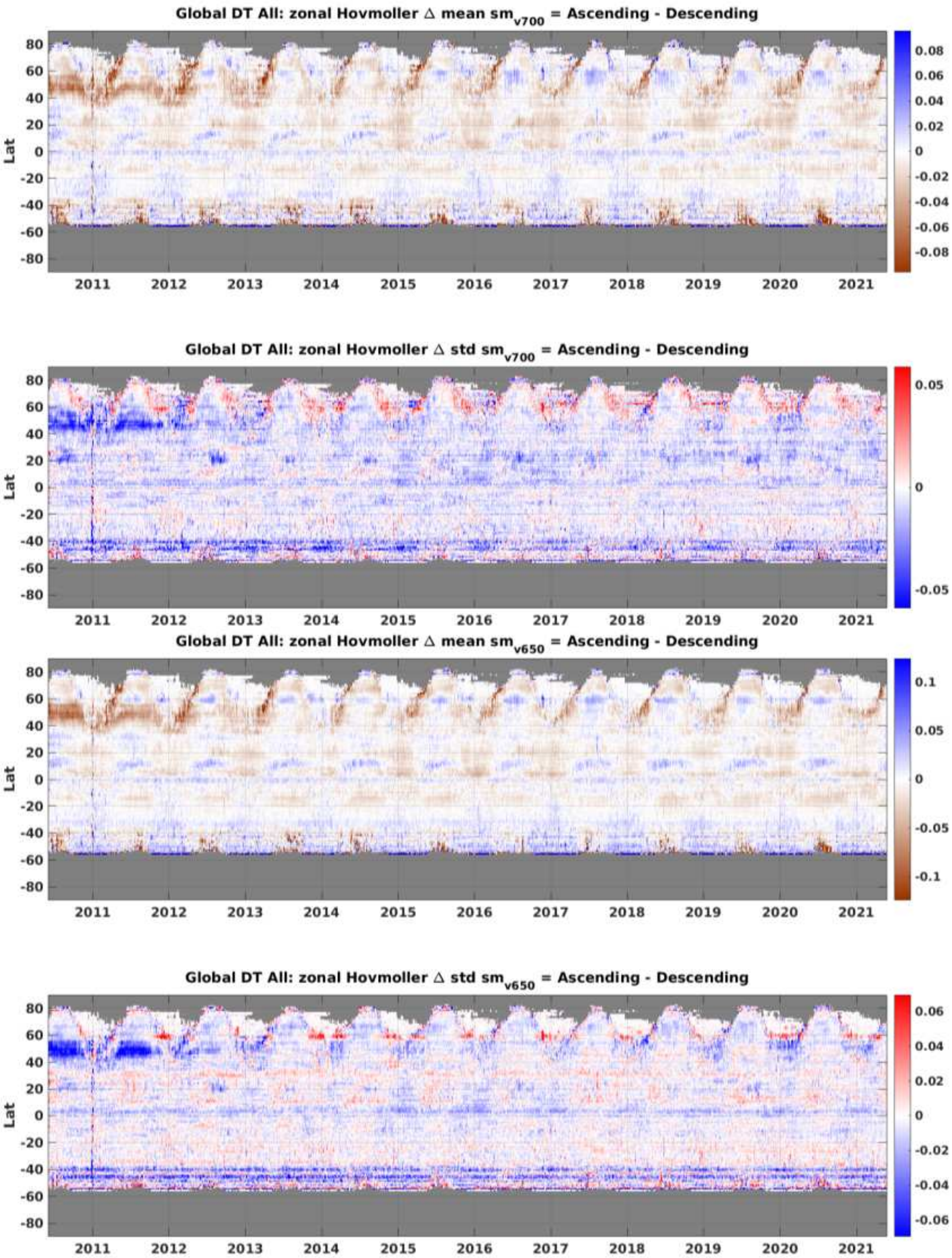

Figure 140: v700 Zonal hovmoller of differences Ascending – Descending for mean SM; 1st and 2nd row v700, 3rd and 4th row v650.

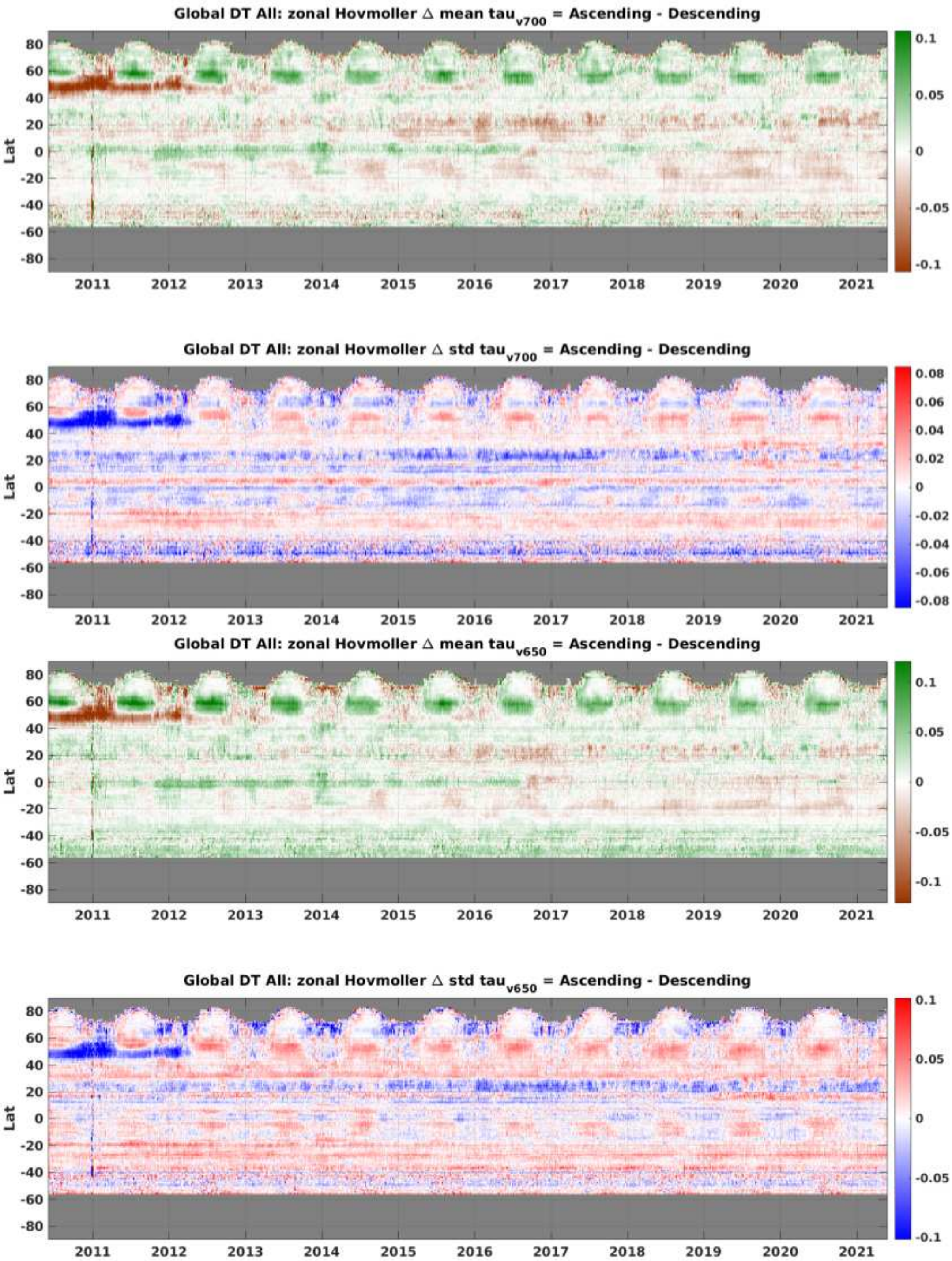

Figure 141: v700 Zonal hovmoller of differences Ascending – Descending for mean TauNadir; 1st and 2nd row v700, 3rd and 4th row v650.

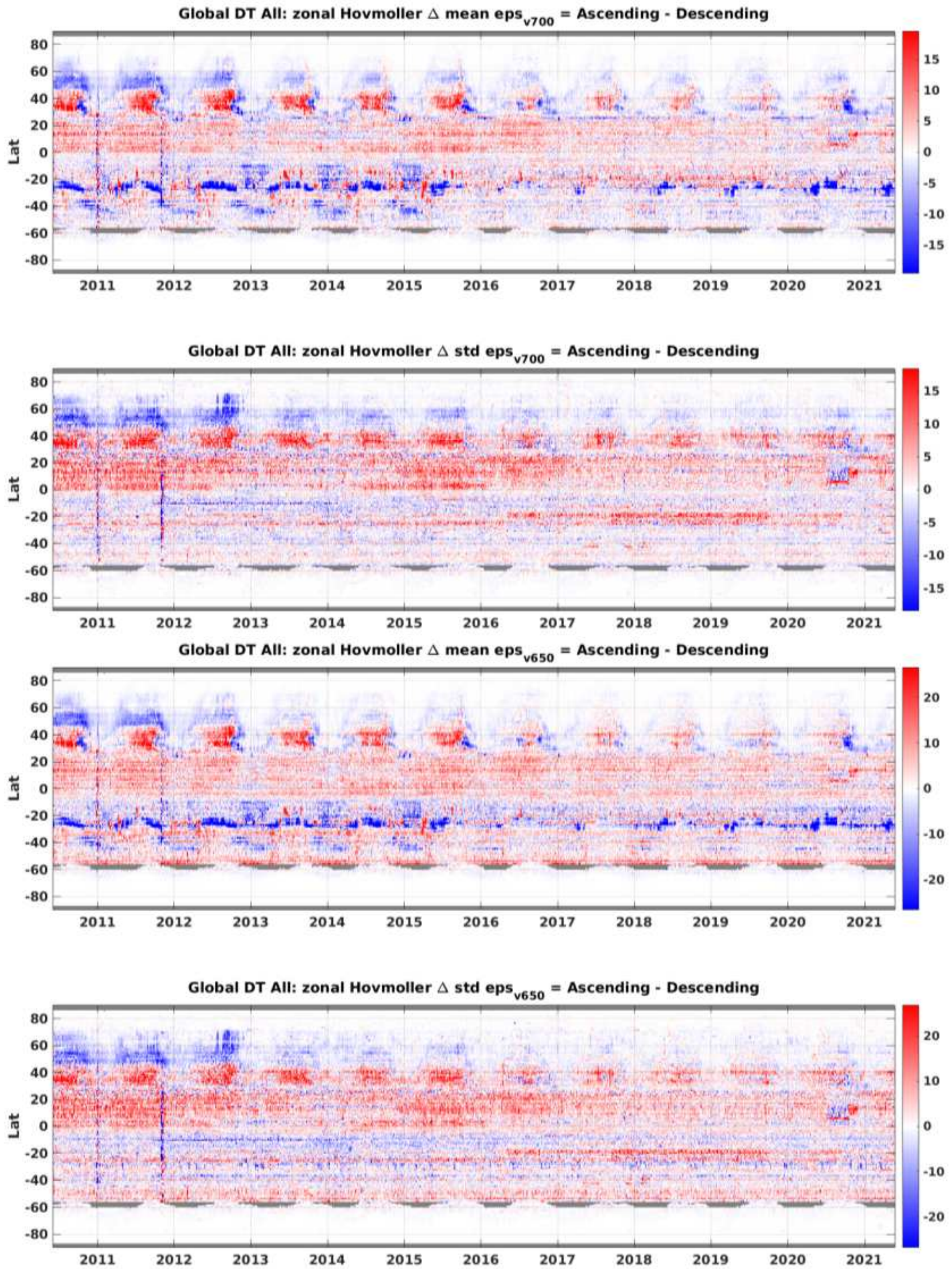

Figure 142: v700 Zonal hovmoller of differences Ascending – Descending for mean ; 1st and 2nd row v700, 3rd and 4th row v650.

5 THEMATIC PERSPECTIVES

5.1 VEGETATION OPTICAL DEPTH

5.1.1 GENERAL VOD VIEWS

This part is dedicated to evaluate the VOD (Vegetation Optical Depth). The first figures present global maps of VOD, averaged over the 2011-2019 period, for both ascending descending overpasses, for versions 650 and 720. The differences (right column). They are some differences depending on the areas of interest but it concerns mostly the transitions between the FFO and FNO. Version 650 had very marked transition in terms of VOD whereas version 720 presents smoother transitions, as can be seen on Figure 144, which is a focus over Africa. This is the effect of the joint FNO+FFO VOD retrieval.

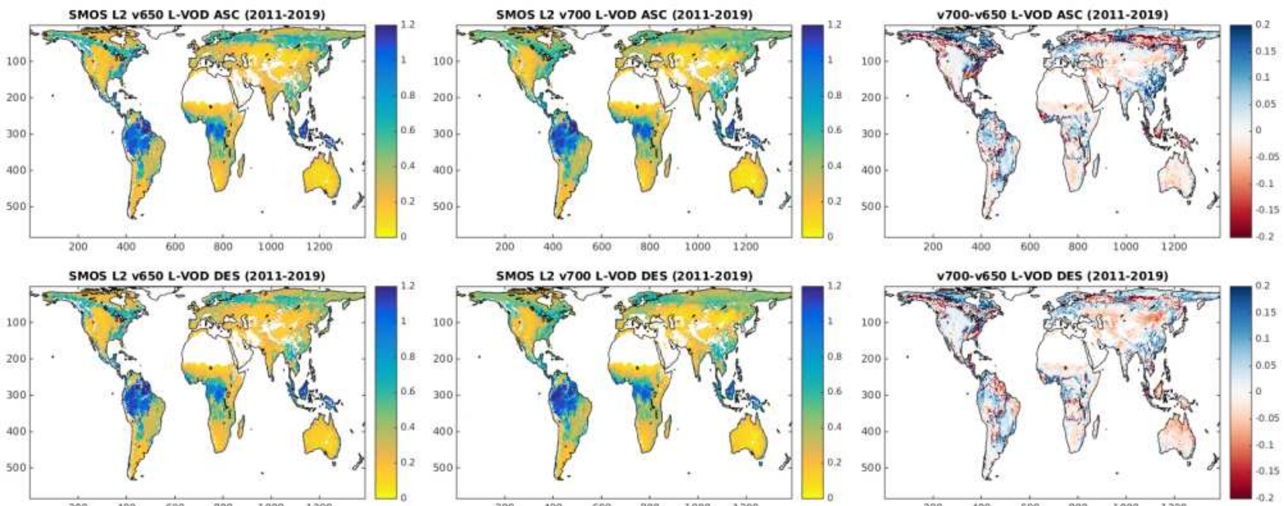

Figure 143: Global map of L-VOD averaged over nine years, a) L2 v650 ASC b) L2 v700 ASC c) difference between L2 v700 ASC and L2 v650 ASC d) L2 v650 DES e) L2 v700 DES f) difference between L2 v700 DES and L2 v650 DES

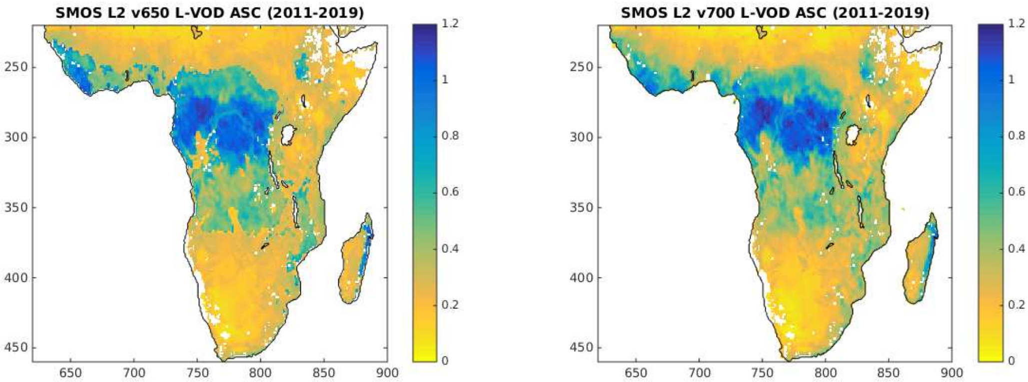

Figure 144: Same as Fig. 1 a) and b) for Africa only. Borders of landcovers are less sharp.

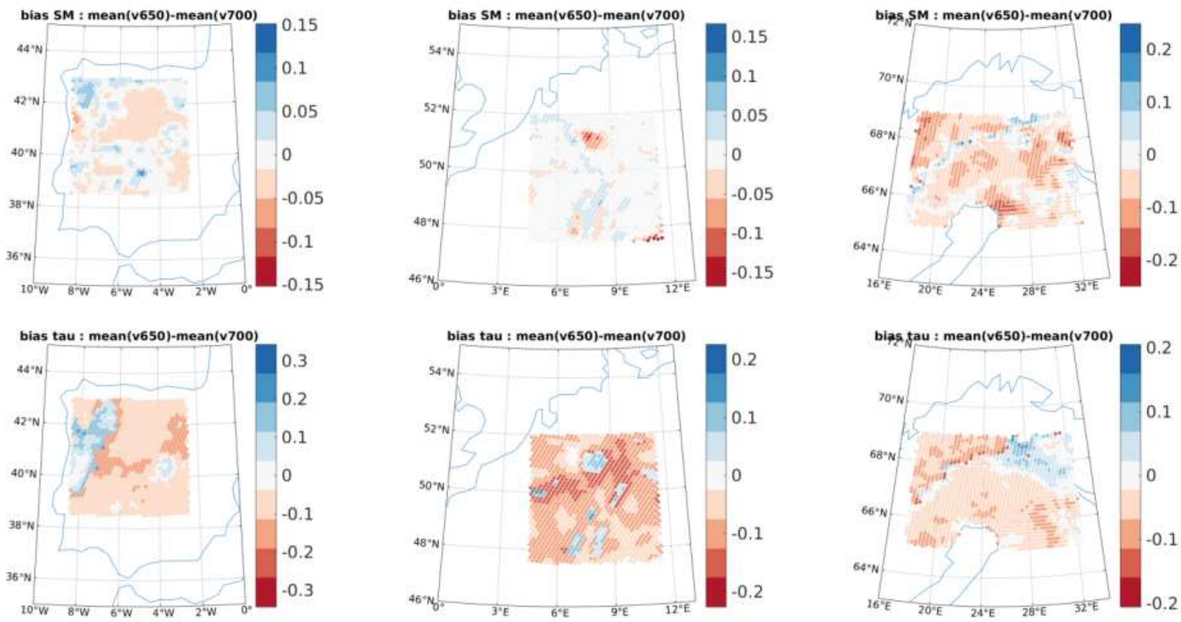

Figure 145: Differences v650 - v700, in terms of SM (top row), VOD (bottom row) for the three areas in Spain, the Netherlands, and North of Finland

This can also be observed in Figure 145, which shows the differences v650 minus v700 in SM and VOD, for the three areas of interest of the Carbon Constellation ESA project. Figure 146 reports the standard deviation of VOD_DQX and one can notice that the VOD_DQX for v700 is higher than for v650, expect over Spain.

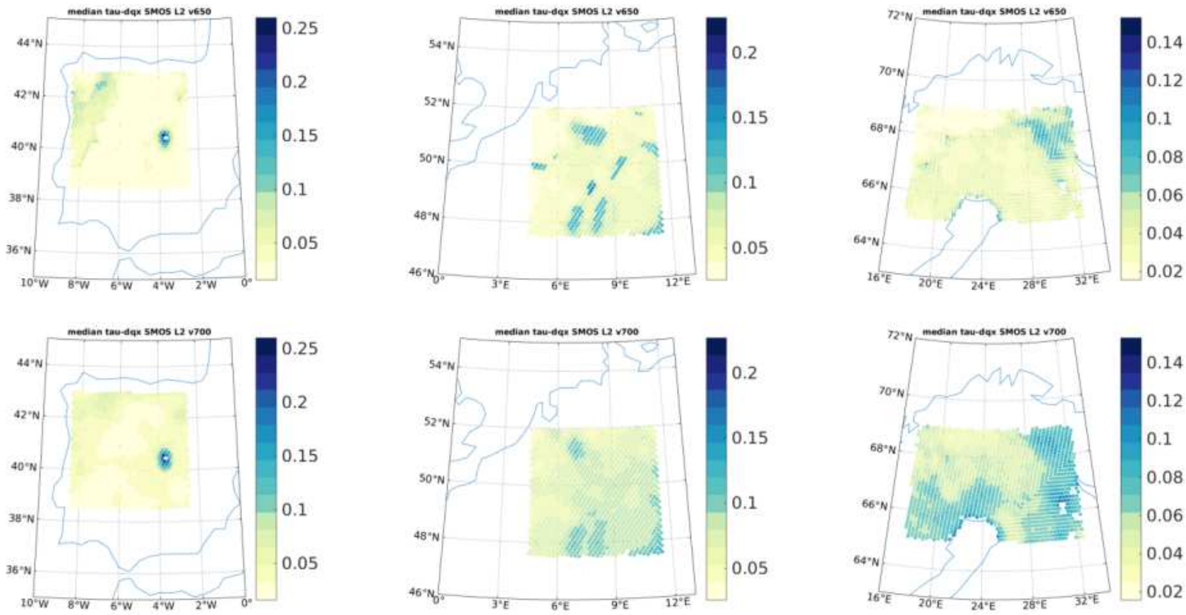

Figure 146: Median Values of SMOS L2 VOD_DQX, for v650 and v700, for Spain, the Netherlands

5.1.2 COMPARISON OF VOD AND AGB

To better assess the evolution of the VOD, it is compared to existing AGB (Above Ground Biomass). The one used here is from ESA CCI biomass project, referred to as GlobBiomass (Santoro et al.). We compared various VOD derived from the L2v650, L2v700, Current files (AUX_DGGCUR) L2v700 and SMOSIC v105. All R coefficients are high showing a good relationship between L-VOD and AGB. The new v700 (2nd column from the left) is clearly an improvement compared to v650, in terms of R and dispersion (less spread). It is confirmed over Amazonia (Figure 146) where the L-VOD v700 performs the best compared to all the VODs.

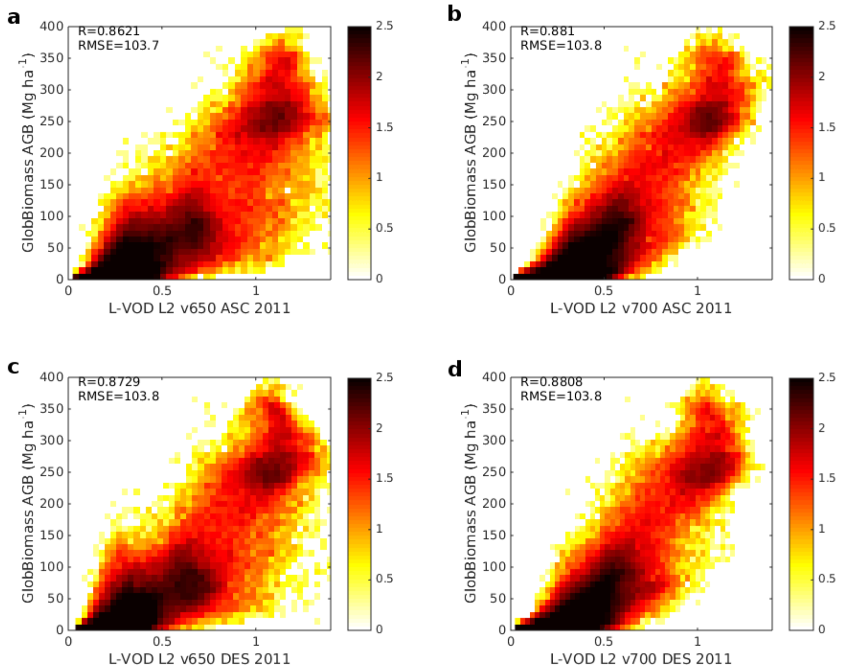

Figure 147: Scatterplot AGB 2010 vs L-VOD 2011 a) L2 v650 ASC b) L2 v700 ASC c) L2 v650 DES d) L2 v700 DES. Global scale.

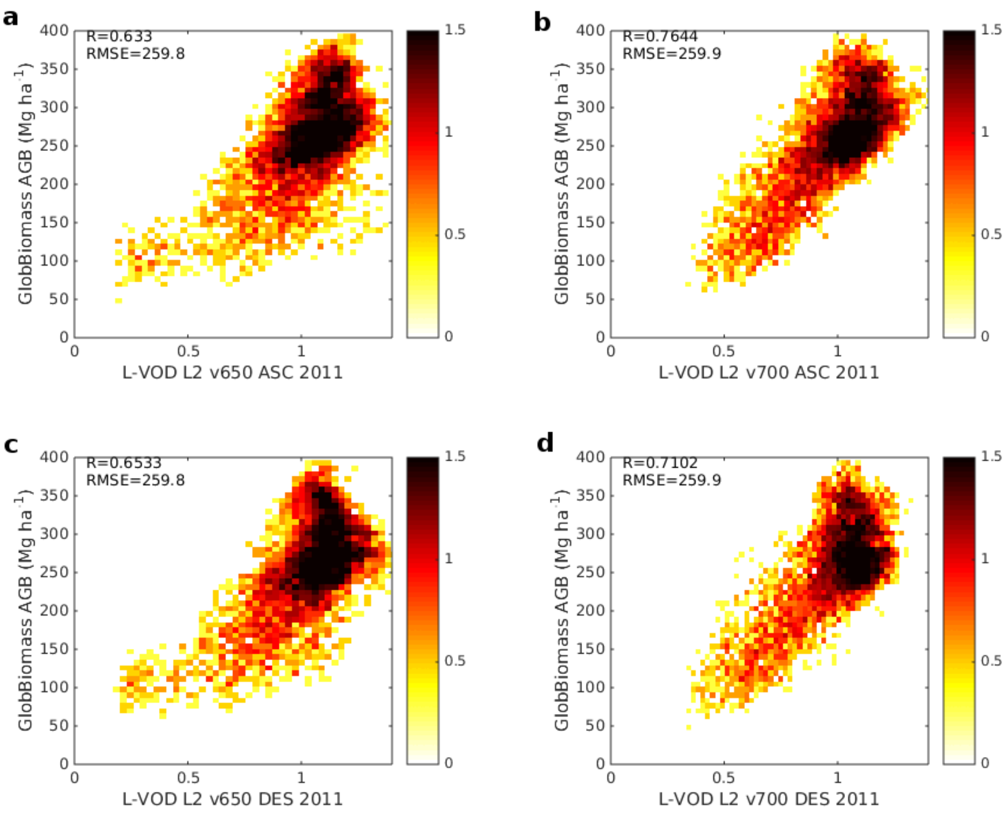

Figure 148: Same as Fig. 3 for the Amazon forest only

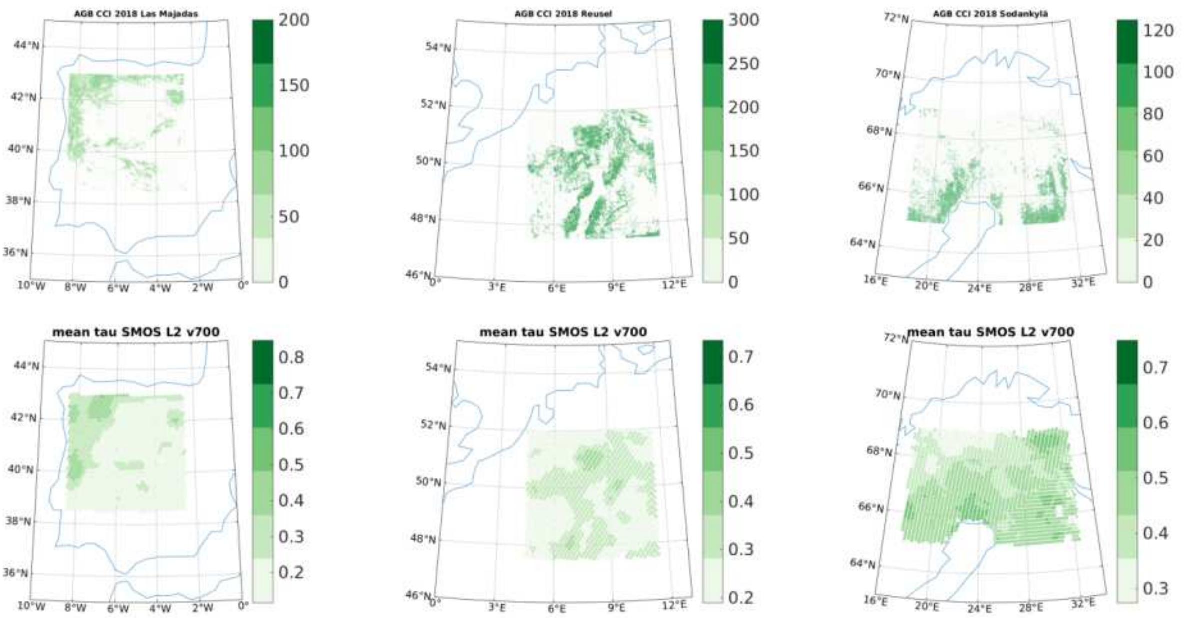

Figure 149: Comparison of L2v700 and above ground biomass (top row) from the ESA-CCI biomass project

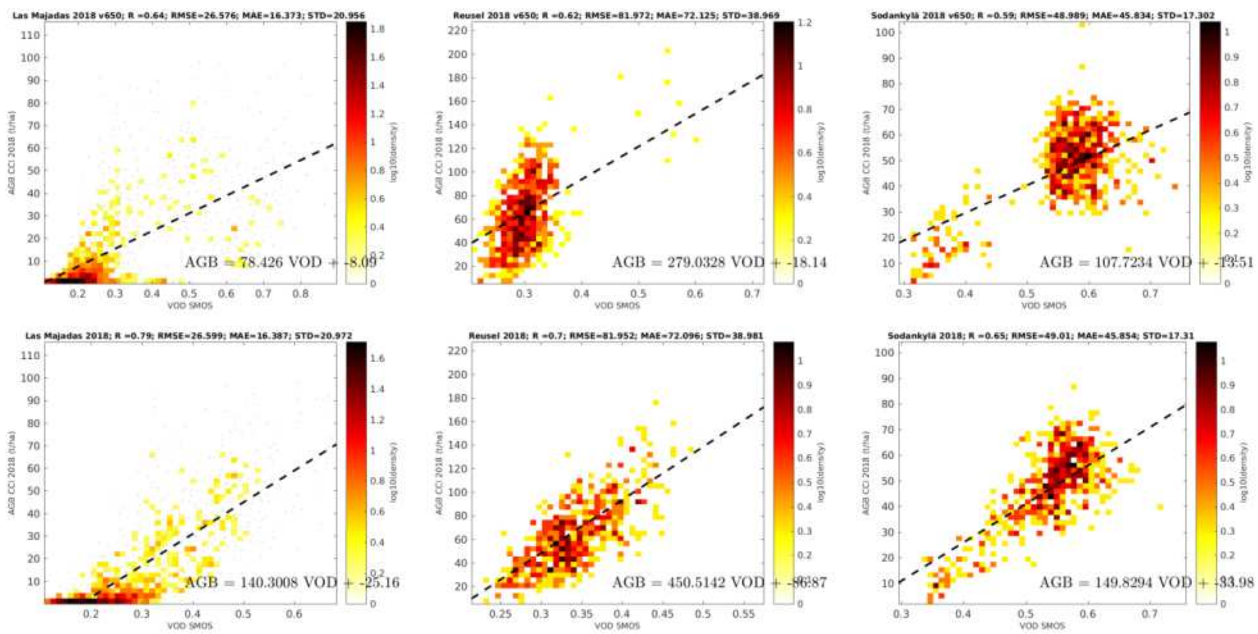

Figure 150: Above Ground Biomass (AGB, for 2018, CCI Biomass) as a function of SMOS VOD (v650 top row, v700 bottom row), for the three sites of Land Carbon Constellation project (from left to right : Mas Majadas in Spain, Reusel in the Netherlands, Sodankyla in Finland)

5.1.3 FOCUS ON VOD TIME SERIES OVER PANTANAL, NORTH-WEST AMAZON AND HARVARD FORESTS

We then present monthly averages as time series for various regions (spatial averages), in the Pantanal (flooded grasslands, South Amercia), North-West Amazon rainforest (South America), Harvard forest (Massachusetts, North America), and Central Congo Basin rainforest (Africa).

Over the Pantanal, all VOD present similar seasonal cycles, with v700 having higher values (~0.1 higher).

However, more investigations is needed over other areas (North West Amazonia, the Havard forest, Congo bassin, as the results between v650 and v700 and very different in terms of seasonal cycles, as they can be opposite. Current and future investigations imply to check SMOS TB.

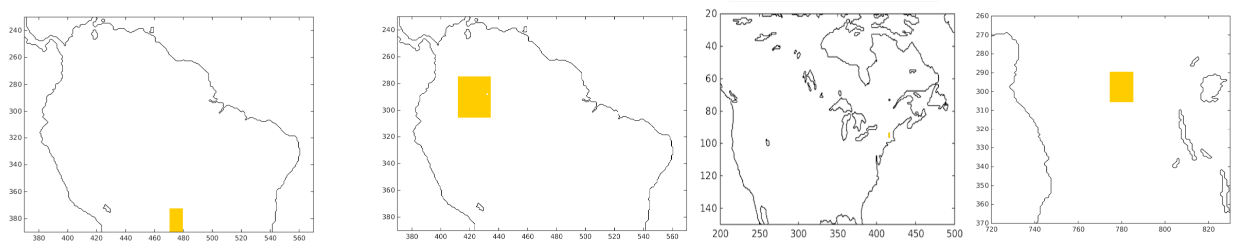

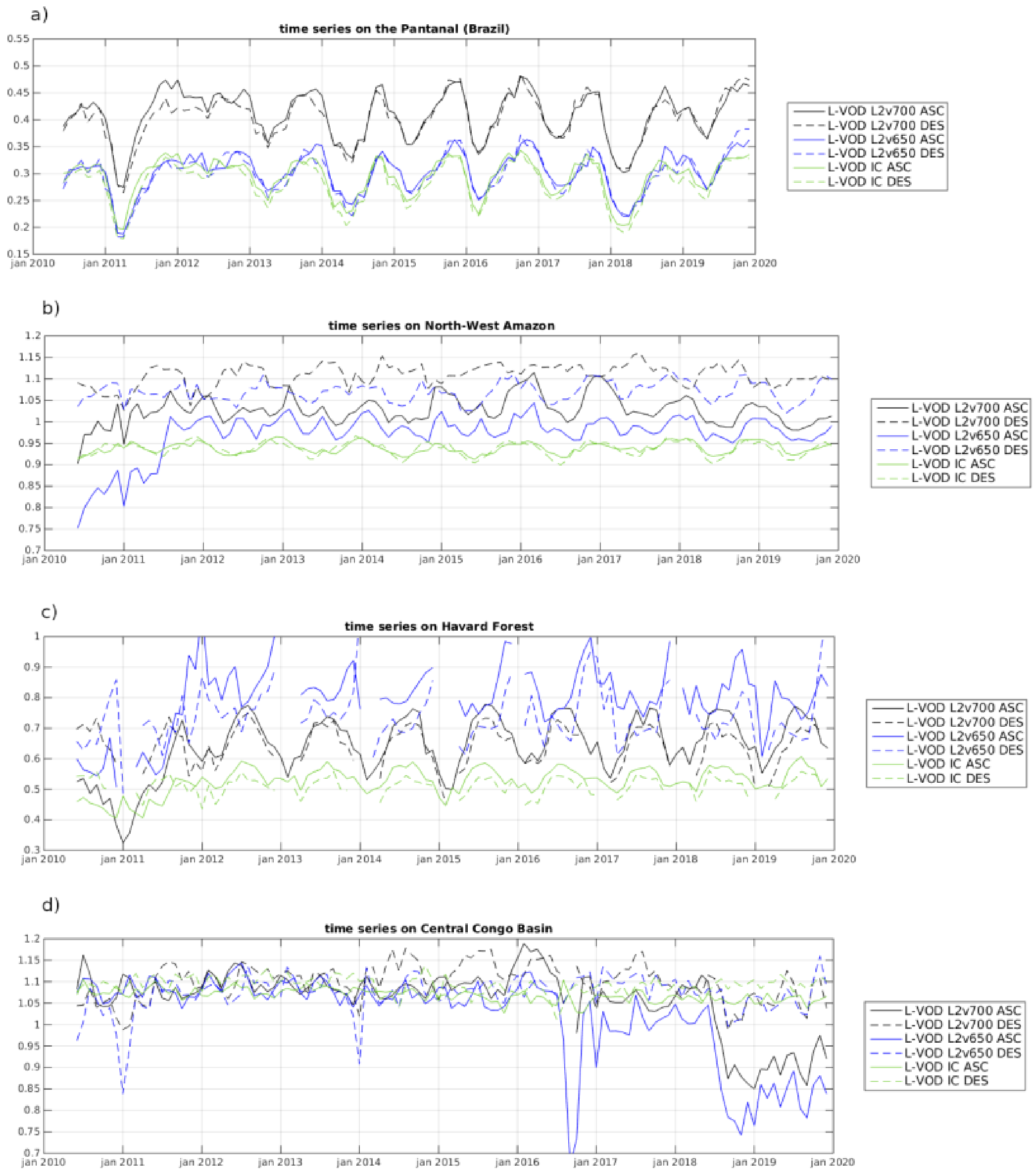

Figure 151: – a) Location of four areas of interest : the Pantanal (flooded grasslands), North-West Amazon rainforest, Harvard forest (Massachusetts), and Central Congo Basin rainforest. b), c), d), e) Time series of L-VOD in these four areas, with L2v700 in black, L2v650 in blue, SMOS-IC v105 in green.

5.1.4 COMPARISON OF VOD WITH GEDI

In this Section, comparisons between the SMOS L-VOD and RH100 and PAI parameters retrieved by Global Ecosystem Dynamics Investigation (GEDI) are reported.

GEDI is a NASA mission aimed at monitoring the Earth ecosystems status with particular focus on deforestation and its impact to the increase of the atmospheric CO_2 concentrations. The GEDI mission is based on a full-waveform LIDAR instrument installed on-board the International Space Station to provide the first global, high-resolution observations of forest vertical structure [AD5]. The GEDI mission is operational since April 2019 and is planned to last for two years, with the capability of producing billions of full waveform observation per year [AD6, AD7].

GEDI is not an imaging instrument, but there are gaps among its ground tracks and between adjacent swaths. The gaps decrease as a function of latitude, mission length and at orbital cross-over points. Anyway, during the planned lifecycle, GEDI will provide a fine mesh of transect observations in order to ensure the mission goal of collecting the first high-resolution lidar observations of the 3D structure of forests on the Earth.

During GEDI's 2 year mission lifetime, waveform measurements are planned to cover the Earth's surface between 51.6°N and 51.6°S latitudes, resulting in approximately 10 billion observations of the Earth's land surface in absence of clouds. The sampling pattern is designed to maximize the geographic coverage of these observations by exploiting the GEDI configuration which is based on three lasers (two full power and a coverage one). The GEDI lasers generate four beams that are dithered to achieve data collection along a swath made of 8 tracks, of 25 m diameter footprints, separated by 600 m in across track direction.

The "coverage" laser is split into two transects that are then each dithered producing four ground transects. The other two lasers are dithered only, producing two ground transects each [AD5].

In this report, we will consider RH100 and PAI parameters measured by GEDI.

The RH100 metric represents the maximum above-ground height of the canopy within a footprint. This parameter has a key role in the analysis of the present report. The plant area index (PAI) is defined as one half of the total of all canopy structural elements (e.g. leaves, branches and trunks) area per unit ground surface.

The GEDI L2B data are provided by NASA as granule products [1]. Each granule contains one orbit in a ±52° range of latitudes. The L2B products are provided as HDF files which contain the lidar parameters and the ancillary information (e.g. geographic coordinates for each footprint, quality flags, etc.) for the four beams of the instruments. Every L2B product contains information sampled on both land and sea and this aspect has been considered in the pre-processing of the data.

The GEDI RH100 L3 product [AD8] is available as an average map of RH100 values from one year of GEDI data. The timeframe is 12 months constrained by the availability of GEDI data, namely from May 2019 to April 2020. The data was averaged to the SMOS spatial resolution and then reprojected on the SMOS DGGs grid.

5.1.4.1 GEDI VS. SMOS ASSOCIATION

The aim of the pre-processing performed in this work is the production of aggregated values of GEDI parameters at the SMOS spatial resolution and the computation of monthly averages of these aggregated data sets. For ensuring the comparability of the GEDI L2B data and the SMOS L2 VOD data a dedicated workflow has been applied.

The workflow consists in the following steps:

- Pre-processing of the GEDI L2B granules in order to eliminate the samples over sea or large inland water areas and lidar beams observations flagged as unsuccessful retrievals.
- Association of the resulting GEDI footprints of each granule to the ISEA4h9 Discrete Global Grid (DGG).
- Taking benefit of the slow variations of SMOS L-VOD and GEDI parameters vs. time, monthly average values of SMOS L-VOD were considered. For each month and SMOS node, a 45 km diameter circle was taken, and the average values of GEDI parameters were computed considering all GEDI footprints which fell within the circle in the considered month.

Outputs of this procedure are monthly average of the RH100 and PAI parameters, ready to be used in further analyses. The work was done for four large continental areas, with coordinate limits specified in Table 9. Within the latitude range covered by GEDI, Europe and Oceania showed a low number of SMOS pixels, particularly for dense forests, and were not included.

Table 9: Considered continental areas for GEDI comparisons and relevant coordinate limits

Area	Lower latitude (°)	Upper latitude (°)	Western longitude (°)	Eastern longitude (°)
North America	20	52	-140	-50
South America	-52	20	-90	-30
Africa	-52	20	-20	50
Asia	-15	52	70	150

SMOS L3 data was averaged to the SMOS spatial resolution and then reprojected on the SMOS DGGs grid. Comparisons against L3 data were done using again the continental areas of Table 9.

5.1.4.2 SPATIAL RESOLUTION ISSUES

Although a correlation between SMOS L-VOD and the GEDI parameters consideredhere (such as RH100 and PAI) is justified by physical considerations, the fundamental problem of spatial resolution must be considered. GEDI footprints are narrow, with about 25 m resolution, 60 m spacing, and a large distance between subsequent orbits.

After applying the procedure described in Section 5.1.4.1, the spatial correlation coefficients (Pearson coefficients) between SMOS L-VOD's and the average values of GEDI parameters were computed for each month and different continents. In order to ensure a sufficient coverage of the SMOS pixels, computations were carried out after excluding SMOS pixels for which the total number of GEDI samples was lower than given thresholds.

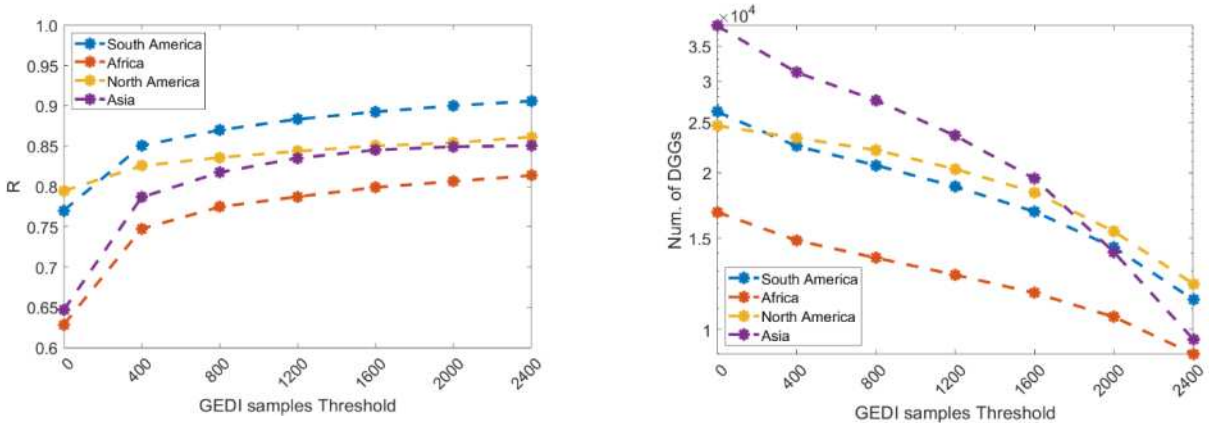

Figure 152: Pearson correlation coefficient of a July 2019 SMOS L-VOD vs GEDI RH100 (cm) regression as a function of the threshold applied to the number of GEDI samples per SMOS pixel. Right: Number of SMOS DGGs.

A quantitative summary of the effects of threshold is reported in Figure 152, in which a regression between SMOS L-VOD and GEDI RH100 was computed. The Pearson correlation coefficients and the number of available SMOS nodes are plotted as a function of the threshold applied to the number of GEDI footprints per SMOS pixel. The cases of July 2019 is considered. Obviously, increasing the threshold produces a decrease in the number of available SMOS nodes, but a significant number (about 10,000 for one month,) is still available for a threshold of 2400. Conversely, increasing the threshold improves the statistical characterization of the extended SMOS pixels. Therefore, the correlation coefficients increase with the threshold, particularly in the range of lower values. For a threshold of 2400, correlation coefficients are higher than 0.8 for all continents It was verified that forcing thresholds higher than 2000-2400 reduces the number of SMOS nodes producing moderate improvements in the correlation while weakening the statistics strength.

Results reported in the subsequent Sections were obtained after eliminating SMOS pixels for which the total number of GEDI samples was lower than 2400.

5.1.4.3 L-VOD VS. RH100 SCATTERPLOTS

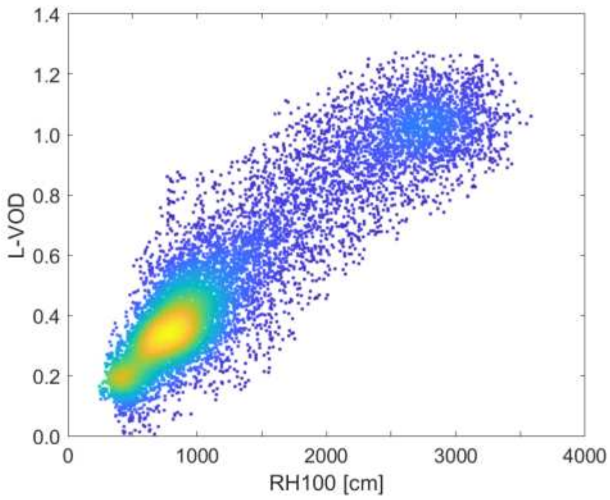

a) South America July 2019

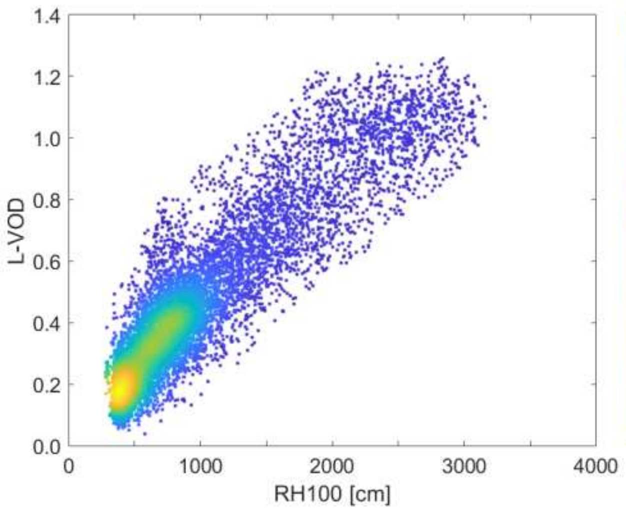

b) South America January 2020

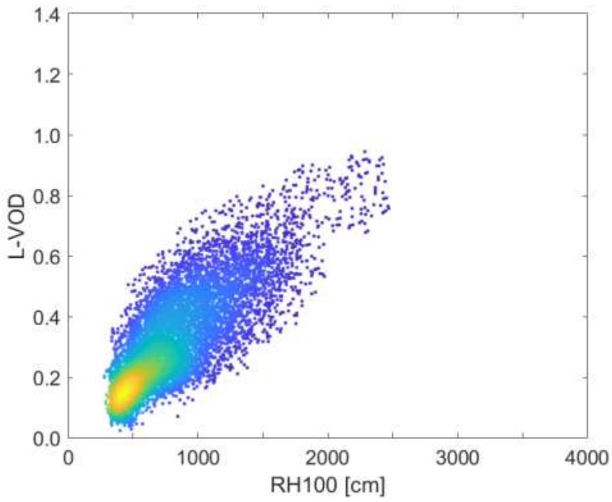

c) Africa July 2019

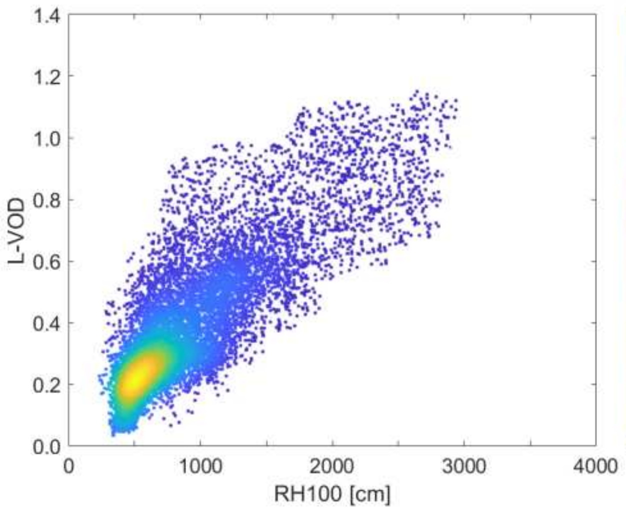

d) Africa January 2020

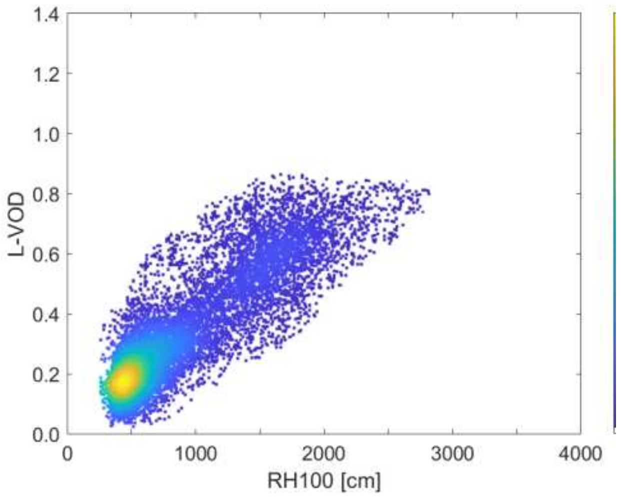

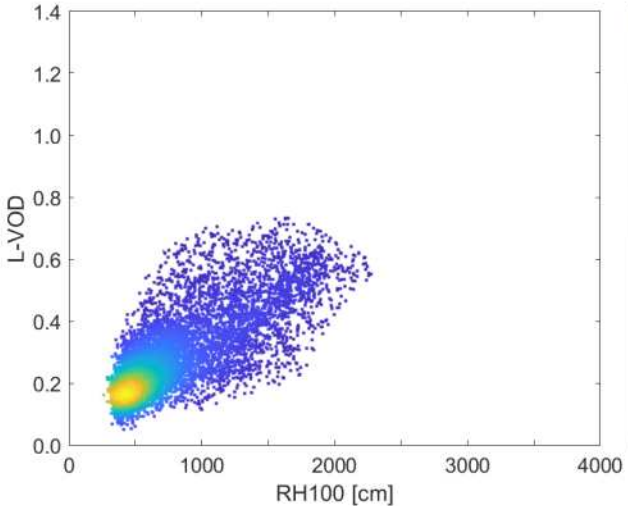

e) North America July 2019

f) North America January 2020

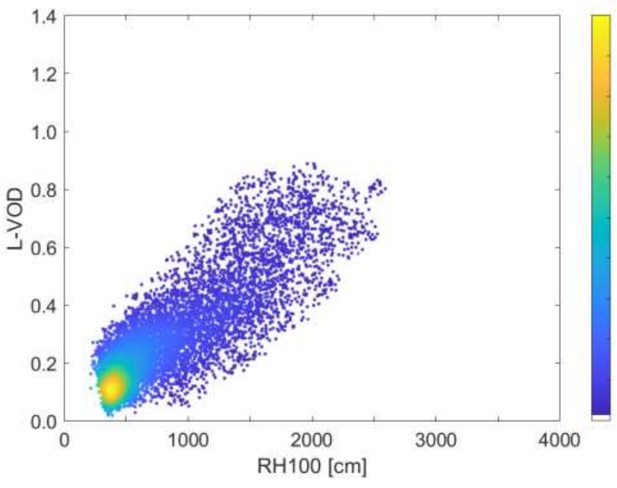

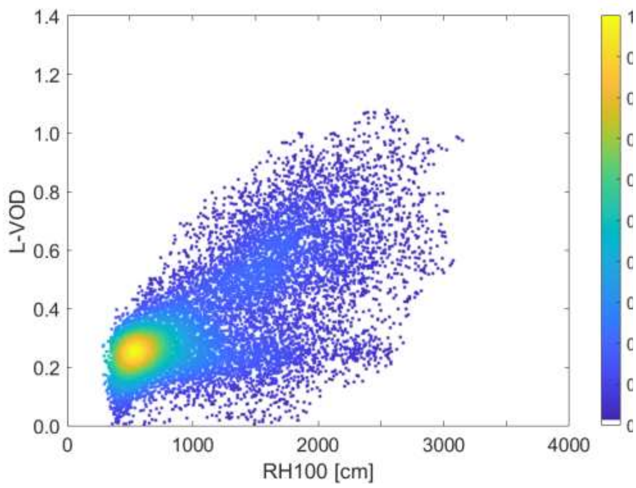

g) Asia July 2019

h) Asia January 2020

Figure 153: Density Scatterplots SMOS L-VOD vs RH100 (cm). From top to bottom: a-b) South America, c-d) Africa, e-f) North America, and g-h) Asia. Left: July 2019. Right: January 2020.

Figure 153 reports scatterplots of SMOS L-VOD vs. GEDI RH100 (cm) obtained considering all available SMOS pixels, for July 2019 and January 2020 and the continental areas indicated in Table 9. Relevant correlation coefficients will be given in subsequent Sections.

In the figures, the color codes represent the values of density (in fraction) of the SMOS pixels involved.

In July 2019 all scatterplots show a significant increasing trend of L-VOD vs. RH100. The best results are achieved over South America, where several samples are available for both low vegetation and dense forests. For Africa and Asia, the dense forests are located in the Equatorial latitudes (Congo basin and Indonesian islands, respectively), for which GEDI orbits provide a limited number of samples, as already found in [AD6]. For North America the RH100 and L-VOD ranges are limited.

Seasonal changes, from July to January, mostly produce effects in Boreal forests of North America and Asia. Here low temperatures, often associated with snow and soil freezing, mostly reduce L-VOD, while defoliation of deciduous forests could affect both L-VOD and RH100.

The recent study of Schwank & al. [AD9] (an advancement of the Technical Note SO-TN-ESLG-GS-0007) has laid the ground to explain the distinct drop in L-VOD when canopy temperature falls below the freezing point. In this study, a novel physics-based model is developed and evaluated to assess L-VOD sensitivities to canopy temperature. The model is compared to L-VOD derived from close-range and SMOS L3TB over the "Sodankylä grid cell". It is demonstrated that L-VOD are maximal at around 0°C and decrease when canopy temperature is moving away from zero degree Celsius. This characteristic L-VOD temperature response is explained by freezing tree sap-water and the dependence of water permittivity on temperature. It explains the larger seasonal dynamics in L-VOD observed by Mialon & al. [AD10]. for boreal forests than for temperate forests

5.1.4.4 REGRESSION ANALYSIS OVER DIFFERENT CONTINENTS

The present study can be used to investigate a possible role of GEDI parameters in the estimation of the prior value of L-VOD, which is used in SMOS L2 algorithm, or in downscaling the retrieved L-VOD. To this aim, we have computed the coefficients of a regression such as:

$$\text{L-VOD} = b' \, \text{RH100} + b'' \qquad (1)$$

The investigation was carried out for each month and each continent. Only cases in which the number of GEDI samples per SMOS pixel was higher than 2400 and number of available SMOS pixels was higher than 5000 were considered.

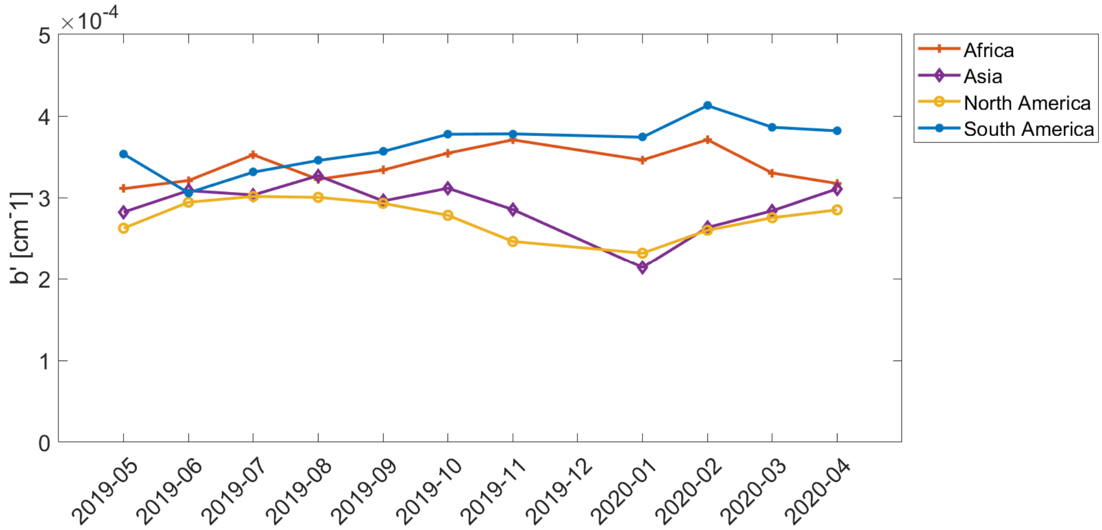

Figure 154: Temporal trends of *b'* (cm^{-1}) coefficient (Eq. 1) for four continental areas (v700).

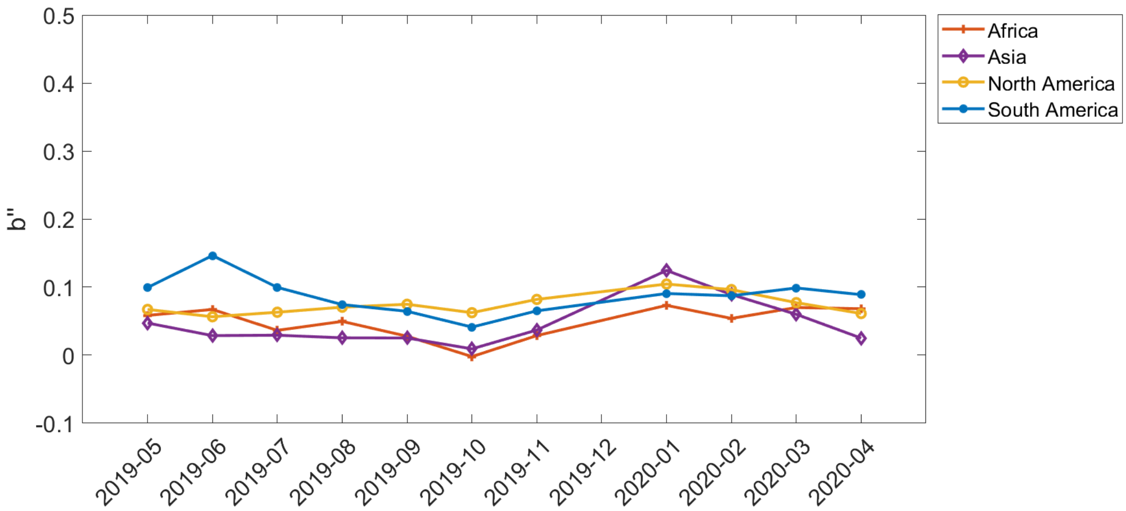

Figure 155: Temporal trends of *b''* coefficients (Eq. 1) for four continental areas (v700).

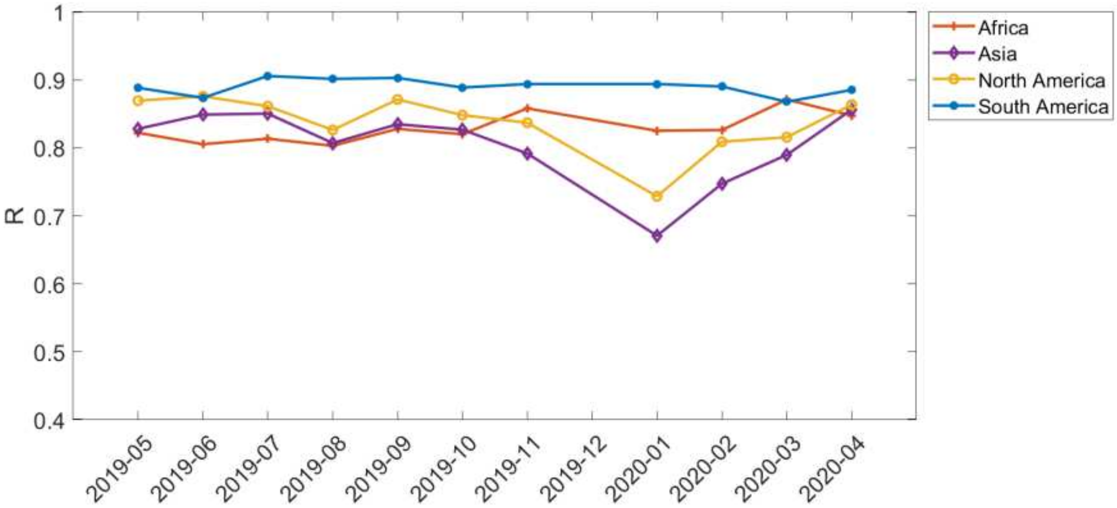

Figure 156 Temporal trends of Pearson correlation coefficient (Eq. 1) for four continental areas (v700).

Results obtained for *b′*, *b″* and Pearson correlation coefficient are reported in Figure 153, Figure 154, Figure 155 and Figure 156 respectively.

December 2019 was not included, since the number of available SMOS pixels was lower than 5000 for all continents.

In the time interval from May to September the *b′* coefficients of the different continents are relatively close to each other. In the subsequent months, seasonal effects are observed in Boreal Forests of North America and Asia, with *b′* reaching a minimum in January.

According to Figure 155, *b″* values (representing the intercept of the linear trend) are inside a limited 0 - 0.1 range in almost all cases. This indicates that the linear trend is followed and saturation effects are moderate for all cases.

Correlation coefficients reported in Figure 156 are higher than 0.7, except for Asia in January 2020.

The same analysis was repeated with 650 version of SMOS L-VOD. Results are reported in Figure 157, Figure 158 and Figure 159. b″ values (Figure 158) are similar to the ones obtained with the version 700 (Figure 155), while b′ values for the different considered areas (Figure 157) show a larger spread with respect to ones of v700 (Figure 154). Finally, all correlation coefficients obtained with 650 version (Figure 159) are lower than ones of 700 (Figure 156).

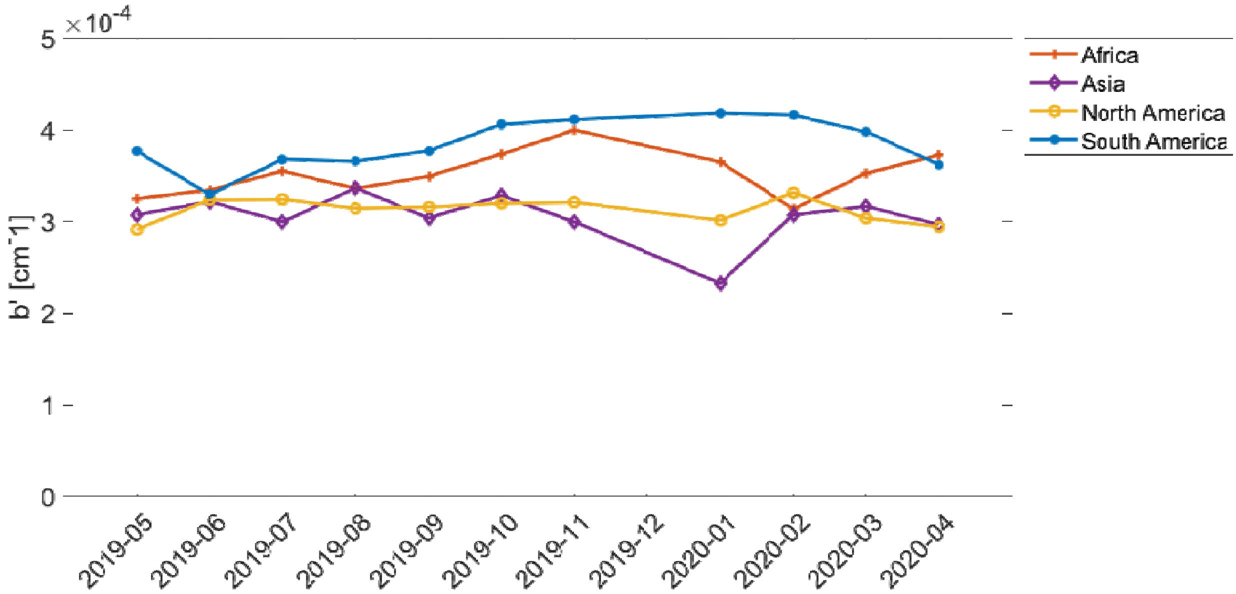

Figure 157: Temporal trends of *b'* (cm^{-1}) coefficient (Eq. 1) for four continental areas (v650).

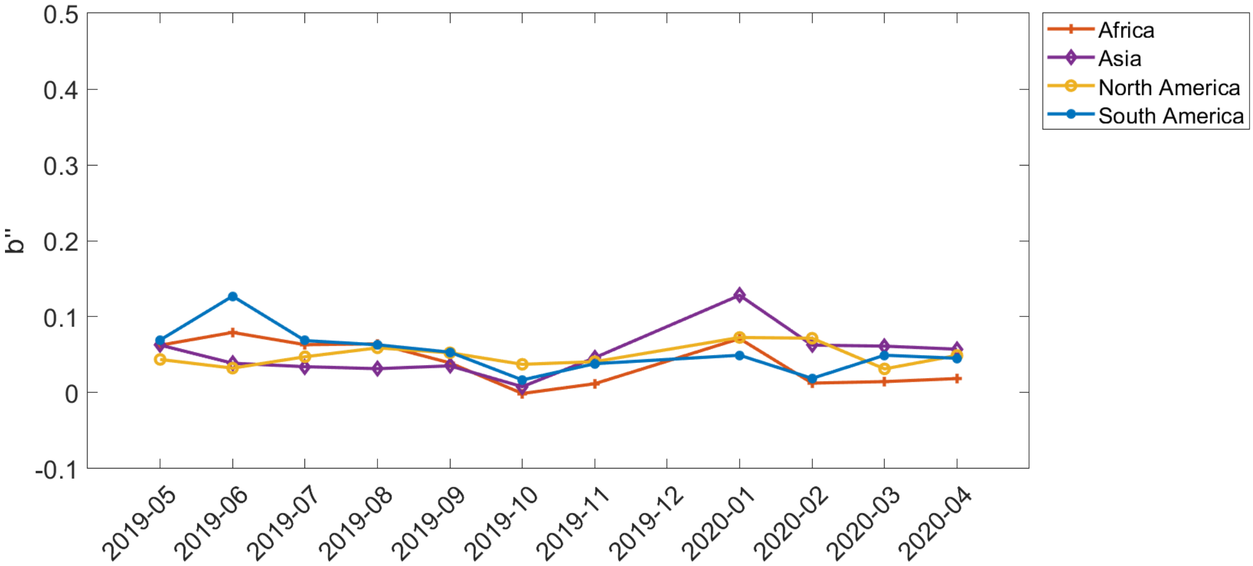

Figure 158: Temporal trends of *b″* coefficients (Eq. 1) for four continental areas (v650).

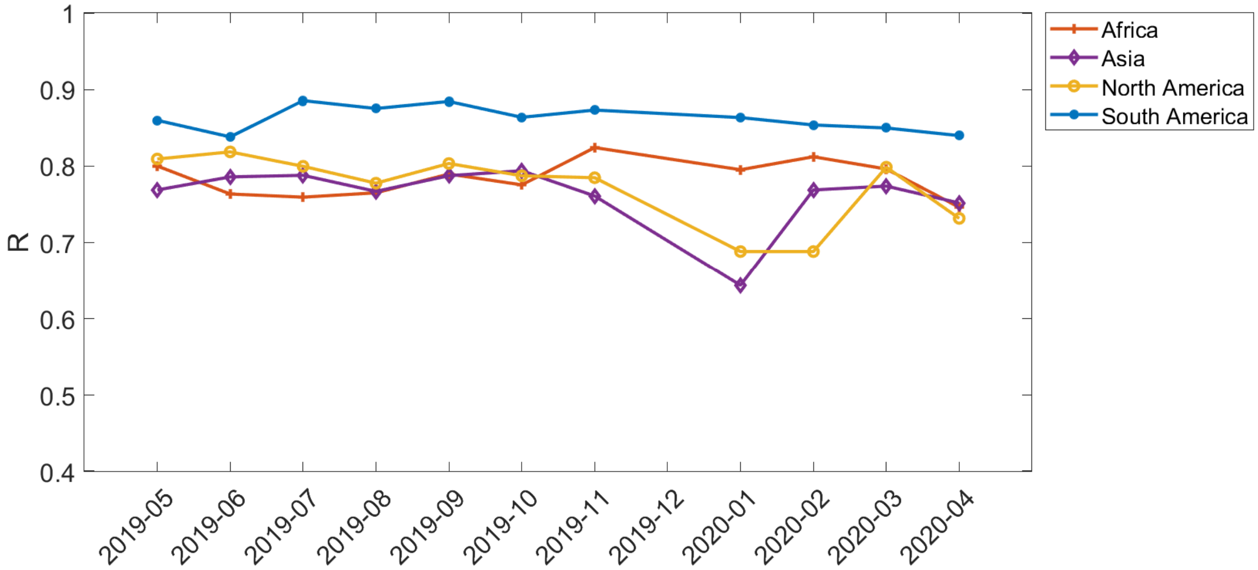

Figure 159: Temporal trends of Pearson correlation coefficient (Eq. 1) for four continental areas (v650).

5.1.4.5 CORRELATION COEFFICIENTS OF L-VOD WITH RH100 AND PAI

Pearson correlation coefficients of the regression of L-VOD versus RH100 and PAI for July 2019 and January 2020 are summarized in Table 10.

Table 10 Pearson correlation coefficients of the regression of L-VOD (retrieved by v700) versus RH100 and PAI for July 2019 and January 2020

	RH100 July 2019	RH100 January 2020	PAI July 2019	PAI January 2020
North America	0.86	0.73	0.78	0.64
South America	0.91	0.89	0.89	0.88
Africa	0.81	0.83	0.80	0.83
Asia	0.85	0.68	0.83	0.75

In July 2019 all coefficients are higher than 0.80 for RH100 and 0.77 for PAI. The best results are achieved in South America, characterized by a large fraction of pixels with large forests, well captured both by SMOS L-VOD and GEDI parameters. In all continents, the replacement of RH100 with PAI does not produce improvements.

For North America and Asia/Oceania seasonal effects are clearly visible, producing an appreciable worsening in the correlation coefficients of January, with respect to the ones of July. This issue was already discussed previously. Conversely, results are stable for South America and Africa, mostly covered by evergreen vegetation.

Table 11: Pearson correlation coefficients of the regression of L-VOD (retrieved by v650) versus RH100 and PAI for July 2019 and January 2020

	RH100 July 2019	RH100 January 2020	PAI July 2019	PAI January 2020
North America	0.80	0.69	0.71	0.58
South America	0.88	0.86	0.86	0.86
Africa	0.76	0.79	0.74	0.79
Asia	0.79	0.64	0.76	0.70

The Pearson correlation coefficients obtained using previous v650 version of SMOS L2 algorithms are reported in Table 11. A comparison between Table 10 and Table 11 indicates that the new algorithm produces evident improvements in all cases.

5.1.4.6 COMPARISON OF L-VOD WITH RH100 FROM GEDI L3 PRODUCT

The GEDI RH100 L3 product is available as an average map of RH100 values from one year of GEDI data. The timeframe is 12 months constrained by the availability of GEDI data, namely from May 2019 to April 2020. The data was scaled to the SMOS DGG grid before testing the correlation with the average VOD values in the same time period of the GEDI L3 product. Only v700 data were considered in this case. In Figure 160 the GEDI RH100 L3 at SMOS resolution in reported.

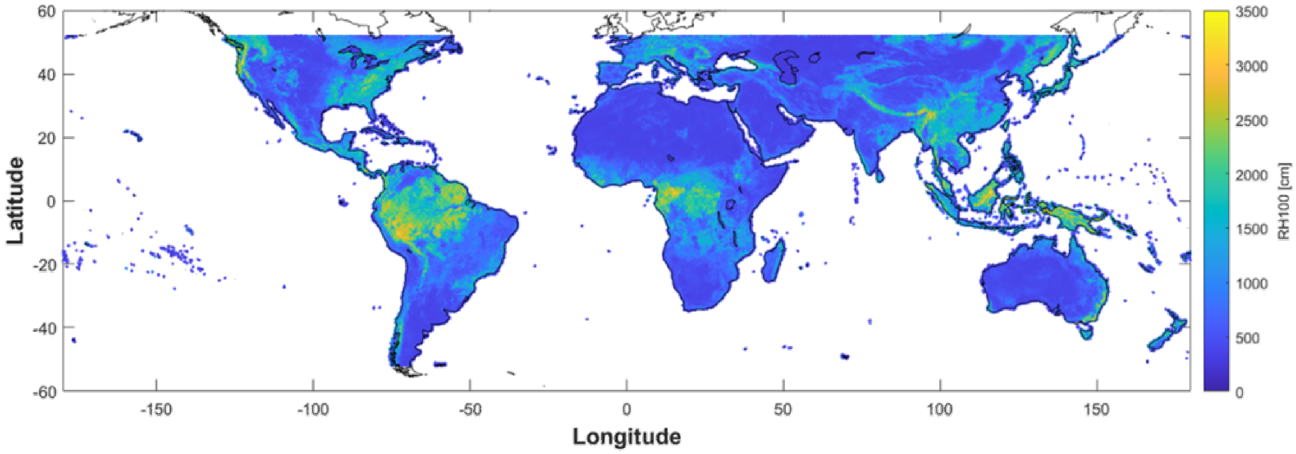

Figure 160: GEDI L3 RH100 at SMOS resolution (01/05/2019 - 30/04/2020)

The correlation between SMOS L-VOD and RH100 was extended to L3 data. To this aim, the time interval between May 2019 and April 2020 was considered. The correlation analysis was conducted only over the SMOS pixels for which the total number of L2 GEDI samples was higher than 2400.

Results are summarized in Table 12, reporting the Pearson correlation coefficients. Results are comparable to the L2 ones reported in Table 11 for July 2019 and generally better than L2 ones for January 2020.

Table 12: Pearson correlation coefficients of the regression of L-VOD (retrieved by v700) versus RH100 (GEDI L3). Time interval: May 2019-April 2020

	RH100
North America	0.88
South America	0.88
Africa	0.83
Asia	0.84

5.2 CRYOSPHERE

5.2.1 INTRODUCTION

This section aims to study and compare the retrievals related to the cryosphere. The first part of this section concentrates on two media: snow and the soil freeze-thaw state. The second part concentrates on comparisons over Greenland. In the first part we consider land areas over 30 degrees latitude excluding Greenland.

5.2.2 SOIL FREEZE & THAW AND SNOW MEDIA

The variables of interest are limited to the dielectric constant and vegetation optical depth. First, these variables are studied separately for both versions 650 and 700, addressing the question whether they behave "reasonably". Second, the variables are compared between the versions to detect possible differences. We are also interested in any strange or unexpected behavior of these variables.

As the context of this section is cryosphere, we will consider the cases where decision tree (DT) values are between 5 and 12. Furthermore, the DT values are grouped into three groups corresponding to snow (SN), frost (RZ),and soil and forest (NO/FO).Table (X) summarizes these DT groups.

Table 13: Grouped decision tree (DT) branches used in the following sections.

DT group used here	N°	Retrieval case
Snow (SN)	5	All wet snow
	6	All mixed snow
	7	Wet snow pollution
	8	Mixed snow pollution
Frost (RZ)	9	All frost
	10	Frost pollution
Soil and forest cover (NO/FO)	11	Forest cover
	12	Soil cover

Our focus is on areal comparisons, either global or local. To this end, variables of interest are averaged over some time period. Maps generated this way are then compared to each other. Most of the results shown are averaged over a period of seven days. It is important to note, that since we limit our comparisons to some DT branch(es) and compare averaged values, it might be that for different versions, the averaged values contain retrievals from different times within this period.

For general inspection and comparison, we make a visual inspection of the retrieval maps as well as look at the histograms of the variables. We compare the (empirical) cumulative distribution functions (CDF) between versions 650 and 700. This is quite crude comparison but will give an idea of the behavior and differences between different versions.

To further study the behavior of the retrievals, we compare both versions 650 and 700 to external data, namely SMOS L3FT product as well as ECMWF snow water equivalent (SWE) estimate. These two are of interest when studying dielectric constant. For vegetation optical depth such comparisons were not done at this time.

5.2.3 DIELECTRIC CONSTANT

5.2.3.1 GLOBAL MAPS AND TIMESERIES

Areal coverage of the main DT branches – temporal evolution for winter period 2018-2019 is presented in following four maps from early October to mid-May. Each map contains the weekly average of the dielectric constant (real part) for selected DT branches.

- In general, areal coverage for chosen DT follows expected logic. Areal coverage for soil/forest (NO/FO) DTs decreases as the winter progress. During winter months, most of the northern latitudes fall into snow (SN) or frost (RZ) DT groups.
- The thresholds for DTs are derived from ECMWF temperature and snow information. For RZ DTs the threshold temperature is set to 270 K (STL1). For dry snow the threshold is set to -12^{o}C (snow skin or air temperature?), wet snow threshold temperature is set to -2^{o}C. Soil frozen DTs are thus selected if soil temperature is low enough and there is either no snow or dry snow cover. During winter period the selected DT branches are mostly either SN DTs or RX DTs at high latitudes, as expected.
- The weekly mean dielectric constant (real part) is highest for NO/FO and lowest for RZ as expected.

Interesting observations from the areal coverage maps

- In Canada on Northwest Territories, particularly, on region between Great Slave Lake and Great Bear Lake, the dielectric constant is on average higher than on the surrounding areas.
- In Finland and on Central Siberia, NO or FO DT is occasionally selected throughout the winter period

Based on the observations above, three areas were selected for regional analysis. These areas were

- Finland and its surroundings– latitude and longitude range: 60-70N; 15-35E
- North America(Alaska and Canada) – 55-71N; 50-170W
- Central Siberia – 60-80N; 70-120E

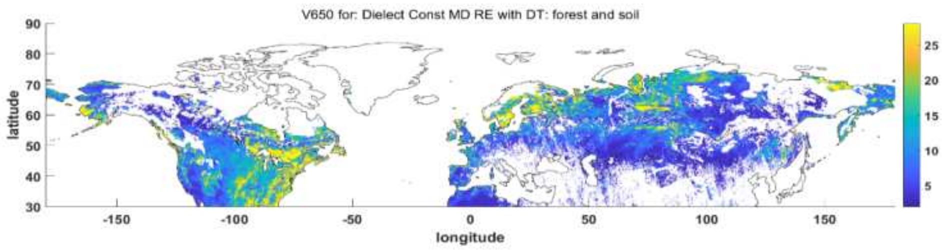
V650 for: Dielect Const MD RE with DT: forest and soil
latitude
90
80
70
60
50
40
30
-150
-100
-50
0
50
100
150
longitude
25
20
15
10
5

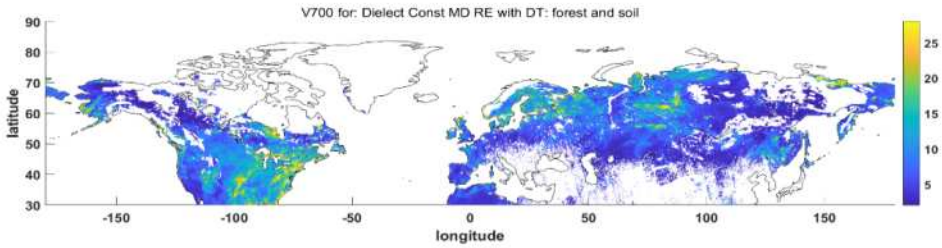
V700 for: Dielect Const MD RE with DT: forest and soil
latitude
90
80
70
60
50
40
30
-150
-100
-50
0
50
100
150
longitude
25
20
15
10
5

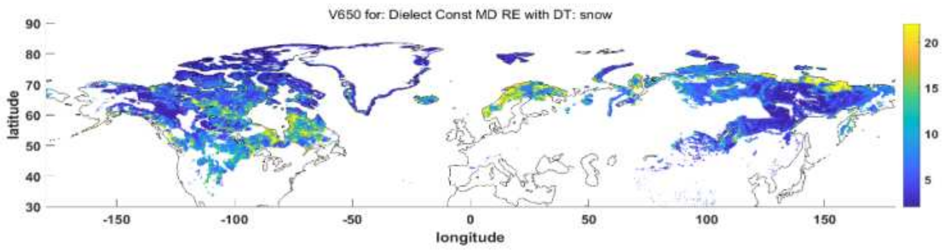
V650 for: Dielect Const MD RE with DT: snow
latitude
90
80
70
60
50
40
30
-150
-100
-50
0
50
100
150
longitude
20
15
10
5

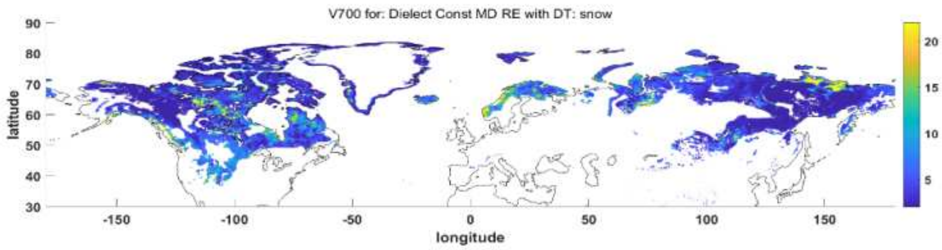
V700 for: Dielect Const MD RE with DT: snow
latitude
90
80
70
60
50
40
30
-150
-100
-50
0
50
100
150
longitude
20
15
10
5

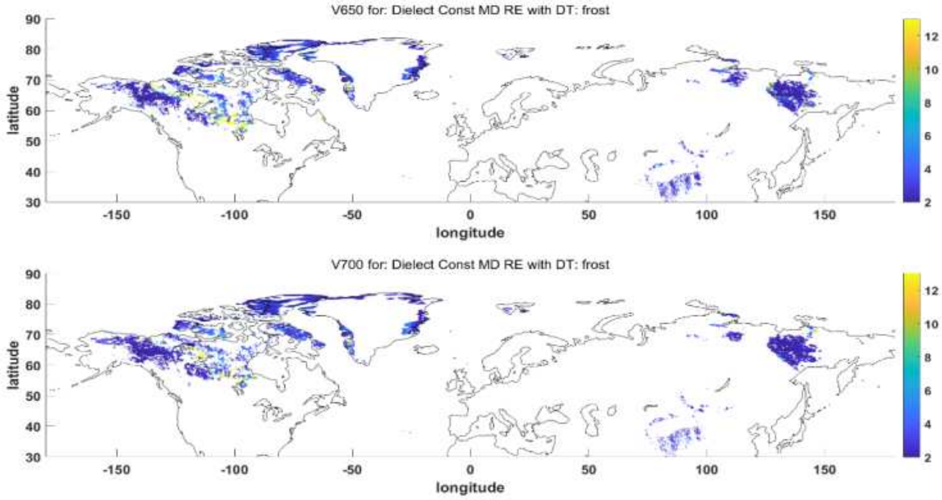

Figure 161: Dielectric constant real part, 7-Oct-2018 – 13-Oct-2018, top: forest and soil (FN & FO), middle: snow, bottom: frost

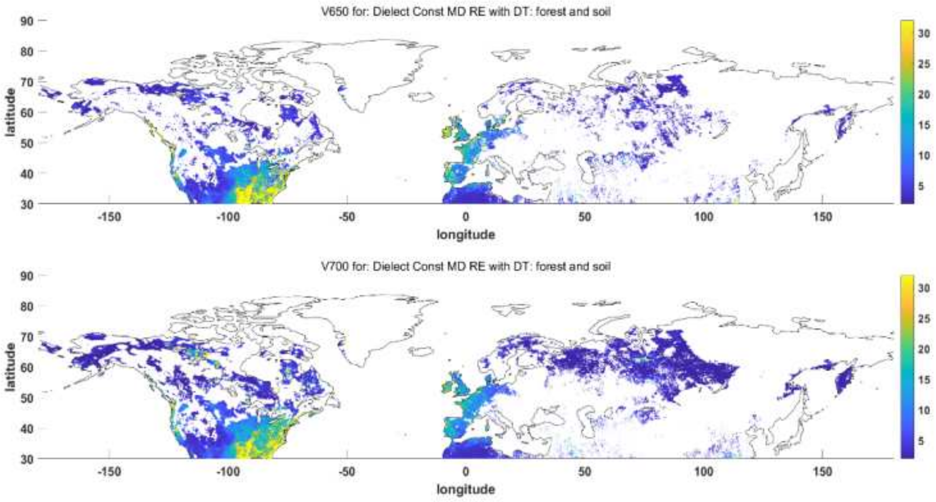

V650 for: Dielect Const MD RE with DT: forest and soil
V700 for: Dielect Const MD RE with DT: forest and soil
latitude
longitude

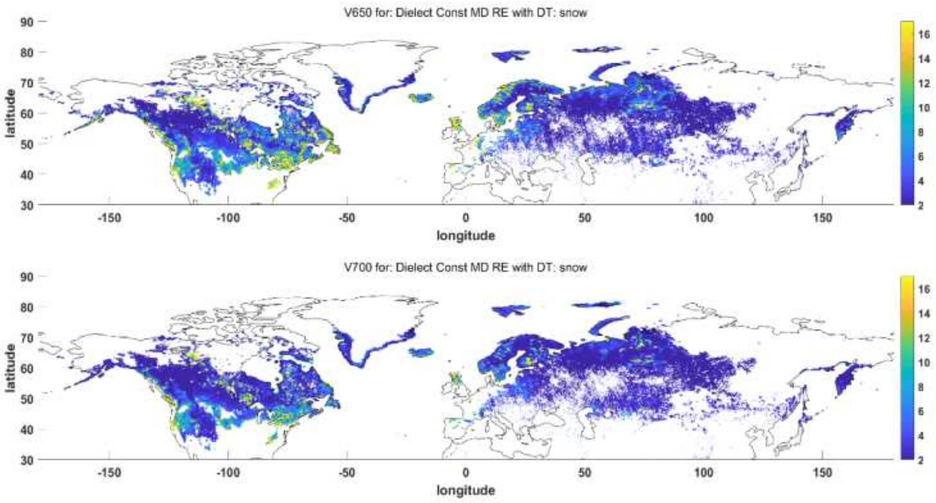

V650 for: Dielect Const MD RE with DT: snow
V700 for: Dielect Const MD RE with DT: snow
latitude
longitude

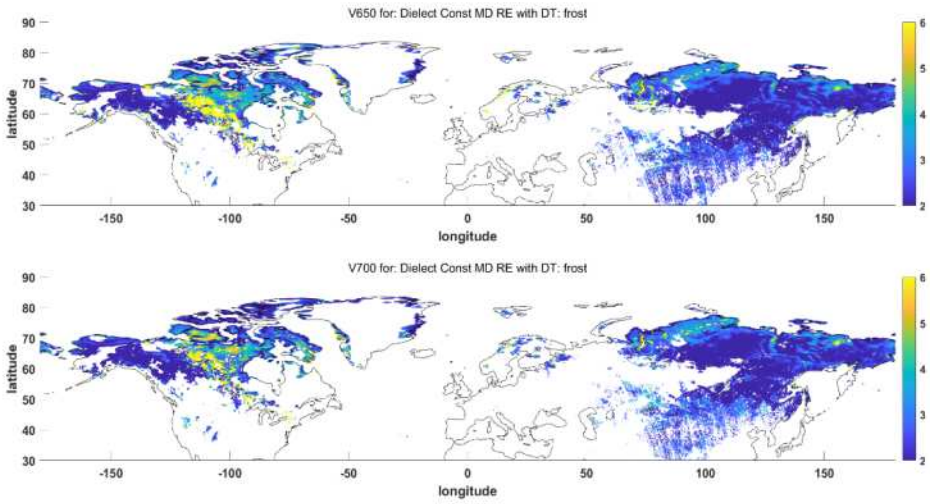

Figure 162: Dielectric constant real part, 16-Dec-2018 – 22-Dec-2018, top: forest and soil (FN & FO), middle: snow, bottom: frost

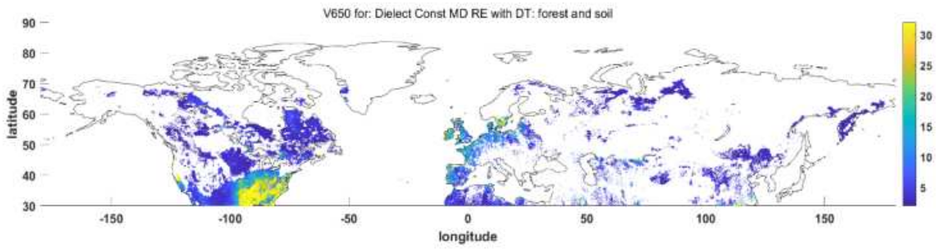

V650 for: Dielect Const MD RE with DT: forest and soil
latitude
longitude

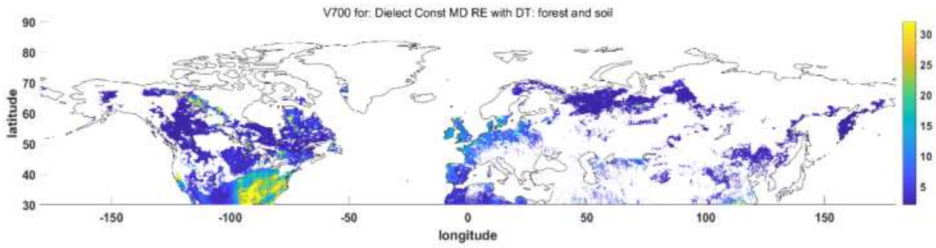

V700 for: Dielect Const MD RE with DT: forest and soil
latitude
longitude

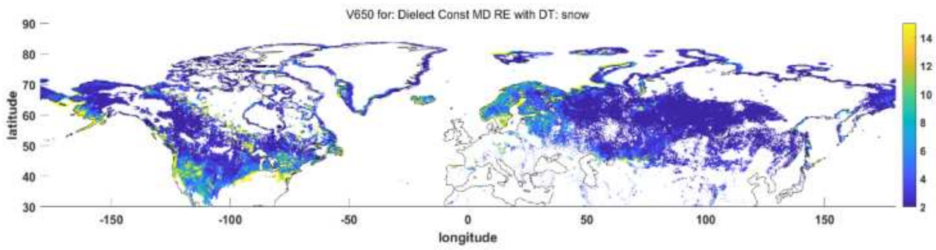

V650 for: Dielect Const MD RE with DT: snow
latitude
longitude

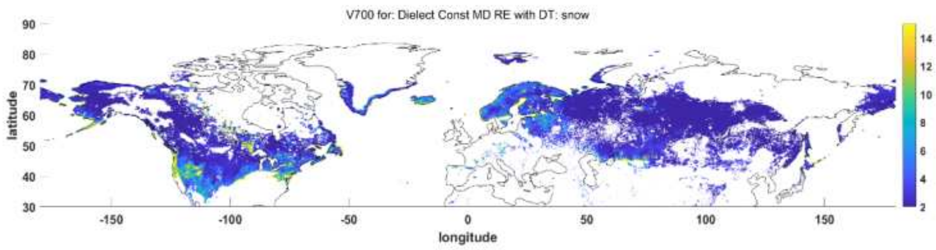

V700 for: Dielect Const MD RE with DT: snow
latitude
longitude

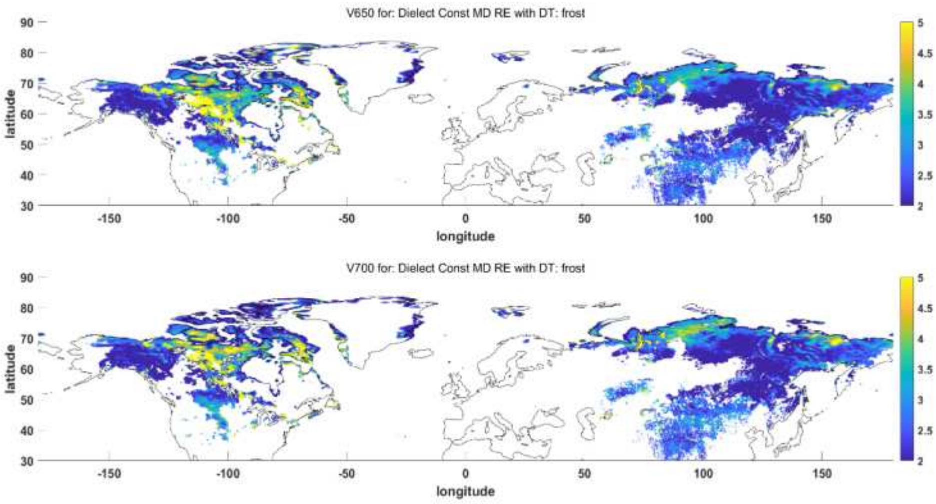

Figure 163: Dielectric constant real part, 24-Feb-2019 – 2-Mar-2019, top: forest and soil (FN & FO), middle: snow, bottom: frost

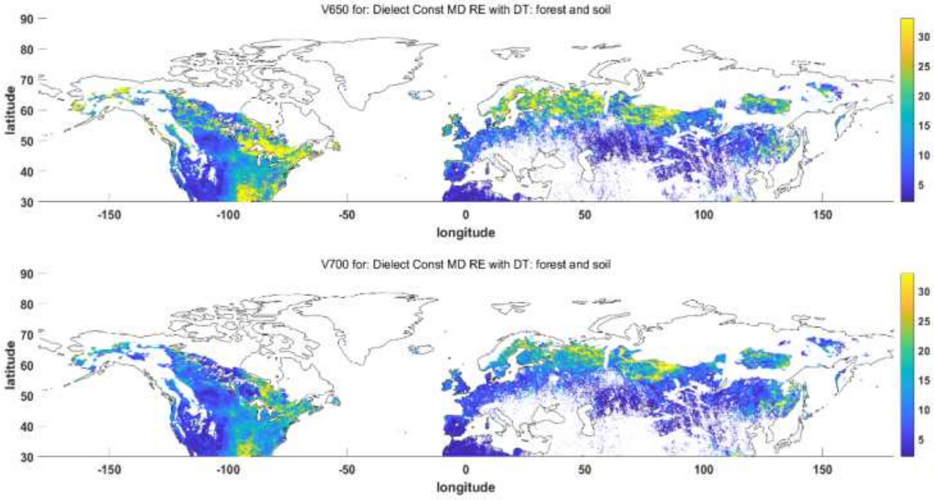

V650 for: Dielect Const MD RE with DT: forest and soil
V700 for: Dielect Const MD RE with DT: forest and soil
latitude
longitude

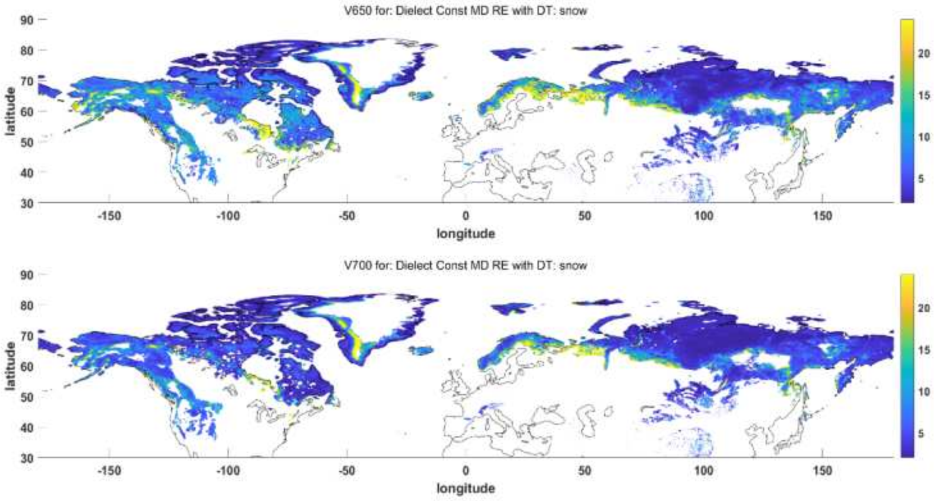

V650 for: Dielect Const MD RE with DT: snow
V700 for: Dielect Const MD RE with DT: snow
latitude
longitude

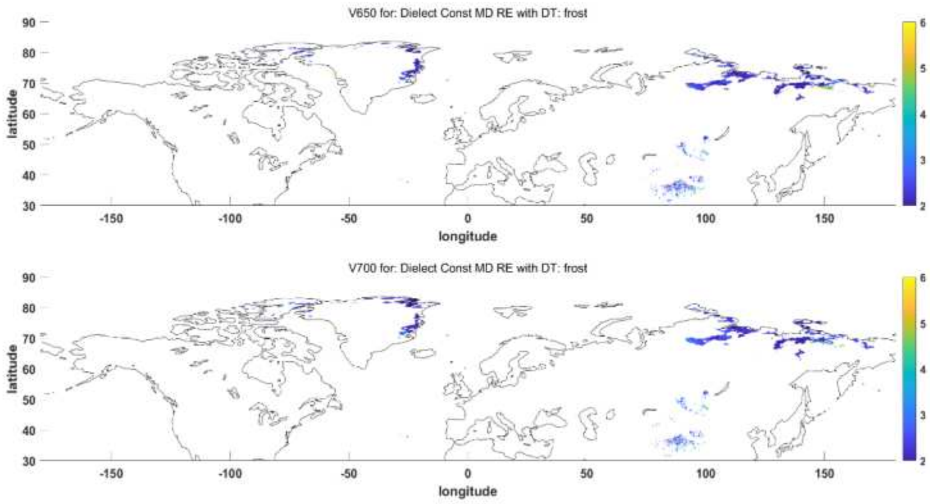

Figure 164: Dielectric constant real part, 12-May-2019 – 18-May-2019, top: forest and soil (FN & FO), middle: snow, bottom: frost

Below are shown time series from 30-Oct-2018 to 18-May-2019 for the Northern hemisphere, including land areas at latitudes above 30 degrees. The time series consist of weekly averaged values of dielectric constant (real part), air temperature (two-meter height), soil temperature (level 1 – soil layer from 0 cm to 7 cm) and snow water equivalent (SWE). Auxiliary data is acquired from ECMWF data used for SMOS level 2 Processor for Soil Moisture. Weekly averaged values include all data falling into the DT group that is under investigation. At the bottom panel in each time series figure is indicated the number of observations. Both v650 (blue color) and v700 (red color) are included in time series. Forest cover (FO) and soil cover (NO) data (based on DT used) are shown separately. All snow DTs are grouped as well as all frost DTs. The largest difference between the two versions (v650 vs. v700) is for FO DT. This includes the number of total observations and the absolute change in dielectric constant.

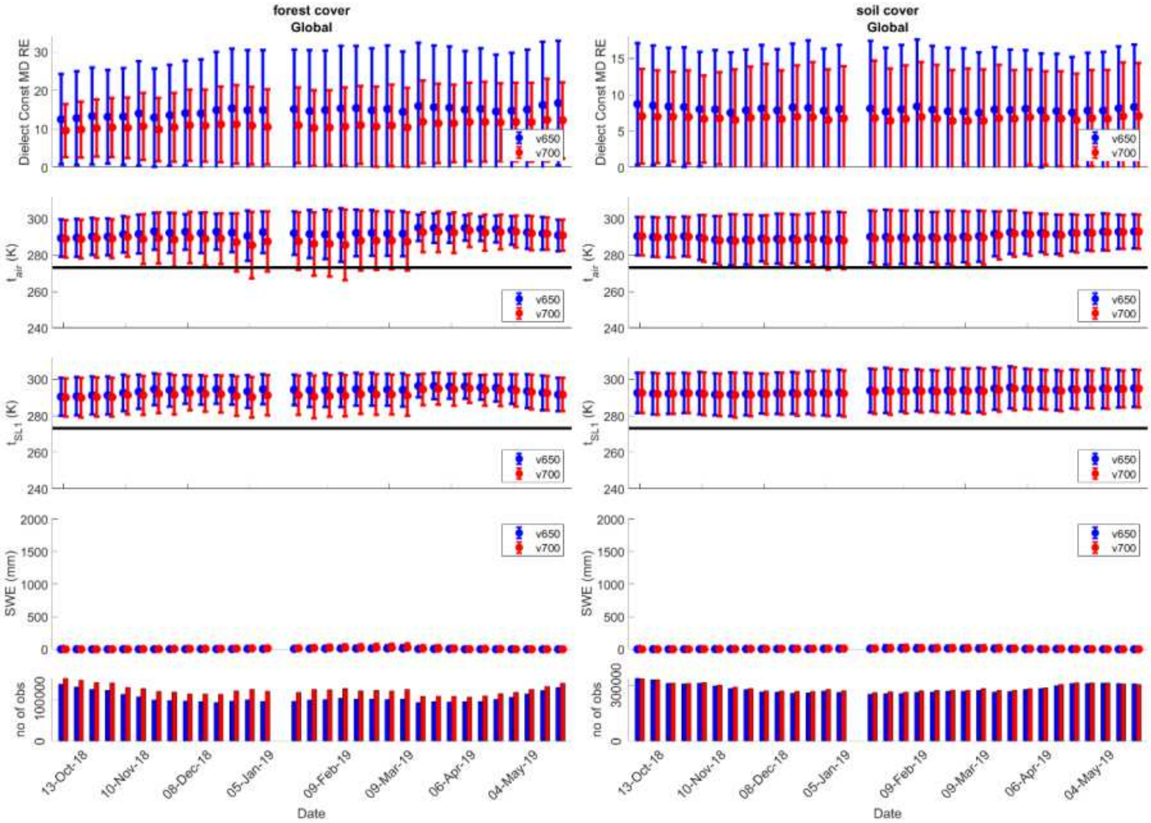

Figure 165: Period: 30-Oct-2018 – 18-May-2019, forest cover (left) and soil cover (right)pixels (DTs: 11 and 12). From top to bottom: real part of dielectric constant; air temperature at 2 m height; soil temperature level 1 (0-7 cm layer); number of observations. Blue markings: version 650, red markings: version 700

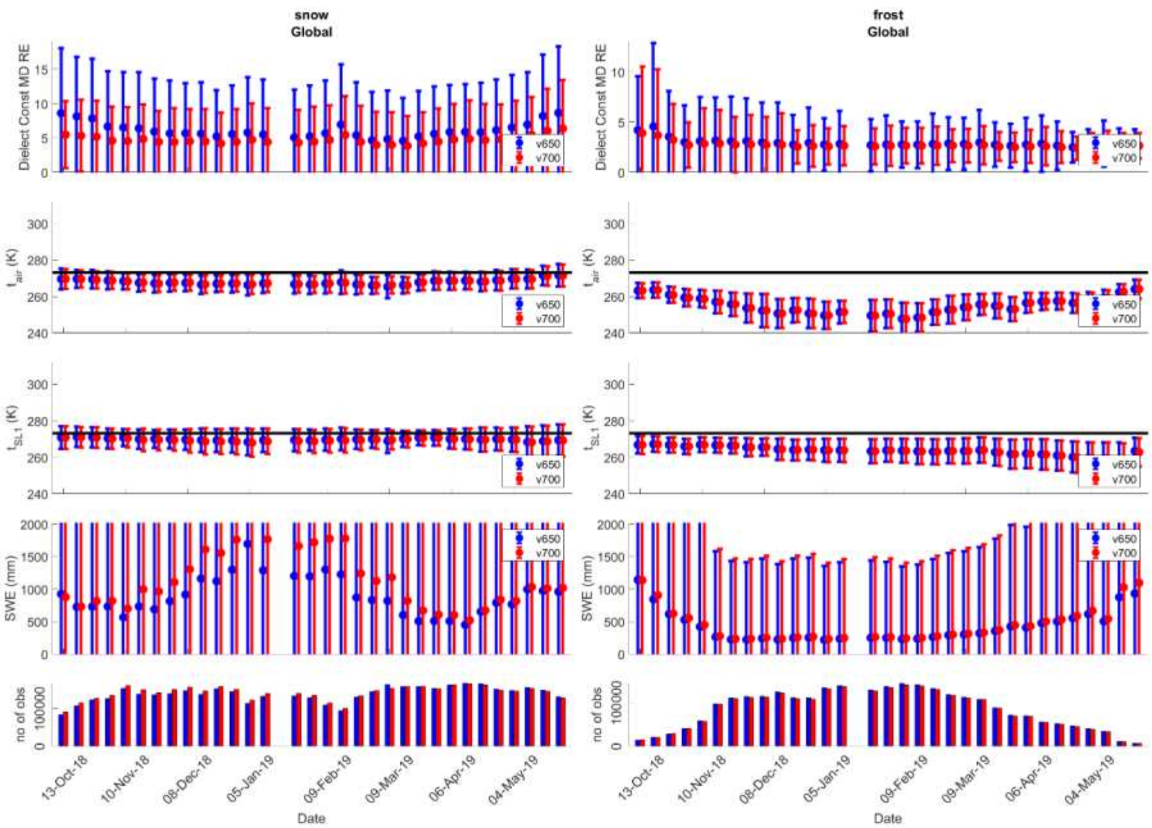

Figure 166: Period: 30-Oct-2018 – 18-May-2019, snow cover pixels (DTs: 5-8) (left) and frost cover pixels (DTs: 9-10) (right). From top to bottom: real part of dielectric constant; air temperature at 2 m height; soil temperature level 1 (0-7 cm layer); number of observations. Blue markings: version 650, red markings: version 700

5.2.4 REGIONAL RESULTS

5.2.4.1 NORTH AMERICA

Example maps of weekly averaged dielectric constant (real part) from North America are shown below. They cover period from 9th to 15th December 2018. Three different DT groups are shown – top: all data falling into nominal soil cover (NO) or forest cover (FO) DT; middle: all data falling into snow (SN) DTs; and bottom: all data falling into frozen soil (RZ) DTs. There is always a separate map for v650 dataset and v700 dataset on top of each other (v650 top, and v700 bottom). The example maps are chosen to illustrate the occasionally visible area having higher dielectric constant. This area is in Northwest Territories in mid-Canada. Characteristics for this area are also following:

- There are more retrievals from NO/FO DTs in v700 dataset than in v650 dataset. Also, on average the dielectric constant is higher for v700 than for v650 dataset.

- However, there are more retrievals from SN and RZ DTs in v650 dataset and on average the dielectric constant is also higher for v650 compared to v700.

It seems that some retrievals falling to NO/FO DT in v700 are considered to belong to SN or RZ DTs in v650.

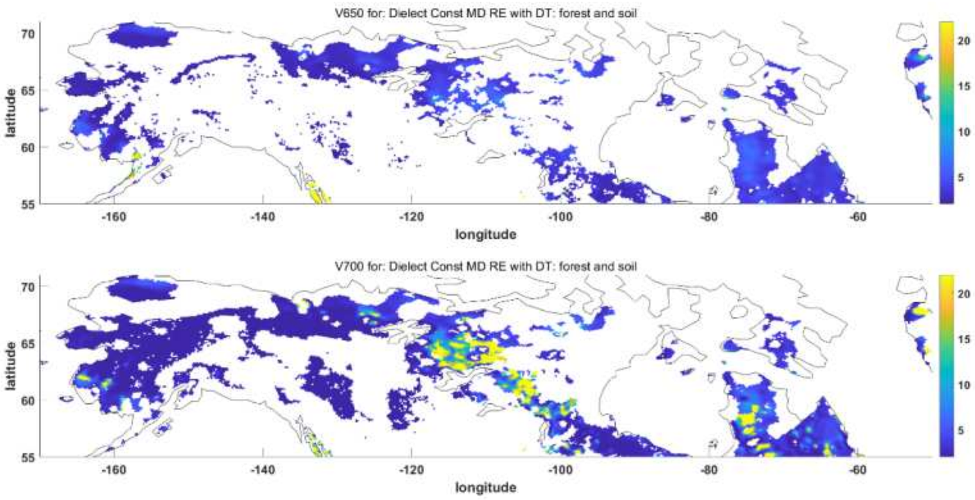

V650 for: Dielect Const MD RE with DT: forest and soil
latitude
longitude
70
65
60
55
-160
-140
-120
-100
-80
-60
20
15
10
5
V700 for: Dielect Const MD RE with DT: forest and soil
latitude
longitude

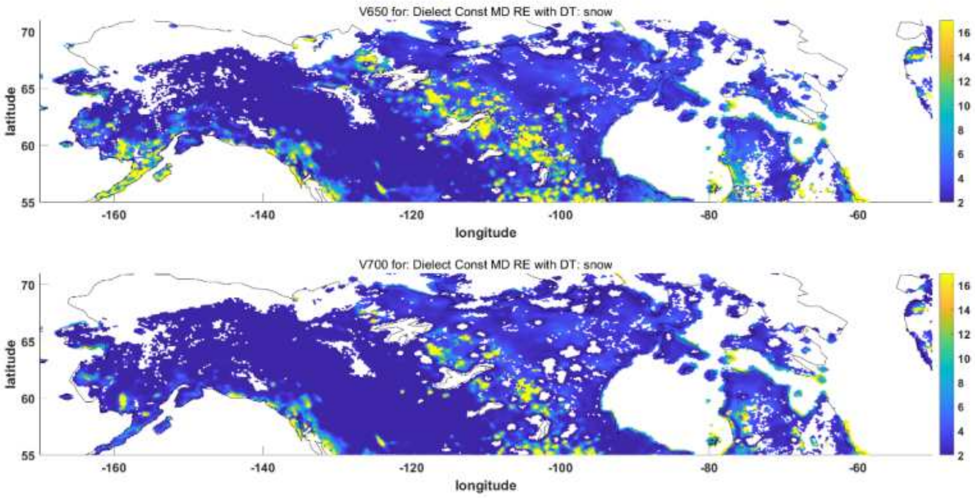

V650 for: Dielect Const MD RE with DT: snow
latitude
longitude
70
65
60
55
-160
-140
-120
-100
-80
-60
16
14
12
10
8
6
4
2
V700 for: Dielect Const MD RE with DT: snow
latitude
longitude

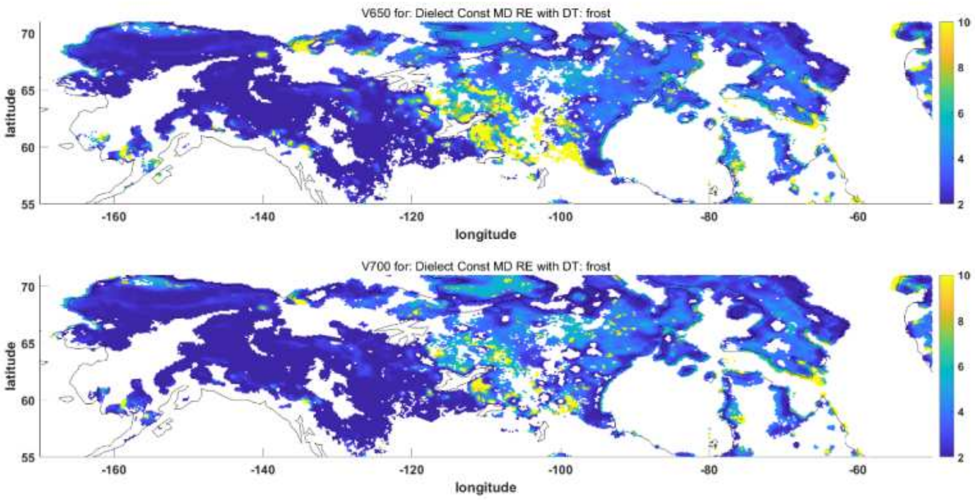

Figure 167: **Dielectric constant real part for North America test area, 9-Dec-2018 – 15-Dec-2018, top: forest and soil (FN & FO), middle: snow (SN), bottom: frost (RZ)**

Time series for North America region.

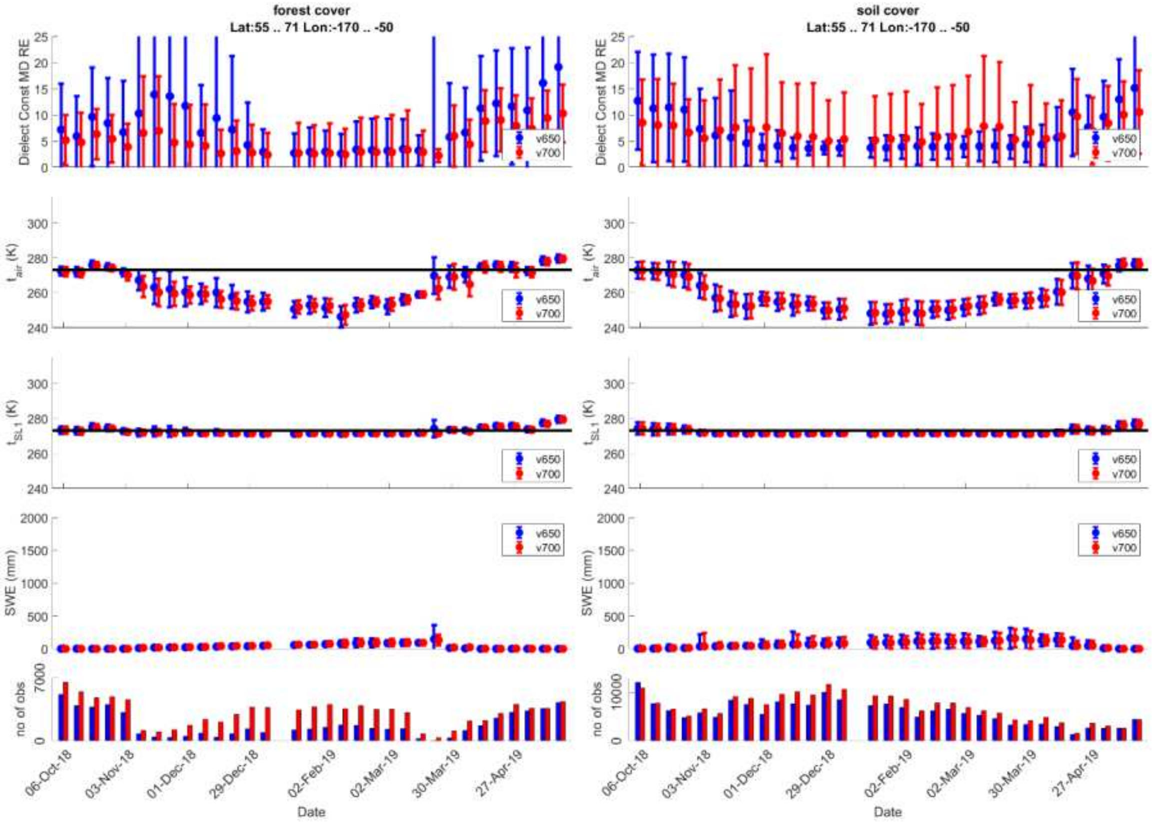

Figure 168: Areal coverage: North America, period: 30-Oct-2018 – 18-May-2019, forest cover (left) and soil cover (right) pixels (DTs: 11 and 12). From top to bottom: real part of dielectric constant; air temperature at 2 m height; soil temperature level 1 (0-7 cm layer); number of observations. Blue markings: version 650, red markings: version 700

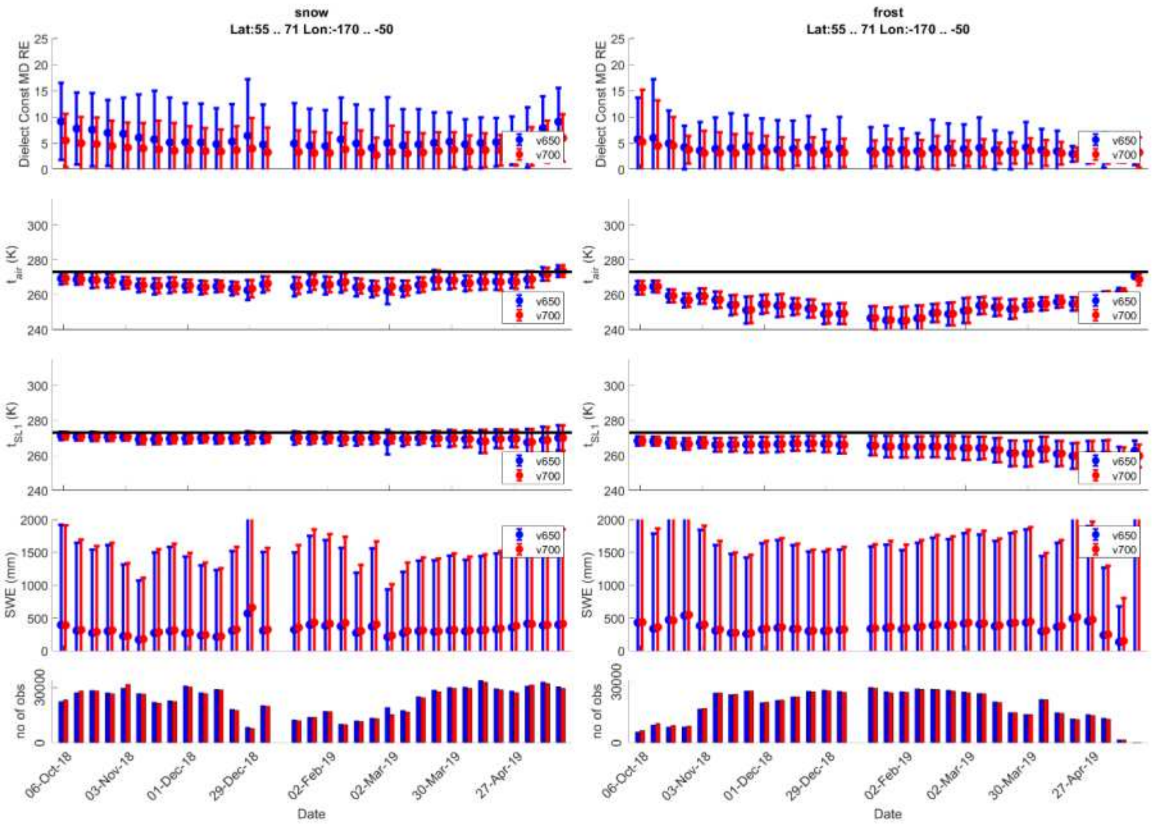

Figure 169: Areal coverage: North America, period: 30-Oct-2018 – 18-May-2019, snow cover pixels (DTs: 5-8) (left) and frost cover pixels (DTs: 9-10) (right). From top to bottom: real part of dielectric constant; air temperature at 2 m height; soil temperature level 1 (0-7 cm layer); number of observations. Blue markings: version 650, red markings: version 700

5.2.4.2 FINLAND

Example maps from test area Finland covers period from 17th to 23rd February 2019. They are same as for North America test area. The amount of data falling into NO/FO DTs is clearly visible even in the North part of the chosen test area. There are more NO/FO retrieval decisions in v700 dataset compared to v650 dataset.

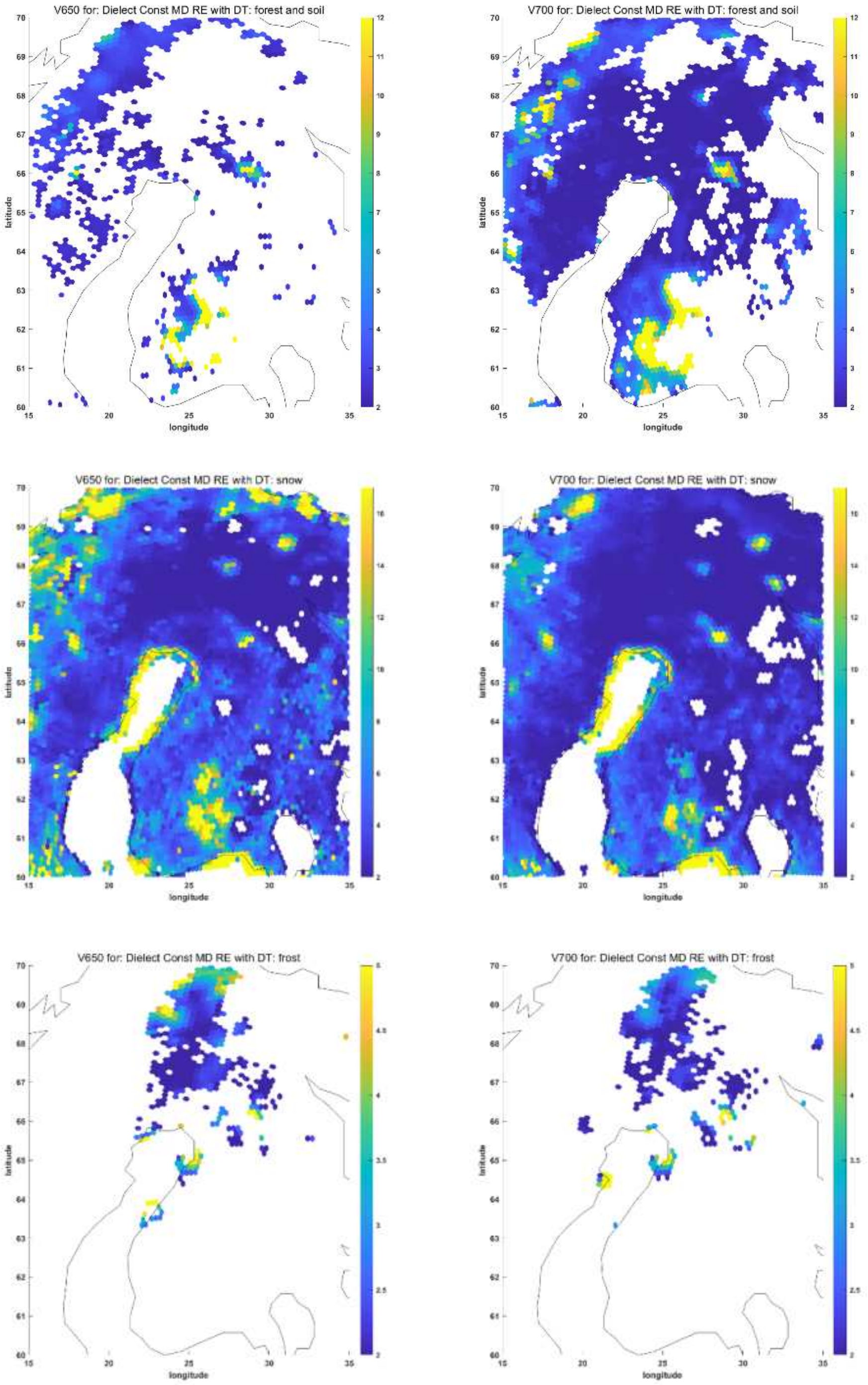

Figure 170: Dielectric constant real part for Finland test area, 17-Feb-2019 – 23-Feb-2019, top: forest and soil (FN & FO), middle: snow (SN), bottom: frost (RZ)

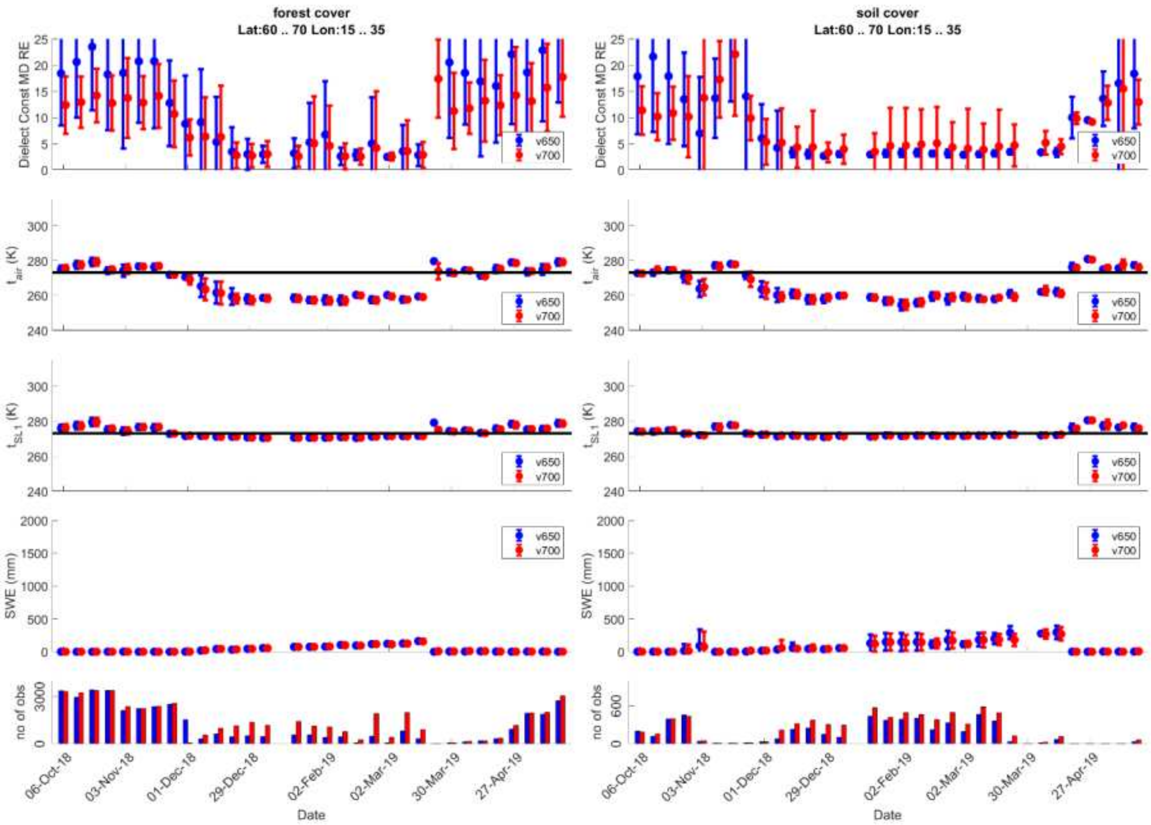

Figure 171: Areal coverage: Finland and its surroundings, period: 30-Oct-2018 – 18-May-2019, forest cover (left) and soil cover (right) pixels (DTs: 11 and 12). From top to bottom: real part of dielectric constant; air temperature at 2 m height; soil temperature level 1 (0-7 cm layer); number of observations. Blue markings: version 650, red markings: version 700

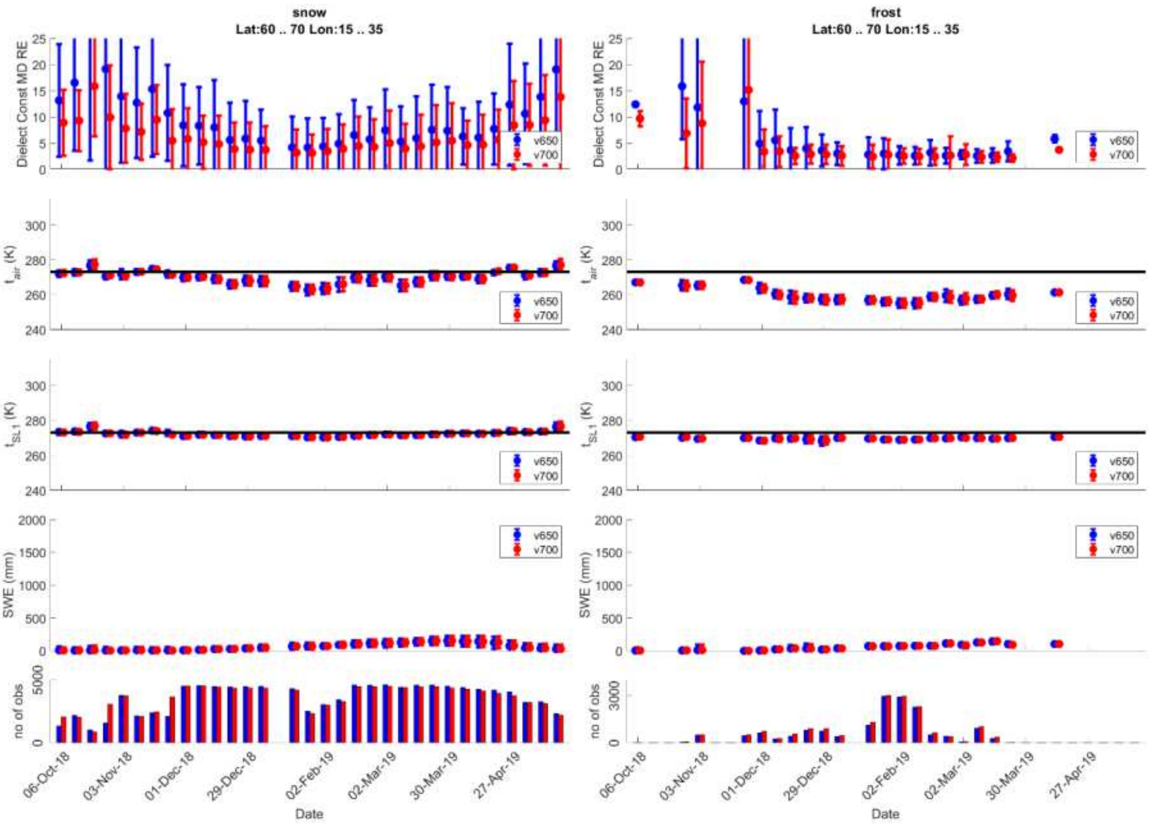

Figure 172: Areal coverage: Finland and its surroundings, period: 30-Oct-2018 – 18-May-2019, snow cover pixels (DTs: 5-8) (left) and frost cover pixels (DTs: 9-10) (right). From top to bottom: real part of dielectric constant; air temperature at 2 m height; soil temperature level 1 (0-7 cm layer); number of observations. Blue markings: version 650, red markings: version 700

5.2.4.3 CENTRAL SIBERIA

Example maps from Central Siberia test area cover also period from 17th to 23rd February 2019. Again, some retrievals are using NO/FO DTs.

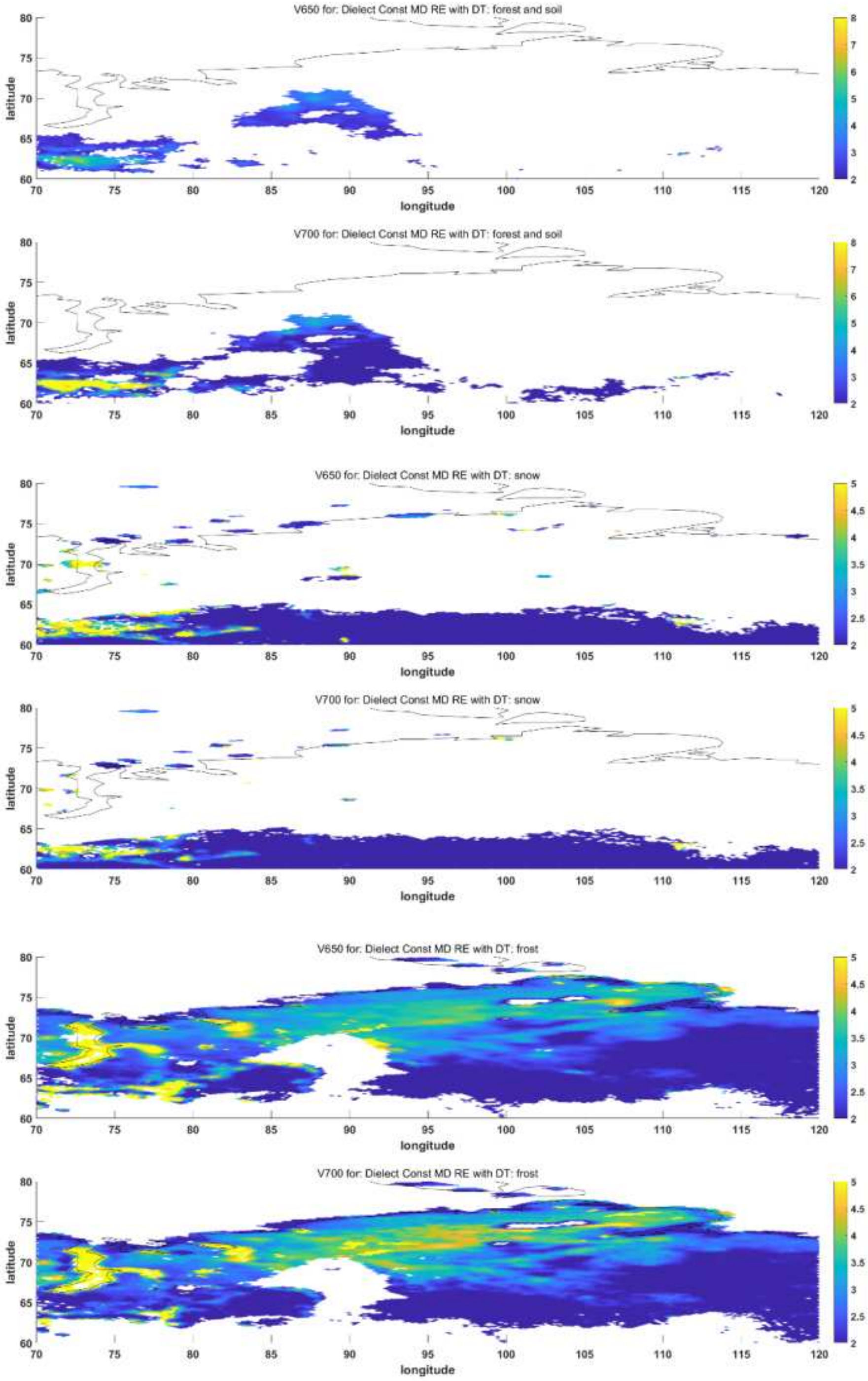

Figure 173: Dielectric constant real part for Central Siberia test area, 17-Feb-2019 – 23-Feb-2019, top: forest and soil (FN & FO), middle: snow (SN), bottom: frost (RZ)

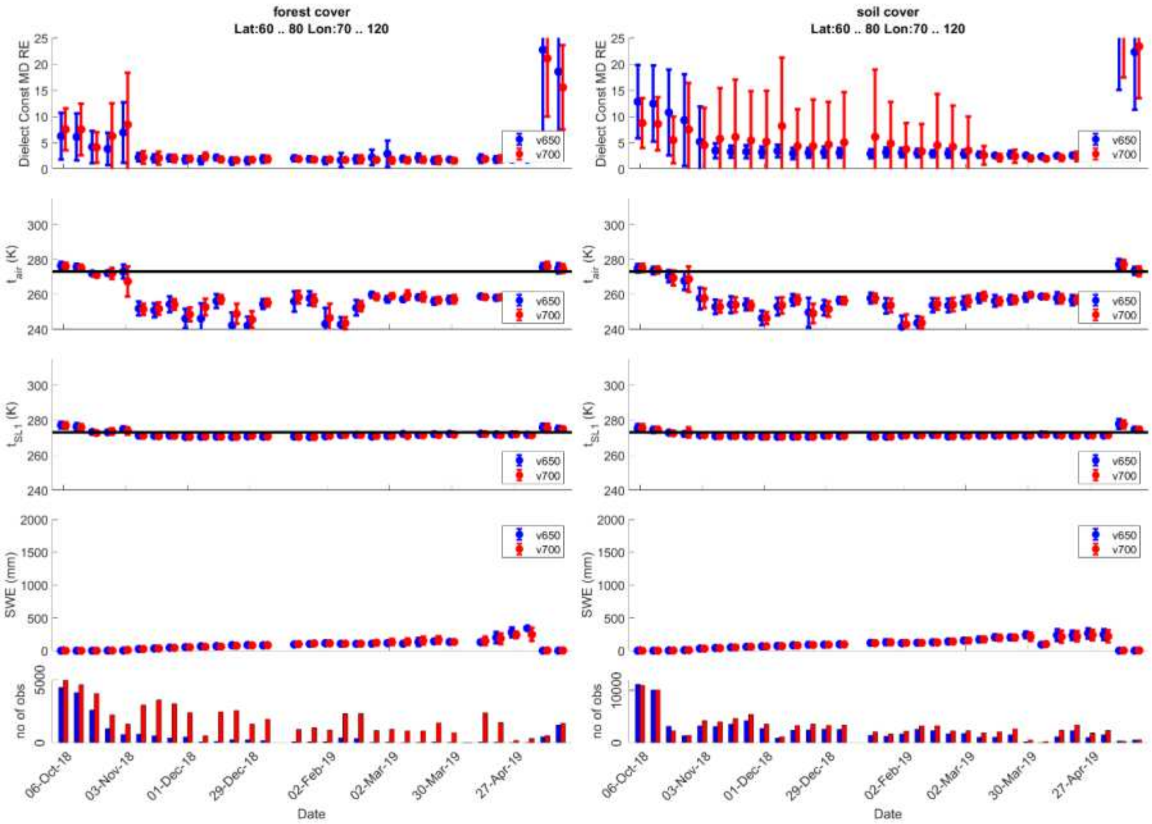

Figure 174: Areal coverage: Central Siberia, period: 30-Oct-2018 – 18-May-2019, forest cover (left) and soil cover (right) pixels (DTs: 11 and 12). From top to bottom: real part of dielectric constant; air temperature at 2 m height; soil temperature level 1 (0-7 cm layer); number of observations. Blue markings: version 650, red markings: version 700

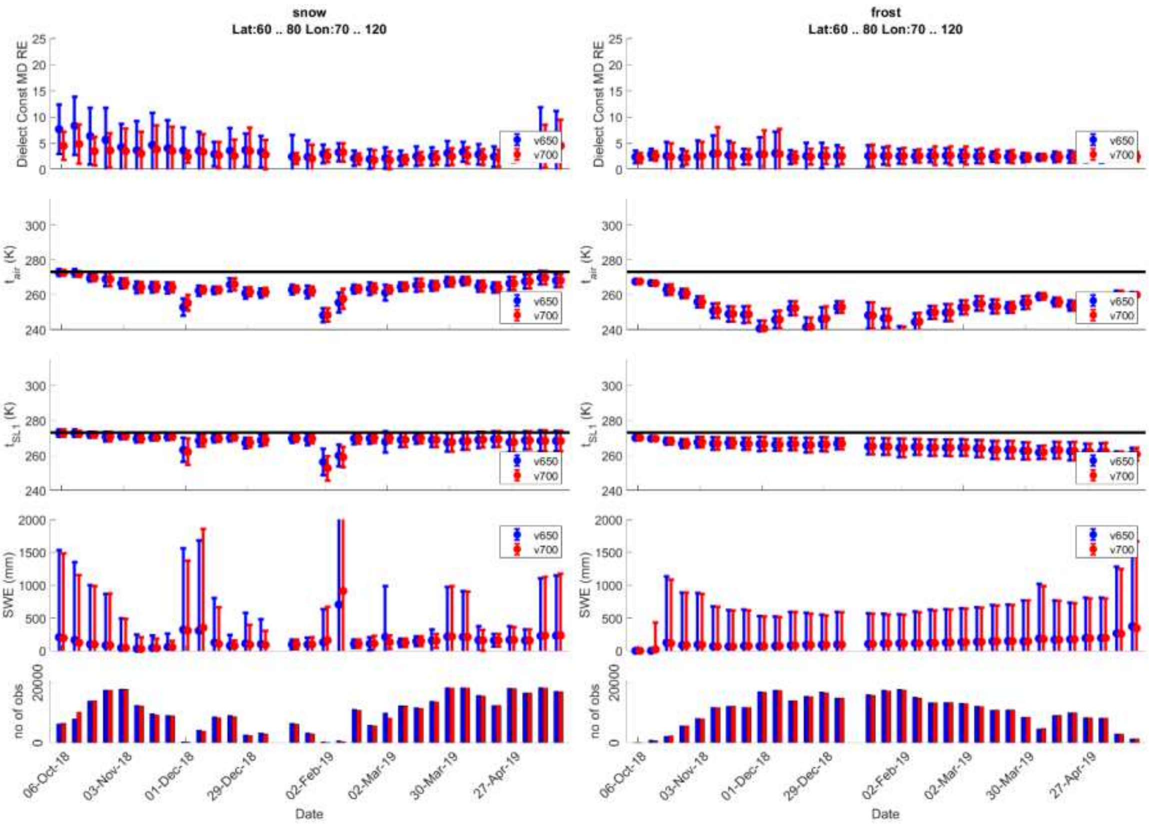

Figure 175: Areal coverage: Central Siberia and its surroundings, period: 30-Oct-2018 – 18-May-2019, snow cover pixels (DTs: 5-8) (left) and frost cover pixels (DTs: 9-10) (right). From top to bottom: real part of dielectric constant; air temperature at 2 m height; soil temperature level 1 (0-7 cm layer); number of observations. Blue markings: version 650, red markings: version 700

5.2.5 COMPARISON TO L3FT AND ECMWF SWE

To study the behavior of the dielectric constant retrievals, we compare it to two other variables: SMOS level 3 freeze-thaw produce (L3FT) and ECMWF snow water equivalent estimate (ECMWF SWE).For freeze-thaw state, we hypothesize that the retrievals of the dielectric constant have higher values for thaw, and lower value for freeze state. This stems from the assumptions that the retrieved dielectric constant value is connected to the dielectric constant of the ground, from which one would expect described behavior under different freeze-thaw states. The retrieved dielectric constant is also compared to SWE values. In Lemmetyinen et al., 2016, it was observed that omitting the dry snow can decrease the retrieved dielectric constant value by approximately 35%. Therefore, we are motivated to study if such decrease is visible by comparing the retrievals to the corresponding SWE values. In practice, we will compare weekly average maps of different variables to each other. For this comparison, we have generated weekly maps from autumn 2015 to spring 2016. Figure 176 shows example maps from the variables under interest.

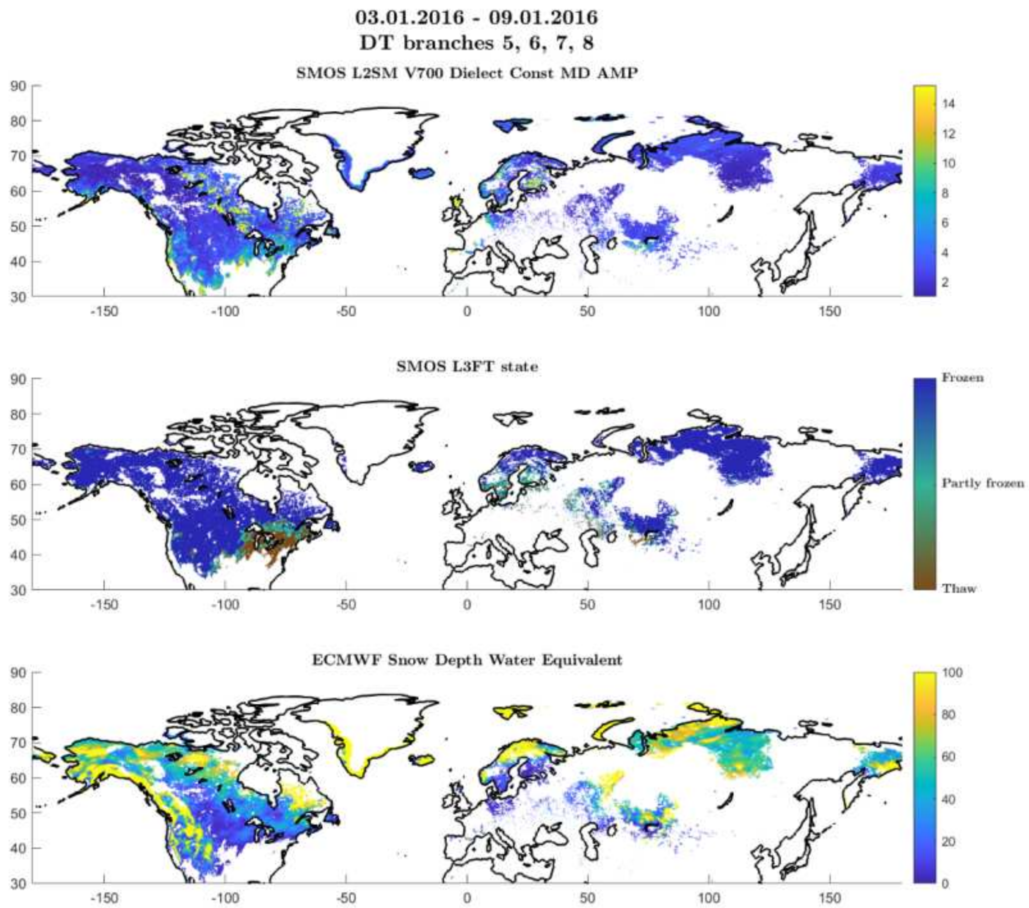

Figure 176: Averaged global maps for 1) L2SM v700 Dielectric constant amplitude, 2) SMOS L3FT freeze-thaw state, 3) ECMWF snow water equivalent estimate, limited to decision tree values 5,6,7, and 8

As a practical notion, the above maps show values only for those points where the dielectric constant was retrieved within this period. The ECMWF SWE estimate was averaged over the same time instances as the dielectric constant retrievals were, but for L3FT the averaging was done over all the available values. For more detailed comparisons, we now limit our focus on an area around Finland. We will show different comparisons as maps, histograms, and plots for some specific week, and then summarize the results over the whole period of interest in different tables.

5.2.5.1 FINLAND, DECISION TREE VALUES 5, 6, 7, AND 8 (SNOW CONDITIONS)

In this subsection we focus on the general area around Finland, and decision tree values 5, 6, 7, and 8, which indicate snow conditions. The following two figures show the areal maps of the retrieved dielectric constant for both versions 650 and 700, as well as the corresponding L3FT and ECMWF SWE maps. Already some differences can be seen between the versions 650 and 700. The behavior of "hot spots" in the maps seems different (e.g., coast of Norway and south-east Finland).

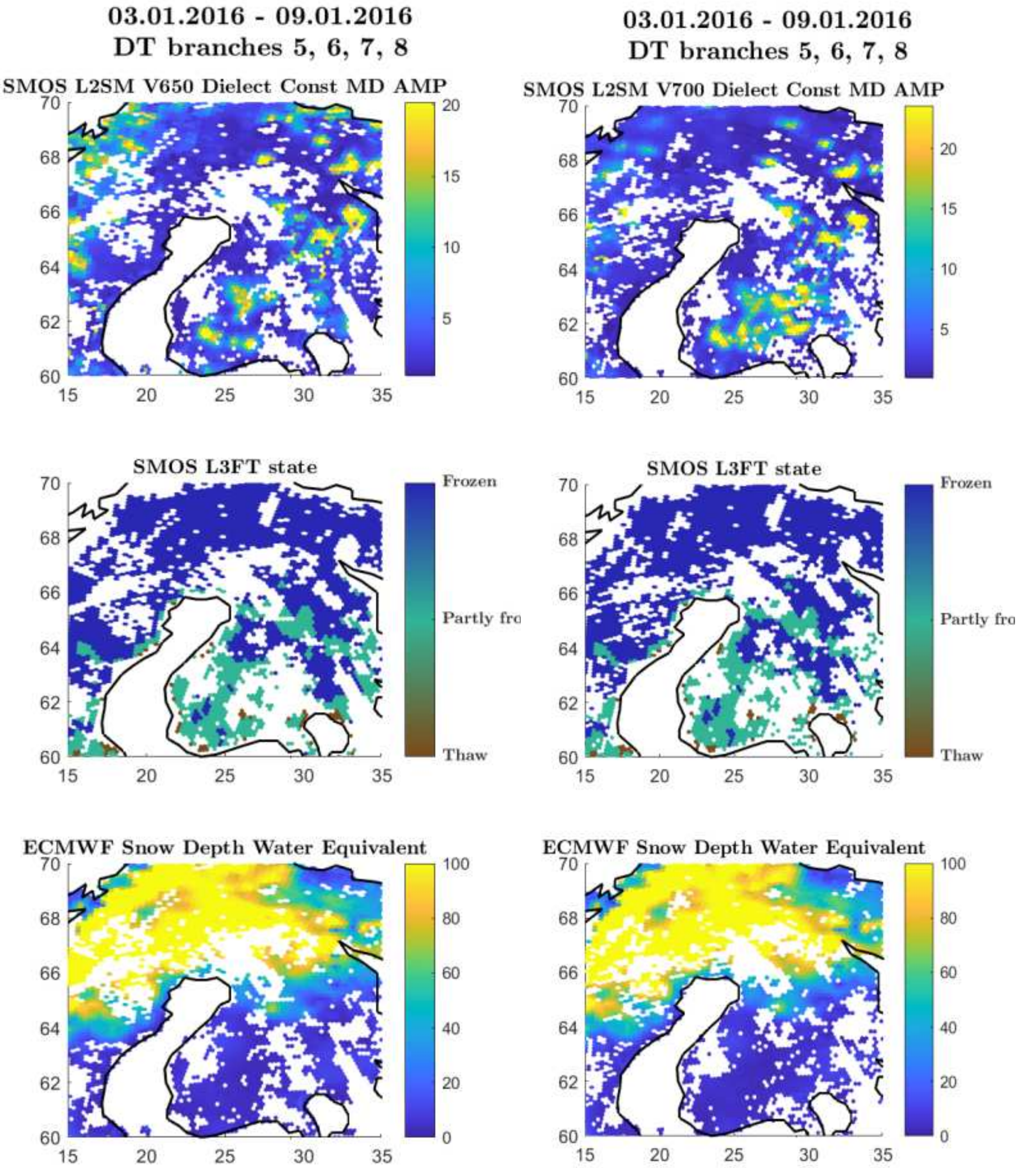

Figure 177: Southern Finland maps of retrieved v700 (top right) vs. v650 (top left) for DT 5,6,7,8 along with frozen and thaw state maps and AUX_ECMWF SD maps for the period 03.01.2016 – 09.01.2016

The below figure shows the differences between versions 650 and 700, comparing the distribution of data (shown in above maps), in histograms and comparing the empirical cumulative distribution functions (CDF).

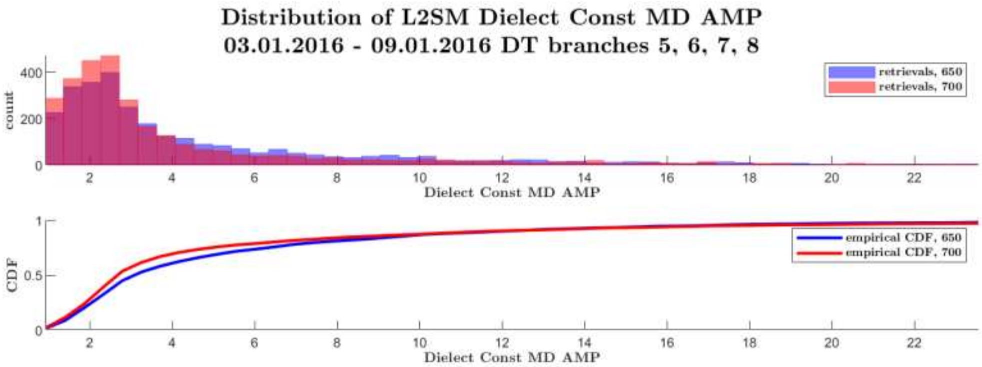

Figure 178: Distributions (top) of and ecfd (bottom) of retrieved v700 (red) vs. v650 (blue) for DT 5,6,7,8 over Southern Finland and for the period 03.01.2016 – 09.01.2016

This type of comparison for each week within the period of interest is summarized in the table below. The relative differences (v650 – v700 divided by v650) is computed for the means, standard deviations, and counts (number of retrievals within this period). The relative differences are colored yellow when greater than 15 % (650 has higher values) and green when smaller than -15% (700 has higher values). This comparison indicates that most of the time version 650 attains higher values than the version 700.

Table 14: Comparison of the statistics for averaged retrieved dielectric constant amplitude within the general area around Finland, restricted to the decision tree values 5, 6, 7, and 8 (snow conditions). Coloring: yellow – relative difference > 15 %, green –relative difference < -15 %.

start date	mean 650	mean 700	relative difference	standard deviation 650	standard deviation 700	relative difference	count 650	count 700	relative difference
30.8.15	18,95	15,74	17 %	4,38	2,83	35 %	149	150	-1 %
6.9.15	18,13	15,07	17 %	5,44	3,43	37 %	148	150	-1 %
13.9.15	23,99	18,63	22 %	6,02	3,71	38 %	92	94	-2 %
20.9.15	23,29	19,32	17 %	8,07	4,34	46 %	92	94	-2 %
27.9.15	15,48	11,69	24 %	8,03	6,38	21 %	701	902	-29 %
4.10.15	14,44	9,19	36 %	10,81	7,22	33 %	1338	1348	-1 %
11.10.15	20,98	11,63	45 %	17,07	8,15	52 %	1163	1162	0 %
18.10.15	17,8	11,29	37 %	10,4	6,08	42 %	873	888	-2 %

25.10.15	15,12	9,17	39 %	12,14	7,04	42 %	2557	2562	0 %
1.11.15	17,2	12,01	30 %	14,23	8,65	39 %	2279	2411	-6 %
8.11.15	12,6	8,12	36 %	12,41	7,49	40 %	3141	3161	-1 %
15.11.15	10,81	7,28	33 %	11,27	6,59	42 %	4039	4048	0 %
22.11.15	11,25	7,57	33 %	9,61	6,24	35 %	4434	4432	0 %
29.11.15	11,32	6,85	39 %	9,5	5,49	42 %	4160	4155	0 %
6.12.15	12,29	8,22	33 %	12,83	9,02	30 %	3963	3987	-1 %
13.12.15	8,72	7	20 %	8,89	8,55	4 %	4249	4263	0 %
20.12.15	14,18	8,79	38 %	16,21	8,68	46 %	4006	4050	-1 %
27.12.15	7,66	6,53	15 %	8,99	8,54	5 %	4429	4418	0 %
3.1.16	5,32	4,87	8 %	6,6	6,07	8 %	3094	3145	-2 %
10.1.16	3,22	2,91	10 %	3,62	3,46	4 %	3063	3106	-1 %
17.1.16	3,91	3,09	21 %	4,08	2,93	28 %	2324	2481	-7 %
24.1.16	5,74	4,31	25 %	6,26	4,95	21 %	4503	4426	2 %
31.1.16	4,88	4,76	2 %	4,66	5,46	-17 %	4510	4460	1 %
7.2.16	9,44	6,12	35 %	8,2	5,77	30 %	4584	4550	1 %
14.2.16	5,34	4,71	12 %	5,28	5,21	1 %	4514	4495	0 %
21.2.16	4,97	4,67	6 %	5,42	6,2	-14 %	4528	4492	1 %
28.2.16	4,84	4,52	7 %	6,51	7,03	-8 %	4488	4454	1 %
6.3.16	6,25	4,47	28 %	6,1	5,64	8 %	4583	4439	3 %
13.3.16	7,78	5,33	31 %	8,04	6,15	24 %	4550	4454	2 %
20.3.16	5,07	3,88	23 %	4,86	4,47	8 %	4512	4391	3 %
27.3.16	8,41	5,18	38 %	7,86	5,28	33 %	4504	4340	4 %
3.4.16	7,87	5,32	32 %	6,1	4,92	19 %	4168	4074	2 %
10.4.16	7,11	5,15	28 %	5,91	4,57	23 %	3970	3828	4 %
17.4.16	9,06	5,45	40 %	9,33	5,24	44 %	3080	3037	1 %
24.4.16	10,08	6,95	31 %	8,42	5,46	35 %	3068	3041	1 %
1.5.16	12,82	8,23	36 %	11,17	7,35	34 %	2178	2195	-1 %
8.5.16	15,41	10,62	31 %	11	7,89	28 %	1853	1866	-1 %
15.5.16	16,26	11,22	31 %	10,68	6,82	36 %	1204	1254	-4 %
22.5.16	16,05	11,93	26 %	8,92	7,44	17 %	895	902	-1 %
29.5.16	15,35	12,35	20 %	7,02	6,02	14 %	611	632	-3 %

To compare the retrieved dielectric constant values to L3FT freeze-thaw state estimate, we divide the dielectric constant values into two groups, corresponding to thaw states and freeze states (some retrievals which do not clearly belong to either group are discarded). The following figures show example of such comparison.

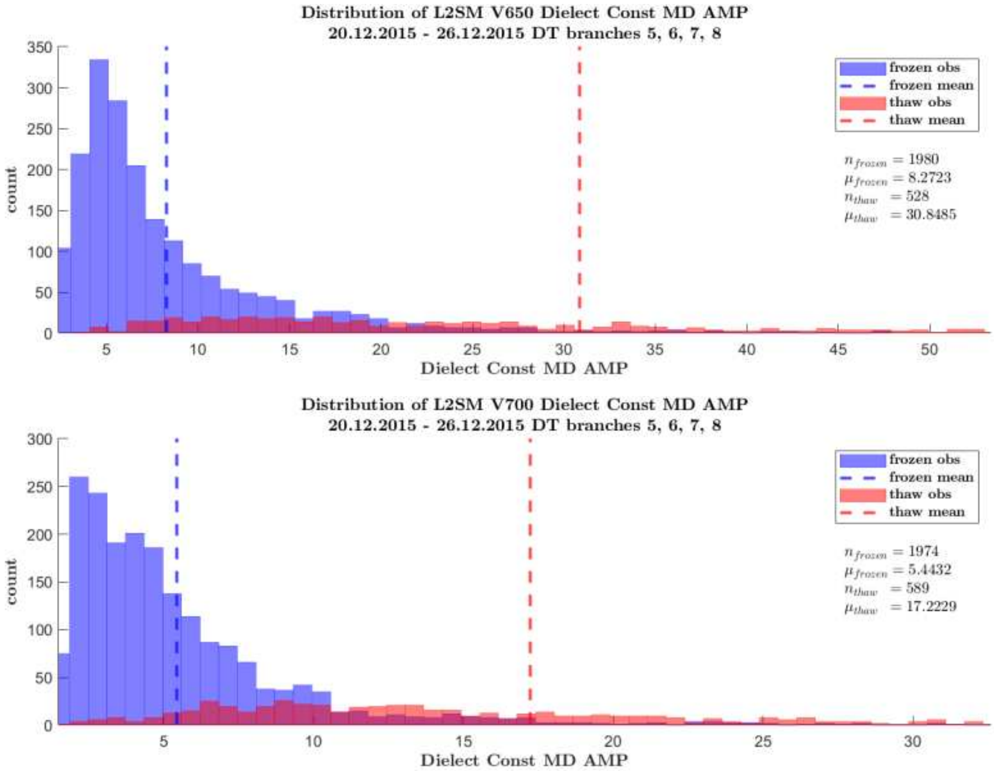

Figure 179: Distribution of retrievals v700 (bottom) vs. v650 (top) for DT 5,6,7,8 along with frozen and thaw state distributions over Southern Finland and for the period 20.12.2015 – 26.12.2015

The overall behavior is as expected: the retrievals associated with frozen ground, on average, have lower values than those associated with thaw ground. However, there is overlapping of the distributions. The retrievals which are associated with thaw ground but have low values are of particular interest. We will later investigate whether snow could lower the retrieved value, being a suspect for such behavior (other possible explanations are the misclassification by L3FT or actual physical behavior, e.g., dry ground). Again, the tables below summarize the similar comparison for other weeks. The coloring in these tables is the following: yellow – values greater than 5, and green – values greater than 10. The coloring indicates fit with hypothesis: values associated with frozen ground are expected to have lower values than those associated with thaw ground. The weeks where either of the frozen or thaw states had less than 100 retrievals, were discarded. Based on these tables, the difference between mean values of the retrieved dielectric constant amplitude between freeze and thaw states seems to be more evident in the version 650. However, both versions follow the general hypothesis and thus it cannot be said which one fits it better.

Table 15: Version 650 dielectric constant amplitude. Comparison of mean values between freeze and thaw states (from L3FT). Yellow - difference greater than 5, Green - difference greater than 10.

start date	thaw mean	frozen mean	difference	thaw count	frozen count
8.11.15	13,42	9,59	3,83	1591	332
15.11.15	12,39	7,13	5,26	1493	797
22.11.15	14,63	7,27	7,36	1024	1433
29.11.15	14,31	7,79	6,52	755	1775
6.12.15	19,57	7,01	12,56	757	1780
13.12.15	11,51	5,84	5,67	905	1825
20.12.15	30,85	8,27	22,58	528	1980
27.12.15	7,84	6,89	0,95	550	2023
3.4.16	14,31	6,42	7,89	113	2539
10.4.16	9,56	5,33	4,23	795	2102
17.4.16	13,83	6,51	7,32	441	1873
24.4.16	12,86	9,77	3,09	541	725
1.5.16	14,43	7,22	7,21	1032	262
8.5.16	18,35	6,78	11,57	1120	164
15.5.16	18,68	7,63	11,05	683	158

Table 16: Version 700 dielectric constant amplitude. Comparison of mean values between freeze and thaw states (from L3FT). Yellow - difference greater than 5, Green - difference greater than 10.

start date	thaw mean	frozen mean	difference	thaw count	frozen count
8.11.15	9,35	4,17	5,18	1608	332
15.11.15	8,62	4,77	3,85	1510	798
22.11.15	11,44	4,53	6,91	1028	1433
29.11.15	10,07	4,81	5,26	756	1774
6.12.15	14,28	4,8	9,48	778	1780

13.12.15	9,24	4,36	4,88	918	1832
20.12.15	17,22	5,44	11,78	589	1974
27.12.15	8,11	5,03	3,08	557	2016
3.4.16	11,78	4,23	7,55	121	2504
10.4.16	7,3	3,91	3,39	784	2082
17.4.16	8,11	4,29	3,82	441	1855
24.4.16	9,37	6,96	2,41	537	723
1.5.16	9,91	4,93	4,98	1058	261
8.5.16	13,51	4,24	9,27	1145	164
15.5.16	14,22	4,91	9,31	736	159

Finally, we will study whether there is a connection between snow and the retrievals of dielectric constant. As we mentioned before, there is a reason to believe that the presence of dry snow has a decreasing effect on the retrieved value when neglected (Lemmetyinen et al., 2016). We will seek evidence for this claim: retrieved dielectric constant values are decreased by the effect of snow. The approach to study this claim is like the previous freeze-thaw comparison; we split the retrievals into two groups, one corresponding to ECMWF SWE estimate values less than 5 mm and the other to values greater than 50 mm and compare the statistics of these two groups. The figures below show histograms of such split as an example.

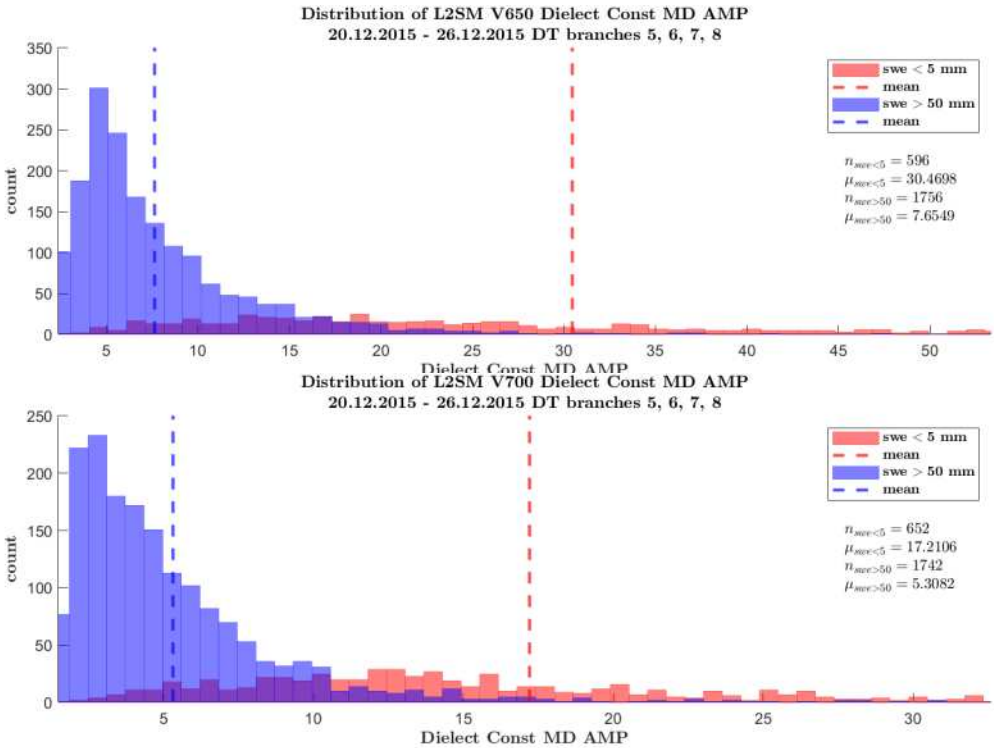

Figure 180: Distribution of retrievals v700 (bottom) vs. v650 (top) for DT 5,6,7,8 along with swe < 5mm and swe>50m distributions over Southern Finland and for the time period 20.12.2015 – 26.12.2015

In this specific case, the difference is clearly visible. However, this is not always the case. The figures below show a less optimistic case from another week. Here the distributions are visually very similar, but for version 700, the mean values differ more. Since the latter figures are from January, the retrievals associated with low SWE values could be associated with frozen L3FT state, explaining the low values. Indeed this comparison should be expanded to take in to account the L3FT state and limit the comparisons only to those values associatedwith either freeze or thaw state.

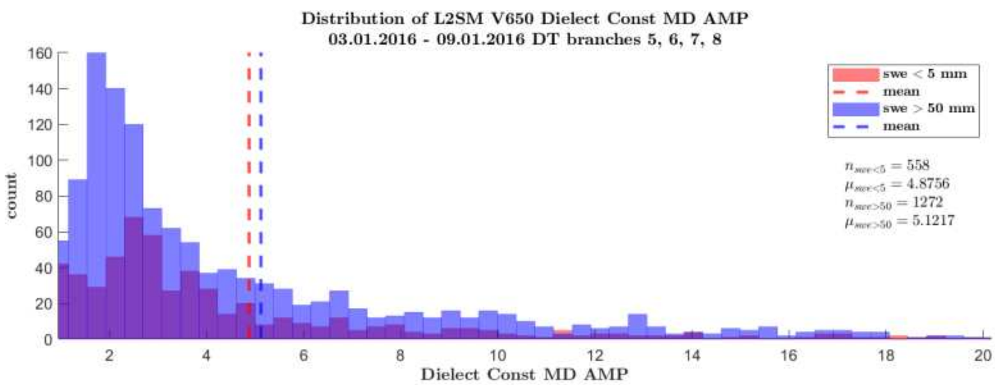

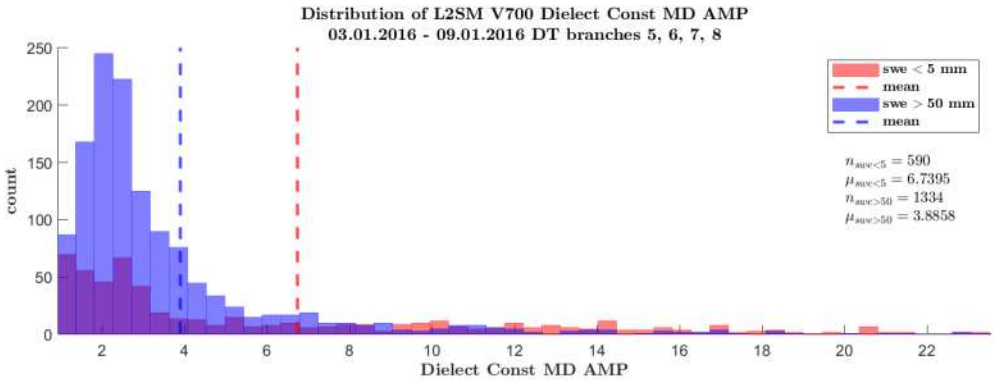

Figure 181: Distribution of retrievals v700 (bottom) vs. v650 (top) for DT 5,6,7,8 along with swe < 5mm and swe>50m distributions over Southern Finland and for the time period 03.01.2016 – 09.01.2016

The above figures indicate that only looking at the mean value of the distributions can be misleading (last histogram shows very overlapping distributions with differing mean values). This suggests a possible benefit from using statistics other than mean to compare, describing the separation of the two groups better. Nevertheless, we will at this time compare the mean values in the tables below. Weeks where either of the groups had less than 100 retrievals, were discarded.

Table 17: Version 650 dielectric constant amplitude, comparison between different snow conditions.Coloring: yellow – relative difference greater than 30%, green – greater than 50%, red – less than 0%.

start date	mean, swe < 5 mm	mean, swe > 50 mm	relative difference	count, swe < 5 mm	count, swe > 50 mm
8.11.2015	14,21	12,72	10 %	936	102
15.11.2015	18,38	8	56 %	644	238
22.11.2015	16,79	6,88	59 %	480	352
29.11.2015	16,18	7,09	56 %	753	718
6.12.2015	24,99	7,03	72 %	604	1170
13.12.2015	12,37	6,6	47 %	746	1508
20.12.2015	30,47	7,65	75 %	596	1756
27.12.2015	7,29	6,89	5 %	1318	1794
3.1.2016	4,88	5,12	-5 %	558	1272
7.2.2016	20,78	7,26	65 %	117	3081
20.3.2016	10,37	4,6	56 %	123	3592
27.3.2016	15,74	7,02	55 %	292	3229
3.4.2016	11,32	7,02	38 %	406	2717

10.4.2016	10,45	5,78	45 %	704	2336
17.4.2016	14,02	7,34	48 %	385	2036
24.4.2016	13,04	8,62	34 %	408	1841
1.5.2016	18,81	9,94	47 %	393	1145
8.5.2016	18,35	10,74	41 %	656	515
15.5.2016	19,3	8,67	55 %	571	246
22.5.2016	18,38	9,98	46 %	550	161

Table 18: Version 700 dielectric constant amplitude, comparison between different snow conditions. Coloring: yellow – relative difference greater than 30%, green – greater than 50%, red – less than 0%.

start date	mean, swe < 5 mm	mean, swe > 50 mm	relative difference	count, swe < 5 mm	count, swe > 5 mm
8.11.2015	8,63	9,6	-11 %	960	101
15.11.2015	9,8	6,61	33 %	622	237
22.11.2015	10,22	5,59	45 %	505	351
29.11.2015	9,47	5,12	46 %	741	715
6.12.2015	16,75	5,05	70 %	622	1181
13.12.2015	9,3	4,62	50 %	693	1502
20.12.2015	17,21	5,31	69 %	652	1742
27.12.2015	8,68	4,63	47 %	1340	1782
3.1.2016	6,74	3,89	42 %	590	1334
7.2.2016	12,55	4,35	65 %	112	3042
20.3.2016	5,44	3,58	34 %	118	3500
27.3.2016	8,94	4,2	53 %	287	3119
3.4.2016	8,53	4,49	47 %	409	2651
10.4.2016	8,18	4,11	50 %	664	2293
17.4.2016	8,61	4,49	48 %	419	2010
24.4.2016	9,83	6,08	38 %	471	1779
1.5.2016	11,11	6,93	38 %	414	1143
8.5.2016	12,06	7,52	38 %	677	514
15.5.2016	13,28	5,38	59 %	628	243
22.5.2016	14,18	6,49	54 %	550	164

Unfortunately, due to the many limitations, the strength of this evidence is rather weak. First, the different instances of data come from DGG pixels having different geophysical properties and states. Second, the errors and uncertainties in the ECMWF SWE estimate will further decrease the strength of the evidence. Third, the presence of snow is connected via air and ground temperature, and other variables to ground permittivity, and therefore there is also an actual physical reason why the observed separation of the two groups should happen. As a conclusion, we observe the expected difference between the two groups, but due to many limitations cannot say whether the difference is physical or underestimation dielectric constant due to the presence of snow. Either a comparison of time series from one DGG pixel with in-situ data, or further enhancement of this approach is needed to better understand the question whether the presence of snow affects the retrievals of dielectric constant.

5.2.5.2 FINLAND, DECISION TREE VALUES 9 AND 10 (FROZEN CONDITIONS)

Like the previous subsection, we will focus on the general area around Finland, and decision tree values 9 and 10, which indicate frozen conditions. The following two figures show the areal maps of the retrieved dielectric constant for both versions 650 and 700, as well as the corresponding L3FT and ECMWF SWE maps. As it was in the previous case, also here the "hot spots" are more visible for the version 700.

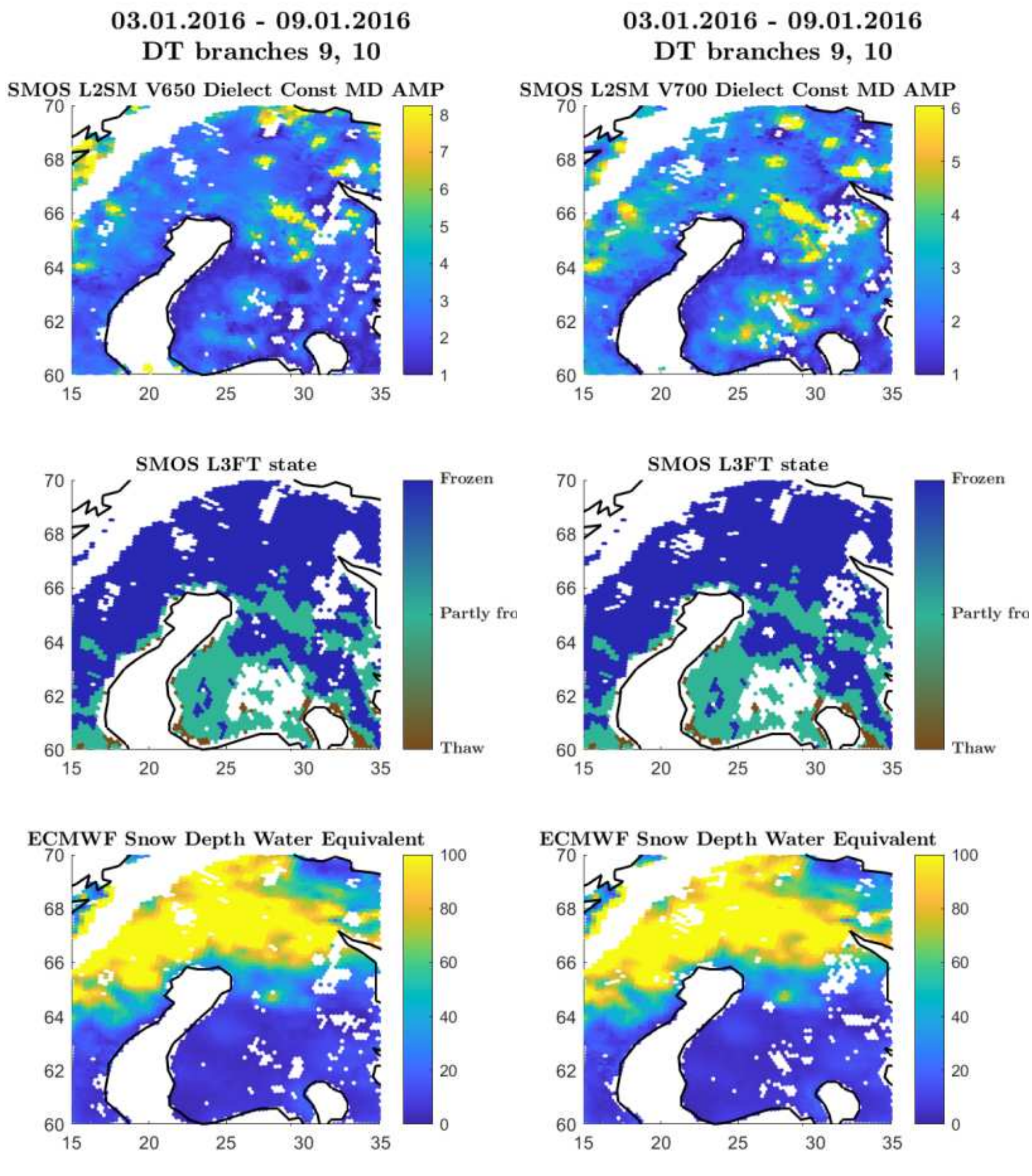

Figure 182: Southern Finland maps of retrieved v700 (top right) vs. v650 (top left) for DT 9, 10 along with frozen and thaw state maps and AUX_ECMWF SD maps for the period 03.01.2016 – 09.01.2016

As an example, the figure below shows a comparison of distribution of the retrieved values. For this week, the two versions are distribution wise very similar.

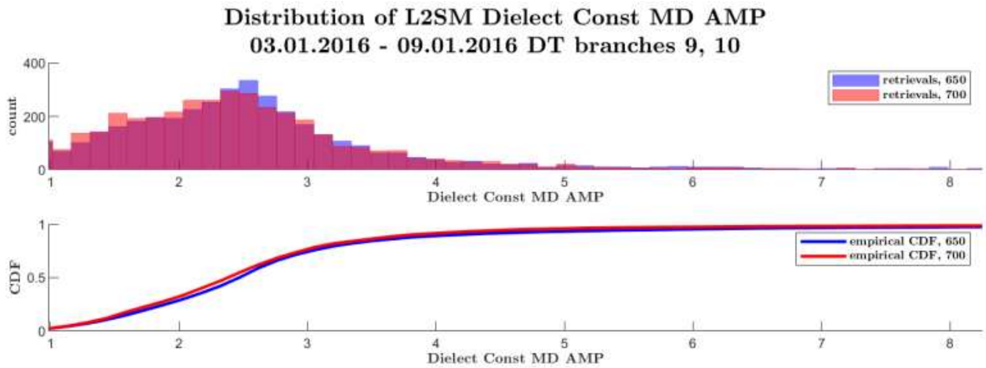

Figure 183: Distributions (top) of and ecfd (bottom) of retrieved v700 (red) vs. v650 (blue) for DT 9, 10 over Southern Finland and for the period 03.01.2016 – 09.01.2016

The following table summarizes similar comparison for every week within the period of interest. The coloring is the following: yellow for values of relative difference larger than 15% (650 has higher values) and green for values smaller than -15% (700 has higher values). The relative difference columns in the table refer to the previous two columns, respectively. As it was the case when comparing retrievals for decision tree branches 5, 6, 7, and 8, it is also now visible that on average, the version 650 has higher values than 700. Also, for the standard deviation (within the area of interest, shown in the maps), 650 attains higher values than 700. What is different from the earlier comparison with decision tree branches 5, 6, 7, and 8, is that the version 700 seems to have often considerably more retrievals than the version 650 (last three columns).

Table 19: Comparison of the statistics for averaged retrieved dielectric constant amplitude within the general area around Finland, restricted to the decision tree values 9 and 10 (frozen conditions). Coloring: yellow – relative difference > 15 %, green – relative difference < - 15 %.

start date	mean 650	mean 700	relative difference	standard deviation 650	standard deviation 700	relative difference	count 650	count 700	relative difference
30.8.15	18,32	10,91	40 %	9,1	3,9	57 %	4057	3994	2 %
6.9.15	17,95	11,27	37 %	9,5	4,36	54 %	4118	4058	1 %
13.9.15	19,81	12,31	38 %	10,98	4,9	55 %	4100	4046	1 %
20.9.15	22,99	15,48	33 %	13,59	6,77	50 %	4029	4024	0 %
27.9.15	19,93	13,47	32 %	10,67	5,22	51 %	4063	4041	1 %
4.10.15	15,02	10,42	31 %	9	5,34	41 %	3766	3983	-6 %
11.10.15	16,77	9,86	41 %	9,63	4,26	56 %	3291	3358	-2 %
18.10.15	19,14	12,1	37 %	10,7	5,17	52 %	3720	3779	-2 %
25.10.15	19,14	13,16	31 %	12,41	7,02	43 %	3529	3733	-6 %

1.11.15	17,77	11,48	35 %	10,61	5,3	50 %	3598	3685	-2 %
8.11.15	18,7	12,74	32 %	11,5	7,02	39 %	2824	3003	-6 %
15.11.15	17,87	11,81	34 %	13,13	7,97	39 %	1473	1705	-16 %
22.11.15	9,25	7,45	19 %	11,11	10,45	6 %	756	1154	-53 %
29.11.15	24,5	13,9	43 %	16,04	10,12	37 %	779	1019	-31 %
6.12.15	29,81	18,06	39 %	18,64	10,17	45 %	1144	1269	-11 %
13.12.15	11,71	8,79	25 %	15,22	10,45	31 %	2061	2730	-32 %
20.12.15	27,85	15,45	45 %	18,39	10,63	42 %	1306	1649	-26 %
27.12.15	7,96	7,54	5 %	13,73	12,65	8 %	1082	1616	-49 %
3.1.16	4,35	4,72	-9 %	7,5	6,71	11 %	1247	1670	-34 %
10.1.16	3,21	4,05	-26 %	1,63	4,72	-190 %	656	857	-31 %
17.1.16	3,06	3,9	-27 %	1,44	4,08	-183 %	620	913	-47 %
24.1.16	2,93	3,43	-17 %	0,6	2	-233 %	112	270	-141 %
31.1.16	2,98	3,12	-5 %	1,63	2,38	-46 %	316	582	-84 %
7.2.16	8,69	4,26	51 %	12,07	3,89	68 %	68	208	-206 %
14.2.16	3,07	4,09	-33 %	0,59	1,59	-169 %	63	129	-105 %
21.2.16	2,7	2,72	-1 %	1	1,81	-81 %	679	1431	-111 %
28.2.16	2,7	2,77	-3 %	0,76	1,98	-161 %	625	1208	-93 %
6.3.16							0	0	
13.3.16	18,5	7,46	60 %	11,24	4,86	57 %	4	5	-25 %
20.3.16	3,79	3,8	0 %	4,96	5,14	-4 %	607	1058	-74 %
27.3.16	14,51	11,43	21 %	9,83	6,22	37 %	150	182	-21 %
3.4.16	18,59	16,04	14 %	11,78	8,2	30 %	280	282	-1 %
10.4.16	14,13	10,95	23 %	11,57	7,6	34 %	1044	1015	3 %
17.4.16	16,67	11,74	30 %	12,39	7,49	40 %	1204	1154	4 %
24.4.16	19,38	13,72	29 %	13,8	8,46	39 %	1673	1778	-6 %
1.5.16	27,21	16,9	38 %	14,74	7,54	49 %	2410	2396	1 %
8.5.16	28,33	16,36	42 %	13,84	6,98	50 %	2841	2819	1 %
15.5.16	24,77	15	39 %	12,34	5,82	53 %	3355	3366	0 %
22.5.16	23,16	15,05	35 %	11,94	5,81	51 %	3591	3561	1 %
29.5.16	22,93	13,02	43 %	11,93	3,95	67 %	3657	3648	0 %

Next, we will compare the retrieved dielectric constant values between L3FT freeze-thaw state estimates. As before, we split the dielectric constant values into two groups, corresponding to thaw states and freeze states (some retrievals which do not clearly belong to either group are discarded). The following tables show the results for this comparison. The tables are a slightly different format compared to the case where we studied different decision tree branches. In the decision tree branches 9 and 10 we expect most of the retrievals to be associated with frozen estimate from L3FT.We will color the deviations from our expectations as red: for "thaw mean" column values less than 10, for "frozen mean" values greater than 10. These limits are arbitrary but might give an idea where to aim our focus.

Table 20: Version 650 dielectric constant amplitude retrievals restricted to decision tree values 9 and 10. Comparison of mean values between freeze and thaw states (from L3FT). Coloring: red – thaw values < 10 or frozen values > 10.

start date	thaw mean	thaw count	frozen mean	frozen count
4.10.2015	20,94	7		0
18.10.2015	19,25	6		0
25.10.2015	13,02	412	24,1	5
1.11.2015	28,09	38	8,26	79
8.11.2015	6,36	29	9,59	332
15.11.2015	4,53	61	7,13	797
22.11.2015	8,52	74	7,27	1433
29.11.2015	1,68	1	7,79	1775
6.12.2015		0	7,01	1780
13.12.2015	6,78	313	5,84	1825
20.12.2015		0	8,27	1980
27.12.2015	5,78	375	6,89	2023
3.1.2016	1,86	97	5,08	1745
10.1.2016	1,71	1	2,97	2210
17.1.2016		0	3,57	1767
24.1.2016		0	5,2	3505
31.1.2016		0	4,52	3571
7.2.2016		0	8,72	3557
14.2.2016	6,04	11	4,74	3524
21.2.2016	3,82	7	4,43	3546

28.2.2016		0	4	3549
6.3.2016		0	5,35	3586
13.3.2016		0	6,62	3562
20.3.2016		0	4,06	3480
27.3.2016		0	6,43	3159
3.4.2016		0	6,42	2539
10.4.2016		0	5,33	2102
17.4.2016		0	6,51	1873
24.4.2016		0	9,77	725
1.5.2016		0	7,22	262
8.5.2016		0	6,78	164
15.5.2016		0	7,63	158
22.5.2016		0	7,59	14

Table 21: Version 700 dielectric constant amplitude retrievals restricted to decision tree values 9 and 10. Comparison of mean values between freeze and thaw states (from L3FT). Coloring: red –thaw values < 10 or frozen values > 10.

start date	thaw mean	thaw count	frozen mean	frozen count
4.10.2015	20,62	10		0
18.10.2015	24,03	7		0
25.10.2015	13,42	414	18,67	5
1.11.2015	20,21	81	6,06	79
8.11.2015	6,4	21	4,17	332
15.11.2015	3,65	52	4,77	798
22.11.2015	7,74	89	4,53	1433
29.11.2015	1,49	1	4,81	1774
6.12.2015		0	4,8	1780
13.12.2015	7,36	322	4,36	1832
20.12.2015		0	5,44	1974
27.12.2015	6,11	365	5,03	2016
3.1.2016	1,87	94	4,33	1779
10.1.2016	1,24	4	2,79	2325

17.1.2016		0	2,95	1946
24.1.2016		0	4,01	3514
31.1.2016		0	4,2	3553
7.2.2016		0	5,57	3550
14.2.2016	5,29	11	4,05	3517
21.2.2016	3,37	6	4	3536
28.2.2016		0	3,58	3543
6.3.2016		0	3,85	3551
13.3.2016		0	4,4	3539
20.3.2016		0	3,1	3422
27.3.2016		0	3,81	3095
3.4.2016		0	4,23	2504
10.4.2016		0	3,91	2082
17.4.2016		0	4,29	1855
24.4.2016		0	6,96	723
1.5.2016		0	4,93	261
8.5.2016		0	4,24	164
15.5.2016		0	4,91	159
22.5.2016		0	4,29	14

There are many weeks where there is only a small number of retrievals associated with thaw ground. However, there are still more than what we would expect. Also, the mean values for the measurements associated with thaw ground seem to have rather low values (colored red in the tables). The following figures show an example of such week, starting from 27.12.2015.

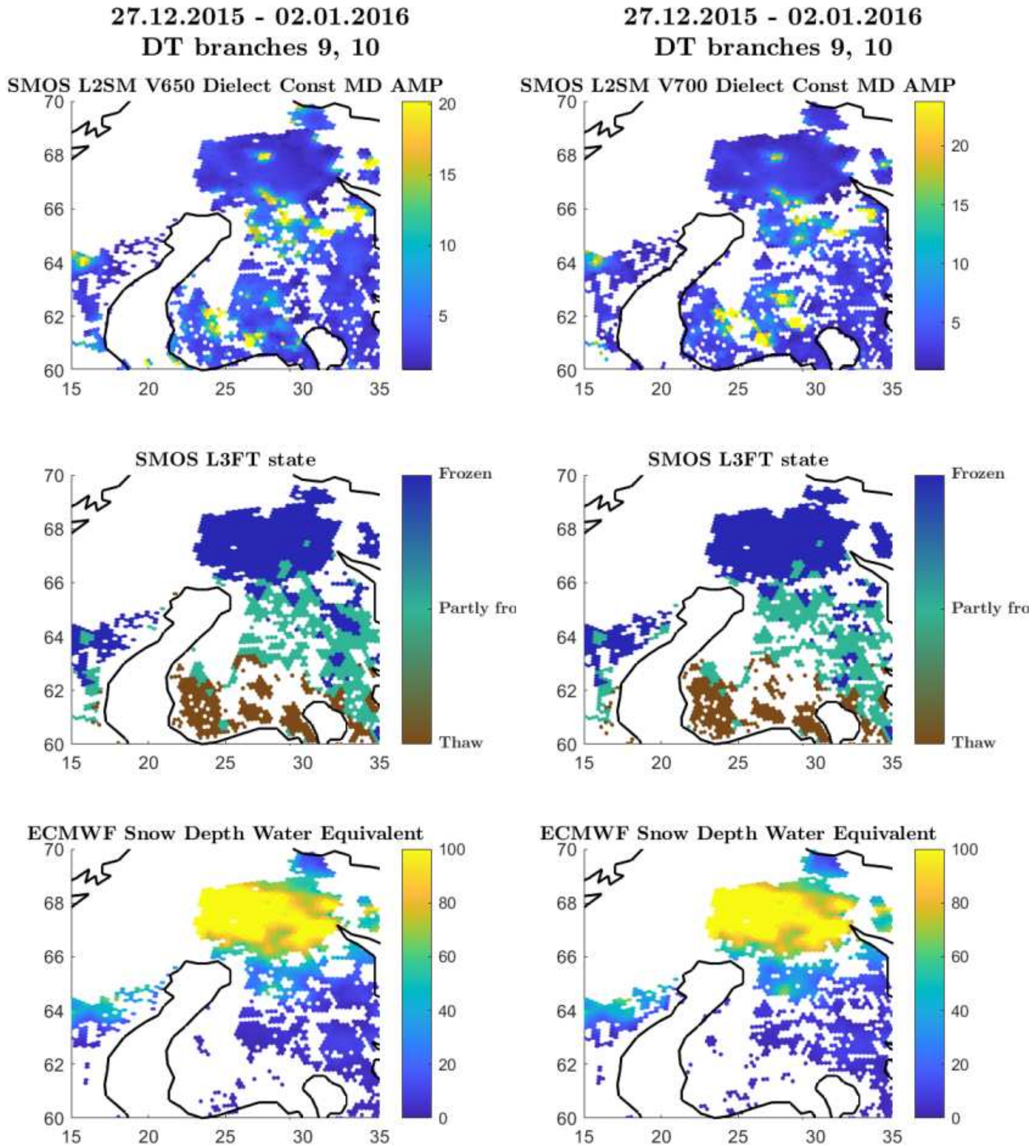

Figure 184: Southern Finland maps of retrieved v700 (top right) vs. v650 (top left) for DT 9, 10 along with frozen and thaw state maps and AUX_ECMWF SD maps for the period 27.12.2015 – 02.01.2016

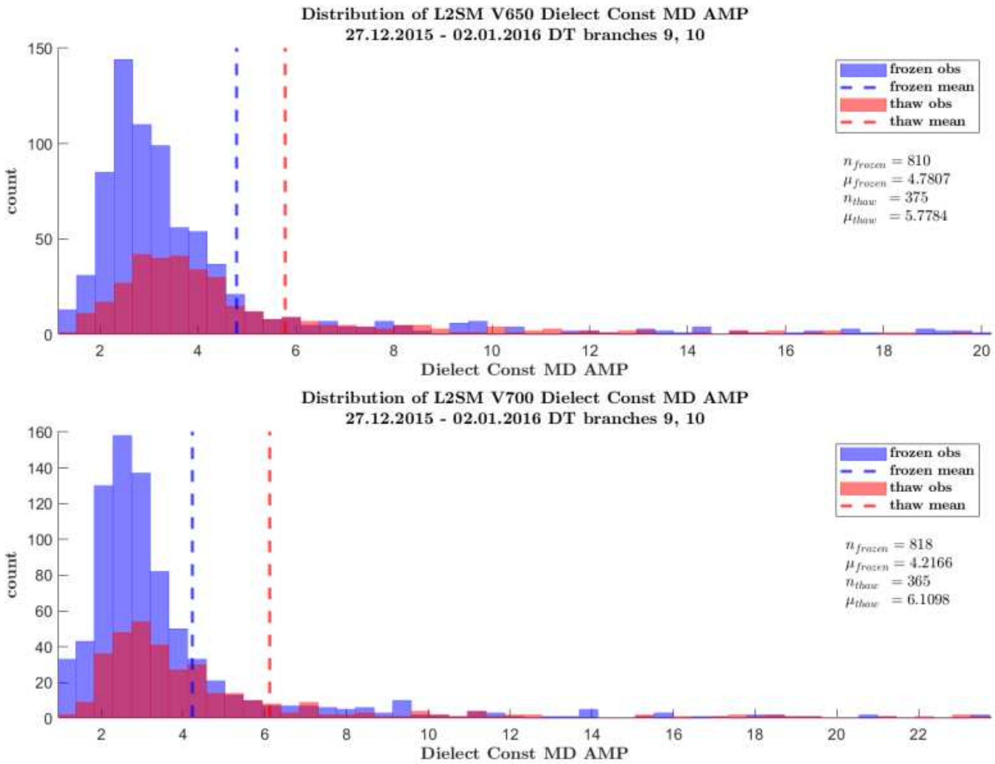

Figure 185: Distribution of retrievals v700 (bottom) vs. v650 (top) for DT 9, 10 along with frozen and thaw state distributions over Southern Finland and for the period 27.12.2015 – 02.01.2016

The maps above show that the retrievals associated with thaw ground (southern Finland) are not affected by snow. This indicates a disagreement between the retrieved dielectric constant values and L3FT estimates, as from thaw ground without the presence of snow, one would generally expect higher dielectric constant values. This disagreement is present in both versions 650 and 700, and it cannot be said to be stronger in one or the other. As this is only one example of such disagreement, it would require a further study to determine whether such disagreements occur and how frequently. This, and the cause of the disagreement are not studied further at this time.

Finally, we will make a similar comparison between ECMWF SWE estimate and the retrievals of dielectric constant as before. Again, we split the retrievals into two groups, one corresponding to SWE values less than 5 mm and the other to SWE values greater than 50 mm and compare the statistics of these two groups. The figures below show histograms of such split as an example.

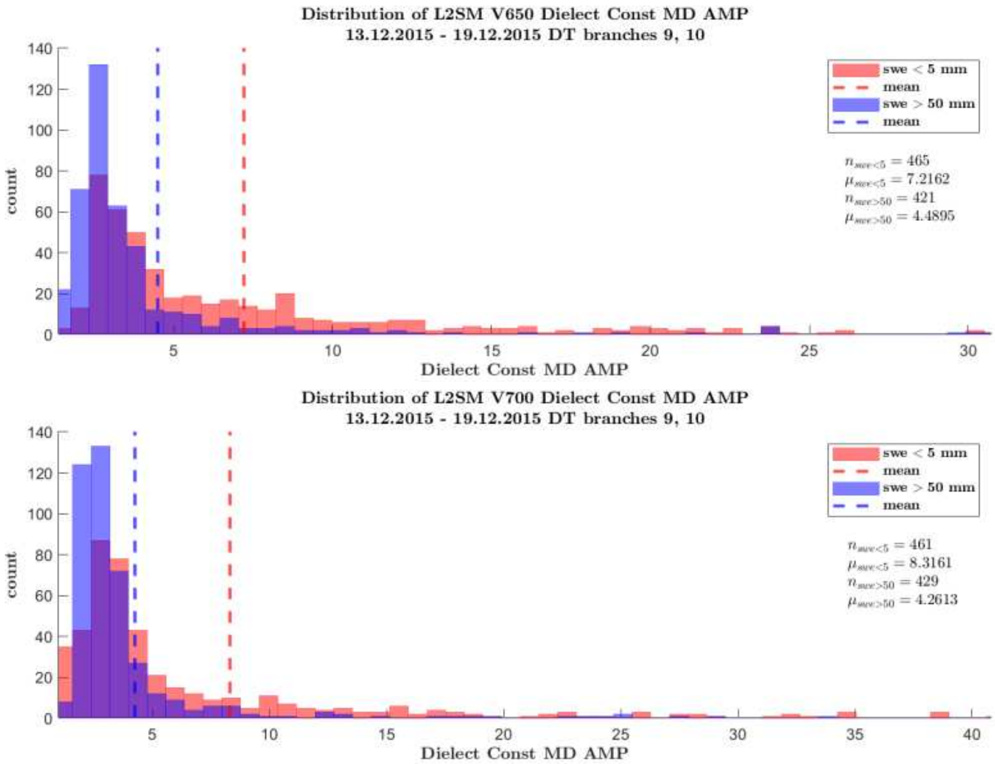

Figure 186: Distribution of retrievals v700 (bottom) vs. v650 (top) for DT 9, 10 along with swe < 5mm and swe>50m distributions over Southern Finland and for the time period 13.12.2015 – 19.12.2015

The below table provides a summary over the whole period of interest. Weeks where there were less than 100 retrievals in either class are discarded. The same limitations hold as before when it comes to this comparison. On the one hand, we expect that the other geophysical factors affecting the distributions are more controlled within frozen decision tree branches. On the other hand, a small number of weeks where a comparison is possible, it is again hard to make conclusions. Although frozen decision tree branches (9 and 10) might provide more stability into the comparison, the small number of available weeks would require this comparison to be extended into a larger period. This should be considered in the possible future comparisons.

Table 22: Version 650 dielectric constant amplitude, comparison between different snow conditions. Coloring: yellow – relative difference greater than 30%, green – greater than 50%, red – less than 0%.

start date	mean, swe < 5 mm	mean, swe > 50 mm	relative difference	count, swe < 5 mm	count, swe > 50 mm
13.12.2015	7,22	4,49	38 %	465	421
27.12.2015	5,05	4,26	16 %	899	601

3.1.2016	2,35	3,4	-45 %	390	1474

Table 23: Version 700 dielectric constant amplitude, comparisonbetween different snow conditions.Coloring: yellow – relative difference greater than 30%, green – greater than 50%, red – less than 0%.

start date	mean, swe < 5 mm	mean, swe > 50 mm	relative difference	count, swe < 5 mm	count, swe > 50 mm
13.12.2015	8,32	4,26	49 %	461	429
27.12.2015	5,76	3,71	36 %	895	601
3.1.2016	2,34	3,09	-32 %	360	1482

5.2.5.3 SODANKYLÄ, SIMPLE TIME SERIES INSPECTION

To see if the effect of snow in the retrieval of dielectric constant is visible on a local scale, we do a visual comparison of time series from the Sodankylä DGG pixel. In the above plots a time series of the versions 700 and 650 are plotted next to in-situ snow depth (measured at FMI weather station at Tähtelä, Sodakylä) and colored according to in-situ ground temperature (measured at 5 cm depth), which is averaged over four in-situ sites (located around Sodankylä region) with codes DIS0001, DIS0002, IOA0007, and LEN0001.

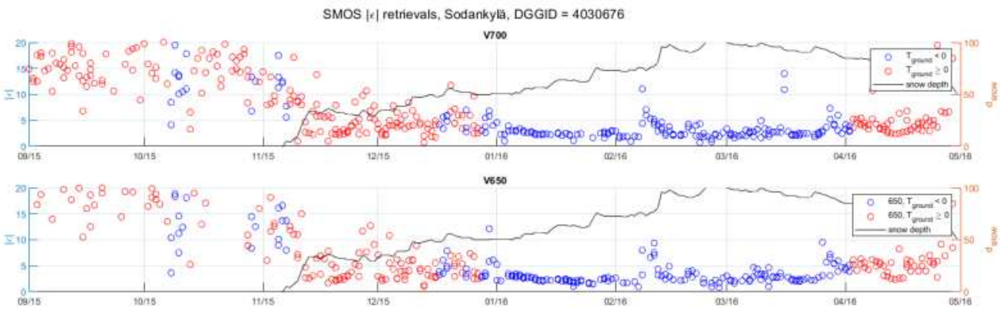

Figure 187: v700 (top) vs. v650 (bottom) retrievals time series at Sodankylä identified with positive ground temperature >0°C (red marker) and negative < 0°C (blue marker) along with snow depth (black).

The above figure shows a decrease in the dielectric constant values at the same time as the snow starts to appear, while the ground temperature indicates above zero temperature. However, below we show another time series, with slightly changed temperature threshold. From this figure it cannot be said that the decrease would be caused by appearance of snow. Therefore, when taking the representativeness uncertainties of the in-situ sites into account, it is not possible to conclude about the effect of snow on the retrieved value of dielectric constant.

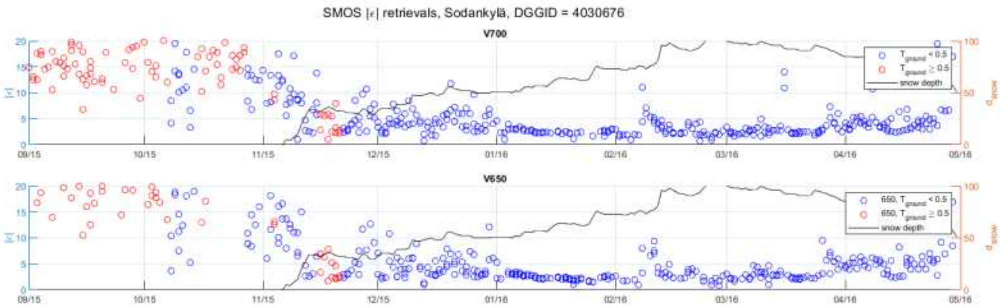

Figure 188: v700 (top) vs. v650 (bottom) retrievals time series at Sodankylä identified with ground temperature > 0.5°C (red marker), < 0.5°C (blue marker) along with snow depth (black).

5.2.6 VEGETATION OPTICAL DEPTH

For vegetation optical depth, we will only look at the summary tables below. These contain the weekly averaged value from the general area around Finland, like the previous comparison of dielectric constant. The only clear trend visible is that for decision tree branches 9 and 10 (frozen conditions), the version 700 has more retrievals than the version 650. The same was observed earlier when comparing dielectric constant.

Table 24: Comparison of weekly averaged VOD retrievals, restricted to the decision tree branches 5, 6, 7, and 8 (snow conditions). Coloring: yellow –relative difference < -15 %, green – relative difference > 15 %.

start date	mean 650	mean 700	relative difference	standard deviation 650	standard deviation 700	relative difference	count 650	count 700	relative difference
30.8.15	0,35	0,43	-23 %	0,06	0,07	-17 %	149	150	-1 %
6.9.15	0,32	0,4	-25 %	0,07	0,08	-14 %	148	150	-1 %
13.9.15	0,36	0,42	-17 %	0,06	0,07	-17 %	92	94	-2 %
20.9.15	0,33	0,39	-18 %	0,07	0,07	0 %	92	94	-2 %
27.9.15	0,41	0,5	-22 %	0,12	0,16	-33 %	701	900	-28 %
4.10.15	0,47	0,57	-21 %	0,15	0,14	7 %	1337	1348	-1 %
11.10.15	0,45	0,55	-22 %	0,13	0,13	0 %	1163	1162	0 %
18.10.15	0,39	0,51	-31 %	0,11	0,13	-18 %	873	888	-2 %
25.10.15	0,56	0,63	-12 %	0,19	0,18	5 %	2557	2562	0 %
1.11.15	0,54	0,61	-13 %	0,19	0,16	16 %	2279	2411	-6 %
8.11.15	0,59	0,62	-5 %	0,2	0,18	10 %	3124	3148	-1 %
15.11.15	0,57	0,59	-4 %	0,15	0,17	-13 %	4023	4030	0 %

22.11.15	0,56	0,57	-2 %	0,14	0,15	-7 %	4411	4421	0 %
29.11.15	0,59	0,59	0 %	0,14	0,14	0 %	4153	4145	0 %
6.12.15	0,58	0,59	-2 %	0,14	0,16	-14 %	3960	3984	-1 %
13.12.15	0,56	0,54	4 %	0,17	0,18	-6 %	4196	4203	0 %
20.12.15	0,57	0,57	0 %	0,14	0,17	-21 %	4003	4048	-1 %
27.12.15	0,57	0,54	5 %	0,18	0,2	-11 %	4235	4300	-2 %
3.1.16	0,54	0,49	9 %	0,22	0,23	-5 %	2602	2529	3 %
10.1.16	0,48	0,42	13 %	0,23	0,23	0 %	1206	1223	-1 %
17.1.16	0,48	0,44	8 %	0,24	0,22	8 %	1151	1227	-7 %
24.1.16	0,5	0,44	12 %	0,2	0,2	0 %	4183	4110	2 %
31.1.16	0,45	0,43	4 %	0,19	0,19	0 %	4375	4353	1 %
7.2.16	0,54	0,5	7 %	0,16	0,15	6 %	4533	4504	1 %
14.2.16	0,52	0,48	8 %	0,18	0,18	0 %	4345	4364	0 %
21.2.16	0,5	0,47	6 %	0,18	0,19	-6 %	4441	4411	1 %
28.2.16	0,47	0,45	4 %	0,21	0,22	-5 %	4283	4248	1 %
6.3.16	0,56	0,48	14 %	0,17	0,18	-6 %	4531	4379	3 %
13.3.16	0,5	0,46	8 %	0,16	0,16	0 %	4541	4446	2 %
20.3.16	0,45	0,39	13 %	0,17	0,16	6 %	4434	4344	2 %
27.3.16	0,49	0,43	12 %	0,15	0,16	-7 %	4503	4334	4 %
3.4.16	0,46	0,42	9 %	0,13	0,15	-15 %	4167	4073	2 %
10.4.16	0,46	0,44	4 %	0,15	0,16	-7 %	3959	3819	4 %
17.4.16	0,48	0,46	4 %	0,15	0,18	-20 %	3072	3029	1 %
24.4.16	0,46	0,45	2 %	0,14	0,15	-7 %	3067	3037	1 %
1.5.16	0,46	0,45	2 %	0,15	0,16	-7 %	2178	2194	-1 %
8.5.16	0,42	0,44	-5 %	0,12	0,12	0 %	1852	1866	-1 %
15.5.16	0,42	0,47	-12 %	0,12	0,13	-8 %	1204	1254	-4 %
22.5.16	0,37	0,42	-14 %	0,1	0,12	-20 %	895	902	-1 %
29.5.16	0,33	0,39	-18 %	0,09	0,1	-11 %	611	632	-3 %

Table 25: Comparison of weekly averaged VOD retrievals, restricted to the decision tree branches 9 and 10 (frozen conditions). Coloring: yellow – relative difference < -15 %, green – relative difference > 15 %.

start date	mean 650	mean 700	relative difference	standard deviation	standard deviation	relative difference	count 650	count 700	relative difference

				650	700				
4.10.15	0,76	0,77	-1 %	0,03	0,04	-33 %	7	10	-43 %
18.10.15	0,7	0,83	-19 %	0,05	0,09	-80 %	6	7	-17 %
25.10.15	0,58	0,61	-5 %	0,27	0,24	11 %	379	408	-8 %
1.11.15	0,79	0,72	9 %	0,24	0,21	13 %	66	137	-108 %
8.11.15	0,45	0,49	-9 %	0,24	0,28	-17 %	98	69	30 %
15.11.15	0,36	0,36	0 %	0,24	0,23	4 %	152	159	-5 %
22.11.15	0,47	0,47	0 %	0,27	0,22	19 %	424	501	-18 %
29.11.15	0,62	0,54	13 %	0,17	0,13	24 %	23	23	0 %
6.12.15	0,43	0,36	16 %	0,06	0,05	17 %	2	2	0 %
13.12.15	0,52	0,51	2 %	0,24	0,23	4 %	1392	1487	-7 %
20.12.15	0,47	0,43	9 %	0,26	0,22	15 %	69	81	-17 %
27.12.15	0,44	0,45	-2 %	0,22	0,22	0 %	1409	1393	1 %
3.1.16	0,44	0,43	2 %	0,2	0,21	-5 %	1666	1732	-4 %
10.1.16	0,53	0,48	9 %	0,21	0,2	5 %	1267	1566	-24 %
17.1.16	0,46	0,42	9 %	0,2	0,2	0 %	1138	1370	-20 %
24.1.16	0,44	0,39	11 %	0,2	0,19	5 %	768	871	-13 %
31.1.16	0,43	0,4	7 %	0,2	0,18	10 %	327	386	-18 %
7.2.16	0,55	0,61	-11 %	0,37	0,3	19 %	54	43	20 %
14.2.16	0,38	0,37	3 %	0,25	0,27	-8 %	42	36	14 %
21.2.16	0,41	0,37	10 %	0,2	0,12	40 %	82	121	-48 %
28.2.16	0,42	0,35	17 %	0,16	0,13	19 %	265	286	-8 %
20.3.16	0,36	0,33	8 %	0,2	0,17	15 %	206	243	-18 %

5.3 CLIMATOLOGY

This section examines soil moisture trends for selected geographical regions using data from L2SM v650 and v700. For v700 we also consider ascending passes versus descending passes, and the impact of RFI filtering. We use Hovmöller diagrams over specific regions for the period of 2010 to 2020 to depict SM anomalies. The SM anomalies are measured using an average of SMOS Level 2 SM for the years 2012 to 2016. We used 2012 as a starting point for the SM reference set to avoid the strong RFI contamination over northern Canada prior to this year. We use a running window of size 11 (days) to compute each SM sample before averaging over longitudinal bands. Each data point in a Hovmöller plot represents the anomaly of SM average over a specified latitudinal band with respect to reference data (2012-2016).

The purpose of this section is mainly to investigate the differences between v650 and v700, and to unveil possible issues with the v700 product. An investigation of climatological trends is beyond the scope of this document. We have therefore selected a small subset of plots that help emphasize the points we wish to raise here.

For many regions we found that SM trends as indicated by v700 are quite similar to those of v650, except for the fact that v700 plots indicate more retrievals than v650. Figure 189 shows an area in South America where v650 ascending and v700 (both ascending and descending) are in good agreement. Figure 190 shows anomalies over Washington state of US and Vancouver province of Canada where v700 ascending and descending passes give a complete opposite trend for the years 2010 and 2011. This is caused by the RFI sources in northern Canada (switched off in 2011). Figure 191 gives pictures for a region in north India where RFI is strong and we see differences between images before and after RFI filtering and between ascending and descending of v700.

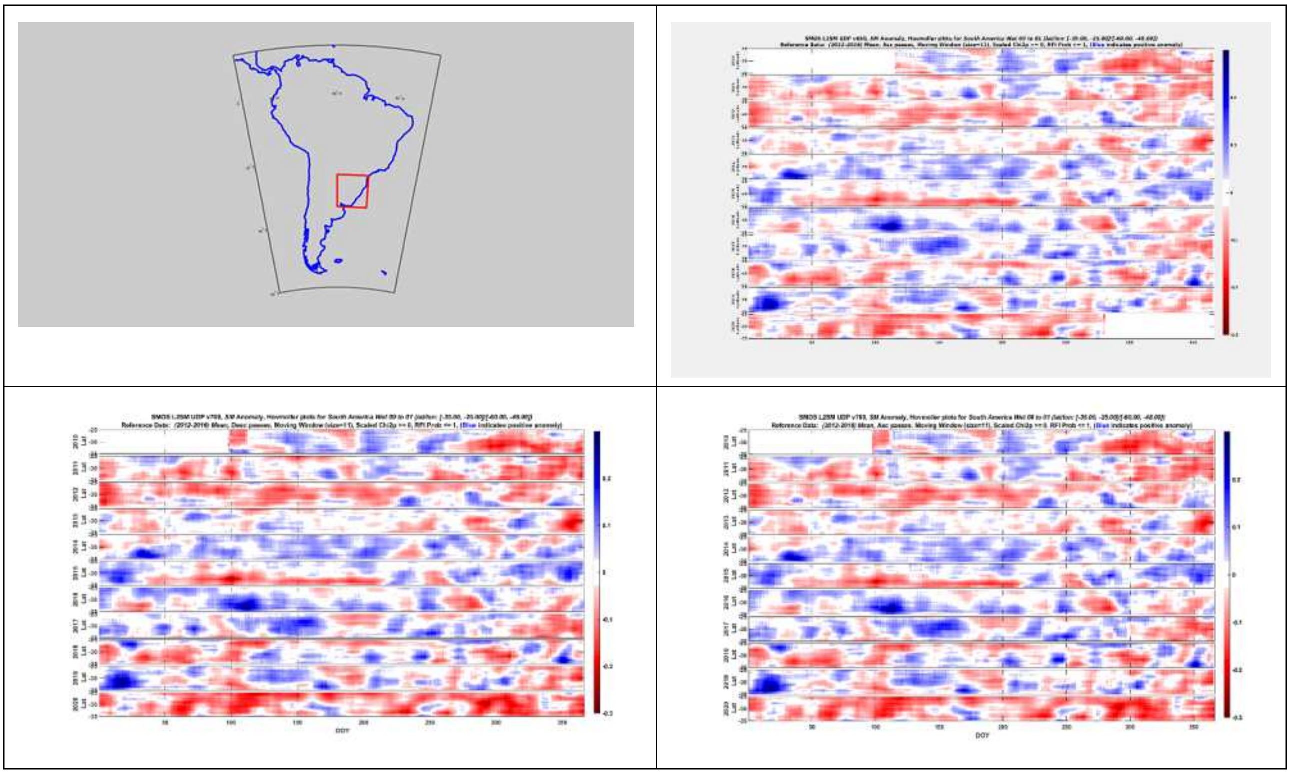

Figure 189: South America SM anomalies (top right) v650 Ascending (bottom left) v700 Descending (bottom right) v700 Ascending. No RFI filtering was applied.

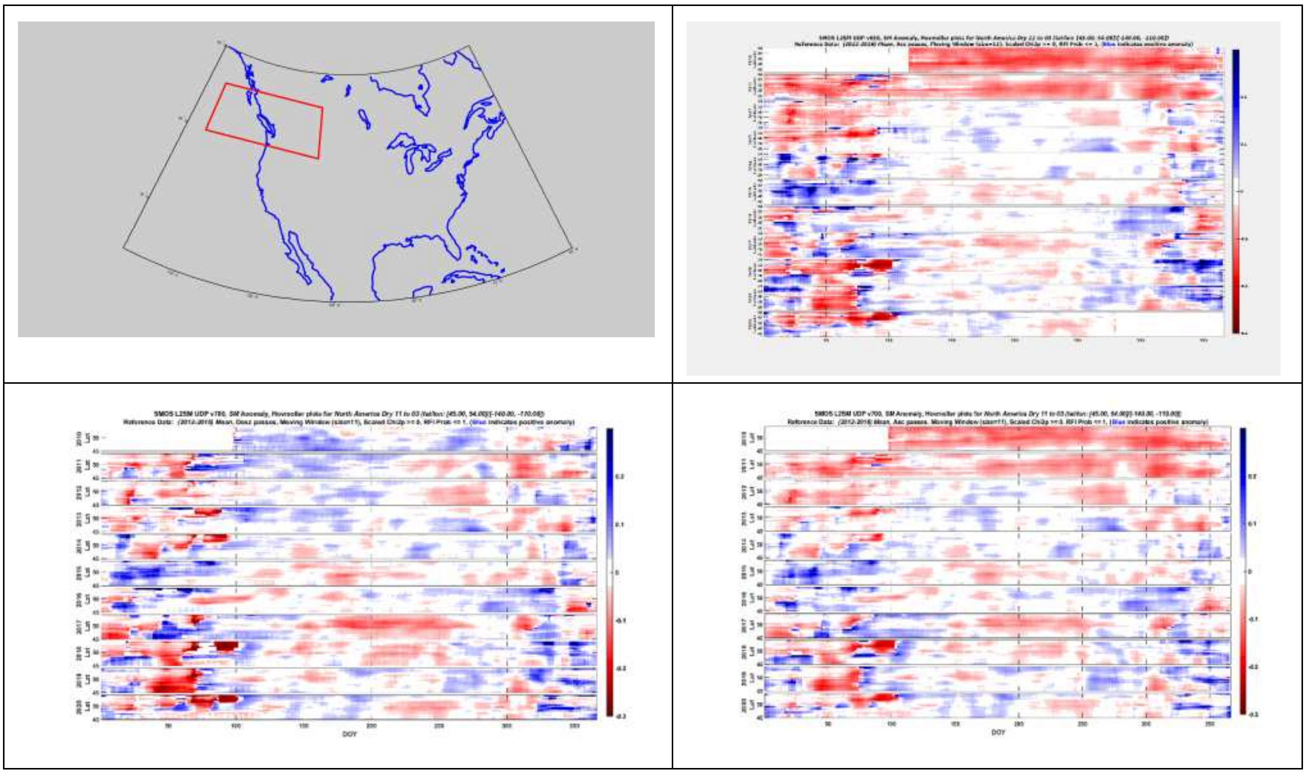

Figure 190: North America SM anomalies (top right) v650 Ascending(bottom left) v700 Descending (bottom right) v700 Ascending. No RFI filtering was applied.

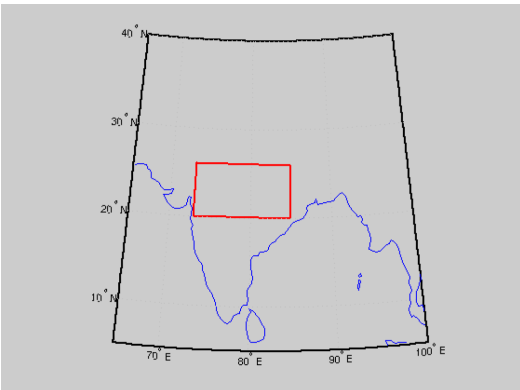

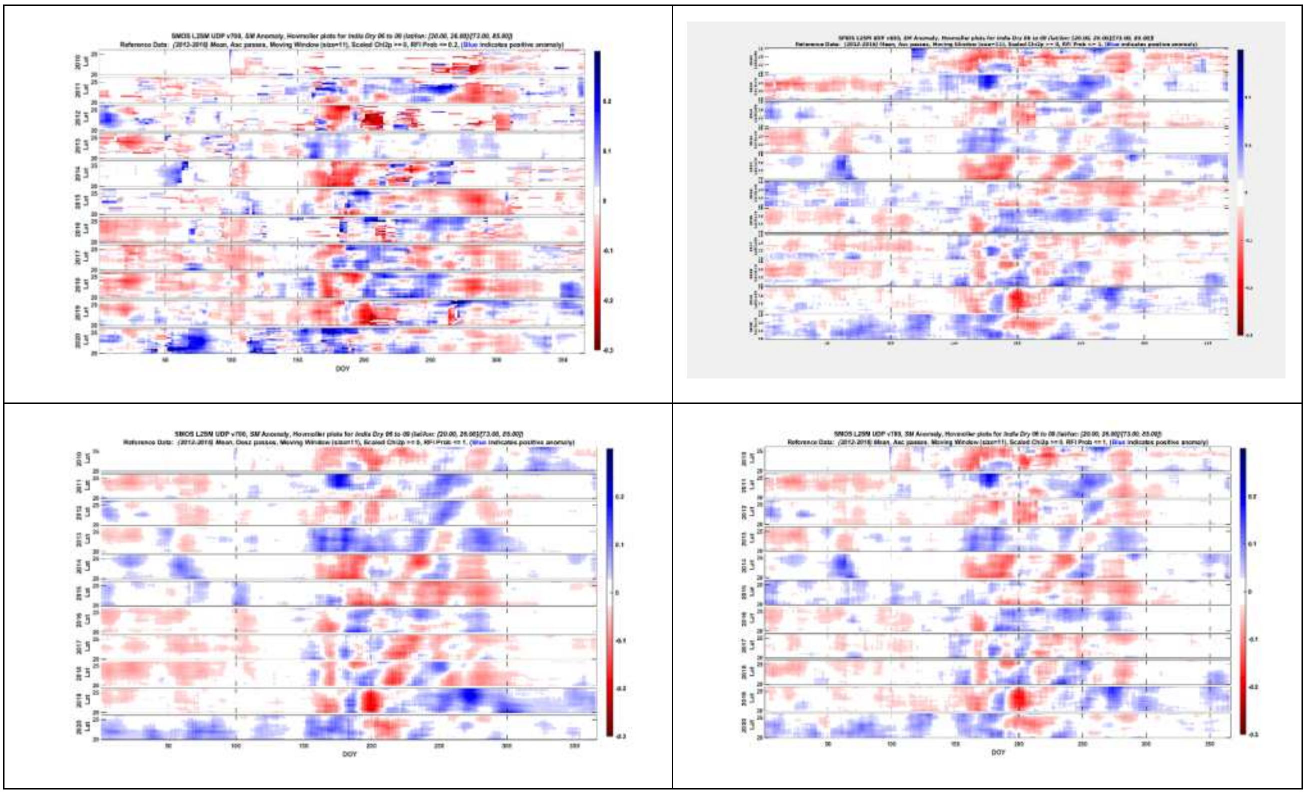

Figure 191: North India SM anomalies (top left) v700 Ascending (RFI <= 0.2), (top right) v650 Ascending, (bottom left) v700 Descending, (bottom right) v700 Ascending.